Permanganate Flushing of DNAPL Source Zones: Experimental and Numerical Investigation

by

Eric David Hood

A thesis
presented to the University of Waterloo
in fulfilment of the
thesis requirement for the degree of
Doctor of Philosophy
in
Civil Engineering

Waterloo, Ontario, Canada, 2000

The University of Waterloo requires the signatures of all persons using or photocopying this thesis. Please sign below and give address and date.

Abstract

In situ chemical oxidation (ISCO) is a potentially effective technology for remediating aquifers contaminated with dense, non-aqueous phase liquids (DNAPLs) such as trichloroethene (TCE) and perchloroethene (PCE). These contaminants dissolve slowly in groundwater; however, the dissolution rate is enhanced by the addition of a concentrated oxidant, such as potassium permanganate, which rapidly degrades these contaminants to carbon dioxide and chloride. The research presented in this thesis focuses on the application and effectiveness of ISCO at the field scale. As part of this research, an ISCO field experiment was completed at an experimental site at Canadian Forces Base Borden. A small DNAPL source zone containing both residual PCE and TCE was flushed with a 8 g/L permanganate solution for 485 days. In addition, a numerical model was developed to simulate field-scale application of the remediation process.

Recycling of the residual permanganate in the extraction wells was used to minimize the mass of the oxidant injected into the treatment zone and the volume of effluent permanganate solution requiring treatment. In total, 892 kg of permanganate were injected into the treatment zone while 303 kg were recaptured by the recycling system. A permanganate mass balance was completed which suggested that much the injected oxidant solution was lost from the treatment zone. The oxidant loss was primarily attributed to downwards vertical flow caused by the density difference between the permanganate solution and the background porewater.

Groundwater monitoring during the oxidant flush focussed on characterizing the spatial distributions of permanganate and chloride in groundwater. While the injection system successfully flushed the source zone with the concentrated permanganate solution, the monitoring data suggested that some of the oxidant migrated below the capture zone of the extraction wells. Measurements of the chloride concentration down-gradient of the source zone were used to indicate the removal of DNAPL mass. Interpretation of the chloride concentrations measured in the extraction wells was complicated by the recycling of chloride along with the residual oxidant and provided little information on the rate of DNAPL mass removal; however, after ~300 days of oxidant injection, the concentration of chloride in the extraction wells was comparable to the background concentration of chloride, suggesting that the rate of DNAPL removal had slowed considerably. Discrete-depth sampling immediately down-gradient of the source zone was used to identify the presence of a high-concentration chloride signature. After 485 days of oxidant injection, high chloride concentrations were only found in samples collected right on the down-gradient edge of the source zone, suggesting that the chloride plume produced by DNAPL removal was small.

The performance of the oxidant flush was assessed by comparing the extent of groundwater contamination before and after the oxidant flush. Specific performance measures included the reductions in DNAPL mass, peak solvent concentration, and solvent plume load. While the

groundwater data indicated that some DNAPL was present in the source, DNAPL was not detected in soil samples collected from the source, emphasising the difficulty of evaluating DNAPL mass in the field. Plume loading was identified as the most useful performance measurement. The oxidant flush reduced the loads of TCE and PCE in the groundwater plume by 99% and 90%, respectively.

A numerical model was developed to simulate the kinetic physico-chemical processes through which enhanced mass transfer occurs. The model was applied to several synthetic scenarios to demonstrate the processes which influence the effectiveness of ISCO. A mass transfer enhancement in a scenario where dissolution was limited by diffusion across a stagnant path length was demonstrated; two-way diffusion of the oxidant towards the DNAPL zone increased the mass transfer rate in inverse proportion to the path length. The effect of several parameters on the effectiveness of ISCO was evaluated by applying the model to a synthetic field scale problem. Dispersivity and oxidation rate had no affect on the performance of ISCO; mass transfer rate, injected oxidant concentration, and hydraulic gradient had varying affects. Remediation appeared to be limited by the oxidant flux into the source zone and the mass transfer rate.

Acknowledgements

Seven years of continuous hard work was only possible with the energy and support of a number of organizations and individuals.

I would like to thank my supervisors, Dr. N.R. Thomson and Dr. G.J. Farquhar, for giving me the opportunity to work with them, and for their professional and personal support. While their contributions were from diverse technical perspectives, they share a common understanding of the need to enjoy work and the value of teaching that made working with them a pleasurable experience.

Research funding from a number of sources, including the Natural Sciences and Engineering Research Council (NSERC) of Canada, the Government of Ontario, and the University Consortium Solvents-in-Groundwater Research Program, is gratefully acknowledged. The sponsors of the Solvent Consortium have included the Boeing Company, Ciba-Geigy Corporation, Dow Chemical Canada/USA, Eastman Kodak Company, General Electric Company, Laidlaw Environmental Systems Ltd., PPG Industries, and United Technologies Corporation. My participation in this program provided me with a unique opportunity to learn within one of the most active groundwater research programs in the world and gain an understanding of the key challenges in the field of contaminant hydrogeology. In addition, the Consortium meetings were an invaluable opportunity for me to develop communication skills.

I would like to thank the members of my thesis examining committee, especially Dr. R.L. Siegrist of the Colorado School of Mines, for their participation and comments on this thesis.

In addition to my efforts, a number of people lent their expertise to the experimental component of this research. In particular, the assistance of Mark Sobon and Bruce Stickney was invaluable. Mark and Bruce made a number of trips to Borden building components of the treatment system and assisting with sampling . In addition, their help in maintaining and operating the analytical equipment in the laboratory is greatly appreciated. Between them, I learned everything I ever wanted to know about gas and ion chromatography. Several other people participated in this research as undergraduate students. Sharla Howard assisted with column studies while James Cullen measured the oxidant demand of a number of samples.

I would like to thank my fellow students in the Water Resources Group for sharing their energy and enthusiasm. I would especially like to thank Dave for the many long discussions in our office and for the opportunity to share in a small way in raising his first daughter. In addition, Fosh contributed significantly over the last 18 months by encouraging me to move forward and finish. The patience of my family is appreciated and I thank them, especially my mother and my grandmother, for their love, unquestioning support, and occasional "loans". Finally, I would like to express my heartfelt gratitude and thanks to Monica Emelko for her encouragement and support throughout these last few years.

TABLE OF CONTENTS

LIST OF FIGURES

LIST OF TABLES

Chapter 1
Introduction

Groundwater is an important resource throughout North America. In the U.S., groundwater accounts for approximately 53% of the drinking water supply (Moody, 1990). While surface water supplies are more available in Canada, a significant number of municipalities and individual rural homeowners rely on groundwater supplies. Groundwater supplies are a valuable resource due to their widespread availability in many regions, reliability during drought periods, typically good quality, and low treatment costs.

Over the last twenty five years, public concern about the quality of drinking water derived from groundwater sources has focussed on contamination by organic compounds. Quality surveys of groundwater-based drinking water supplies have identified volatile organic compounds (VOCs) as the most common contaminants (Westrick et al., 1984). These compounds are frequently cited as problematic pollutants in groundwater at industrial sites (Roberts et al., 1982; Grubb and Sitar, 1994). The widespread extent of VOC contamination may be attributed to the particular chemical and physical characteristics of some common VOC contaminants which are immiscible and denser than water (Schwille, 1988). Termed "dense, non-aqueous phase liquids" or DNAPLs, these compounds have low aqueous solubilities that exceed health-based regulatory criteria by as much as five orders of magnitude. In porous media aquifers, DNAPLs migrate downward as a consequence of their density and laterally in response to small differences in soil properties. This movement continues until the pressure and gravity forces

driving DNAPL flow are balanced by the resisting capillary forces.

The prevalence of contamination by DNAPLs are only partially explained by their unusual physico-chemical properties. The numerous commercial and industrial applications of these compounds are an important contributor to widespread contamination. Approximately 20 million tons of VOCs are annually produced in the U.S. and are used in industrial applications including degreasing metals, cleaning electronic components, dissolving rubber, and dry cleaning operations as well as in the extraction of products from fish meal, leather, seeds, and coffee beans (Barbee, 1994). VOCs are also used as intermediates in a variety of chemical manufacturing processes. Contamination by VOCs may also occur in agricultural regions. The U.S. Environmental Protection Agency (USEPA) has listed several VOCs, including common groundwater contaminants such as trichloroethylene (TCE) and perchloroethylene (PCE), as inert agents in some agricultural pesticide formulations (USEPA, 1987). Mackay and Smith (1990) suggested that groundwater impacts may be significantly underestimated due to limited monitoring of these compounds in agricultural areas.

The DNAPL compounds TCE and PCE are of particular interest given their prevalent occurrence in groundwater. A national survey of U.S. groundwater-derived drinking water supply systems identified TCE and PCE as two of the three most frequent contaminants (Westrick et al., 1984). Their occurrence was respectively reported in 4.6% and 3.2% of randomly sampled supply systems serving less than 10,000 persons, and in 11.3% and 11.3% of systems serving more than 10,000 persons. A similar survey of U.S. Superfund cleanup sites, Resource Conservation and Recovery Act site monitoring programs, and municipal landfill monitoring programs observed that PCE and TCE were the two most frequently detected organic compounds (Plumb, 1991).

1.1 Research needs

The physico-chemical properties and widespread use of DNAPLs such as TCE and PCE have resulted in intensive aquifer remediation efforts in North America and Europe. The need to

develop and evaluate strategies for aquifer remediation has necessitated investigative studies of numerous remediation technologies. The selection of a remediation technology for a particular contaminated site is often controlled by the identification of DNAPL source zones, as well as the cost, acceptability, and effectiveness of the remediation technologies under consideration. While cost and acceptability may be clear criteria, the meaning of technology "effectiveness" is subject to interpretation and can lack relevance. For example, if remediation efficacy is based purely on DNAPL mass removal, the potential for chronic groundwater contamination resulting from a minute remaining fraction may be overlooked. Generally, the goal of remediation is to return a contaminated aquifer to a useful condition but whether this requires removal of all contaminant mass is uncertain.

Further compounding the difficulty of selecting an appropriate remedial strategy has been sparse performance testing of some innovative technologies. The DNAPL remediation technologies developed in the last decade have been rigorously tested at only a couple small-scale sites and few data describing their operation, monitoring, and performance are available. It is critical that the criteria for assessing technology performance and the limitations of remediation technologies be clearly defined so that the long term costs and potential benefits of applying these technologies can be assessed.

In situ chemical oxidation (ISCO) is a potentially effective technology for remediation of aquifers contaminated with DNAPLs such as TCE and PCE that may be particularly suited to removing the DNAPL phase (i.e. residual and free product) as opposed to the sorbed and dissolved phases of these contaminants. The advantage of this technology is the rapid chemical reaction that occurs between the oxidant and the aqueous phase contaminant. The rate of mass transfer from the non-aqueous to aqueous phase increases in the presence of the oxidant, suggesting that ISCO may be an effective and rapid means of removing DNAPL mass from contaminated aquifers. Various oxidants have been proposed as flushing reagents; however, research initiated in 1989 at the University of Waterloo has focussed on the use of potassium permanganate ($KMnO_4$) with promising results. At that time, neither bench nor pilot scale

evaluations of permanganate had been performed. While some controlled experimental work had been completed to evaluate the effectiveness of ISCO when this thesis research began in 1993, little design, performance, and cost information was available with respect to field application of in situ chemical oxidation.

1.2 Research goals and objectives

The goal of this research was to investigate the applicability and efficacy of in situ flushing with potassium permanganate as a remediation strategy for the removal of DNAPLs from porous media. To meet this goal, the following specific objectives were defined:

- based on data available in the literature, develop a general conceptual model of the ISCO remediation technology;
- design and operate a field-scale ISCO system under realistic hydraulic and hydrogeologic conditions;
- develop general monitoring approaches for use in treatment system design and ISCO remediation operation and performance evaluation;
- assess the efficacy of ISCO for chlorinated ethene remediation in porous media;
- derive kinetic expressions to describe the chemical reactions and interphase mass transfer processes occurring during an oxidant flush that are consistent with the existing field and laboratory data and incorporate these expressions into an existing comprehensive flow and transport model; and,
- provide an overall conceptual framework for successful implementation of this technology.

1.3 Thesis organization

The experimental and numerical assessment of ISCO was accomplished using a stepwise

progression of research activities. Chapter 2 presents a theoretical framework for evaluating ISCO in the context of the current conceptual understanding of DNAPL migration, groundwater plume formation, and site remediation. A fundamental understanding of the DNAPL paradigm is provided through a review of mechanisms of source zone formation, mass transfer processes, and VOC solubility. Chemical reaction stoichiometry and kinetics relevant to potassium permanganate are summarized and the current range of DNAPL remediation technologies are examined, with particular emphasis on the results of ISCO experimental investigations. Chapter 3 summarizes the hydrogeologic studies completed at the Emplaced Source (ES) site at CFB Borden, and provides a detailed description of the pilot ISCO treatment system operated at this site. The significance of these results are discussed in the context of the conceptual model of the remediation process. Chapter 4 presents the development of a comprehensive numerical model that includes the generalized stoichiometry and kinetics for a multi-component DNAPL source zone, demonstrates several transport processes affecting the performance of ISCO, and examines the sensitivity of the model to key model and design parameters. Finally, Chapter 5 presents the conclusions of the research and presents recommendations for future research.

Chapter 2
Theoretical and Experimental Background

2.1 Introduction

Groundwater remediation technologies can only be appropriately applied when a robust conceptual model of the site hydrology and contaminant transport is developed, and the physico-chemical interactions between the treatment technology and the hydrogeological system are considered. In the case of ISCO using permanganate, this may be accomplished by integrating the primarily physical phenomenon of contemporary hydrogeology embodied in the DNAPL paradigm (Pankow and Cherry, 1996) with the existing chemical literature describing the reactivity of permanganate.

Critical hydrogeological phenomena that must be considered for the successful implementation of ISCO include an understanding of the factors that influence DNAPL migration in the subsurface and the impact of the treatment process on groundwater flow. DNAPL migration and groundwater flow are related and necessitate knowledge of the processes by which plumes of contaminated groundwater form. This interaction between the free product (contaminant) and the flowing groundwater can be described by the processes of solubility and dissolution (or mass transfer).

The appropriate application of ISCO also requires an appreciation of the chemical interactions of the concentrated oxidant solution and the reaction products with the aquifer geochemistry in

addition to the contaminants, and the linkage of these processes with physical phenomena (e.g., groundwater flow). In the case of permanganate, the theoretical basis of industrial applications (e.g., the fields of chemical synthesis, aquaculture, drinking water treatment, etc.) provides initial insight into this oxidant's potential efficacy for groundwater remediation. The various chemical reactions that occur during in situ permanganate oxidation can be partially extrapolated from the existing knowledge of permanganate chemistry and from the limited body of work specifically examining the use of permanganate in groundwater remediation.

Concurrent consideration of the hydrogeological and chemical components of ISCO provides the fundamental theoretical basis necessary for the appropriate selection and application of the ISCO technology for groundwater remediation. This chapter presents a general discussion of the physical mechanisms that control DNAPL distribution in the subsurface and a conceptual framework for the factors that affect solubility and mass transfer rates. The relevant chemistry discussed includes a review of the reactivity of permanganate (MnO_4^-) with organic and inorganic compounds, including the oxidation of soil organic matter. In addition, the mechanism, stoichiometry, and kinetics of the oxidation reactions with chlorinated alkenes are discussed and current source zone treatment technologies are reviewed with an emphasis on field experiments examining the application of hydrogen peroxide and permanganate. Finally, conceptual models describing the physico-chemical processes controlling the effectiveness of ISCO and their impact on groundwater chemistry during and following treatment are presented.

2.2 Conceptual model of DNAPL contamination

2.2.1 Physical processes

Backed by extensive empirical evidence, a conceptual description of the mechanisms resulting in aquifer contamination by DNAPLs has developed over the last two decades. This model, which implies that remediation technologies are limited in their ability to remediate groundwater to a pristine state (Pankow and Cherry, 1996), forms a basis for developing conceptual models of the ISCO remediation process.

A generic case of groundwater contamination by a DNAPL in a heterogenous unconfined aquifer underlain by an impermeable aquitard is presented in Figure 2.1. Following the release of a finite volume of the DNAPL (pure phase) at the water table, the free product migrates through the aquifer due to pressure gradients and the density contrast between the DNAPL and the porewater. The distribution of the pure phase is controlled by the spatial distribution of the permeability of the porous media, which is a function of the geologic stratigraphic and depositional environment, and the capillary forces that resist entry of the DNAPL into a porous media. The displacement pressure required for a non-wetting phase to enter a porous media can be correlated with the permeability using the J-function (Leverett, 1941),

$$P_d^{\cdot} = P_d \left(\frac{k\phi^{\cdot}}{k^{\cdot}\phi} \right)^{0.5} \tag{2.1}$$

where P_d, k, ϕ is the displacement pressure, permeability, and porosity of a known sample, $P_d^{\cdot}$ $k^{\cdot}$ and $\phi^{\cdot}$ are the displacement pressure, permeability ,and porosity of a scaled soil, which indicates that the entry pressure increases as the permeability decreases. Since permeability contrasts of several orders of magnitude are not uncommon within a relatively homogeneous aquifer, the Leverett scaling function suggests that finer-grained soil types will act as capillary barriers and divert DNAPL flow laterally until the entry pressure of the lower permeability zone is exceeded.

DNAPL releases can result in trapped non-aqueous phase mass. While some of this mass remains in the vadose zone, frequently much of the DNAPL mass is below the water table as is distributed as either low saturation residual or high saturation "pools" perched above lower permeability porous media. The spatial distribution of DNAPL mass in the porous media is a function of the interaction between resisting and driving forces controlling DNAPL flow and the spatial variability of soil properties within the aquifer.

A limited number of controlled experiments to evaluate the distribution of DNAPL in natural

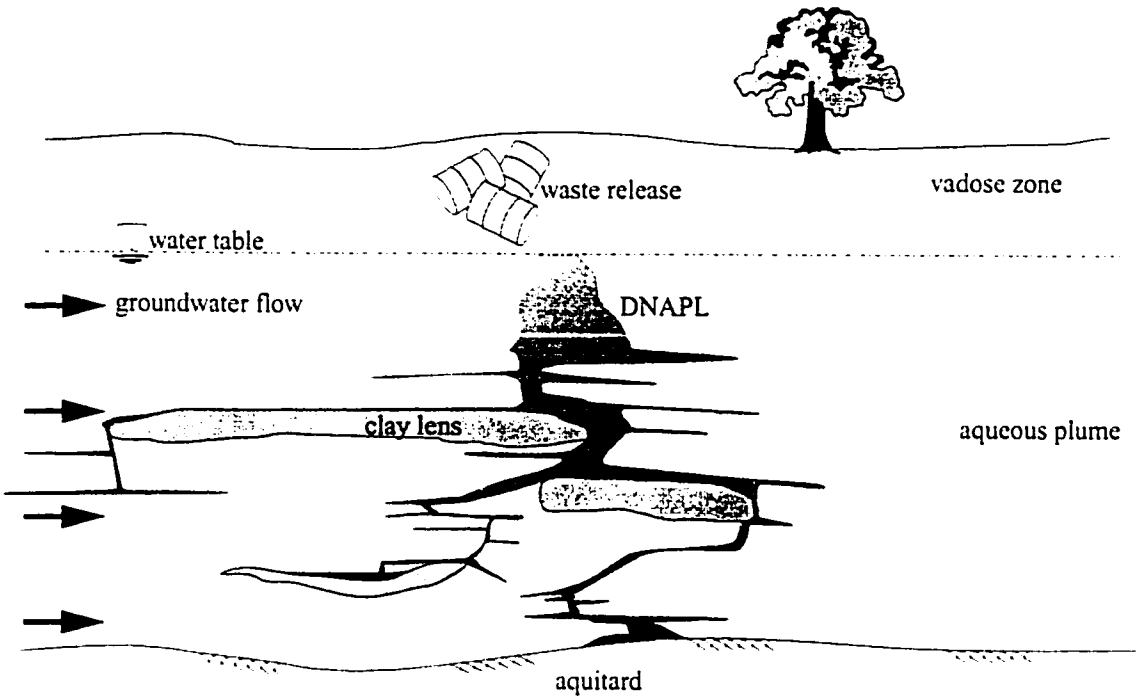

Figure 2.1 Idealized DNAPL source zone distribution and solvent plume formation.

porous media have been conducted at laboratory and field scales. Schwille (1988) conducted the first extensive experiments of two-phase flow in saturated and unsaturated porous media as well as in parallel plate fractures. In one series of experiments, a thin glass trough containing homogeneous sand was partially filled with water to form vadose and saturated zones while a horizontal hydraulic gradient was induced by tipping the trough. Various chlorinated solvents, including PCE, were spilled into the vadose zone. After flow of the pure phase ceased, most of the solvent mass was present in a pool at the bottom of the trough (Schwille, 1988). From photographs of the spill it was evident that preferential lateral spreading above the pool occurred along thin heterogeneities, which resulted from the packing process used to place the sand.

In a smaller scale laboratory experiment, Kueper et al. (1989) infiltrated PCE into a sand-packed and water-saturated parallel plate cell containing silica sand heterogeneities. Permeability contrasts (and the corresponding contrasts in entry pressure) of less than an order of magnitude

in the sands were capable of inducing lateral flow and inhibiting further downward flow. Upon reaching a heterogeneity for which insufficient displacement pressure precluded penetration, the non-wetting fluid would build-up pressure with a corresponding increase in saturation, forcing lateral flows. After the pressure exceeded the displacement pressure, flow through the low permeability lens would occur; however, since the permeability of the lens was unable to support the relatively large DNAPL fluid flux, lateral spreading within the low permeability lens occurred (Kueper and Frind, 1991).

As a result of strict regulatory prohibitions on intentionally contaminating aquifers, few field experiments have been conducted to evaluate the flow behaviour of DNAPLs in a natural porous media. Most of these experiments were conducted in an unconfined sand aquifer at a research site at Canadian Forces Base (CFB) Borden, Ontario, Canada. DNAPL experiments at this site have included two releases of 6 L of PCE into the vadose zone (Poulsen and Kueper, 1992), a release of 231 L of PCE into a saturated zone contained inside a 3 x 3 x 3.4 m steel sheetpile walled cell (Kueper et al., 1993), and a release of 770 L of PCE into a saturated zone within a 9 x 9 m cell (Brewster and Annan, 1994). In the vadose zone experiments, Poulsen and Kueper (1992) demonstrated that capillary forces dominated multi-phase flow based on the observed distribution of residual PCE. Excavation and mapping of the release revealed a complex residual distribution resulting from visible heterogeneities in the sand at the millimetre scale. Measured residual DNAPL contents ranged from 0.1% to 9.0% (v/v); however, the stained PCE was not visually evident in a large fraction of the porous medium within the spill zone (Poulsen and Kueper, 1992). A similarly complex PCE residual distribution was observed in the saturated zone experiment with PCE saturations ranging from 1 to 38.1% (Kueper et al., 1993). In a manner similar to the trough experiments reported by Schwille (1988) , a pool of 9 L of PCE formed in a cobbled sandy-silt layer immediately above the clay aquitard underlying the test cell (Kueper et al., 1993). In the 9 x 9 m cell experiment, Brewster and Annan (1994) used geophysical methods to observe a PCE spill redistributing over time into nine separate pools located at various depths within the cell, including a large pool located directly upon the underlying aquitard.

The Borden experiments suggested that immobile DNAPL residues in the subsurface may be broadly characterized by their processes of formation. Residual DNAPL consisting of small disconnected blobs (Figure 2.2) is formed by non-aqueous phase imbibition followed by drainage and is controlled by processes occurring at the pore scale. The residual volumetric saturation following drainage is related to the maximum saturation achieved during imbibition and is controlled by the smallest pore penetrated in the porous media (Kueper et al., 1993).

In contrast, DNAPL pool formation is dominated by macroscale changes in permeability and entry pressure resulting from the geological structure of the aquifer (Figure 2.3). Several mechanisms can result in the formation of pools above a lower permeability horizon. A pool can form within a high permeability, low entry pressure lens, even in a relatively homogeneous

Figure 2.2 Disconnected blobs of immobile residual DNAPL in glass beads (from Schwille, 1989).

Figure 2.3 A DNAPL pool above a lens of finer-grained glass beads with a higher entry pressure (from Schwille, 1989).

porous media (e.g., the Borden aquifer) containing only small contrasts in entry pressure. The lens imbibes the non-aqueous phase to a maximum saturation and partially drains once the DNAPL release into the subsurface ends. Pools can also form above a low permeability material with an entry pressure exceeding the available capillary pressure. In either case, if lateral DNAPL movement is limited by either low permeability or high entry pressures, the pressure of the non-aqueous phase will increase and will penetrate increasingly smaller pores. Accordingly, high volumetric saturations can develop without an opportunity for non-wetting phase drainage.

2.2.2 Chemical processes

Effective solubility

Following formation of a DNAPL source zone, an aqueous phase plume of solvent-contaminated water forms as a result of dissolution. Quantitative predictions of dissolution rates are complicated by a decrease in solubility that occurs with DNAPLs formed of more than one pure phase component, a relatively common phenomenon (Feenstra, 1990). The effective aqueous solubility of a DNAPL mixture containing n components may be determined using an analog of Raoult's Law,

$$C_{n,e}^{sat} = \gamma_n X_n C_{n,0}^{sat} \tag{2.2}$$

where $C_{sat,n}^{e}$ is the effective aqueous phase solubility of component n in the non-aqueous phase mixture, γ_n is aqueous phase activity coefficient, X_n is the mole fraction of n in the mixture, and $C_{sat,n}^{0}$ is the solubility of pure component n (Pankow and Cherry, 1996). Equation (2.2) assumes equilibrium partitioning between the aqueous and non-aqueous phases. A possible simplifying assumption for (2.2) is that the activity coefficients of the components are unity (ideal solution). Lesage and Brown (1994) observed aqueous activity coefficients for a mixture of trichloroethane (TCA), PCE, toluene, and CFC-113 ranging from 0.9 to 3.2, exceeding the expected range of $0<\gamma_n<1.0$. The largest deviations from ideality were for the two least soluble components (PCE and CFC-113) and were attributed to a PCE/CFC-113 solubility enhancement caused by interactions between these compounds, and TCA and toluene. The assumption of ideality may be valid for non-aqueous phase mixtures of chemically similar components (Mackay et al., 1991; Banerjee, 1984) and likely contributes minimal error relative to other hydrogeologic uncertainties.

Feenstra (1990) proposed using (2.2) as a basis for interpretating aqueous phase VOC concentrations from pump and treat systems and suggested a procedure to estimate the DNAPL mass remaining in the source area. Broholm et al. (1993) monitored dissolution from a three component DNAPL source in a field experiment to test the hypothesis of Feenstra (1990) and reported that (2.2) provided a reasonable estimate of the remaining DNAPL mass in spite of what was thought to be non-equilibrium dissolution resulting from a highly variable DNAPL

distribution. The Raoult's Law approach for estimating the effective solubility of DNAPLs has also been employed in a number of modelling studies. Frind et al. (1999) accurately simulated dissolution from an emplaced residual DNAPL source in the CFB Borden sand aquifer over a two-year period. Equation (2.2) was also successfully employed by Geller and Hunt (1993) to model non-equilibrium mass transfer from a toluene-benzene residual NAPL mixture applied to a porous medium contained within a glass column. The relative success of these studies suggests that Raoult's Law, while a simplified approach, is an adequate model of multi-component DNAPL solubility.

Dissolution mass transfer

Over the last two decades, modelling approaches for dissolution have changed from assumptions of local equilibrium partitioning (Johnson and Pankow, 1992) to highly rigorous, experimentally-derived mass transfer correlations (Powers et al., 1994), and recently, back to the realization that equilibrium conditions prevail for some conditions and modelling scales (Frind et al., 1999). The process of dissolution mass transfer is generally considered a function of the effective solubility and diffusivity of the DNAPL components, the distribution of the pure phase, and the rate of groundwater flow through the contaminated zone (Pankow and Cherry, 1996). A variety of conceptual models exist to describe mass transfer rate, but the most commonly applied is the stagnant film model (Figure 2.4; Miller et al., 1990) where a boundary

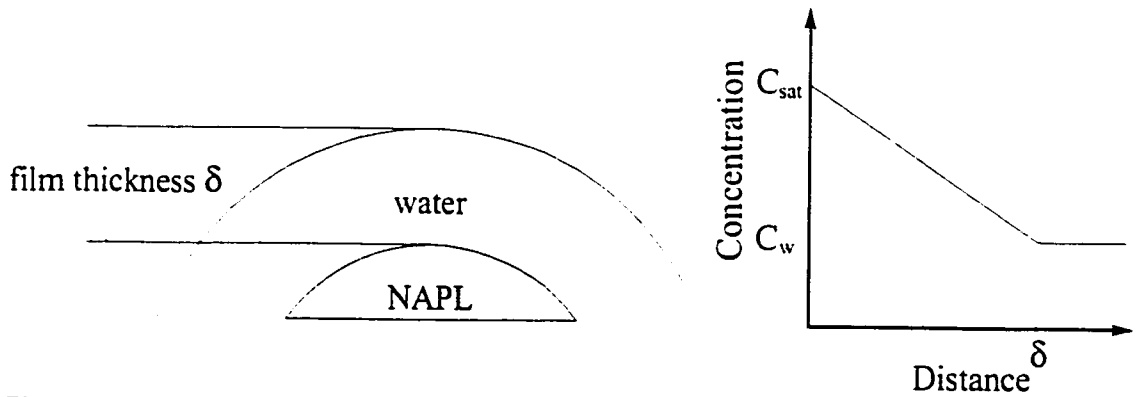

Figure 2.4 Conceptual representation of the concentration profile in the stagnant film model describing dissolution mass transfer rates.

layer of water with a thickness of δ at the DNAPL/water interface provides a diffusive resistance to mass transfer. This resistance is incorporated into an expression for the mass flux, given by Fick's First Law,

$$N = -D_L \frac{\partial C_w}{\partial x} \tag{2.3}$$

where N is the flux per unit area of NAPL:water interface, D_L is the aqueous phase free diffusion coefficient, and C_w is the bulk water concentration. If a linear concentration gradient through the film thickness is assumed, (2.3) is equivalent to,

$$N = -D_L \frac{C_w - C_{sat}^e}{\delta} = K(C_{sat}^e - C_w) \tag{2.4}$$

where C_{sat}^e is the effective solubility, and $K = D_L/\delta$ is defined as the mass transfer coefficient. In practice, the mass transfer flux is expressed as a mass flux per unit volume of porous media (V) such that,

$$J = N\frac{A_{nw}}{V} = K\frac{A_{nw}}{V}(C_{sat}^e - C_w) = \lambda(C_{sat}^e - C_w) \tag{2.5}$$

where λ is the lumped mass transfer rate coefficient and A_{nw} is the phase interface surface area. Since in practice the surface area of the DNAPL/water interface and the boundary layer thickness are not measurable, the lumped mass transfer coefficient is typically treated as either a calibration coefficient or is empirically determined.

Treating λ strictly as a calibration coefficient, simplified expressions for the mass transfer rate coefficient have been proposed. Guiguer (1993) employed,

$$\lambda = \alpha S_{nw}^{\beta} \tag{2.6}$$

where α and β are calibration parameters and S_{nw} is the volumetric saturation of the non-aqueous phase. Similarly, Sleep and Sykes (1990) used a lumped mass transfer coefficient that was equivalent to a special case of (2.6) with β=0.

Extensive experimental efforts have resulted in the development of several empirical correlations for λ that are expressed in terms of a modified Sherwood number $Sh=\lambda d_{50}/D_L$ (Powers et al., 1994), where d_{50} is the median particle diameter of the porous media. Powers et al. (1994) conducted extensive experiments with sand-packed columns containing residual saturations between 3.9-6.5% of styrene flushed at Darcy velocities ranging from 3.52-15.20 m/d and reported,

$$Sh=4.13Re^{0.598}\delta_n^{0.673}U_i^{0.369}\left(\frac{S_{nw}}{S_{nw_0}}\right)^{\beta_4} \tag{2.7}$$

with,

$$\beta_4=0.518-0.114\delta-0.10U_i \tag{2.8}$$

and,

$$Re=\frac{v\rho_w d_{50}}{\mu_w} \tag{2.9}$$

where Re is the Reynold's number, δ_n is normalized grain size ($\delta=d_{50}/d_m$, where d_m is defined as 0.05 cm), S_{nw_0} is the initial non-wetting phase saturation, S_{nw} is the current non-wetting phase saturation, U_i is the uniformity index ($U_i=d_{60}/d_{10}$), v is the average linear groundwater velocity, and ρ_w and μ_w are the density and viscosity of the water phase.

Another correlation developed using a similar experimental approach was presented by Miller et al. (1990). Using notation consistent with that of Powers et al. (1994), the Sherwood number was given by,

$$Sh = 12(\phi - S_{nw})Re^{0.75}S_{nw}^{0.60}Sc^{1.2} \tag{2.10}$$

where Sc is the Schmidt number ($Sc=\mu_w/(\rho_w D_L)$) and ϕ is the porosity.

Based on the relationships previously discussed, Frind et al. (1999) employed a mass transfer term of the form,

$$\lambda^n = \frac{Sh\, D_L^n}{(d_{50})^2}\left(\frac{f^n S_n}{S_{n_0}}\right)^{\beta^n} \tag{2.11}$$

where f^n is the local volume fraction in the NAPL of component n and determined that values of the Sherwood number in the range $10^{-5}<Sh<10^{-2}$ provided results corresponding closely to the observed data. Unlike the other correlations, (2.11) was developed considering a non-aqueous phase consisting of multiple components.

In the absence of empirical data describing dissolution from a spatially heterogeneous DNAPL source, it is difficult to select an appropriate mass transfer term except on the basis of ease of parameter selection. While the expression of Guiguer (1993) (Equation 2.6) may fit most dissolution data, it is not physically-based and the parameters can only be determined through calibration. Of the remaining mass transfer rate terms, equations (2.10) and (2.11) reduce the calibration uncertainty but still require *a priori* estimates of either the Schmidt or Sherwood numbers. In the absence of additional sensitivity analyses of these parameters, the most appropriate means of evaluating the mass transfer rate coefficient may be the expression developed by Powers et al. (1994) (equation 2.7).

In the case of DNAPL pools, mass transfer rate coefficient expressions such as (2.7) may be of limited utility in describing dissolution DNAPL pools. Sale (1999) hypothesized that solute transport processes played a significant role in determining the rate of DNAPL depletion (Figure 2.5). Assuming equilibrium mass transfer, advection and dispersion could limit aqueous phase mass removal rates from pores containing DNAPL. Since the relative water phase permeability within the pool is lowered due to the presence of the non-wetting phase, the advective flux will be limited by the low Darcy flux, the small cross section of the pool (b) exposed to flow, and

the low contaminant solubility. Accordingly, mass transfer may be controlled by dispersive mixing. Since the stratigraphy of many unconsolidated deposits is dominated by horizontally-oriented bedding planes resulting in similarly oriented pools, dispersive mixing is primarily through transverse vertical dispersion, a process which is on the scale of aqueous phase diffusion (Rivett et al., 1992). In this case, complete mass depletion from pool would require an extended periods ranging from decades to centuries (Johnson and Pankow, 1992). This conceptual analysis suggested that pool dissolution rates may be insensitive to the mass transfer rate coefficient in comparison to vertical transverse dispersivity.

2.3 Reactivity and chemistry of permanganate

2.3.1 Reactivity of permanganate with organic/inorganic compounds

The existing knowledge of the reactivity of permanganate, primarily from the chemistry

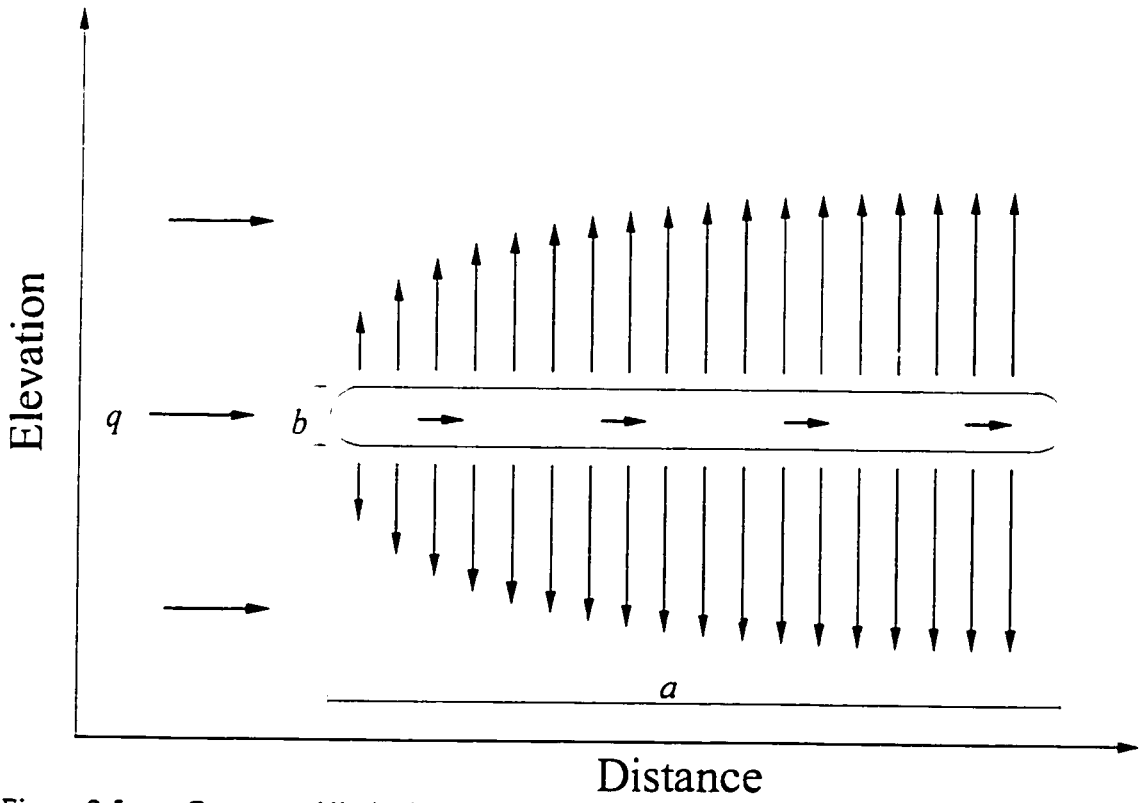

Figure 2.5 Conceptual limitation of transport processes on mass transfer rates from a cross-section of a DNAPL pool in saturated porous media.

literature, is somewhat limited by the focus on organic product synthesis rather than degradation and the tendency to study compounds rarely encountered at contaminated sites. The principal contribution of the chemistry literature is the understanding of the reactivity of permanganate with inorganic compounds and natural organic matter, and the development of analytical methods. Water treatment applications, included those examining the treatment of chlorinated solvents, constitute the primary source of reactivity data.

Potassium permanganate is widely recognized as the reagent in the Baeyer test for the presence of unsaturated organic compounds (Stewart, 1973). The physical and chemical properties of permanganate provide a starting point for understanding the effects of permanganate on aquifer geochemistry and its role as a reagent in a treatment process (Table 2.1). Several physical properties are dependent upon permanganate concentration, including absolute viscosity and solution density. Hydraulic conductivity increases in proportion to oxidant concentration but the net effect is minor (Figure 2.6). The maximum solubility of potassium permanganate is strongly dependent upon temperature and at a typical groundwater temperature of 10°C it is 42 g/L.

Table 2.2 Summary of the physical and chemical properties of permanganate (*from Carus Chemical, 1998*).

Molecular weight	158.03 g/mol
Solid density	2.703 g/cm^3
Bulk density	~1605 kg/m^3
Aqueous solubility ($KMnO_4$)	S=30.55+0.796T+0.0392T^2 (T *in °C*)
	S=62.9 g/L at 20°C
Aqueous solubility ($NaMnO_4$)	900 g/L at 20°C
Aqueous specific gravity	S_g=1.000+0.007C (*where C is the concentration of* $KMnO_4$ *[%w/w]*)
Specific conductance	S_c*(mS/cm)*=0.7002C+0.0915 *(where C is the concentration of* $KMnO_4$ *[%w/w])*
Average Mn-O bond distance	1.629 ± 0.008 Å
Average O-Mn-O bond angle	109.4 ±0.7°

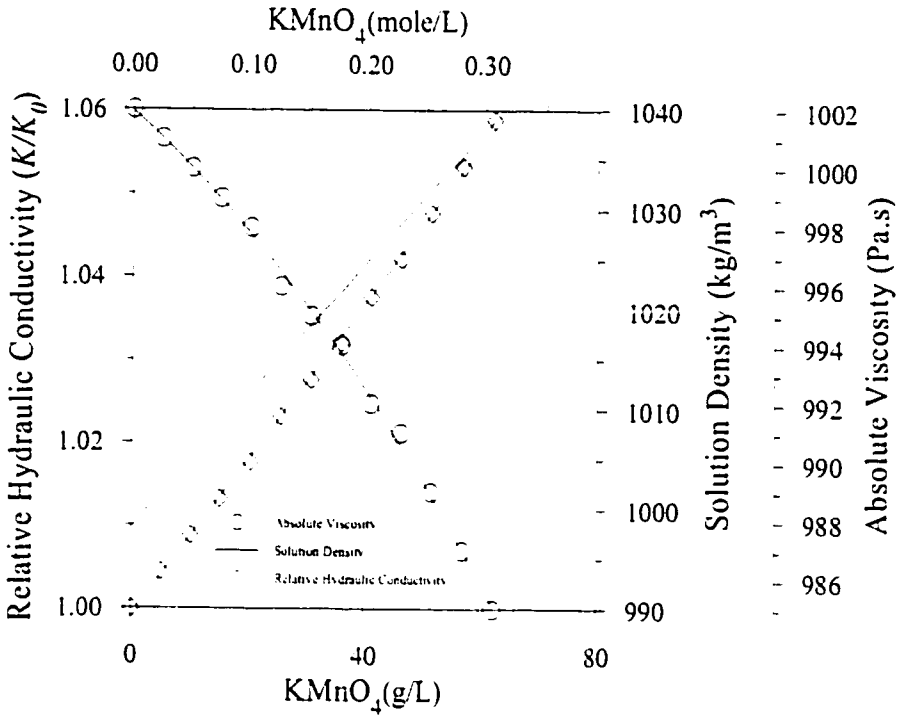

Figure 2.6 Dependence of absolute viscosity and solution density on potassium permanganate concentration and the calculated change of the aqueous phase hydraulic conductivity ($K=k\rho g/\mu$) relative to pure water.

Permanganate has been used to treat wastes and contaminants in addition to TCE and PCE. In drinking water treatment, permanganate oxidation is used to remove trihalomethane precursors (Singer et al., 1980; Moyers and Wu, 1985), taste and odour compounds (Middlemas and Ficek, 1986) and iron and manganese (Ficek, 1986). Wastewater treatment applications have included the removal of phenols (Vella et al., 1990), chlorinated phenols (Vella and Munder, 1991), and cyanides (de Renzo, 1978) although little is known about the reaction mechanisms involved.

Manganese in drinking water has aesthetic impacts, especially discolouration (Carlson and Knocke, 1999). Permanganate is frequently used for Mn(II) removal through oxidation of either aqueous or adsorbed Mn^{2+} on glauconite cation exchange media (greensand) and the formation

of additional Mn(IV) oxide by,

$$2MnO_4^- + 3Mn^{+2} + 2H_2O \rightarrow 5MnO_2(s) + 4H^+ \quad (2.12)$$

which is known as the Guyard reaction (Stewart, 1973). Permanganate is used in a similar application to remove soluble iron following the reaction,

$$3Fe^{2+} + MnO_4^- + 4H^+ \rightarrow MnO_2(s) + 3Fe^{3+}(s) + 2H_2O \quad (2.13)$$

which is also the basis of a volumetric method for measuring manganese concentration. Mn(II) results from dissolution of manganese oxide minerals which include pyrolusite (MnO_2(s), also known as birnessite or vernadite), and manganite (MnOOH). In the absence of oxygen, MnO_2(s) is among the strongest oxidants present in natural groundwater systems. Dissolution of MnO_2(s) is a reduction process where the dioxide acts as a oxidant according to,

$$MnO_2(s) + 4H^+ + 2e^- \rightarrow Mn^{2+} + 2H_2O \quad (2.14)$$

Several analytical methods other than direct spectrophotometric determination employ the intense purple colour of permanganate as an indicator. For example, the rather violent reaction with hydrogen peroxide,

$$2MnO_4^- + 5H_2O_2 + 6H^+ \rightarrow 2Mn^{2+} + 5O_2 + 8H_2O \quad (2.15)$$

is the basis of a volumetric method for determining the concentration of H_2O_2. Beck (1968) described an amperometric method for measuring permanganate concentration with phenylarsene oxide (PAO) as the titrant, where,

$$3C_6H_5AsO + 2KMnO_4 + 4H^+ \rightarrow 3C_6H_5AsO(OH)_2 + 2KOH \quad (2.16)$$

PAO has been used as a quenching agent to stop oxidation so that the reductant concentration may be determined (G. Hoag, personal communication, 1998). Titration of permanganate solutions with oxalate also relies on the disappearance of the permanganate colour as an

indicator following the reaction,

$$5MnO_4^- + 5C_2O_4^{2-} + 16H^+ \rightarrow 2Mn^{2+} + 10CO_2 + 8H_2O \qquad (2.17)$$

The stability of aqueous MnO_4^- solutions is of concern from an analytical perspective. Stewart (1973) suggested that autocatalytic decomposition of near-neutral permanganate solutions occurred according to,

$$2MnO_4^- + H_2O \rightarrow 2MnO_2(s) + 2OH^- + \frac{3}{2}O_2 \qquad (2.18)$$

This reaction, however, is extremely slow and solutions can remain stable for several years if carefully prepared (Rees, 1987). Decomposition is catalysed by solid phase MnO_2 and sunlight, suggesting that careful filtration to remove dust and isolation from light will minimize decomposition (Rees, 1987).

Removal of permanganate from solution is possible using a reductant such as thiosulphate which forms the insoluble Mn(IV) dioxide according to,

$$3S_2O_3^{2-} + 8MnO_4^- + H_2O \rightarrow 8MnO_2(s) + 6SO_4^{2-} + 2OH^- \qquad (2.19)$$

$MnO_2(s)$ may be readily coagulated, flocculated and removed by settling. Schnarr (1992) employed this reaction to determine the concentration of permanganate by titrating with a standardized thiosulphate solution; however, this is not a viable analytical approach since the precipitation of $MnO_2(s)$ interferes with visual determination of the permanganate endpoint.

With hydrochloric acid (HCl) and permanganate a rapid reaction occurs,

$$2KMnO_4 + 8HCl \rightarrow 3Cl_2(g) + 2MnO_2(s) + 4H_2O + 2KCl \qquad (2.20)$$

which produces chlorine gas in addition to manganese dioxide; however, given the reactivity of $Cl_2(g)$ in aqueous solution, this is unlikely to be problematic in a groundwater environment.

In fact, qualitative evidence suggesting that chlorine residuals can re-oxidize $MnO_2(s)$ to form permanganate was observed during the current research.

In most porous media, the presence of carbonate minerals results in some alkalinity and near neutral pH as a result of carbonate equilibria with calcite. At near neutral pH the half-reaction for the reduction of permanganate is,

$$MnO_4^- + 4H^+ + 3e^- \rightarrow MnO_2(s) + 2H_2O \qquad (2.21)$$

For this half-reaction, the reaction potential is given as (Eilbeck, 1987),

$$E = E_0 - \log\frac{[MnO_4^-][H_2O]}{[H^+]} \qquad (2.22)$$

This expression suggests that the half-reaction potential depends directly on the permanganate concentration and solution pH and indicates, consistent with permanganate's insolubility in most organic phases, that water is involved in the oxidation process (Stewart, 1973).

In general, $KMnO_4$ is a specific oxidant which is reactive with a number of organic and inorganic substrates; however, limited information is available describing degradation rates and reaction products. Degradation rates of organic compounds are usually faster in alkaline solution due to ionization (Stewart, 1973). Several studies have indicated that organic compounds are completely oxidized to inorganic products by $KMnO_4$. Both phenolic compounds and anilines are rapidly degraded to CO_2 while aromatics such as xylene, toluene and benzene were progressively more stable (Stewart, 1973). Methane is completely oxidized by permanganate to CO_2 under acidic conditions (Belavin et al., 1990). Rinehart (1973) observed that oxidation of either primary and secondary alcohols produced CO_2. Other compounds, however, may be only partially degraded. Oxidation of aromatic hydrocarbons by permanganate results in the formation of the corresponding carboxylic acids (Lee, 1980). Oxidation of the pesticides Diquat and Paraquat produced oxalate and ammonia (de Renzo, 1978).

Lunn et al. (1994) recommended permanganate oxidation for the disposal of a variety of organic wastes and developed a laboratory-scale treatment process. Application of this method to degrade dibenz(a,j)acridine, dibenz(a,h)acridine, dibenzo(c,g)carbazole, and dibenzo(a,i)carbazole resulted in a solution that was non-mutagenic with less than 0.1% of the original organic material remaining; however, no assessment of the reaction products was completed.

Qualitative evidence of permanganate oxidation of benzene, toluene, xylene, chloroform, and cyclohexane was reported by Truax (1993). No evidence of oxidation of 1,1,1-TCA and chlorobenzene was noted. Tratnyek et al. (1998) observed that halogenated alkanes (1,1,1-TCA and 1,1-DCA), methanes (CH_2Cl_2 and $CHCl_3$), and CFC-11 were completely unreactive with permanganate while several reports, discussed in detail in Section 2.3.3, have confirmed that the chlorinated alkenes (including PCE, TCE, and the DCE isomers) are rapidly mineralized to CO_2.

The few studies of degradation products and the limited mechanistic understanding of the reactions provides only a rudimentary assessment of the reactivity of permanganate with groundwater contaminants that emphasizes the specificity of permanganate. While some compounds may be completely degraded to inorganic products like CO_2, others result in stable organic products or are completely recalcitrant. The formation of a stable organic product would only be acceptable if the product was less toxic than the parent or had a limited environmental fate through either biotic or abiotic degradation processes. The current use of permanganate to treat wastewaters containing phenols or chlorophenols (Vella et al., 1990; Vella and Munder, 1991) and the reported degradation of aromatic and polyaromatic hydrocarbons suggests that these compounds may be amenable to permanganate degradation in groundwater though no assessment of reaction products has been performed. In many cases, complete degradation to inorganic products appears to be contaminant-specific and difficult to predict without direct experimental data. Unfortunately, wide gaps in the experimental data

exist and the reactivity of few common groundwater contaminants has been evaluated. While the chlorinated alkenes are reactive (described in detail in Section 2.3.3), permanganate appears to have no effect on either chlorinated alkanes or methanes and little is known about the reactivity of any other groundwater contaminant including the chlorobenzenes, aromatic hydrocarbons, polycyclic aromatic hydrocarbons, and the polychlorinated biphenyls. Of the few reactions known to degrade contaminants, little is known about the reaction kinetics with the exception of the chlorinated ethenes. The gaps in reactivity and kinetic data for an oxidant known to completely degrade at least several contaminants indicates that additional experimental evaluations are necessary to completely assess the applicability of permanganate oxidation as a treatment process. These evaluations should include identification of reaction products and an assessment of the toxicity relative to the parent contaminant. In addition, an understanding of the degradation rates of oxidizable compounds is critically required to identify groundwater contaminants for which permanganate may be an effective in situ oxidant.

2.3.2 Reactivity with porous media

Soils have a complex composition that typically includes both inorganic and organic components. While the inorganic fraction primarily consists of carbonate and silicate minerals, it can also include mineral species containing reduced forms of manganese and iron. The organic fraction of typical aquifer materials is composed of a poorly defined group of compounds known as humic substances (Hayes, 1989). Humic substances are large complex macromolecules with molecular weights ranging from 200-20,000 g/mol. The structure and composition of the humic material is often inferred from an analysis of the products formed during oxidation of clean soil by permanganate; typical products include mono- and di-carboxylic acids, CO_2, and oxalic acid with reported yields of CO_2 accounting for 26-42% of the available organic carbon mass (Aiken et al., 1985; Hayes et al., 1989).

Humic substances and reduced mineral species provide a natural reductive capacity which results in oxidant consumption, implying that oxidant will be consumed during the initial phases of an oxidant flush until the reduction capacity is satisfied. The extent to which aquifer solids

act as reductants, termed either the reduction capacity or natural oxidant demand, is an important design component of ISCO. Reduction capacity, which can be expressed in terms of either a specific oxidant mass or electron transfer equivalence necessary to completely oxidize a unit mass of porous media, may vary throughout the aquifer due to spatial variability in the soil composition. Spatial and temporal gradients in measured Eh values were observed by Barcelona et al. (1989), who suggested that some regions of an aquifer may be more oxidized relative to others. While the pore water and the solid fraction of a bulk aquifer sample both exert an oxidant demand, the reduction capacity of uncontaminated pore water is insignificant relative to the solid phase (Barcelona and Holm, 1991) although this may not be true for all groundwater environments (e.g., wetland recharge zones). Reduction capacities of dry sand and gravel samples from both aerobic and anaerobic aquifers were measured using dichromate digestion and compared to the reduction capacity calculated using measured Fe(II) and total organic carbon (modelled as phthalic acid [$C_8H_6O_4$]) concentrations. Good agreement between the measured and calculated reduction capacities was reported suggesting that Fe(II) and TOC were the only significant contributors to the reduction capacity of the bulk aquifer although S(II) mineral phases may be significant reductants in some sands (Barcelona and Holm, 1991). Redox disequilibrium between the porewater and the porous media can occur (Barcelona and Holm, 1991), implying that spatially-variable aquifer redox measurements are not necessarily correlated with the natural oxidant demand and that direct measurements using sediment samples may be the only means of estimating the natural oxidant demand.

Based on a single column measurement, Schnarr (1992) reported an oxidant demand of 42 g $KMnO_4$/kg of dry sand for a sample from the Borden aquifer; however, this result was not supported by the results of a field experiment where ~7.5 m^3 of the same soil was flushed with permanganate (Schnarr et al., 1998). On the basis of the laboratory-measured oxidant demand of 42 g $KMnO_4$/kg sand and a bulk sand density of 1.81 g/cm^3, the field experiment would have required 570 kg of oxidant; however, only 45 kg $KMnO_4$ were required to completely remove the 1 L PCE source zone and oxidize the aquifer solids. Based on the $KMnO_4$ monitoring data from this field site the oxidant demand of the sand was 3.1 g $KMnO_4$/kg sand, suggesting either

an error in the column measurement by Schnarr (1992) or high spatial variability. It should be noted that samples collected from the same location in the Borden aquifer but at different depths have variable organic carbon contents with relatively high *foc* in shallow samples, possibly resulting from the inclusion of small fragments of weathered vegetation particles in the soil samples.

As part of the present research, two measurement techniques for soil oxidant demand were compared. The first method is a standard method promulgated by the British Standards Institution (1975) that is based on a procedure developed by Walkley and Black (1935). The method consists of complete sample oxidation by an acidified dichromate solution (chromic acid) and subsequent volumetric determination of the amount of consumed dichromate. The second method, developed in the course of the present research, emulated field conditions by packing a small column with a representative soil sample and flushing the sample with a concentrated permanganate solution. A description of these methods and the results of NOD measurements using these methods are presented in detail in Appendix A. The average specific oxidant demand, calculated using replicated measurements with six different sand samples, was 65 g $KMnO_4$/kg sand/%*foc*, which generally agrees with the average specific oxidant demand of 108 g $KMnO_4$/kg sand/%*foc* of three sand samples measured by Barcelona and Holm (1991).

In addition to acting as a sink for permanganate, the reaction of permanganate with organic material in soil results in the formation of potentially problematic reaction products. At near neutral pH manganese dioxide (MnO_2), a dark brown to black precipitate, is the dominant manganese product (Equation 2.15) and has been observed as a coating (indicated by the brown staining) on porous media and dolomite fracture surfaces (Tunnicliffe, 1999). This precipitate may result in changes in aquifer porosity and permeability, and, given reducing redox conditions favouring MnO_2(s) dissolution, produce a Mn^{2+} plume.

Few studies have been performed to characterize the effect of permanganate flushing on porosity and permeability resulting from deposition of MnO_2(s) produced by oxidation of the

DNAPL source and soil organic matter. Assuming that the natural oxidant demand is rapidly converted to a stoichiometric quantity of MnO_2(ρ=5.08 g/cm^3), oxidation of soil organic matter will only slightly decrease the total porosity over the range of soil organic contents typically observed in unconsolidated granular deposits (Figure 2.7). In contrast, complete oxidation of a residual DNAPL and deposition of MnO_2(s) may result in a porosity increase since the DNAPL phase is replaced by a stoichiometric quantity of comparatively dense MnO_2(s). For example, the volume of MnO_2(s) produced by oxidizing TCE and PCE is 41% and 23%, respectively, of the original solvent volume. In the case of soils containing carbonates, the effective porosity increase will be even larger since the acid produced by the degradation reaction will dissolve these minerals.

While the expected changes in porosity can be readily approximated based on reaction stoichiometry, means of estimating the impact of precipitate formation on bulk permeability are limited (other than direct measurement). Several approaches correlate permeability with other common soil properties, such as grain size, porosity, and uniformity coefficient, including the Hazen and Carmen-Kozeny equations. Amer and Awad (1974) suggested the relationship,

$$k = A\left(\frac{e^3}{1+e}\right) U^B d_{10}^C \qquad (2.23)$$

where A, B, and C are fitting coefficients, U is the uniformity coefficient, and e is the void ratio, which is a function of porosity. These approaches rely on the properties of naturally formed geologic material and do not account for structural changes in pore morphology and connectivity and deposition of MnO_2(s) particles by physical and chemical processes. The severe silica sand cementation was observed by MacKinnon (1999) suggests that the change in permeability may be more complex than suggested by a simple grain diameter model. Physical removal may also play a role in of MnO_2(s) deposition through mechanical filtration if particle attachment preferentially occurs at pore throats and restricts pore connectivity. In addition to decreasing the permeability, the formation of an MnO_2(s) film around a drop of pure phase PCE observed by Tunnicliffe (1998) suggests that mass transfer processes may also be effected.

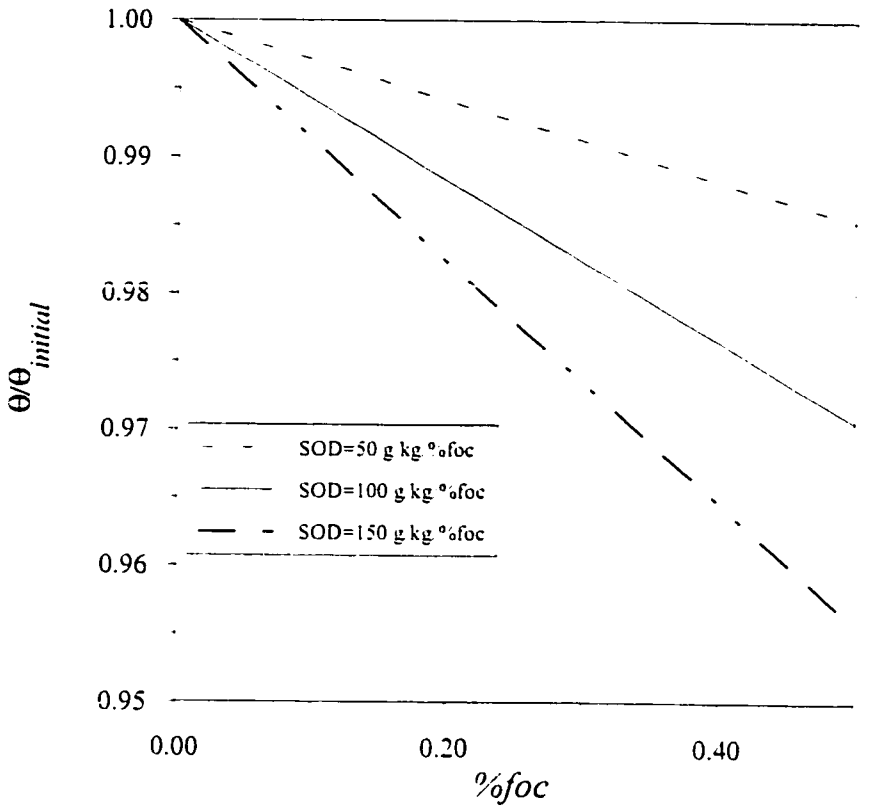

Figure 2.7 Calculated change in porosity as a result of the precipitation of MnO_2 by the natural oxidant demand.

Urynowicz and Siegrist (2000) examined the enhancement in mass transfer rate resulting from permanganate addition and observed that the mass transfer rate decreased over time, suggesting that the formation of the film added a mass transfer resistance.

In a limited set of experiments, Schnarr (1992) observed that oxidant flushing of columns packed with Borden sand resulted in a mean porosity reduction of 5.6% (four samples). The porosity reduction may have included gas-phase carbon dioxide in addition to manganese dioxide. In contrast, the mean hydraulic conductivity actually increased following the oxidant flush. While less than the hydraulic conductivity of clean sand, the oxidant flush increased the hydraulic conductivity by 14.5% (two samples) as pure phase PCE was removed and replaced

by precipitate. While complicated by the inclusion of the pure phase, these experiments suggest that changes in permeability and porosity result from complex pore-scale interactions that depend upon the initial distribution of the pure phase contaminant.

2.3.3 Reactivity of permanganate ion with chlorinated alkenes

Mechanism

In industrial synthesis, oxidation of alkenes is frequently used to produce glycols (Rinehart, 1973); however, yield of this product is often limited by complete mineralization to carbon dioxide. A review of likely reaction mechanisms of the oxidation of chlorinated alkenes by Yan and Schwartz (1999) was built upon mechanisms reported by Wiberg and Saegebarth (1957) and Lee (1980) (Figure 2.8). The initial step involves the formation of a cyclic hypomanganate ester with two possible reaction pathways resulting in complete mineralization. Under one mechanism, the cyclic ester is hydrolysed, forming a glycol aldehyde, which could be further oxidized to oxalic acid. Alternatively, cleavage of the double bond within the hypomanganate ester could result in the production of a formaldehyde with rapid conversion to formic acid. Both oxalic and formic acids are carboxylic acids which are readily mineralized by

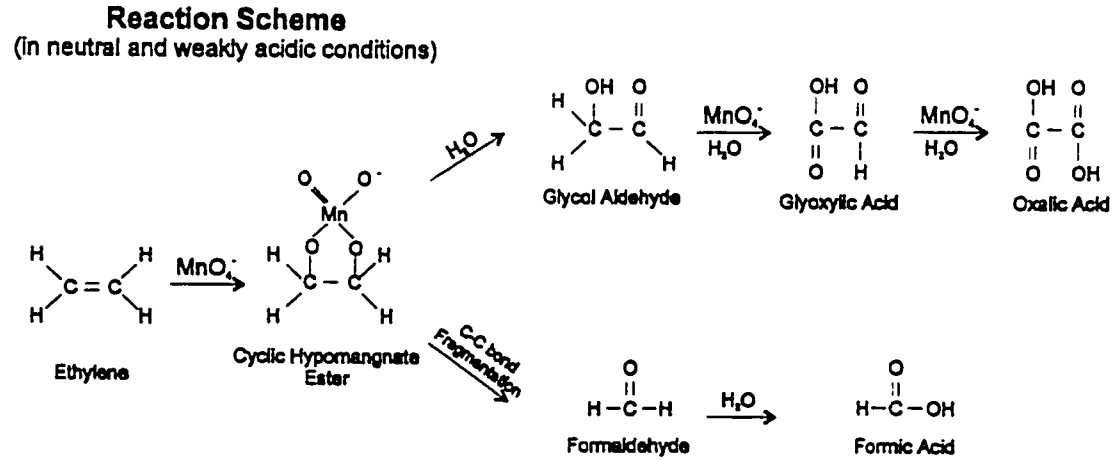

Figure 2.8 Reaction mechanism for the oxidation of halogenated alkenes by permanganate in near-neutral solution (from Yan and Schwartz, 1999).

permanganate to CO_2. Experimental confirmation of these reaction pathways was completed by Yan and Schwartz (1998) who determined that the principal carboxylic acids formed were formic, oxalic, and glyoxylic acid and that these acids were eventually converted to CO_2.

Stoichiometry

The stoichiometry of the oxidation reaction between $KMnO_4$ and an organic compound may be determined using mass and charge balances. Given the reported half reaction for the reduction of permanganate under near neutral pH (Equation 2.21), the half reactions corresponding to chlorinated alkenes like TCE and PCE may be derived by calculating the change in oxidation state for the two carbon atoms (+II to +IV) such that,

$$C_2Cl_3H + 4H_2O \rightarrow 2CO_2 + 3Cl^- + 9H^+ + 6e^- \quad (2.24)$$

$$3C_2Cl_4 + 12H_2O \rightarrow 6CO_2 + 12Cl^- + 24H^+ + 12e^- \quad (2.25)$$

Combined with the half-reaction for permanganate reduction, the overall stoichiometric equations describing the oxidation of PCE and TCE by permanganate under near-neutral ($3<pH<12$) conditions are,

$$3C_2Cl_4 + 4MnO_4^- + 4H_2O \rightarrow 6CO_2 + 12Cl^- + 4MnO_2(s) + 8H^+ \quad (2.26)$$

and,

$$C_2Cl_3H + 2MnO_4^- \rightarrow 2CO_2 + 3Cl^- + 2MnO_2(s) + H^+ \quad (2.27)$$

Complete mineralization of 100 mg/L of TCE or PCE results in equivalent chloride concentrations of 81 or 86 mg/L, respectively.

Using a similar approach, the overall reactions for the dichloroethylene isomers and vinyl chloride are,

$$3C_2Cl_2H_2 + 8MnO_4^- + 2H^+ \rightarrow 6CO_2 + 6Cl^- + 8MnO_2 + 4H_2O \quad (2.28)$$

and,

$$C_2ClH_3 + 2MnO_4^- \rightarrow 2CO_2 + Cl^- + 2MnO_2 + 3H^+ \quad (2.29)$$

It should be noted that this approach for developing stoichiometric equations results in potential equations which are only complete from a mass and electron transfer perspective and are not necessarily either thermodynamically or kinetically feasible.

If the oxidation reaction is assumed to occur at low pH (pH<3), the half reaction involving a five electron exchange,

$$MnO_4^- + 8H^+ + 5e^- \rightarrow Mn^{+2} + 4H_2O \quad (2.30)$$

occurs and the overall reactions for PCE and TCE become,

$$5C_2Cl_4 + 4MnO_4^- + 4H_2O \rightarrow 10CO_2 + 20Cl^- + 4Mn^{2+} + 8H^+ \quad (2.31)$$

$$5C_2Cl_3H + 6MnO_4^- + 3H^+ \rightarrow 10CO_2 + 15Cl^- + 6Mn^{2+} + 4H_2O \quad (2.32)$$

These reactions (Equations 2.31 and 2.32) require less oxidant per mole of solvent species degraded than the comparable reactions at neutral pH and may result in an unexpected oxidant sink if they were to occur. In contrast to the neutral pH reactions, the oxidation of alkenes under low pH conditions does not produce MnO_2(s) although this could form once the pH was buffered by the alkalinity of the aquifer.

The stoichiometry of the overall oxidation reactions the degradation of TCE and PCE at neutral pH provide some insight on the applicability of permanganate flushing. These reactions result

in the production of highly soluble carbon dioxide and hydrogen ions, indicating that significant pH decreases may occur adjacent to regions of high DNAPL saturation that result in a buffering response through dissolution of carbonate minerals. In carbonate aquifers, stoichiometric increases in the concentration of Ca^{2+} are likely with possible effects on the porosity and permeability of the aquifer. At the same time, the formation of Cl^- provides a simple reaction tracer not commonly found in groundwater at significant concentrations.

The combination of low pH and excess Cl^- may result in the formation of HCl, suggesting that additional oxidant may be required to react with the acid following Equation (2.20); however, this is likely a negligible effect since HCl is a strong acid ($K_a=10^3$). Decreases in pH as low as pH of 1 have been observed adjacent to a PCE pool in an unbuffered silica sand (MacKinnon, 1999). This phenomena may have two important consequences for the reaction chemistry immediately adjacent to DNAPL contaminants. In many aquifers a substantial fraction of carbonate minerals are present that will buffer the pH. The depletion of carbonate and gas binding from CO_2 exsolution may change the hydraulic properties of the porous media as well as the solution fluid properties (e.g., permeability, viscosity, interfacial tension, and density). High acidic conditions further complicate the solution chemistry since the oxidation half-reaction is more likely to produce Mn^{2+} which will subsequently be reoxidized by residual permanganate once the pH is buffered by the aquifer solids. A similar solubility enhancement may be expected for other metal species. In addition, it is uncertain whether permanganate is the active oxidant in highly acidic solutions. Stewart (1973) suggested that at low pH the equilibrium,

$$H^+ + MnO_4^- \rightarrow HMnO_4 \qquad (2.33)$$

forms permanganic acid, a reportedly stronger oxidant than permanganate although little is known about the its reactivity.

Several researchers have examined the theoretical basis for the assumption of complete mineralization. Schnarr et al. (1998) conducted mass balances on porous media columns

flushed with $KMnO_4$. Mass balances on carbon (both inorganic and organic) and chloride in the column's effluent indicated that the proposed stoichiometries for chlorine and carbon were generally correct. Similar results using chloride mass balances were obtained by Vella and Veronda (1992) and Yan and Schwartz (1999), although both Vella and Veronda (1992) and Schnarr (1992) observed chloride concentrations that were slightly in excess of the stoichiometric amount, suggesting a possible analytical bias in the ion-specific electrode analytical method for chloride used in both studies.

Kinetics

Reaction kinetics are an essential component of the evaluation of contaminant degradation in the slow-moving groundwater environment. The kinetic rate law describing bimolecular and irreversible homogenous oxidation of an organic solute by aqueous permanganate in a homogeneous solution has the general form,

$$r_C = \frac{dC}{dt} = -k_C[C]^{\alpha}[MnO_4^-]^{\beta} \tag{2.34}$$

where r_C is the decay rate (expressed as a change in concentration of C per change in time t), k_C represents the specific reaction rate constant, and α and β are the reaction orders with respect to $[C]$ and $[MnO_4^-]$. Table 2.2 presents a summary of experimentally determined kinetic rate data. These data, which are primarily available for TCE and PCE, indicate that the oxidation rate of the chlorinated alkenes varies inversely with the degree of chlorination as a result of electron deficiencies in the carbon-carbon double bond of the higher chlorinated species (Yan and Schwartz, 1999). Regression of the grouped reaction rate data (Figure 2.9) suggested that the appropriate rate expressions (in units of M and min) for TCE and PCE are,

$$r_{TCE} = -k_{TCE}[TCE][MnO_4^-]^{\beta} = -32.8[TCE][MnO_4^-]^{0.96} \tag{2.35}$$

and,

$$r_{PCE} = -k_{PCE}[PCE][MnO_4^-]^{\beta} = -2.4[PCE][MnO_4^-]^{0.99} \tag{2.36}$$

Table 2.1 Summary of reported rates for the oxidation of chlorinated alkenes by potassium permanganate.

Alkene	*Rate Law*	*Oxidant Dose (mM)*	*Source*
PCE	$r=-0.17[PCE]$ (min^{-1})	63.3	Truax (1993)
PCE	$r=-0.34[PCE]$ (min^{-1})	126.6	Truax (1993)
PCE	$r=-0.37[PCE]$ (min^{-1})	189.8	Truax (1993)
PCE	$r=-2.5[PCE][KMnO_4]$ $(M^{-1} min^{-1})$	31.0-193.0	Hood et al. (2000)
PCE	$r=-0.5[PCE][KMnO_4]$ $(M^{-1} min^{-1})$	0.07-0.7	Tratnyek et al. (1998)
PCE	$r=-0.0027\pm0.00018[PCE]$ (min^{-1})	1	Yan and Schwartz (1999)
TCE	$r=-1.89[TCE]$ (min^{-1})	63.3	Truax (1993)
TCE	$r=-4.35[TCE]$ (min^{-1})	126.6	Truax (1993)
TCE	$r=-8.40[TCE]$ (min^{-1})	189.8	Truax (1993)
TCE	$r=-0.039\pm0.0006[TCE]$ (min^{-1})	1	Yan and Schwartz (1999)
TCE	$r=-1.78\times10^{-3}[TCE]$ (min^{-1})	0.03	Vella and Veronda (1992)
TCE	$r=-2.87\times10^{-3}[TCE]$ (min^{-1})	0.06	Vella and Veronda (1992)
TCE	$r=-6.40\times10^{-3}[TCE]$ (min^{-1})	0.16	Vella and Veronda (1992)
TCE	$r=-1.50\times10^{-2}[TCE]$ (min^{-1})	0.32	Vella and Veronda (1992)
TCE	$r=-53.4\pm1.8[TCE][KMnO_4]$ $(M^{-1} min^{-1})$	1.58-6.33	Huang et al. (1999)
1,2-cisDCE	$r=-0.055\pm0.003[cDCE]$ (min^{-1})	1	Yan and Schwartz (1999)
1,2-transDCE	$r=-1.80\pm0.12[tDCE]$ (min^{-1})	1	Yan and Schwartz (1999)

where the reaction rate of TCE is ~14 times higher than the reaction rate of PCE. The reaction order of TCE (β_{TCE}) was significantly different from unity ($n=8$, $p=0.05$), while β_{PCE} was indistinguishable from unity ($n=13$, $p=0.05$); however, the small variation from unity suggests that assuming that the rates are second order overall is an appropriate simplification that results in negligible error.

It is important to distinguish between the rate of oxidation, expressed by (2.35) and (2.36), and the rates of formation of reaction products such as chloride. Stoichiometrically the rate of chloride production can be related to the rate of contaminant oxidation; this linkage, however, assumes that the reaction mechanism excludes intermediate rate-limiting reaction steps. Yan and Schwartz (1999) demonstrated that the rates of TCE oxidation and Cl^- formation were identical, suggesting that dechlorination of the intermediate products was rapid relative to TCE

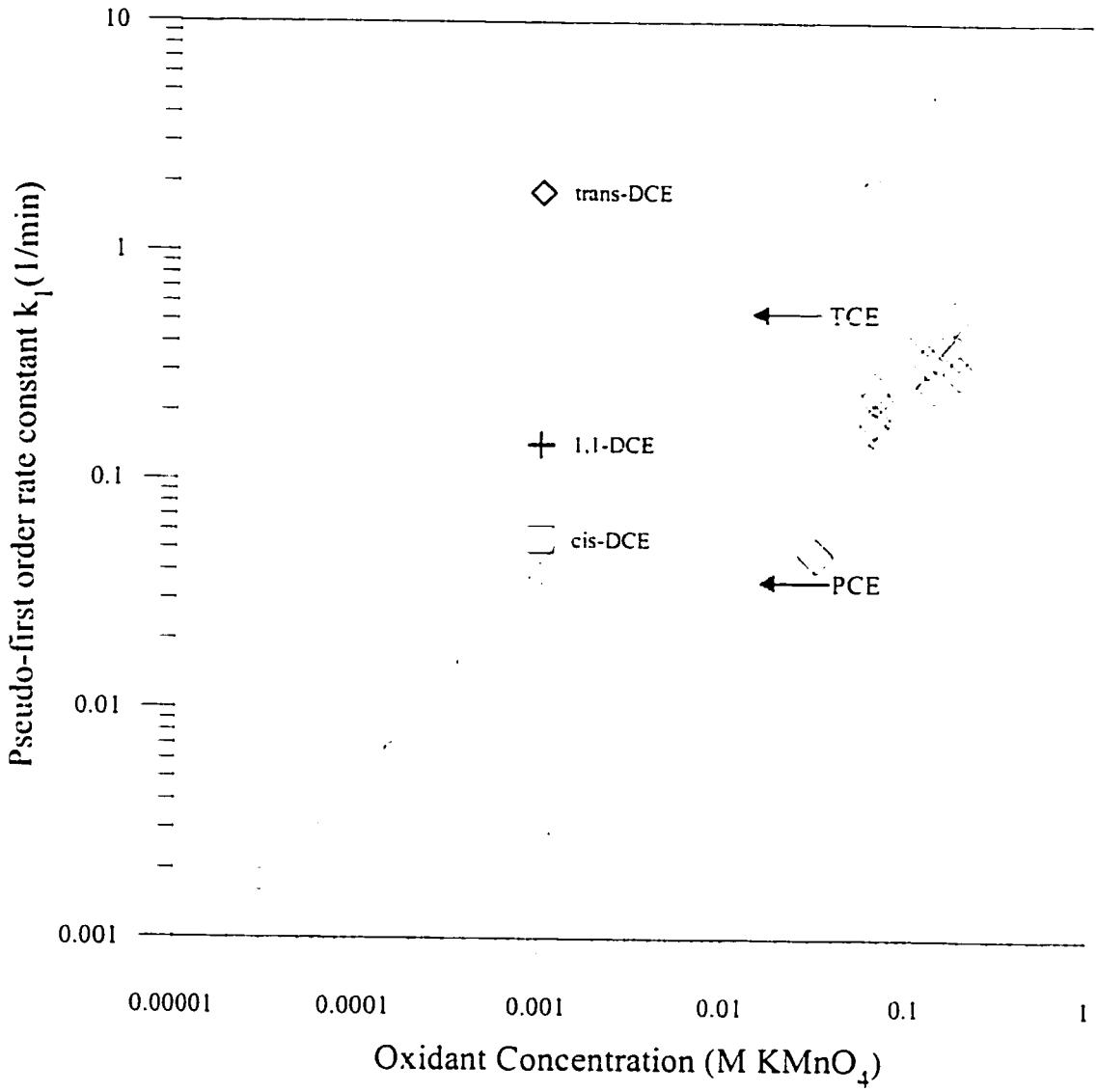

Figure 2.9 Summary of experimentally determined reaction rates for the oxidation of chlorinated alkenes by potassium permanganate.

oxidation.

Factors potentially impacting the reaction rate include pH and temperature. Yan and Schwartz (1999) observed that the rate coefficient for TCE was constant over the range $4.2 \leq pH \leq 8$, suggesting that the reaction mechanism was independent of pH. The rate of TCE degradation is sensitive to temperature with an activation energy of 35±2.9 kJ/mol, corresponding to an

increase in reaction rate by a factor of 1.7 for an increase in temperature from 10°C to 20°C (Huang et al., 1999).

2.4 DNAPL remediation technologies

Understanding the range of existing remediation strategies for DNAPL source zones provides information on the potential applicability and limitations of *in situ* chemical oxidation. The most common treatment approach at DNAPL sites has been the operation of a pump and treat system (Mackay and Cherry, 1989; National Research Council, 1994) but several new technologies have emerged which can complement existing pump and treat systems by focussing on the removal of pure phase contaminants. These source technologies fall within three general categories which include containment, mobilization, and treatment.

2.4.1 Pump and treat remediation

Pump and treat systems consist of hydraulic plume capture by extraction wells with above-ground treatment of the captured water. As a DNAPL remediation technology, pump and treat is limited by low contaminant solubility, large treatment volumes, slow desorption from aquifer solids, contaminant storage in low permeability zones, and large masses of non-aqueous phase liquid present in the aquifer (Doty and Travis, 1991). When pooled DNAPL is present in an aquifer, complete remediation of groundwater by pump and treat is considered to be unachievable (Mackay and Cherry, 1989). A survey of sixteen pump and treat operations throughout the United States noted that at 25% of the examined sites, operations continued after treatment periods twice as long as projected (Doty and Travis, 1991); estimated treatment durations had not been exceeded at the remaining sites. Cherry et al. (1992) indicated that no instances of complete aquifer restoration by a pump and treat system have been documented.

A comprehensive survey of remedial programs evaluated the performance of pump and treat remediation at seventy-six sites in the U.S. (National Research Council, 1994). Of these, six had met site-specific cleanup goals; however, in each of these six cases, all or some of the contaminants were biodegradable compounds, such as aromatics, ketones or alcohols, and none

had DNAPL contaminants. Of the seventy-six sites, 80% were thought to have a non-aqueous phase liquid present; the majority of these were either LNAPL in porous media, DNAPL in fractured rock, or DNAPL in porous media (National Research Council, 1994). The historical record of the performance of pump and treat systems suggests that while this technology may effectively contain groundwater plumes, pump and treat will be unable to achieve aquifer restoration within a feasible time period. As an alternative to pump and treat, a number of complementary technologies have been developed. These include, for example, the use of permeable treatment walls (Starr and Cherry, 1993; Pankow et al., 1993), biodegradation (Grubb and Sitar, 1994), and air sparging (Johnson et al., 1993); however, these technologies focus on limiting the migration of the groundwater plume and do little to address the source of contamination. Recognizing that treatment times will be long, considerable emphasis has been placed on the development of passive and semi-passive plume remedial techniques which require a minimum commitment of resources to operation and/or maintenance.

2.4.2 Source containment

Source containment technologies minimize the mobility of contaminants in the groundwater flow system. Containment may be achieved by reducing the permeability of the contaminated zone by either heating it into a molten slag and allowing it to cool (vitrification) or injecting a solidifying compound such as cement (Grubb and Sitar, 1994). At several sites, hydraulic disconnection from the surrounding aquifer has been achieved by constructing cutoff walls composed of continuous sealable sheetpiling, injected grout or comparable sealant, or trenched bentonite slurry. Both grout injection and slurry walls have been used at field sites with application limited by cost, required depth of installation, and durability (Grubb and Sitar, 1994). Within the contained zone, a small-scale pump and treat system may be used to maintain an inward hydraulic gradient.

2.4.3 Source mobilisation

Mobilisation technologies attempt to remove DNAPL by either physically moving the pure phase through the aquifer or by enhancing the contaminant's solubility in the aqueous phase.

Some efforts are usually made to pump pure phase DNAPL (e.g., Smith and Sykes, 1988) but this approach is limited by the large velocities required to displace the DNAPL which are only generated in the immediate vicinity of the well screen. Mercer and Cohen (1990) suggested that methods used for LNAPL collection (e.g., interception trenches, pumping wells, etc.) may be applicable to DNAPL collection systems; however, the depths at which mobile DNAPL is found may preclude these measures. DNAPL recovery from aquifers may be accomplished by pumping DNAPL alone using a pumping system controlled by down-well free product sensors (Michalski et al., 1995), by pumping wells intended as DNAPL production wells operating at rates low enough to produce both DNAPL and water (Oolman et al., 1995), or pumping groundwater extraction wells and separating co-produced DNAPL (Connor et al., 1989).

Several approaches have been proposed to enhance the efficacy of pump-and-treat systems by increasing the effective aqueous solubility of individual DNAPL components; these include flooding of the DNAPL source zone with a surfactant solution (Underwood et al., 1993), and alcohol flooding or cosolvency (Brandes and Farley, 1993). These technologies may be limited in applicability since the mechanisms which increase solubility can decrease the water/NAPL interfacial tension and potentially remobilise the pure phase. Surfactant flushing has been used for remediation of hydrocarbons and DNAPL at a number of sites (Grubb and Sitar, 1994). For example, Fountain et al. (1996) removed 61 L of a 231 L PCE spill in the Borden aquifer after flushing 14 pore volumes of a 2% surfactant solution. A limitation of both surfactant and cosolvent flushing is the requirement to either recycle or treat a waste stream containing very high concentrations of the contaminant and the solubilizing agent.

Several enhanced mobilization techniques have been proposed, including alcohol flooding and steam injection, that rely on mobilizing the contaminant in either the pure phase contaminant or a non-aqueous phase mixture. These techniques risk unfavourable DNAPL mobilization deeper into the aquifer. Steam injection (e.g., She and Sleep, 1999) uses concurrent vapourization of the source zone and vacuum extraction of the contaminated gas to remove DNAPL mass while alcohol flooding relies on mobilization of a DNAPL/alcohol mixture with

extraction by conventional extraction wells. Both technologies have been demonstrated at the pilot scale (Grubb and Sitar, 1994).

Source mobilisation is infrequently used since large quantities of DNAPL may not be identified as existing at a particular site. At sites where DNAPL is known to be present, recovery of a substantial volume of the pure phase may be accomplished; however, the immobile residual DNAPL can remain a source of chronic contamination (Connor et al., 1989; Cherry et al., 1990; Michalski et al., 1995; Oolman et al., 1995). It is likely that the reported successes in pumping pure phase are a function of the extremely large volumes of DNAPL found in pools in these aquifers. The extremely high non-wetting phase saturations that occur at these sites are readily detected using conventional monitoring approaches (resulting in incontrovertible identification of these sites as DNAPL sites) and provide a large reservoir of mobile DNAPL mass. Despite removing a large fraction of the total mass, the remaining DNAPL may act as a long term plume source.

2.4.4 Source treatment

Biological remediation

Various strategies have been utilized to treat aqueous phase contamination by transformation of the contaminant to less toxic products using microbiological processes. Concentrations of chlorinated solvents near the solubility limit are generally thought to inhibit metabolic processes in the microflora capable of actively degrading chlorinated organics (Pankow and Cherry, 1996). Regardless of inhibition, the slow biological reactions expected are unlikely to significantly accelerate source zone dissolution. As a consequence, biological techniques are generally not considered applicable to DNAPL removal although are potentially highly effective at containing plume migration.

In situ reduction

While numerous researchers have proposed dehalogenation technologies for chlorinated solvent remediation, the most common remediation approachs involve a solid phase catalyst (e.g., zero

valent iron (Gillham and Burris, 1992), palladium/H_2 (Lowry et al., 1998)). Approaches employing aqueous flushing reagents have included colloidal zero-valent iron particles (T. McAlary, personal communication, 2000), dithionite ($Na_2S_2O_4$; Tratnyek et al., 1998), redox couples such as vitamin B_{12} and titanium citrate (Lesage et al., 1996), and other porphyrin compounds such as heme (Larson and Cervini-Silva, 1998). While the current widespread use of Fe^0 in permeable reactive barriers has demonstrated the effectiveness of this approach as a plume containment technology in the short term, long term performance analyses have yet to be conducted. Of the remaining reduction approaches, only vitamin B_{12} has been tested at the pilot scale for DNAPL removal.

2.5 In situ chemical oxidation

While ISCO is a relatively new technology, several groups in Canada and the U.S. are engaged in research activities involving laboratory and field experimentation as well as modelling efforts. The majority of work has evaluated peroxide as the flushing reagent; however, several researchers are now examining permanganate.

Cowie and Weider (1986) were the first to apply ISCO with a concentrated peroxide solution. Potassium permanganate was first suggested as a flushing reagent for in situ groundwater remediation by Cho and Bowers (1991) while the first experimental investigations were conducted by Schnarr and Farquhar (1992). Alternative oxidants to permanganate include ozone, peroxide, and Fenton's reagent, all which can participate in reactions producing hydroxyl radicals, a powerful oxidant.

2.5.1 Alternative oxidants: ozone, peroxide, and Fenton's reagent

Ozone and peroxide are individually strong oxidants; they are primarily employed in water treatment processes in a complex series of reactions that result in the formation of highly reactive free hydroxyl radicals (OH•). Reaction rate constants for hydroxyl radicals with organic substrates are high, ranging from 10^9-10^{10} $M^{-1}s^{-1}$ (Glaze and Kang, 1988), making this a potentially effective oxidant for in situ groundwater treatment. Several processes are known

to produce these radicals, including generation by ozone with hydrogen peroxide (O_3/H_2O_2), ultraviolet light with peroxide (UV/H_2O_2), and peroxide in solution with ferrous salts such as $FeSO_4$ (Fe^{2+}/H_2O_2), which is also known as Fenton's reagent. UV/H_2O_2 oxidation processes are not relevant to in situ groundwater treatment since direct UV irradiation of the waste stream is required.

Ozone is frequently used in drinking water treatment disinfection, taste and odour control, and trihalomethane precursor removal. Montgomery (1985) discusses a reaction pathway, postulated by Hoigné and Bader (1976), where O_3 either participates in direct oxidation, a slow and highly selective reaction, or rapid decomposition to form OH•. Decomposition is promoted by the presence of hydroxyl radicals, organic radicals or high concentrations of hydroxide ions (Montgomery, 1985). In groundwater the low aqueous solubility of ozone, comparable to that of oxygen, will limit the oxidant mass delivered to a DNAPL source zone, suggesting that ozone may not be particularly useful for DNAPL mass removal.

While OH• formed by either O_3/H_2O_2 or Fe^{2+}/H_2O_2 is a strong and non-selective oxidant for many organic compounds, it is competitively scavenged by carbonate and bicarbonate, resulting in radical forms of these species. This reaction limits the effectiveness of the hydroxyl radical since many sediments contain a significant carbonate mineral fraction. The reaction rates of carbonate and bicarbonate with OH• are 4.2×10^8 $M^{-1} \cdot s^{-1}$ and 1.5×10^7 $M^{-1} \cdot s^{-1}$, respectively, resulting in significant radical abstraction given the concentration of these species relative to those of typical groundwater contaminants. As a result, hydroxyl radical oxidation processes in typical water treatment processes are more effective at pH<6.3 where carbonic acid is the dominant carbonate species (Montgomery, 1985). In the range 6.3<pH<10.3, bicarbonate is the dominant species, while above pH 10.3 scavenging of hydroxyl radicals by CO_3^-, the more reactive carbonate species, will predominate. Glaze and Kang (1988) suggested that this effect in O_3/H_2O_2 treatment processes was offset by the reaction of ozone with hydroxyl ions which resulted in further hydroxyl radical formation.

The majority of oxidation technologies for conventional water treatment and in situ groundwater remediation have emphasized either hydrogen peroxide or hydrogen peroxide with a catalyst promoting hydroxyl radical formation. For example, O_3/H_2O_2, and Fe^{2+}/H_20_2 are used effectively for a broad range of contaminants in drinking water and wastewater applications. In principle, the primary controls on the rate of contaminant degradation are the rates of hydroxyl radical formation and abstraction which are influenced by catalyst concentration, organic substrate concentration, alkalinity, and pH. Glaze and Kang (1988) investigated O_3/H_2O_2 oxidation processes and observed that increasing bicarbonate alkalinity decreased TCE and PCE degradation rates due to radical scavenging. Consistent degradation rates were reported in a similar study by Bellamy et al. (1991). In an O_3 system where direct oxidation by both O_3 and the hydroxyl radical was known to occur, contaminant degradation rates were insensitive to pH (Glaze and Kang, 1988). The authors attributed this result to the increasing rates of radical scavenging by carbonate, which has a lower reaction rate with the hydroxyl radicals, offsetting the increased rate of radical formation at high pH (Glaze and Kang, 1988). This study separated the effectiveness of the active oxidant (OH•) from the solution pH and demonstrated the effect of carbonate and bicarbonate on hydroxyl radical abstraction.

In a review of conventional advanced oxidation processes, Venkatadri and Peters (1993) suggested that the pH adjustments required for in situ groundwater application of Fenton's reagent could be an economic impediment. These authors primarily surveyed water treatment literature applying to waste streams with typically low alkalinity and no solid carbonate fraction. Adjustment of pH in these weakly-buffered waste streams would optimize the rates of hydroxyl production and contaminant degradation by decreasing hydroxyl radical scavenging by converting carbonate to carbonic acid and increasing the solubility of Fe(II). Similar adjustments in aquifers containing large quantities of carbonate minerals would require sufficient acid addition to completely exhaust the carbonate mineral reservoir, producing high temperatures, high partial pressures of CO_2 and high alkalinity. Otherwise, if a low pH was not achieved, the high alkalinity could limit contaminant degradation rates through OH• scavenging. Secondary side effects of acid addition could include heat generation, CO_2 exsolution causing

gas binding, mobilization of metal species sensitive to pH, and DNAPL remobilisation through the reduction in interfacial tension caused by the high aqueous concentration of CO_2.

A number of studies have specifically examined groundwater contaminant degradation using H_2O_2 or Fe^{2+}/H_2O_2 in porous media. The most common of these studies have been laboratory investigations using a variety of approaches including batch reactors, mixed soil slurry reactors, and columns packed with soil. While batch and slurry reactors permit careful control of experimental conditions, columns closely model the actual field situation by including the limitations on oxidant supply to the contaminant imposed by groundwater flow. Ravikumar and Gurol (1994) used H_2O_2 and Fe^{2+}/H_2O_2 in a bench-scale column study to oxidize TCE and pentachlorophenol. The iron content of the sand media in columns flushed with only H_2O_2 catalysed decomposition of the peroxide resulting in the formation of hydroxyl radicals (Ravikumar and Gurol, 1994); however, the natural iron content of the sand (800 mg/kg) was less effective than 50 mg/L $FeSO_4$ in catalysing the reaction. Mineral-induced catalysis has been observed by other investigators including Watts et al. (1999).

Gates and Siegrist (1995) used H_2O_2 to oxidize TCE contaminated clay soils in bench scale experiments simulating in situ soil mixing and oxidant addition. Reductions of TCE concentration as high as 98% were observed and demonstrated the potential effectiveness of this oxidation without pH adjustment. Peroxide concentrations as high as 7.3% were used to provide oxidant doses up to 28.3 g H_2O_2/kg soil. Decreases in pH from 6 to 5.3 were interpreted as resulting from Fenton reactions between the H_2O_2 and iron minerals plus the production of CO_2 from the oxidation reactions. Increases in the aqueous total organic carbon concentration were observed concurrent with increased oxidant addition and were thought to reflect partial oxidation of organic matter present in the soil resulting in soluble organic products (i.e., carboxylic acids).

Taken together, these studies suggest that hydroxyl radicals generated using Fenton's reagent have significant potential as effective oxidants in groundwater remediation. However,

eliminating the pH adjustment step usually included may prove an equally effective approach. This approach would avoid the cost of the acid required for pH adjustment, have less impact on the aquifer geochemistry, and reduce the heat and gas generated by acid addition and carbonate dissolution. Additionally, less peroxide would be required since hydroxyl scavenging by carbonates would be minimized. While some decrease in contaminant degradation rates may result, the effect of this on DNAPL mass removal rates is not known; however, anecdotal reports have suggested that the effect may be negligible since Fenton's reagent often requires the addition of a "stabilizer", usually a phosphate salt, to reduce the rate of hydroxyl radical formation so that the radicals are not depleted before reaching the contaminated soil.

2.5.2 ISCO experiments

While several studies have characterized reaction kinetics (see Section 2.3.3), few laboratory trials have examined the effectiveness of ISCO and attempted to assess the physico-chemical processes limiting the rate of DNAPL mass removal. Schnarr (1992) reported high removals of PCE from contaminated soils and observed that the effectiveness of the oxidant flush was dependent on the oxidant concentration and the flushing rate. In another comprehensive study examining the effect of a permanganate flush on a DNAPL pool, a physical model was constructed consisting of a silica sand aquifer above a silica flour aquitard (MacKinnon, 1999). A DNAPL pool was formed by injecting 2224 mL of pure PCE into the base of the aquifer through a small drivepoint piezometer. The pool was flushed with 10 g/L permanganate for 150 days at a flow rate corresponding to a Darcy velocity of 0.09 m/day. The oxidant flush removed 45% of the PCE mass from the aquifer, while the steady-state aqueous mass flux from the solvent pool decreased by a factor of four. The decrease in PCE mass transfer rate was attributed to the formation of dense $MnO_2(s)$ precipitates above the DNAPL pool. These few, highly controlled experiments suggested that while the effectiveness of ISCO was highly dependent upon the DNAPL distribution, significant benefits could be achieved without complete removal of the DNAPL.

Several field trials evaluating ISCO have been attempted using a variety of oxidant delivery

techniques. The field experiments have focussed on estimating contaminant mass removal, assessing technology effectiveness, and providing design recommendations for full scale application. Additional field experiments are currently underway in the Borden aquitard and at several industrial sites; however, data produced by these studies is not published.

The earliest report of in situ oxidation described flushing a 17,000 gallon release of a 50% formaldehyde solution with concentrated peroxide solution (Cowie and Weider, 1986). The first peer-reviewed report of in situ oxidation using permanganate was a summary of field experiments conducted at the Borden research site (Schnarr et al., 1998). Two experiments were conducted within a double-walled sheetpile cell (1 x 2.5 x 3 m) that isolated the experimental zone from the surrounding aquifer system. The experimental cell was equipped with injection and extraction wells and three multilevel samplers between the source zone and the extraction wells. In the first of two experiments, Schnarr (1992) built an artificial DNAPL zone of residual PCE that consisted of 1.6 kg of PCE in a box shape (0.3 x 0.3 x 0.35 m) below the water table in the upper third of the cell (non-aqueous phase saturation of 8%). The cell was continuously flushed with an oxidant solution (10 g/L $KMnO_4$) at a mean flow rate of 71 L/day. After 120 days of oxidant injection the remaining oxidant solution was displaced by injecting clean water. During this period permanganate, chloride and PCE were monitored in the extraction wells and the multilevel sampling piezometers. Chloride profiles from extraction wells were used to calculate a cumulative chloride mass balance which indicated that ~92% of the initial PCE mass could be accounted for by chloride production (Figure 2.10). Further, both soil and groundwater samples taken during the subsequent clean water flush suggested that the PCE was completely removed.

The second field experiment used a different source configuration and employed an improved dosing method. The source consisted of a 7.9 L equal mass mixture of TCE and PCE that was slowly injected into the cell through six small stainless steel injection points over 120 hours (Schnarr et al., 1998). In contrast to the earlier work, this experiment was an attempt to examine the effect of oxidant flushing on a heterogeneously distributed (pooled) DNAPL

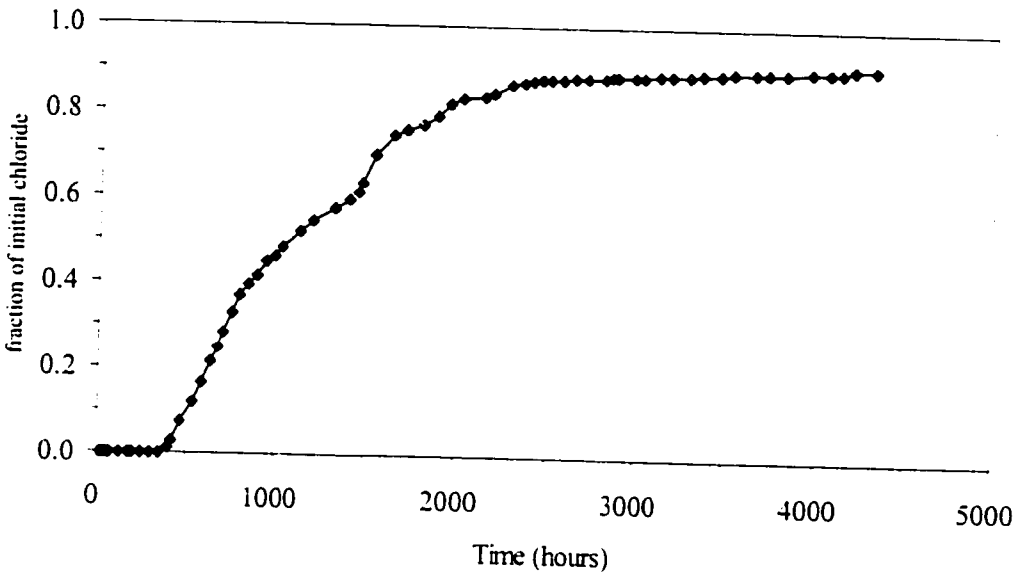

Figure 2.10 Fraction of initial PCE DNAPL source, expressed on an equivalent chloride basis, removed during permanganate flush (from Schnarr, 1992).

source. Oxidant recycling was used to reduce the mass of oxidant required. Chloride and solvent concentrations in the effluent were monitored over 250 days while the source was flushed with a 10 g/L oxidant solution injected at 48 L/day. Due to concurrent oxidant and chloride recycling, the chloride mass was calculated based on the average Cl^- concentration in the cell at the end of the oxidant flush. This estimate indicated that chloride in the cell accounted for ~62% of the stoichiometric chloride mass in the initial DNAPL source; however, it was evident that oxidation of the solvent was continuing in the upper third of the cell. A water flush of the cell provided further information on the effectiveness of the experiment. Clean water was injected into the cell for 180 days to remove excess oxidant and manganese dioxide deposits. During the flush, low concentrations of TCE and PCE were detected. These data suggested that the initial rapid production of chloride was consistent with source removal from zones of low non-wetting phase saturation that rapidly dissolved while the decrease in chloride production was characteristic of slow dissolution from pooled DNAPL. As a second measure of the effectiveness of the oxidant flush, effluent solvent data from the extraction wells indicated the average concentration had decreased by a factor of 10^1-10^2.

Cline et al. (1997) treated a low permeability soil contaminated with TCE by mixing the oxidant and soil in situ using both H_2O_2 and $KMnO_4$ as oxidants. In the peroxide test, large mixing blades with injection ports injected 10% v/v H_2O_2 to depths of 1.5 m in a saturated clay soil. With an effective mixing diameter of 3.1 m, each treatment location was mixed for 60 minutes. Average TCE removals (initial concentration 10-20 ppm) of 72% were reported; however, these were only estimates since it was difficult to collect representative samples from the large volume of soil mixed within each column. At another site with an unsaturated clay soil (*foc*=1%) contaminated with up to 2000 mg/kg of total VOC (primarily TCE and 1,1-DCE), a large auger with oxidant injection ports was used to mechanically mix a 0.5-12% w/w permanganate solution with the soil. The mixed column was 14.3 m deep with a diameter of 2.4 m. Estimated TCE removals from the two soil columns were 65% and 68%. Permanganate was observed to disappear from soil samples collected 3-5 days after treatment, likely reduced by natural organic matter.

Zhu et al. (1998) injected fresh water containing dissolved chlorine dioxide into a karst aquifer contaminated with petroleum, an approach of limited applicability due to the potential formation of trihalomethanes resulting from reactions between the chlorine residual and natural organic matter. Concentration reductions of 60-80% were observed in monitoring wells during the period of chlorine dioxide injection. No clear mechanism causing this decrease was identified and it may have resulted from simple dilution.

The field experiments described above demonstrate the potential strengths and limitations of in situ oxidation technologies. While it is clear that under ideal conditions complete removal of a contaminant can be achieved (e.g., Schnarr et al., 1999), the benefits from partial DNAPL removal resulting from mass transfer and oxidant mixing limitations are uncertain. Mixing and mass transfer limitations are common to essentially every oxidant flushing scheme (except the in situ mixing system employed by Cline et al., 1997) and result from weak dispersion and the influence of the DNAPL distribution on the overall mass transfer rate.

The buffering capacity of the aquifer is important design consideration. In the case of permanganate, carbonates will buffer the acid produced by oxidizing chlorinated alkenes. If the carbonates are primarily in the form of calcite or dolomite, oxidation of TCE or PCE by permanganate will result in elevated concentrations of Ca^{2+} or Mg^{2+}. In the case of ISCO using Fenton's reagent with acidification, the buffering response may limit contaminant degradation rates. In the specific case of Fenton's reagent, it may be that addition of an iron salt is unnecessary if sufficient iron or other hydroxyl catalysing metal species are present in the porous media. In aquifers where a carbonate mineral phase is present, the improvement in Fe(II) solubility resulting from the lowered pH may be offset by increased radical scavenging by carbonate species.

These experimental results demonstrated that complex contaminant distributions will make it difficult to design, monitor, and assess the performance of in situ treatment systems. Clear measures of the benefits based on DNAPL mass removal and on the reduction in the concentration of the groundwater plume are necessary. Since DNAPL removal will be difficult to measure and achieve, an assessment of the benefits of an oxidant flush should emphasize the reductions in the concentration and the mass load of the contaminant in the groundwater plume.

2.5.3 Oxidant flushing system design

Delivery of oxidant to the contaminated media is a significant design problem that is exacerbated by geologic heterogeneity and the spatial extent of the source zone. Faced with a specific reaction chemistry, several approaches have been suggested to utilize oxidants as part of a in situ treatment process

Plume remediation requires in situ mixing of the contaminant plume and the injected oxidant solution and is difficult to achieve since little dispersive mixing occurs in groundwater. A possible means of adding dilute oxidant to a plume is through an interception wall. Wilson and Mackay (1995) tested a passive diffusion apparatus installed in a wall composed of closely spaced, large diameter wells that added oxygen to stimulate biodegradation. Testing of the

apparatus with permanganate is currently underway. In this case, mixing will be limited if the permanganate reacts with natural oxidant demand rather than the contaminant plume. Ozone may be more effective since direct ozone oxidation would tend to result in biodegradable organic products with molecular oxygen available for aerobic biodegradation.

Above-ground treatment of groundwater using oxidation is potentially feasible as part of a pump and treat system. Design of an oxidant reactor would require selection of an oxidant dose and contact time resulting in either negligible oxidant residual and complete contaminant removal or addition of excess oxidant, complete contaminant removal, and residual oxidant removal with either re-injection or disposal of the treated effluent. The economic viability of constructing a reactor with the necessary contact time will be controlled by the reaction rates. In the case of permanganate, the reaction rate is slow relative to hydroxyl radical reactions and large reactor volumes would be required. Inclusion of facilities for removing and handling $MnO_2(s)$ solids would incur additional cost.

Ozone is a potentially effective oxidant for treatment of contaminated groundwater; however, as previously stated, it is unlikely that ozone could be used for in situ DNAPL remediation since the low solubility of ozone in water would permit only small mass fluxes of the oxidant into the contaminated zone. Ozone has been used with some success as a "polishing" agent to treat soil contaminated with low levels of pentachlorophenol and polyaromatic hydrocarbons. Marvin et al. (1999) performed a one month pilot test of ozone injection through an air sparging system in a stratified sand aquifer and observed an 82% reduction in the average groundwater concentration. While O_3 was assumed to be the sole oxidant, oxidation by both O_3 and $OH\bullet$ could be expected in natural waters (Glaze and Kang, 1988).

While schemes to remediate aqueous plumes must overcome the difficulty of mixing the oxidant and contaminant with complex oxidant dosing strategies, in situ chemical oxidation of DNAPL source zones has only two primary modes of application. The most common, known as active flushing, involves flushing a concentrated oxidant solution through a DNAPL zone

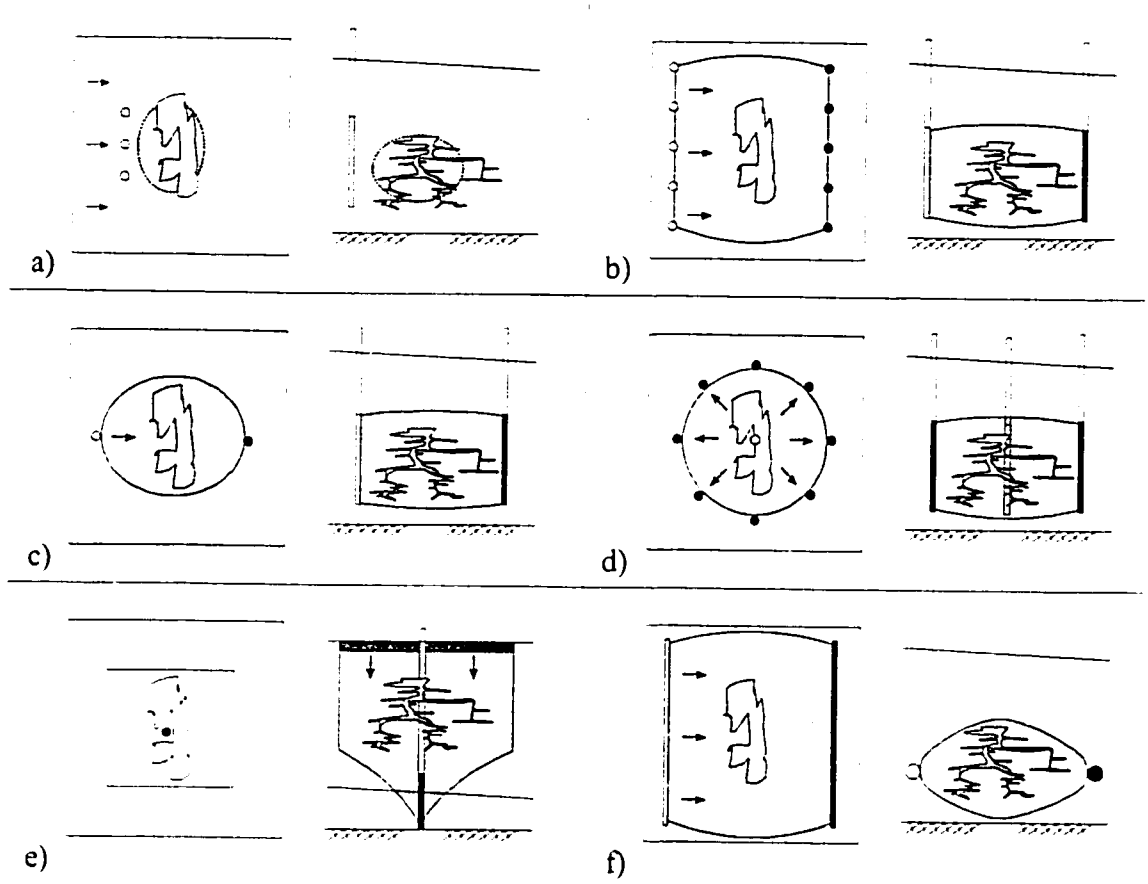

Figure 2.11 Conceptual oxidant delivery schemes (plan and profile) for a) passive flushing; b) parallel vertical wells; c) doublet; d) radial; e) vadose zone infiltration; and f) horizontal wells. Shown are the injection wells (light grey), extraction wells (black) and treatment zone volume (shaded).

under a forced gradient while passive flushing uses the natural flow system to provide contact between the contaminant and the oxidant (Figure 2.11a). In either case, transport of the oxidant to the contaminant is achieved through the hydraulic gradient driven advection, density-driven advection, or dispersive mixing.

Active oxidant flushing requires a means of injecting oxidant solution as well as extracting the residual oxidant solution, aqueous phase contaminant, and reaction products. Regardless of the

particular injection system, active systems flush the contaminated zone with the required oxidant solution and contain any contaminants within the treatment zone. The choice of injection and extraction approach is dictated by cost, depth of contaminant, aquifer hydrogeology, operational and maintenance flexibility, and site accessibility. A further consideration is the impact of density-driven advection on the flow of the oxidant solution within the treatment zone. Possible design options include the installation of horizontal wells, conventional vertical wells, drivepoint tools, and infiltration galleries.

Design alternatives for conventional well injection and extraction systems include the well pattern or geometry in addition to the well type. Parallel lines of wells at right angles to groundwater flow (Figure 2.11b) are likely to provide a more effective flush than a doublet covering a relatively small lateral area (Figure 2.11c). Geometries such as the radial recirculation cell (Figure 2.11d) or five-spot well pattern require drilling within the source zone and can result in oxidant short-circuiting between wells.

For any alternative the design should be conservative in the sense that, given a degree of performance uncertainty, the actual zone of contamination is completely contained within the flushed volume. Accordingly, alternatives with a larger number of injection points provide better operational flexibility. For example, the injection or extraction flow rates in individual wells may be changed to either reduce the volume of oxidant solution required or to provide additional advection in lower permeability zones. Stagnation zones, which form between adjacent vertical wells, are a limitation since these zones result in complex flow fields that are difficult to characterize using conventional hydraulic monitoring techniques.

At sites where the primary target of remediation is within the vadose zone or a shallow aquifer, infiltration galleries may be employed. Consisting of a constructed system allowing gravity-driven flow from a constant head surface, infiltration galleries promote downwards flow through the vadose zone (Figure 2.11e). Alternatively, oxidant injection in the vadose zone may be achieved with either conventional wells or drive points (MacKay et al., 1998) with recovery

of the oxidant solution by conventional wells screened in the saturated zone.

In thin aquifers, horizontal wells can potentially flush the entire thickness without forming stagnation zones between injection points but offer little ability to change the flow field in response to operational monitoring. The most likely configuration, similar to that used by West et al. (1998), would involve parallel extraction and injection wells oriented at right angles to the direction of groundwater flow (Figure 2.11f). Contrary to the approach of West et al. (1998), who were concerned with potential DNAPL remobilisation (O.R. West, personal communication, 1999), injection at the up-gradient well would take advantage of the existing gradient. The dosing apparatus for a single injection well would be less complicated relative to that the number of conventional vertical wells required to provide the same flushing capacity; however, as stated previously, the design concept is operationally inflexible. Without the use of specialized packer systems, there are limited means of monitoring or controlling the distribution of flow within the screened interval. Variations in well screen efficiency and aquifer hydraulic conductivity could result in the injected solution short-circuiting through the highest conductivity pathway, an effect reported by West et al. (1998) who attributed differential advancement of the permanganate front into the aquifer to spatial variability in hydraulic conductivity.

2.5.4 Conceptual model: mass transfer during ISCO

The studies completed to date provide a conceptual framework to describe the rapid process of DNAPL mass removal and form the basis for the quantitative modelling approach developed later in this thesis. A conceptual macroscale hypothesis for the physico-chemical processes controlling DNAPL dissolution and oxidation is built upon the widely-accepted stagnant film model of dissolution (Figure 2.12). As clean water flows through porous media contaminated with DNAPL, a concentration gradient of the aqueous solvent is established at the phase interface. As the solubility limit of the solvent in the bulk aqueous phase is achieved, the concentration gradient of the solvent becomes small. In the case of an oxidant flush, the aqueous concentration of the solvent is decreased by the oxidation reaction, increasing the

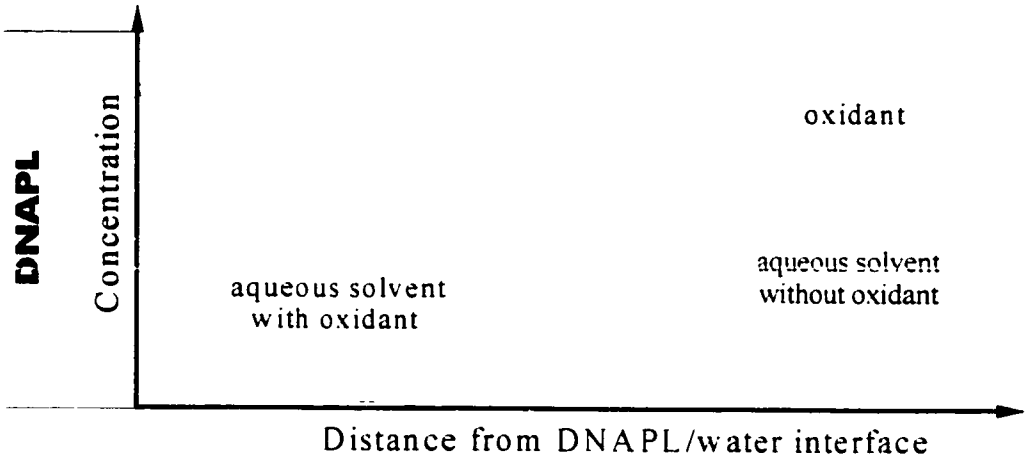

Figure 2.12 Conceptual model describing the macroscale process of DNAPL mass removal from the phase interface during oxidant flushing.

solvent concentration gradient through the stagnant film and the mass flux from the DNAPL into the aqueous phase. If the reaction kinetics are slow, the decrease in bulk aqueous concentration occurs further away from DNAPL/water interfaces, precluding any increase in the mass transfer rate. For a rapid reaction the solvent concentration at the interface is driven to zero, suggesting that the maximum dissolution rate depends only upon the effective solubility and the mass transfer rate coefficient. Since the only equilibrium possible during an oxidation reaction occurs when either of the two reacting species is completely degraded, it is evident that the local equilibrium assumption is an inappropriate model to describe this process. As a further consequence of the reaction, macroscale diffusive transport of the oxidant species toward the DNAPL/water interface is enhanced in proportion to the mass transfer rate.

The conceptual model describing enhanced DNAPL dissolution caused by oxidant flushing has several implications. First, it suggests that in hydrogeologic environments where solvent mass removal is essentially diffusive (e.g., low permeability lenses, aquitards, and hydraulically isolated aquifer pockets), oxidant flushing will significantly enhance remediation of these zones provided the path length from the DNAPL interface to the advective region is short. For long

path lengths, the solvent concentration gradient will be small and the corresponding dissolution enhancement negligible. A brief quantitative analysis of the effect of the diffusion path length on the enhancement of dissolution is presented in Chapter 4.

The second implication is that successful prediction of overall rates of mass removal requires kinetic expressions for both macro-scale non-equilibrium dissolution and oxidation. While sufficient data is available to adequately characterize oxidation reaction rates for several contaminants, limited data are available quantitatively describing non-equilibrium dissolution from DNAPL pools. During a water flush, the mass transfer rate coefficient may be sufficiently fast that some macro-scale local equilibrium occurs; however, the dissolution enhancement observed in the oxidation studies previously described suggests that mass transfer rates controlled DNAPL removal under some conditions (i.e., DNAPL pools). The high water phase permeability of residual source zones, which have high specific surface areas favouring dissolution, allows high advective fluxes of oxidant to the DNAPL which minimizes oxidant depletion and results in high reaction rates. In DNAPL pools with high saturation, the opposite conditions exist and mass transfer will control the maximum rate of mass removal.

2.5.5 Conceptual model: field application and monitoring of ISCO

A qualitative description of the trends in the solvent, oxidant, and chloride concentration expected during an oxidant flush with permanganate are presented in Figure 2.13. This conceptual model is based on a generic site consisting of a sandy aquifer which is contaminated with a source zone with both pooled and residual DNAPL (single component). The aquifer contains no background concentration of chloride in the groundwater and composition of the porous media includes natural organic matter. The oxidant injection system consists of flushing a constant concentration of permanganate through the contaminated zone without recycle of the effluent. During the initial phase of the oxidant flush, oxidant is consumed by the porous media before it reacts with aqueous solvent. Since oxidant is not delivered to the contaminant, the concentration of the solvent in the effluent of the recirculation system reaches a steady-state condition. During this phase of the oxidant flush, above-ground treatment processes are

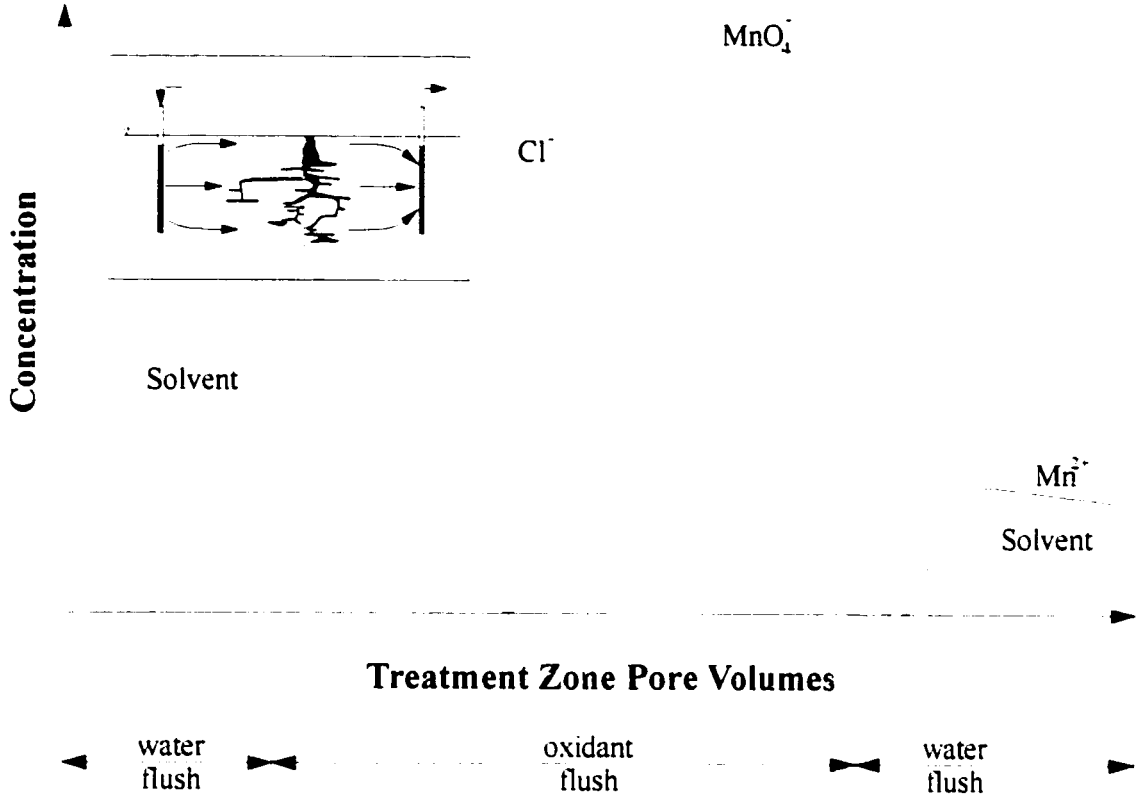

Figure 2.13 Expected variations in extraction well effluent concentrations of solvent, permanganate, chloride, and manganese, assuming a typical treatment scenario (shown in inset). Dashed lines represent inherent uncertainty in technology performance.

required to prevent the solvent from being re-injected, potentially resulting in the deposition of $MnO_2(s)$ in the screens of the injection wells or the surrounding filter packs and reducing the efficiency of the injection wells. Similarly, if the groundwater during this initial phase contained soluble iron and manganese, precipitation of the metals would also occur in addition to $MnO_2(s)$. After the injected oxidant solution reaches the DNAPL source zone, a high concentration of chloride is produced in the effluent flow. The chloride concentration peaks as oxidant migrates through the source zone and produces a significant dissolution enhancement. Shortly after breakthrough of chloride, the effluent solvent concentration becomes non-detectable as the injected oxidant is fully mixed with the groundwater plume from the DNAPL and remains low until the oxidant flush is completed. The breakthrough of the oxidant pulse

in the recirculation system effluent lags the chloride pulse as a result of continued oxidant consumption by the porous media retarding the migration of the oxidant between the source zone and the extraction wells. Once most of the natural organic carbon in the treatment zone is oxidized, the oxidant pulse breakthrough occurs in the effluent flow and reaches a steady concentration. As the oxidant flush continues, the concentration of chloride declines, reflecting a decrease in the mass transfer rate caused by a shift from advection-dominated to diffusion-dominated dissolution processes. During advection-dominated mass removal, the decrease in the mass transfer rate results from the decreased permeability of zones of significant MnO_2(s)deposition, and decreased interfacial surface area available for mass transfer. As long as mass transfer limits the rate of mass removal from the source zone. the addition of the oxidant enhances the rate of DNAPL removal; however, addition of oxidant during the diffusion-limited stage produces a negligible dissolution enhancement.

The mass transfer rate at the end of the oxidant flush will be evident by the chloride concentration; however, estimating the chloride concentration will be complicated by the high detection limit for chloride relative to the comparable regulatory limits for chlorinated ethenes and any existing background chloride concentration. A chloride concentration of zero would suggest that the contaminant was completed removed while a non-zero chloride concentration suggests that solvent was still present in the treatment zone. However, a constant chloride concentration would imply that removal of the remaining mass was limited by diffusion and that addition of the permanganate produced only a small dissolution enhancement. Accordingly, the addition of oxidant to the treatment zone should continue until mass removal is dominated by diffusion. As a convenient endpoint, the oxidant flush should continue until the effluent chloride flux is less than or equal to the steady-state effluent solvent flux (in comparable units) measured before the oxidant flush. In other words, if the chloride flux during the oxidant flush indicates that the rate of contaminant mass removal by the oxidant is less than or equal to the rate of contaminant mass removal before the oxidant flush, the benefit of the oxidant flush is negligible.

Following the oxidant flush, injection of the oxidant solutions is stopped and ambient groundwater is flushed through the treatment zone. During the post-oxidation water flush, the concentrations of permanganate and chloride rapidly decrease as the residual oxidant solution is displaced by ambient groundwater. Once the remaining oxidant removed and aquifer becomes more reducing, reductive dissolution of the manganese dioxide occurs. Simultaneously, any DNAPL remaining in the source zone will be evident by the concentration of the solvent in the effluent groundwater; however, the solvent concentration observed following the oxidant flush should be less than that observed before the oxidant flush.

2.5.6 Conceptual model: removal of manganese dioxide

Manganese is a regulated contaminant in drinking water supplies in many jurisdictions. Usually a parameter of aesthetic concern, the drinking water limit for total Mn is typically 50 µg/L. Dissolution of the precipitate is a redox reaction (Equation 2.13), the extent of which is controlled by redox conditions. While residual permanganate remains in the treatment zone, the oxidizing conditions will inhibit dissolution of the dioxide; however, once the oxidant flush is complete and background aquifer water is flushed though the treatment zone, manganese dioxide can act as an oxidant and produce a Mn^{2+} plume. The concentration of the plume with depend on the redox conditions and the concentration of available reductant. In this half-reaction, manganese dioxide acts as an oxidant in a two electron transfer; the extent and rate of the reaction is dependent upon the availability of a reductant (e.g., dissolved iron, dissolved organic carbon, etc.) as well as the redox environment. Manganese dioxide reacts with both organic and inorganic reductants, any of which could be introduced into the treatment zone in an attempt to accelerate the dissolution process.

Down-gradient of the treatment zone, the mobility of Mn(II) will be dependent upon site-specific factors. The cation may participate in cation exchange processes, including those with naturally occurring manganese dioxide minerals. If redox gradients exist within the aquifer, Mn(II) may be readily oxidized and re-precipitated as $MnO_2(s)$.

Chapter 3
In Situ Oxidation Field Trial

3.1 Introduction

As part of the current thesis research, a field demonstration of *in situ* chemical oxidation was conducted to examine the effectiveness of ISCO at a well-characterized experimental site. The principal objectives of this research component were to evaluate the performance of ISCO under conditions that were representative of the hydrogeology of full-scale field sites, to refine the conceptual model of the ISCO remediation process, and to develop general monitoring approaches applicable to full-scale technology implementation. Significant features of this field experiment included:

- A sheetpile enclosure was not used and oxidant flow in the subsurface was controlled through a network of injection and extraction wells.

- The experiment was conducted in a naturally heterogeneous aquifer. Variability in hydraulic gradient, hydraulic conductivity, and oxidant reduction capacity were not controlled.

- Emphasis was placed on characterizing the pre- and post-oxidant flush solvent plume.

- The source was a relatively homogeneous multi-component DNAPL containing TCE and PCE.

This chapter provides site characterization data, treatment system design, and monitoring data required to appropriately evaluate the experimental objectives and support the numerical simulations presented in the following chapter. Previous studies characterizing the regional and local hydrogeology and experimental work at the Borden research site, are reviewed. The design of the oxidation treatment system, including the oxidant recycling system, the locations of monitoring wells and multilevel samplers, and the processes used for waste treatment, is presented. The field trial results present data from two tracer tests and soil samples collected from the source zone in addition data collected during the oxidant flush, and includes time-series groundwater concentration data from multilevel piezometers and sample points in the oxidant recycling system, synoptic sampling events at the 1-m multilevel fence, drive point profiling data from within the source zone, and soil sampling of the source zone.

3.2 Site location and local hydrogeology

The Canadian Forces Base Borden (Borden), near Alliston, Ontario, is approximately 100 km north of Toronto (Figure 3.1). The University of Waterloo has maintained a research station on the base since the late 1970's and has conducted research ranging from a characterizing landfill contaminant plume to monitoring solvent vapours in the vadose zone (Cherry et al., 1995).

The regional hydrogeology is dominated by an upper, unconfined sand aquifer deposited during the Late Wisconsinian period (10,000-20,000 BP) as glacial retreat formed extensive lakes over much of southern Ontario (Bolha, 1986). These large lakes, fed by meltwater streams with high sediment loads, formed deltaic deposits which were reworked by wave action to form a prograding (well sorted higher in the deposit, poorly sorted deeper) sand deposit. This upper sand unit is underlain by a thick consolidated clay aquitard which forms a leaky upper boundary to a lower semi-confined aquifer. Foley (1992), as part of an hydraulic investigation of the aquitard, completed a 63 m borehole which showed that the local overburden consisted of 60 m of interbedded clays and sand over a limestone bedrock.

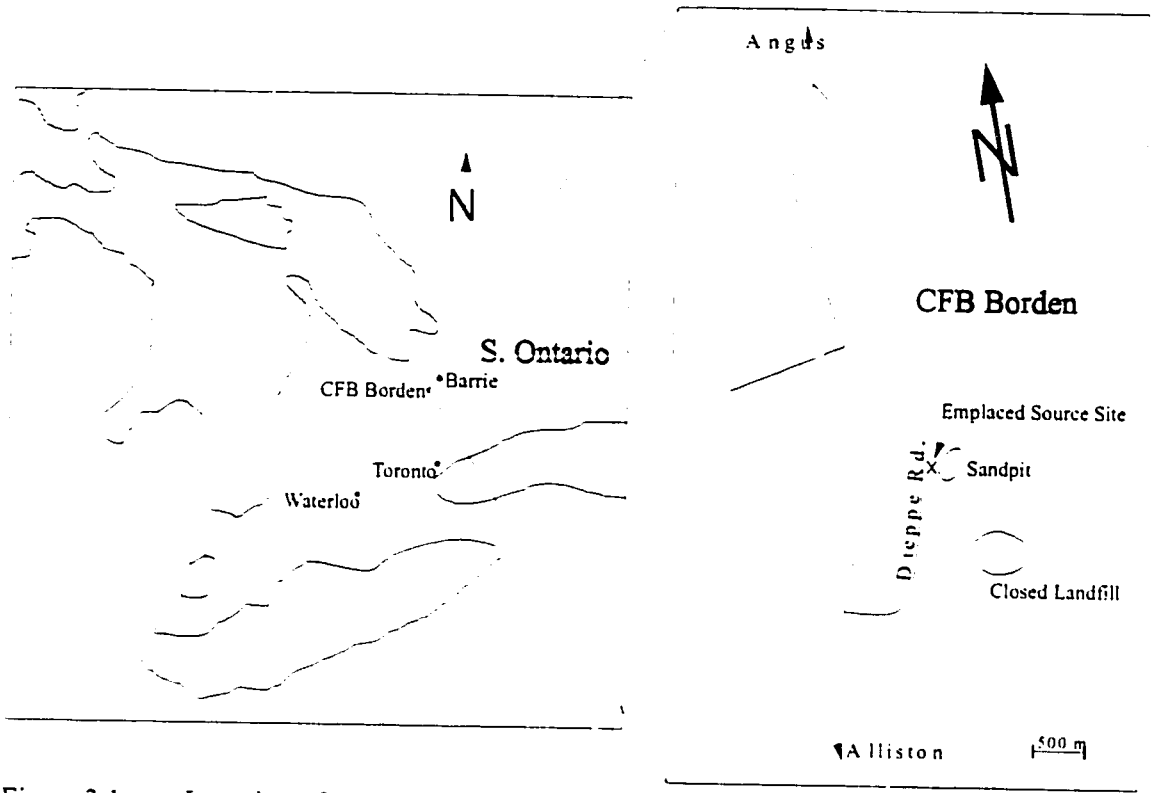

Figure 3.1 Location of experimental site (inset shows emplaced source location within CFB Borden).

The local watershed is dominated by the Pine River on the western limit of Borden which flows to the northeast into the Nottawasaga River. Groundwater flow in the vicinity of the Borden research station is towards the northwest towards the Pine River. Groundwater recharge at the research site is approximately 1.7 mm/month (Solomon et al., 1992); average monthly precipitation for the period 1995 to 1998 was 90 mm/month, above the 30-year climate normal for southwestern Ontario (S.R. Fassnacht, personal communication, 1999).

3.2.1 Characteristics of the Borden upper aquifer

The Borden upper aquifer is an unconfined aquifer consisting of glaciolacustrine sand. The sand is predominantly composed of medium-to-fine grains and, while frequently referred to as a homogenous deposit, contains numerous horizontal bedding features varying in thickness from a few millimetres to a few centimetres (Kueper et al., 1992). The relative homogeneity of the

aquifer and the shallow water table, permitting inexpensive installation of monitoring equipment, have made the Borden aquifer an ideal research site. In the sand pit, immediately to the south of the ES site, the depth to water is usually <0.3 m while at the ES the mean water table is located ~2.6 m below ground surface.

The sand in the upper aquifer is predominantly composed of calcite, quartz, plagioclase, and feldspar minerals with many of the surfaces coated by iron and manganese oxyhydroxides (Ball et al., 1990). The sand has a mean particle density of 2.71 g/cm^3 (dry bulk density of 1.81 g/cm^3), a cation exchange capacity of 0.67 meq/100 g and contains <0.4% clay by mass (Ball et al., 1990). The intraparticle porosity of the Borden sand has been estimated as 1.1-5.3% of the total solids volume (Ball et al., 1990).

Numerous studies have been performed at the Borden research site to characterize the distribution of hydraulic conductivity in the upper aquifer. Rivett et al. (1992) reported a geometric mean hydraulic conductivity of 6.34×10^{-5} m/s, with a range of 1.62×10^{-5} to 3.12×10^{-4} m/s, based on laboratory permeameter measurements of 794 samples from 16 cores taken from the approximate location and elevation of the source. This result was only slightly less than the mean horizontal hydraulic conductivity of 8.2×10^{-5} m/s measured by Sudicky (1986) at a location only 100 m distant. In the same study, Sudicky (1986) estimated the anisotropy ratio to be 1.3 (horizontal to vertical). Turcke and Kueper (1996) performed a similar analysis using cores from a location 60 m to the north-northeast and estimated a mean hydraulic conductivity of 6.97×10^{-5} m/s (642 samples). It should be noted that the permeameter technique employed in each of these studies was likely to underestimate vertical permeability and overestimate horizontal permeability as a result of sample homogenization and repacking (Allen-King et al., 1998). Using a permeameter which measured the hydraulic conductivity of undisturbed cores collected from a location 30 m from those of Sudicky (1986), Tomlinson (1998) reported a mean hydraulic conductivity of 3.3×10^{-5} m/s (576 samples from eleven cores). Consistent with the hypothesized effects of sample homogenization, the mean hydraulic conductivity was lower and the variance higher than those reported in studies using the conventional permeameter

technique. Based on a comparison of the data from Sudicky (1986) and Turcke and Kueper (1996), the distribution of hydraulic conductivity may not be stationary over the short distance between the two study locations (Turcke and Kueper, 1996). A summary of the Borden hydraulic conductivity studies is presented in Table 3.1.

A wide range of porosities for the Borden sand are reported in the literature. In the Borden landfill study conducted during the early 1980's, Macfarlane et al. (1983) measured an average porosity of 0.38 v/v. This estimate was inferred using the saturated and air-dried weight of relatively undisturbed cores and was slightly higher than the value of 0.33 v/v measured during the subsequent Stanford plume experiment (Mackay et al., 1986). Based on subsamples taken from a series of cores within a sheetpile cell, Poulsen and Kueper (1992) reported an average porosity of 0.47 (n=119, σ=0.017). The samples were repacked prior to measurement (Reitsma, personal communication, 1998) and sample disturbance may explain the relatively high estimate. The difference in porosity estimates is of some significance since the Mackay et al. (1986) estimate (θ=0.33 v/v) is widely assumed by other investigators to adequately represent the average porosity throughout the aquifer (e.g., Curtis et al., 1986; Rivett et al., 1992).

Extensive monitoring of magnitude and direction of the hydraulic gradient in the upper aquifer has been performed. Mackay et al. (1986) observed considerable spatial variability in the hydraulic gradient, likely as a result of facilitated recharge and evapotranspiration through the shallow vadose zone in the sand pit. At the ES site, the hydraulic gradient (Figure 3.2) varied seasonally from extremes of 0.34% to 0.64% with an average of 0.51% (n=53, σ=0.07%), while wide variation in the angle of the gradient was also observed (Rivett et al., 1992). The mean direction of the gradient over the monitoring period was N 12.1° W. The peak gradient corresponds to the time of minimum recharge in late winter while the minimum gradient occurs during late summer. Frind et al. (1999) modelled the fluctuation in gradient by fitting a sine function with a yearly period.

In the Stanford plume monitoring field experiment, Freyberg (1986) calculated first moments

Table 3.1 Summary of experimental studies of the distribution and correlation structure of permeability (temperature corrected to 10°C) in the Borden unconfined aquifer.

Parameter		*Source/Measurement method*
Number of samples	576	Tomlinson (1998)
Mean ln(k)	-26.42 m^2 (-5.72 cm/s)	- constant head measurements at 5 cm intervals in undisturbed cores at 20°C
Var. ln(k)	1.11	
Vert. correlation length	0.16 m	
<u>On Section North-South</u>		
Horiz. correlation length	5.57 m	
<u>On Section East-West</u>		
Horiz. correlation length	1.82 m	
Number of samples	642	Turcke and Kueper (1996)
Mean ln(k)	-25.76 m^2 (-4.96 cm/s)	- falling head measurements of 5 cm repacked subsamples at 22°C
Var. ln(k)	0.59	
Horiz. correlation length	4.8 m	
Vert. correlation length	0.16 m	
Number of samples	794	Rivett et al. (1992)
Mean ln(k)	-25.75 m^2 (6.43x10^{-3} cm/s)	- falling head measurements of 5 cm repacked subsamples at 10°C
Range ln(k)	(-31.73 to -24.17 m^2)	
Number of samples	1188	Woodbury and Sudicky (1991)
Mean ln(k)	-25.32 m^2 (-4.62 cm/s)	- reanalysis of data collected by Sudicky (1986)
Var. ln(k)	0.26	
<u>On Section AA'</u>		
Horiz. correlation length	5.1 m	
Vert. correlation length	0.21 m	
<u>On Section BB'</u>		
Horiz. correlation length	8.3 m	
Vert. correlation length	0.34 m	
Number of samples	1279	Sudicky (1986)
Mean ln(k)	-25.33 m^2 (-4.63 cm/s)	- falling head measurements of 5 cm repacked subsamples at 10°C
Var. ln(k	0.38	
Horiz. correlation length	2.8 m	
Vert. correlation length	0.12 m	

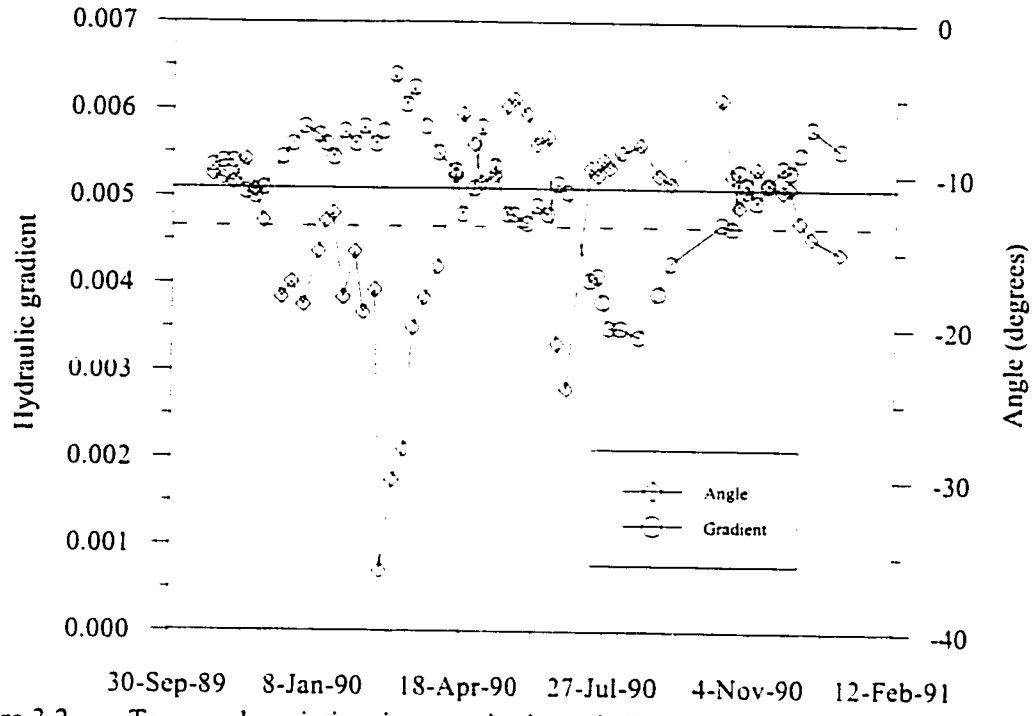

Figure 3.2 Temporal variation in magnitude and direction of hydraulic gradient at the Emplaced Source site (from Rivett et al., 1992).

of the plume monitoring data to estimate a mean groundwater velocity of 9.1 cm/day. The average linear groundwater velocity, estimated with the hydraulic gradient (0.51%), hydraulic conductivity (6.34×10^{-3} cm/day), and porosity (0.33 *v/v*), is 8.5 cm/day (n=53, σ=1.14 cm/day), a result which agrees closely with that measured during the Stanford tracer experiment. In contrast to the relatively high horizontal velocity observed in the Borden aquifer, the average vertical velocity at the water table is only 0.4 m/year (Solomon et al., 1991).

Retardation coefficients for the Borden sand have been measured at both the laboratory and field scales, a summary of which are presented in Table 3.2. Distribution coefficients may be estimated using an empirical correlation with the octanol:water partition coefficient given by Schwarzenbach et al. (1993) as,

$$\log K_{oc} = 0.88 \log K_{ow} - 0.27 \qquad (3.1)$$

and,

$$K_d = K_{oc} foc \tag{3.2}$$

where K_d is the distribution coefficient. The solute retardation factor (R) is (Freeze and Cherry, 1979),

$$R = 1 + \frac{\rho_b K_d}{\theta} \tag{3.3}$$

where ρ_b is the bulk density. Using these equations and typical parameters for the Borden site, retardation factors were estimated using standard values of K_{ow} for TCE and PCE reported by Pankow and Cherry (1996) (Table 3.2).

The retardation estimates in Table 3.2 differ significantly from one another, reflecting differences in experimental conditions and methods. Common laboratory techniques do not allow sufficient time for equilibrium partitioning and tend to underestimate the true partition coefficient (Ball and Roberts, 1991). For example, equilibrium partitioning of PCE to a Borden sand sample may require >20 days (Ball and Roberts, 1991); however, earlier studies used

Table 3.2 Summary of retardation and dispersivity estimates for the Borden unconfined aquifer.

Retardation factor		α_L	α_{TH}	α_{TV}	
TCE	*PCE*	*(m)*	*(m)*	*(m)*	*Source*
1.1	1.4				calculated using Equation 3.3
	3.6±0.3				Curtis et al. (1986)
		0.36	0.04		Freyburg (1986)
	2.7-3.9[a] 2.7-5.9[b]				Roberts et al. (1986), based on a) travel time and b) synoptic sampling
		0.61			Sudicky (1986)
		0.45			Sudicky (1986)
	6				Ball and Roberts (1991)
		0.5	0.05	0	Rajaram and Gelhar (1991)
0.76-1.2	1.2-3.7				Rivett et al. (1991)
		0.30-0.80	0.01		Rivett et al. (1992)

equilibration times as short as five days (Curtis et al., 1986). Field methods of estimating retardation coefficients also have confounding factors. Using 633 days of synoptic sampling data from the Stanford natural gradient tracer test, Roberts et al. (1986) observed gradual increases in the PCE retardation coefficient from 2.7 to 5.9. In this experiment, the observed increase in retardation factor was attributed to the effect of competitive sorption since the PCE plume was not yet separated from the more mobile carbon tetrachloride plume, which suggested that the estimates from later in the experiment were closer to the true single component retardation coefficient. Taken together, these studies suggest that reasonable retardation factors for TCE and PCE would be 1 and 6, respectively.

Various estimates of the magnitude of dispersivity have been made at the Borden field site (Table 3.2). Sudicky et al. (1983) monitored the migration of a chloride tracer pulse over forty days and observed increasing longitudinal dispersivity (α_L) over time to 0.8 m while horizontal transverse dispersivity reached an asymptotic value of 0.03 m. Vertical transverse dispersivity was a weak process attributed primarily to molecular diffusion. Sudicky (1986), Freyburg (1986), and Rajaram and Gelhar (1991) each examined the data set generated by the Stanford tracer experiment. Taken together, these studies are consistent with a longitudinal dispersivity of 0.5 m, a transverse horizontal dispersivity of ~0.05 m, and a negligible transverse vertical dispersivity. Preliminary dispersivity estimates from the ES site are generally consistent with these values of dispersivity, in spite of differences in the design of the experiments. Rivett et al. (1994) used a longitudinal dispersivity of 0.5 m and transverse dispersivity <2 mm to achieve creditable simulated matches to the spatial extent of the source plume with a 2D analytical solution. Rivett et al. (1994) speculated that much of the transverse dispersive behaviour could be attributed to changes in the direction of the gradient, in effect making dispersivity a fitting parameter averaging temporal variations in the boundary conditions as well as the spatial variability of hydraulic properties of the aquifer.

3.2.2 Upper aquifer geochemistry

Background groundwater quality at the ES site was evaluated by Rivett et al. (1992). The upper

aquifer, where the DNAPL source zone is located, is aerobic with a mean dissolved oxygen of 3.6 mg/L. Both sulfate and chloride (<10 mg/L) are present and are associated with a solute plume generated by the closed municipal solid waste landfill 500 m south of the ES site (Macfarlane et al., 1983). The pH of the upper aquifer is slightly alkaline at 7.7, consistent with calcite saturation by the aquifer solids which contain 15.4% calcite by weight (Ball et al., 1990).

Extensive measurements of the organic carbon content of the Borden sand, expressed as a fraction of the dry bulk sand mass (*foc*), have been made by various researchers in the course of both biodegradation and plume retardation studies. Barbaro et al. (1994) measured *foc* contents generally ranging from 0.02-0.05%, with several samples as high as 0.35%, in the upper two metres of the aquifer. These data are consistent with detailed *foc* measurements on a single sand sample taken from the same location with a mean *foc* of 0.021% (n=15, σ=0.006%; Ball et al., 1990). Samples from the ES site area, taken after installation of the source, contained a mean *foc* of 0.035% (n=30, *range*=0.02-0.09%; Rivett et al., 1992). The small differences in *foc* between widely spaced sampling locations imply low spatial variability in natural oxidant demand and retardation coefficients.

3.3 Emplaced source experimental site

3.3.1 Installation of emplaced source

The Emplaced Source, which was installed in October 1989 and used to study the formation and transport of VOC plumes, was used to conduct chemical oxidation field trial reported on in this chapter. An oblong zone of a uniform residual, the initial DNAPL mixture contained 12,540 g PCE, 8,990 g TCE, and 1,450 g chloroform (TCM), resulting in an initial volumetric DNAPL saturation of 5%. Gypsum (~70 kg or 52 g/kg) was added to the source mixture with the purpose of generating a conservative sulfate plume. Following the completion of this study, the source was used in several plume remediation studies, including operation of a pump-and-treat system (Rivett, 1993), installation of a funnel and gate system (Starr and Cherry, 1994) and testing of a field-scale zero-valent iron permeable reactive barrier (O'Hannesin and Gillham, 1992).

The source was installed by excavating to the water table and installing a small sheet pile cell in the excavation. The contaminated sand mixture was packed into a sheet metal form placed in the sheet pile cell. Beneath the form, a steel pan with a ~2 cm lip was placed below the form as a precaution against mobile DNAPL penetrating deeper into the aquifer. Volatilization was minimized by covering the top of the source with a plastic sheet. The cell was backfilled to the top of the form, the form and piling removed, and the remainder of the excavation backfilled.

The limitations of the source emplacement methodology used in 1989 resulted in some significant differences from real field sites. First, the excavation and backfill method used to get the source to depth likely resulted in a different permeability of the sand within the sheetpile zone relative to the surrounding undisturbed aquifer. This zone is likely to have a higher mean horizontal and vertical permeability as a result of homogenization and insufficient compaction of the fill material. The source placement method may also have resulted in permeability changes within the source. Clearly, the presence of the non-aqueous phase would reduce the water phase permeability. In a modelling study of plume transport and DNAPL dissolution, Guiguer (1993) assumed that the initial permeability of the source was 42% of the bulk aquifer permeability. This estimate was based on permeameter measurements of a source zone core and another 1-m down-gradient. Later modelling efforts suggested that the permeability reduction within the source zone was greater than thought by Guiguer (1992). Based on modelling results calibrated using VOC monitoring data from the 1-m fence, Frind et al. (1999) estimated that the hydraulic conductivity of the source may be 10 to 20 times lower than the bulk aquifer conductivity. While the difference between the measured and calibrated permeability was not specifically examined by Frind et al. (1999), it may have resulted from geochemical interactions between the calcite saturated porewater and the solid phase gypsum added to the source zone. As the gypsum dissolved, concurrent calcite precipitation would be necessary to maintain equilibrium molarity of Ca^{+2} (common ion effect), potentially depositing a calcite front on the up-gradient face of the source. The formation of a low conductivity front would decrease the apparent horizontal conductivity, a result consistent the decrease in conductivity simulated by

Frind et al. (1999). It is unlikely that this front was sampled by the vertical cores reported by Guiguer (1992) or in the current study. No direct evidence was collected during the current study supporting this scenario; however, a stainless steel drive-point installed before 1992 and removed from the source in 1998 was covered with a coating of a grey mineral phase, which was tentatively identified as calcite. Based on an average plume SO_4^- concentration of 510 mg/L (Rivett et al., 1992) and assuming uniform flow and stoichiometric precipitation of calcite in exchange for sulfate, ~160 kg of calcite (ρ=2.83 g/cm^3) may have precipitated, an amount equivalent to ~23% of the total pore volume of the source.

A further limitation was the method used to form the residual mixture. The mechanical DNAPL and soil mixing process would result in a residual consisting of uniformly small blobs while a residual generated using imbibition and drainage would result in a wider distribution of blob sizes with varying interfacial areas (Imhoff et al., 1994). Mixing increased the rate of dissolution by creating a DNAPL residual with a comparably high specific surface area, suggesting that the time required for complete mass removal would be short relative to a realistic release containing the same mass.

3.3.2 Pre-oxidation solvent mass estimate

A multilevel piezometer cross section was installed 1-m down-gradient from the source zone (hereafter referred to as the 1-m fence). The experimental work by Rivett et al. (1992) included detailed measurements of solvent mass loading crossing the 1-m fence on thirty-two instances over 1,029 days. Calculated solvent masses remaining after 1,029 days of intensive plume monitoring indicated that 69% of the total mass remained within the ES (Feenstra, 1997).

Frind et al. (1999) completed a rigorous examination of source removal under natural gradient conditions using the ES monitoring data to calibrate a three-dimensional flow and transport model. Frind et al. (1999) determined that 72% of the source mass remained after 1,029 days, a figure which agreed closely with the previous estimate by Feenstra (1997).

The modelling results of Frind et al. (1999) were used to estimate the source mass at the beginning of the oxidation field trial (following 2,400 days of natural gradient source flushing). Their results suggested that the ES contained 9,030 g PCE and 1,620 g TCE at the start of the oxidant flush while chloroform had been completely removed due to its high aqueous solubility.

Water samples for solvent analysis were collected by the Department of Earth Science in 1994 from within the source zone. Vertical concentration profiles of chloroform, TCE, and PCE were compared to their effective solubilities calculated using Raoult's Law for each component (Figure 3.3). These near-solubility data support the modelling results of Frind et al. (1999) whose transport simulations predicted equilibrium solvent dissolution within the source zone. The low concentrations and reversal of the TCE to PCE ratio at the upper and lower edges may reflect preferential depletion of solvent mass at the upper and lower edges of the source, and suggest that the composition of the source was heterogeneous prior to the oxidant flush.

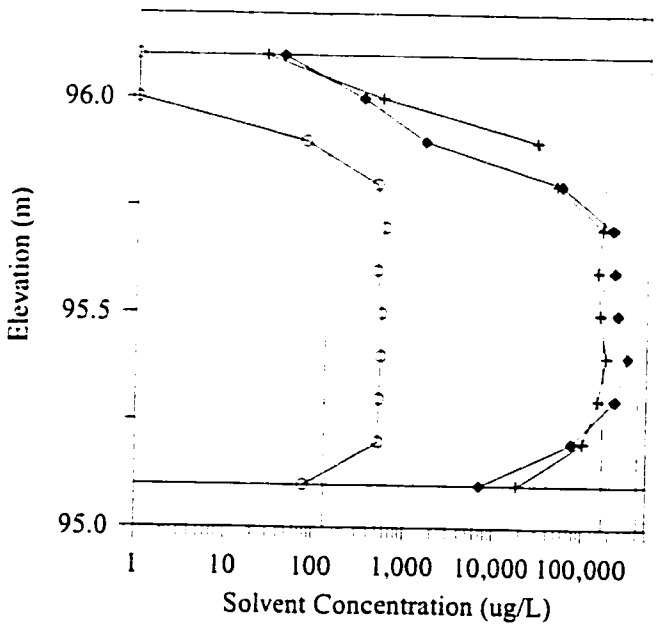

Figure 3.3 Vertical profiles of TCM (○), TCE (◆), and PCE (✚) collected from the ES in October 1994. Horizontal lines indicate the vertical extent of the source. Dashed lines show the effective solubility calculated for each component.

3.4 Design and operation of an in situ oxidation treatment system

The program of field work completed as part of this thesis included:

- characterization of the VOC groundwater plume and completion of a tracer test to evaluate groundwater flow in the treatment zone during the period of November 1995 to January 1996;

- completions of an oxidant flush of the source zone lasting from May 1996 to September 1997 with extraction of residual oxidant from the treatment zone continuing until March 1998;

- repetition of the plume characterization measurements and tracer testing conducted before the oxidant flush during the period of August 1998 to October 1998; and

- the collection of soil cores during excavation of the source in October 1998.

In 1995, a groundwater recirculation system was constructed to provide hydraulic control of the treatment zone, which is the portion of the aquifer, including the contaminated soil, flushed with oxidant. The recirculation system, which was contained in a heated building, consisted of in-ground and above-ground components. Eleven wells were used to inject and extract concentrated oxidant solution from the treatment zone while multilevel piezometers installed during previous investigations were used to monitor the progress of oxidant flush and characterize the VOC plume. The above-ground component of the treatment system included equipment for continuously extracting effluent solution containing reaction products and residual oxidant solution, removing oxidizable contaminants and particles, dosing with additional oxidant, and re-injecting a concentrated oxidant solution. Additional batch processes were used to treat waste oxidant solution.

Six injection and three extraction wells were installed using a direct push technique. The well locations (Figure 3.4) were based on the results of a preliminary flow model which suggested

that this well geometry and the chosen flow rates would increase groundwater velocities in the treatment zone while containing the injected oxidant solution. The recirculation wells were constructed of 5.08 cm (2 in) ID PVC casing with 1.22 m (4 ft) #10 slot screens (Timco, Prairie du Sac, WI). Injection wells were spaced ~0.35 m apart, spanning a total width of 1.95 m, while the vertical extent of screens overlapped the top and bottom of the source zone by ~0.1 m. Two additional extraction wells (BWU and BWL) were installed in August 1996 when it became apparent that oxidant was migrating below the existing extraction wells.

Seven multilevels in the 1-m fence, which were oriented at an approximate right angle to the mean direction of groundwater flow, were used to measure the solvent loading from the source, and to monitor the progress of the oxidant flush (Figure 3.4). The multilevel sample lines were constructed of $^{1}/_{16}$ in ID Teflon tubing with a nylon mesh screen fastened over the bottom end. Fourteen sample lines were attached to a single centre stem constructed of ½ in PVC. The small tubing diameter permitted collection of small sample volumes, which minimized flow disturbance and the volume of purge waste generated during sampling. Multilevel sampling points were spaced ~0.5 m horizontally and 0.2 m vertically.

In the above-ground component of the treatment system, several processes were constructed to recycle and treat excess oxidant solution. Oxidant recycling reduced the amount of solid permanganate necessary to maintain a constant concentration in the injected solution and to minimize the volume of effluent requiring treatment. The waste oxidant treatment system was used to treat the small volume of excess oxidant solution generated during the oxidant flush and to treat the entire effluent flow after the oxidant flush. The above-ground recycling system consisted of a bed filter, equalization tank, oxidant storage column, oxidant dosing pump, and pre-injection filter (Figure 3.5). The bed filter (150 mm of greensand media on a perforated support bed) removed sediment and precipitated particles from the extracted effluent. At the maximum system flow rate, the equalization tank provided a residence time of two days, which was sufficient to degrade any dissolved phase solvent or other oxidizable material in the effluent and settle MnO_2(s) particles. In addition to equalizing the oxidant and chloride concentrations

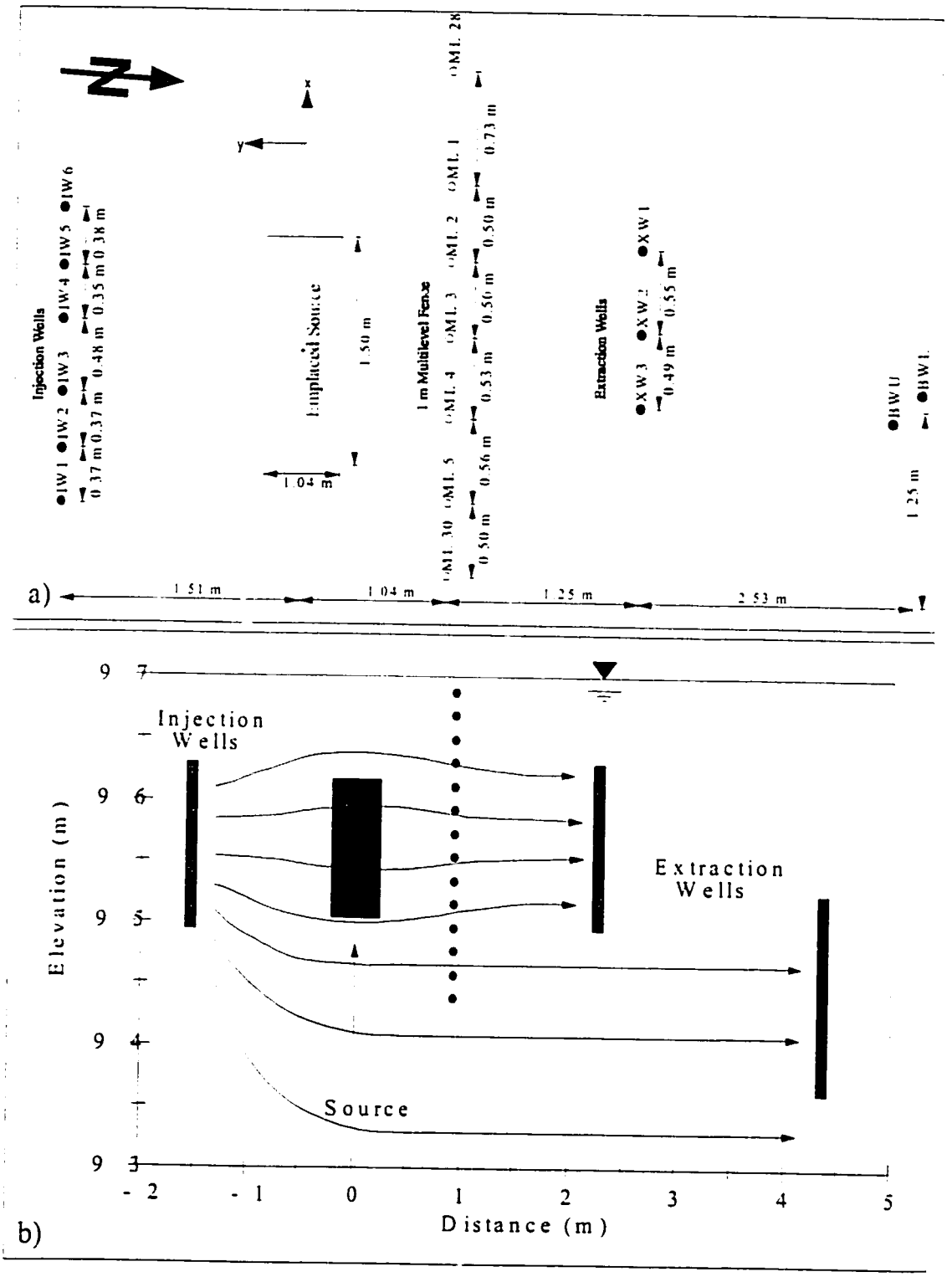

Figure 3.4 Plan (a) and profile (b) drawings of experimental site.

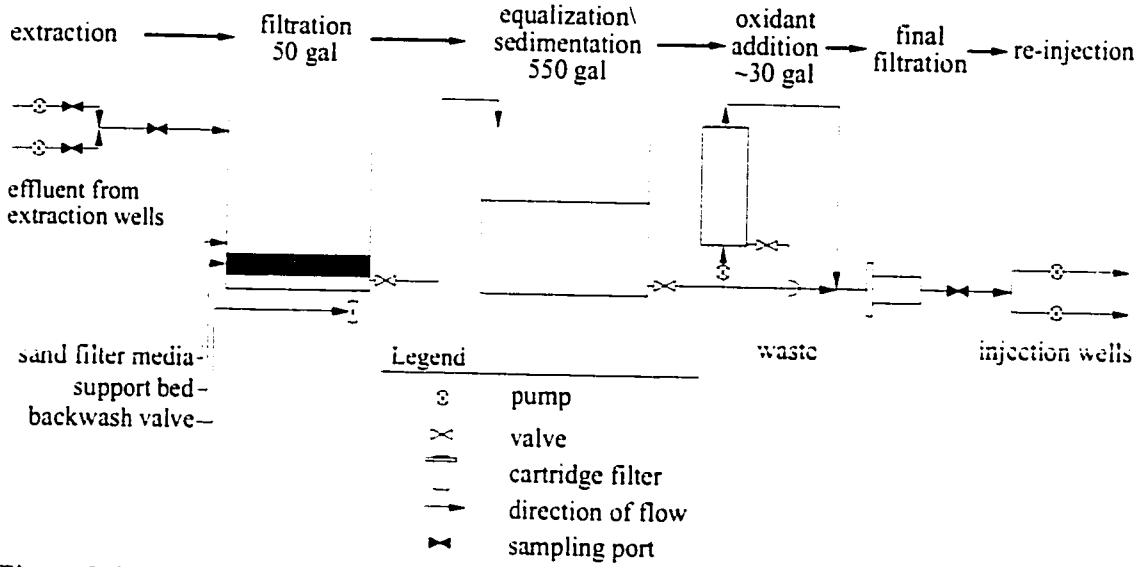

Figure 3.5 Schematic of above-ground apparatus for oxidant dosing and solids removal from recycled oxidant solution.

before injection, the tank also provided bulk fluid storage.

Oxidant dosing used a method similar to that employed by Truax (1993). The oxidant storage column contained flowing-grade solid $KMnO_4$ (Quadra Chemical, Burlington, ON). The dosing pump diverted a portion of the flow from the injection header through the storage column; as this solution passed through the column it became saturated with permanganate (~42 g/L) and was remixed back into the injection header. The flow rate of dosing pump was used to control the oxidant concentration in the feed solution and was manually set based on field measurements of the injected oxidant concentration. Before injection into the individual wells, a standard residential water cartridge filter (Cuno Inc., Meridian, CT) was used to remove particles >2 μm. Flow into the injection wells and from the extraction wells was controlled using 6-600 rpm drives mounted with either peristaltic or diaphragm pump heads.

Oxidant treatment was a comparatively straightforward process but required a high level of operating effort. Waste oxidant solution was treated in batches by reducing the oxidant with granular sodium thiosulphate (VWR Canlab, Mississauga, ON); the solid $MnO_2(s)$ flocs

resulting from the reaction were settled in a 500 gallon HDPE storage tank and the supernate discharged through a bed filter. The thickened sludge was transferred to a second bed filter and dewatered by gravity drainage. The dewatered MnO_2(s) sludge was packed into 5 gallon plastic containers and disposed of by the University of Waterloo (Chemical Waste Pickup, Department of Chemistry).

Four phases of field work were completed at the ES site over the three-year duration of this Borden pilot test (1995-1998). The initial phase of field work examined the characteristics of the solvent plume and the performance of the injection/extraction system. Under natural gradient conditions, a snapshot of samples was collected from the 1-m fence and used to estimate the plume load and peak concentration. Following this, the recirculation system was used to inject a tracer pulse and continuously flush the source with solvent-free groundwater. Three extraction (XW1, XW2, and XW3) and all six injection wells were used. The water supply was obtained from a 5.08 cm (2 in) PVC well located in the sandpit 50 m to the south. Bromide was used as a tracer to avoid interference with high background chloride concentrations. During the tracer test, VOC concentrations in the total extraction flow were monitored to provide a second measurement of plume load. In addition, bromide breakthrough curves in nine multilevel sample points were collected; however, bromide data at the extraction wells were not obtained and estimates of tracer mass recovery or average residence time in the treatment zone could not be determined from this tracer test.

After the tracer test, a concentrated $KMnO_4$ solution was flushed though the source zone. Permanganate and chloride concentrations in the nine multilevels, the extraction wells, and the injection feed were monitored. In addition, periodic sets of samples were collected from multilevels in the 1-m fence and from within the source using the Waterloo profiler (Pitkin et al., 1999) to ascertain the extent of oxidant migration within the treatment zone and to characterize the chloride signature produced by oxidation of the source zone. After the signature was no longer evident (484 days), oxidant injection was terminated and the extraction wells used to remove the oxidant solution remaining in the treatment zone.

After the oxidant flush, measurements of plume load and tracer testing were repeated using the same procedure as in the pre-oxidant flush testing. The tracer test characterized the solvent plume loading from the source zone, evaluated the recovery of the recirculation system, and provided an estimate of the residence time in the treatment zone. The source water used during this test was free of chlorinated solvents and bromide. A tracer pulse was injected into the recirculation system over 4.8 days and then bromide and solvent concentrations were monitored for ninety days in the effluent. The recirculation system was then turned off to form an aqueous phase plume under natural gradient conditions, and a final 1-m fence VOC snapshot was collected.

The final phase of work, completed during the period October 26-30, 1998, assessed the quantity and distribution of VOCs and MnO_2(s) within the source zone. The mass of solvent remaining measured the effectiveness of the treatment process while the MnO_2(s) data was used to infer the effect of the oxidant on the aquifer. Twenty-two 1-m cores were collected from the source zone and subsampled for solvent and MnO_2(s) analyses while permeability tests were performed on two cores.

All data collected during the field experiment are summarized in Appendix B.

3.5 Monitoring and analytical methods

3.5.1 Sampling

With the exception of $KMnO_4$, samples collected at the ES site were transported to the University of Waterloo (Civil Engineering Water Quality Laboratory) and refrigerated at 4°C until analysis for chloride, bromide, or VOC concentrations. Samples for VOC analyses were collected in 40 mL VOA vials and transported in a cooler with icepacks. In the case of profiler samples containing both oxidant and solvent, the oxidation reaction was quenched by adding sodium thiosulphate to each sample vial immediately after sample collection. Due to the reactivity of the oxidant, permanganate analyses were performed on site. Occasional field and

rinse blanks (deionized water) were collected to ensure data reliability.

Injection and extraction wells

Two procedures were used to collect samples from the various wells. Individual extraction wells were sampled using a vacuum manifold system equipped with an electric timer to allow automatic sample collection between site visits. The manifold header was depressurized by ~10 psi (69 kPa) with a vacuum pump. Alternatively, samples were collected from the sampling ports shown in Figure 3.5.

Multilevel piezometer sampling

Multilevels in the 1-m fence were sampled using 125 mL Erlenmeyer flasks connected to the vacuum manifold system. Up to fourteen multilevels could be simultaneously sampled using this technique; however, this method were not used for VOC analysis given the likelihood of sample VOCs being stripped from the samples into the head space. Samples for VOC analysis were collected using the portable vacuum manifold system described by Mackay et al. (1986). Locations of the multilevel sampler points relative to the vertical extent of the source zone are shown in Figure 3.6.

3.5.2 Analytical methods

Perchloroethylene and trichloroethylene

Perchloroethylene, trichloroethylene, and chloroform measurements were performed using an HP 5890 II gas chromatograph (30 m x 0.53 mm ID HP 624 fused silica capillary column) equipped with an HP 7673 autosampler. Flame ionization and electron capture detectors were used in conjunction to analyse VOC concentrations ranging from the aqueous solubility limit to the method detection limit of ~1-ppb. Samples were prepared using the procedure presented in Part 6232 (Trihalomethanes) of Standard Methods (1993). Aqueous samples were extracted with hexane with a solvent/sample extraction ratio of 1 to 6. Samples were shaken vigourously by hand for ~1-min and an aliquot of the hexane was transferred to an autosampler vial with a disposable Pasteur pipette. Concentrations were determined by external standard calibration

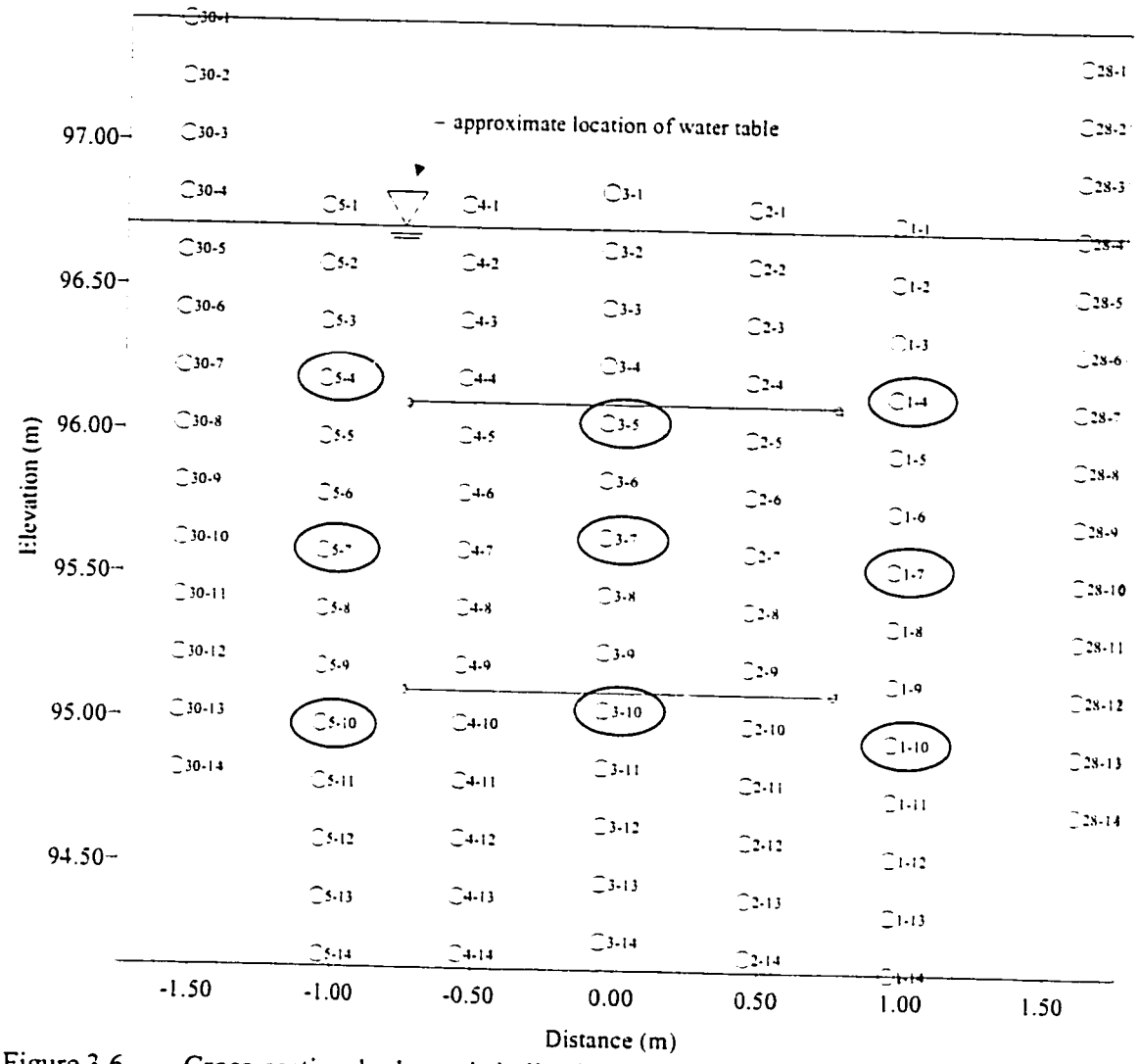

Figure 3.6 Cross-sectional schematic indicating location of multilevel samplers relative to vertical extent of source zone (viewpoint looking up-gradient). The nine highlighted sample locations were used for regular monitoring.

with at least three points.

Concentrations of VOCs were also determined in soil samples from the source. Soil samples were analysed similarly to water samples except that the contaminants were extracted from the bulk porous media with 5 mL of methanol at 75°C for 24 hours and an aliquot of the methanol was analysed. The same procedure was used by Poulsen and Kueper (1992) who reported

quantitative recovery of PCE from synthetic samples containing 1-5% PCE by bulk volume. Sawhney et al. (1988), in an earlier study on the analysis of pesticides in agricultural soils, achieved 95% recovery of adsorbed 1,2-dibromoethane (EDB) from field samples with this extraction procedure and suggested that the procedure would be appropriate for VOCs, like TCE and PCE, that have a hydrophobicity similar to that of EDB. These good recoveries achieved in these studies suggested that the method used for soil analysis would achieve high recovery of sorbed phase halogens.

Chloride and bromide

Analysis of chloride and bromide was completed by ion chromatography, using a method based on Part 4110B (Ion Chromatography with Chemical Suppression of Eluent Conductivity) in Standard Methods (1993). A Dionex DX-300 ion chromatograph, equipped with a SpectraSYSTEM AS3500 autosampler and a conductivity detector, was used with 1.7 mM $NaHCO_3$ and 1.8 mM Na_2CO_3 eluent at a flow of 2 mL/min and 2.5 mM H_2SO_4 regenerant solution at 5 mL/min. To avoid damaging the chromatographic column, residual oxidant in the samples was removed by adding analytical grade sodium thiosulphate (VWR Canlab, Mississauga, ON) to the sample vial to reduce the permanganate to $MnO_2(s)$. Once the solids settled, an aliquot of the supernatant was removed to an autosampler vial using a disposable Pasteur pipette. External calibration standards for chloride and bromide with concentrations ranging from 1 to 100 mg/L were prepared using analytical grade reagents. The conductivity detector provided a slightly non-linear response over this concentration range and a piecewise calibration curve was constructed of two linear regions within the detector response (1-10 mg/L and 10-100 mg/L). In all cases, calibrations were linear functions with r-squared values greater than 0.98. Samples with a concentration above 100 mg/L were diluted. Control standards and blanks were run to confirm calibration and to check for detector drift at a frequency of at least one in twenty-five but little drift in calibration either during a run or between calibrations was observed. The method detection limit for bromide was 0.3 mg/L while the detection limit for chloride was 0.5 mg/L.

$KMnO_4$

The concentration of $KMnO_4$ was spectrophotometrically determined using a Spectronic 20D spectrophotometer set at 525 nm. This wavelength was the most sensitive observed using a UV/VIS scanning spectrophotometer and corresponded to a MnO_4^- peak at 526 nm identified by Stewart (1973). A stock standard, standardized using titration of oxalate (described Method 311B in Standard Methods, 16th ed., 1985) and stored in a brown glass bottle, was prepared by mixing predried reagent grade potassium permanganate in MilliQ water, boiling, and filtering the solution. Calibration with single-use working standards was performed over a concentration range of 4-100 mg/L and was linear on a plot of -log[*T*] (absorption) against concentration. Measurements were only performed over the range 4-40 mg/L.

Total Manganese

Determination of the bulk manganese concentration of soil samples was completed using acid digestion and analysis by inductively coupled plasma (ICP) emission spectroscopy. Samples were stored in precleaned and preweighed 40 mL EPA VOA vials. Samples were dried using a heat lamp in a fume hood (~85 °C) for twelve hours, reweighed and digested using 2 mL of 50% HNO_3 plus 10 mL of 50% HCl over one hour at ~100°C (Standard Method 3030F, Nitric Acid-Hydrochloric Acid Digestion). Following digestion, the samples were diluted with deionized water for a total sample volume of 35 mL.

During analysis, separate analytical lines were used for high sensitivity (20-500 mg/L Mn) and low sensitivity (up to 20 mg/L Mn) calibration curves. Eight calibration standards were run in triplicate, ranging from 1 to 500 mg/L Mn. The method detection limit was determined to be 0.01 mg/L Mn. Every twenty samples, triplicate analysis of a method blank and check standard was performed. A steady decrease in response over time was observed in the ICP analytical data and was corrected using the check standards. After correction the check standards were accurate within 1% of their known concentrations.

Volumetric flow rate

Flow rates from each pump and the total extraction flow were measured volumetrically with a graduated cylinder and stop watch. The measurement error, which was estimated using the resolution of the cylinder and stopwatch, was less than 2%. Average flow between successive sampling events was determined by measuring the initial rate, adjusting the pump controller to the desired flow rate, and then remeasuring the flow rate.

3.6 Pre-oxidant flush testing

3.6.1 Summary of system operation

Under natural gradient conditions, a complete suite of samples was taken from the multilevel fence and analysed for TCE and PCE. Following sample collection, the recirculation system was operated for two weeks to establish a steady-state flow field within the treatment zone. During this phase of the tracer test, samples were collected from the total extraction flow and analysed for VOCs. A reservoir (2500 L capacity) for the injection feed was periodically filled from the up-gradient supply well. Samples from the supply well were analysed for inorganic constituents and were found to contain chloride as high as 6 mg/L but no bromide. The extraction flow, which was not recycled, was treated using serially-connected activated carbon canisters (Stanchem Inc., Mississauga, ON), collected in a reservoir, and then periodically discharged. Following injection of the tracer pulse, the recirculation system was used to recycle the effluent since the onset of extremely cold weather precluded the use of the supply well.

3.6.2 Extraction system tracer testing

A twenty-one hour tracer pulse of bromide (400 mg/L Br^-) was added into the injection wells November 29, 1995, at an average total flow rate of 357±13 mL/min equally divided between the six injection wells (IW1 to IW6). The average total extraction flow rate, equally divided between XW1, XW2, and XW3, was 391±8 mL/min (Figure 3.7).

The tracer solution was prepared by adding pre-weighed portions (130 g each) of sodium bromide (NaBr) to two 50 gal (450 L) polyethylene barrels. The injected mass of NaBr

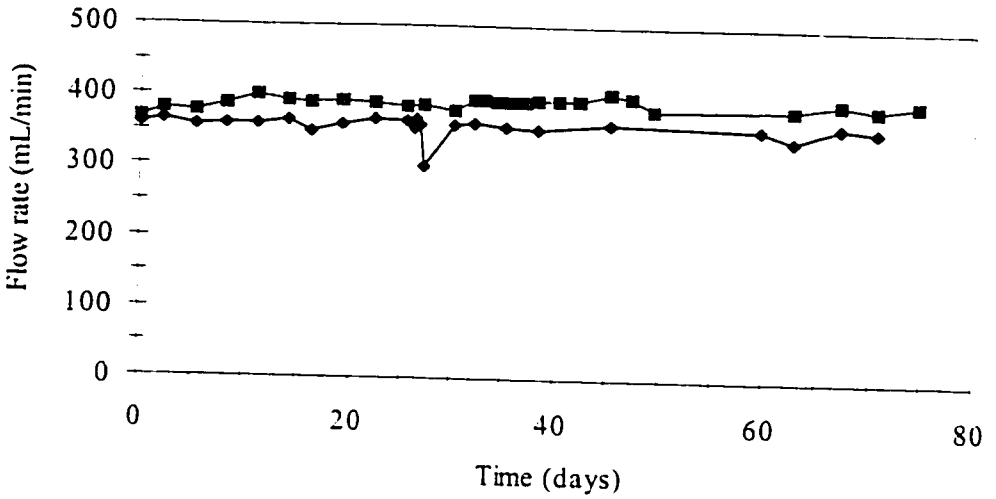

Figure 3.7 Summary of total extraction (■) and injection feed (◆)flow rates from the pre-oxidation tracer test.

corresponded to an equivalent mass of 178.6 g of the bromide anion. Samples were collected at a variable frequency from the nine multilevel sample points highlighted on Figure 3.6 for bromide analysis. Tracer breakthrough curves at each sample point are presented in Figure 3.8.

Average tracer travel times from the injection wells to each of the sampling locations were calculated as the elapsed time between injection of the centre of mass of the input tracer pulse to the centre of mass of the breakthrough curve observed at each monitoring point (Roberts et al., 1986). Travel times were calculated using,

$$t_c = \sum_{i=0}^{n} (C_i/C_0)t_i \Big/ \sum_{i=0}^{n} (C_i/C_0) \qquad (3.4)$$

where t_c is the travel time of the centroid, C_0 is the input tracer concentration, and C_i is the tracer concentration at time t_i (note that t_0 occurs at the midpoint of the injected tracer pulse). The tracer test data were consistent with the presumed decrease in permeability of the source zone.

The calculated average travel times (Table 3.3) suggested that the faster groundwater velocities occurred below and towards the east side of the source. The faster travel times to the sampling

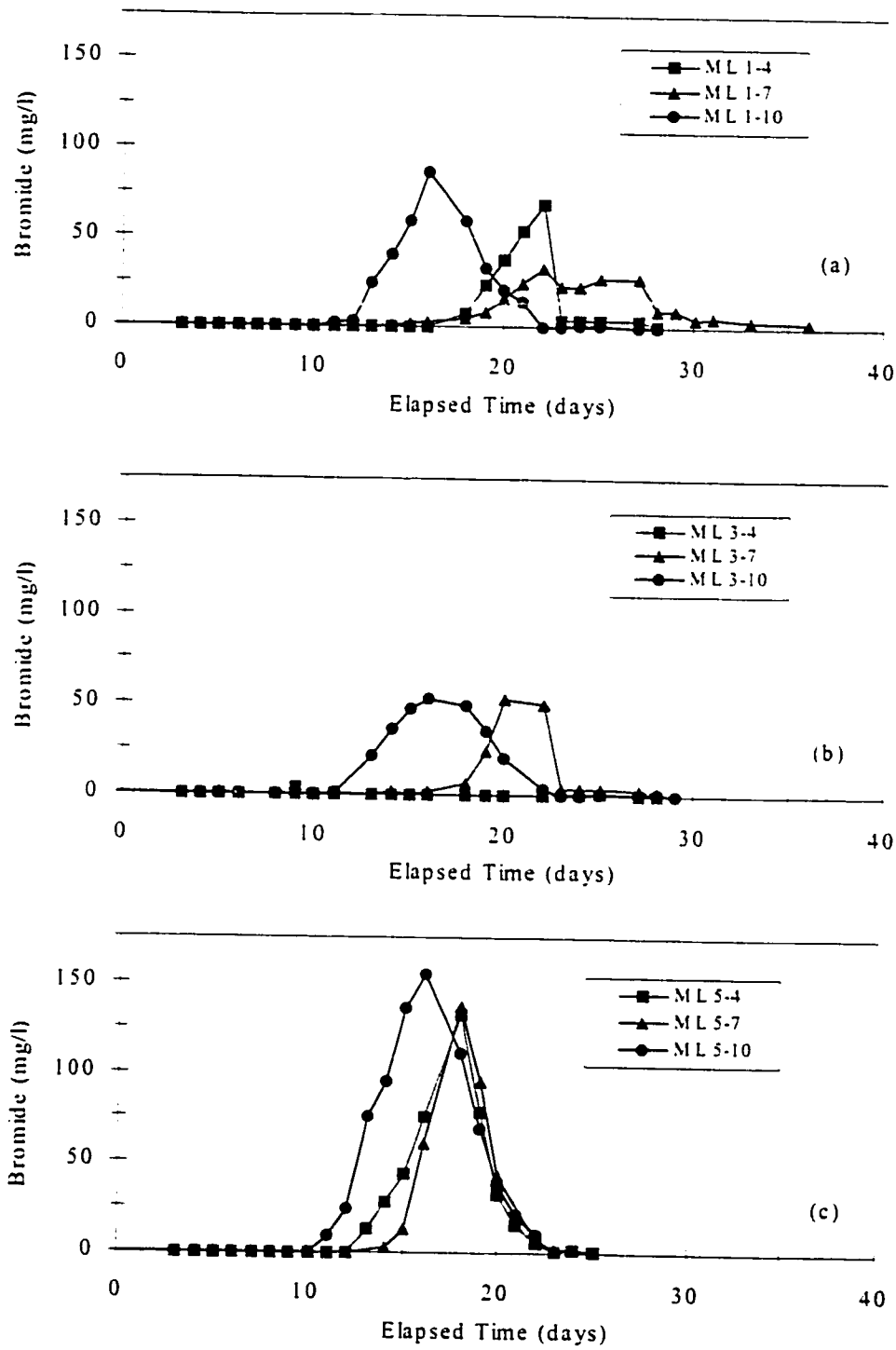

Figure 3.8 Tracer breakthrough profiles in a) ML1, b) ML3, and c) ML5 during the pre-oxidation tracer test (C_0=400 mg/L). Sampling locations are shown in Figure 3.6.

points located below the source were consistent with a portion of the tracer pulse migrating through the more permeable aquifer below and to the side of the less permeable source zone on route to these multilevel points.

Table 3.3 Travel times (days) for tracer pulse centroids monitored at the 1-m fence (see Figure 3.6 for locations relative to source).

Multilevel ID	ML1	ML3	ML5
Point 4	21.2	-	17.5
Point 7	24	20.8	18.2
Point 10	16.5	16.6	16.1

The mean travel times to each multilevel sampling point corresponded to an average groundwater velocity of 13 cm/day (mean travel time of 18.9 days) between the injection wells and the 1-m fence. This estimate should be considered to be the minimum velocity since the flow field between the injection wells and 1-m fence was non-uniform due to heterogeneity, the influence of the hydraulic gradient, and forced-gradient groundwater flow. In comparison to the mean ambient groundwater velocity of 8.5 cm/day calculated in Section 3.2.1, the forced-gradient system employed in this study resulted in a 53% increase in the average groundwater velocity within the treatment zone.

The tracer data suggested that the injected tracer pulse was effectively delivered to the source zone. With the exception of the sampling point positioned just above the source zone (ML3-4), tracer pulses were observed on all sides of the source zone, confirming that the injection wells spanned a sufficient width to flush the source and that the injected tracer solution moved through the treatment zone towards the source.

3.6.3 Solvent plume loading

Multilevel snapshot plume loading

The total advective-dispersive aqueous phase mass flux of the solvent plume from the source zone is given by,

$$J_i = q_i C - \theta D_{ij} \frac{\partial C}{\partial x_i} \tag{3.5}$$

where q_i is the component of the Darcy flux [L T^{-1}], C is concentration [M L^3], θ is the porosity, and D_{ij} is the dispersion coefficient [L^2 T) (note that J_T has units of [M T^{-1} L^{-2}]). The plume loading ($L=JA$, where A is the cross-sectional area), or the integrated solute mass flux over a finite xz plane, was estimated by assuming uniform groundwater flow normal to the plane such that the total flux is given by,

$$J_y = q_y C - \theta D_{yx} \frac{\partial C}{\partial x} - \theta D_{yy} \frac{\partial C}{\partial y} - \theta D_{yz} \frac{\partial C}{\partial z} \tag{3.6}$$

Neglecting the dispersive flux components, a reasonable assumption considering the comparatively large advective flux, and integrating the spatial distribution of the advective mass flux over the xz plane (at y = 1.04 m, the location of the 1-m fence), the plume load was given by,

$$L = \int_{-z_0}^{+z_0} \int_{-x_0}^{+x_0} J_y \, dx dz = q_y \int_{-z_0}^{+z_0} \int_{-x_0}^{+x_0} C(x,z) dx dz \tag{3.7}$$

In the absence of specific hydraulic monitoring data, the average hydraulic gradient and conductivity were used to estimate the Darcy flux normal to the 1-m fence.

Prior the start of the tracer test described in the previous section, the plume's solvent load under natural gradient flow was determined with Equation 3.7 by collecting a snapshot of samples from the 1-m fence (Figure 3.9). The peak concentrations of TCE and PCE in the 1-m fence samples were 142 mg/L and 61 mg/L, respectively. The TCE plume loading was estimated to be 861 mg/day while the PCE loading was 880 mg/day. The plume snapshots were centred on the west side of the source, consistent with the mean gradient slightly to the north-west. The high TCE and PCE concentrations were generally consistent with near-equilibrium dissolution

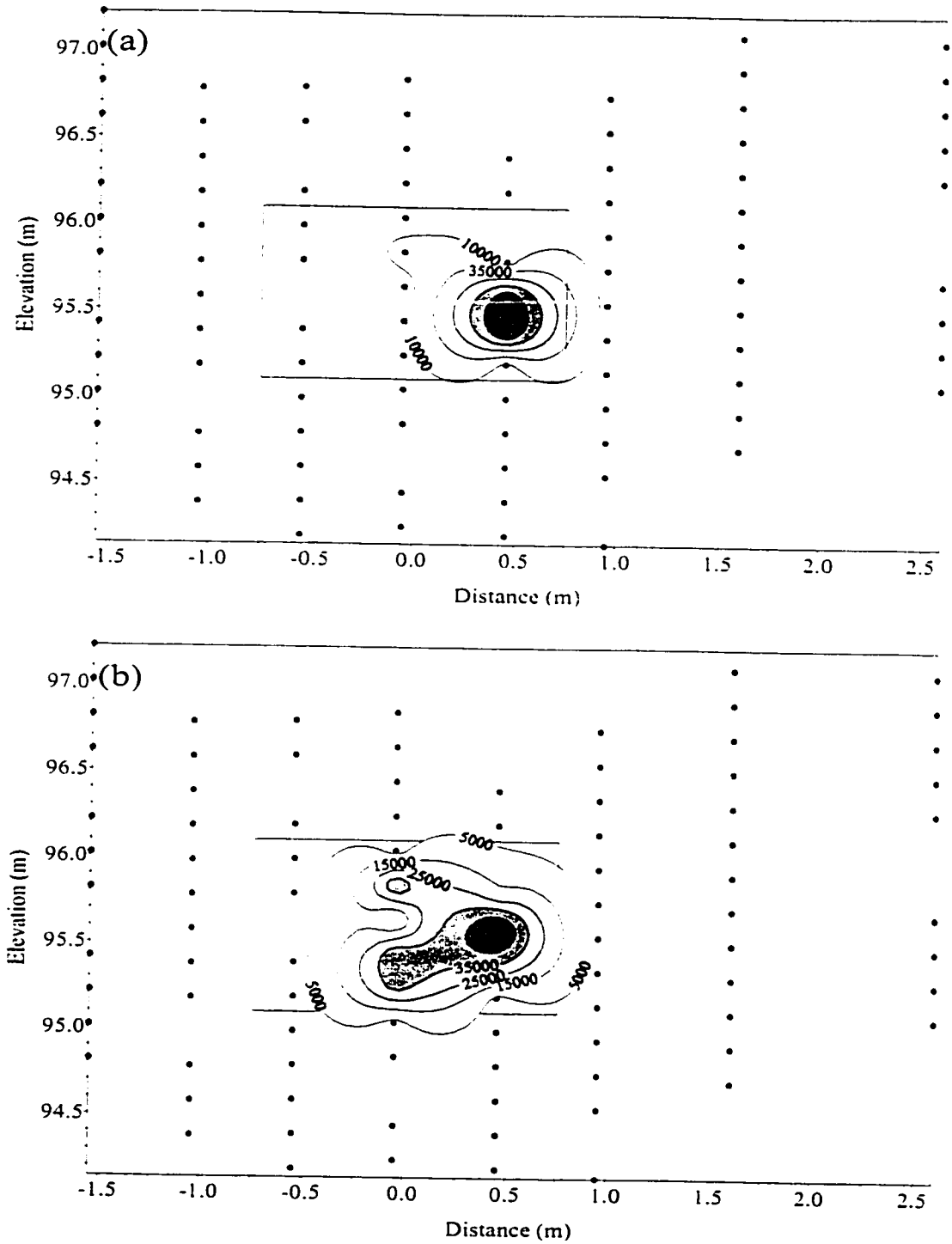

Figure 3.9 Pre-oxidant flush snapshot of (a) TCE and (b) PCE (contours in µg/L) collected from the 1-m fence in October 1995 (points indicate sample locations shown in Figure 3.6).

of the non-aqueous phase in the source.

Extraction system solvent loading

The solvent loading in the total extraction flow during the tracer tests was calculated as,

$$L = \sum_{i=1}^{n} C_i Q_i \Big/ n \tag{3.8}$$

where Q_i is the total extraction flow at time i, and n is the number of measurements. The initial effluent VOC concentrations were relatively high, indicating that initially the effluent was from the core of the VOC plume. As groundwater from the background aquifer entered the extraction wells, effluent TCE and PCE concentrations stabilized at 4.8 and 4.6 mg/L (Figure 3.10). The mass loads for TCE and PCE in the extraction system effluent were 2,099 mg/day and 2,218 mg/day, respectively. The total solvent concentration was stoichiometrically equivalent to 6.5 mg/L of chloride or a total chloride loading of 3,585 mg/day.

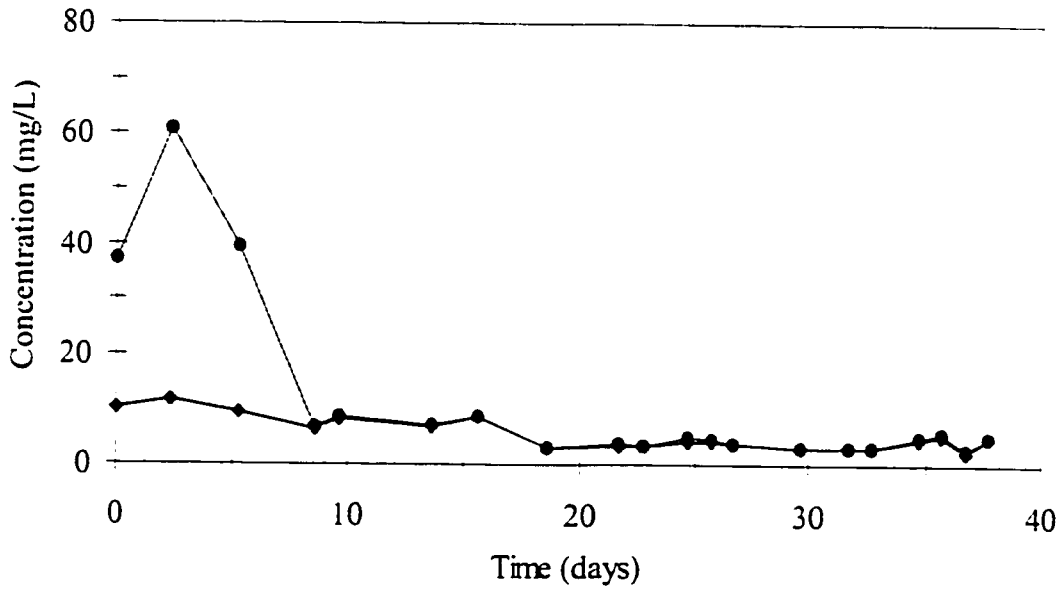

Figure 3.10 Concentration of TCE (●) and PCE (◆) in the total extraction flow during the pre-oxidation tracer testing.

Using a simplified calculation procedure based on Raoult's Law, the molar concentration ratio of the DNAPL constituents in the aqueous phase were calculated. Effective solubilities were estimated using the solubility data employed by Frind et al. (1999). Assuming that the molar concentration ratio of TCE and PCE in the total extraction flow represented the ratio of their effective solubilities, the estimated initial mole ratio of PCE to TCE in the source zone DNAPL mixture at the start of the oxidant flush in 1996 was 4.0, which agreed closely with the mole ratio of 4.5 calculated using the simulated source depletion data reported by Frind et al. (1999).

3.7 Oxidant flushing

3.7.1 Summary of system operation

The potassium permanganate (the "oxidant") flush was initiated May 14, 1996 and operated continuously using a total of 892 kg of $KMnO_4$ over 484 days. The intended oxidant concentration in the feed solution was 10 g/L; however, this was difficult to control and considerable variability occurred. Sources of variation included blockage of the oxidant storage column, depletion of the solid permanganate stored in the column, and the low frequency of site visits to reset the dosing pump rate. In response to early monitoring results suggesting that poor oxidant recovery was occurring, the injection and extraction flow rates were lowered and additional recovery wells installed (BWU and BWL) to minimize oxidant migration below the existing extraction system. After injection of the oxidant solution ended, the extraction system was run for another 177 days to remove the residual oxidant and chloride remaining in the subsurface. During this time, the injection wells were not used and the treatment zone was flushed with background aquifer water.

The monitoring program during this phase included regular sample collection from the injection feed, the total extraction flow, the individual extraction wells, and the nine multilevel points shown in Figure 3.6. Periodically, samples were collected from all the sampling points of selected multilevels in the 1-m multilevel fence. The goal of the monitoring strategy was to determine the effectiveness of the injection system in flooding the source zone with the oxidant and to determine whether a chloride signature, indicative of DNAPL mass removal, was present.

The number of extraction wells used to contain the oxidant solution varied over the course of the field trial. Initially, only XW-1, -2, and -3 were used; however, after some oxidant was observed down-gradient of these wells, BWU and BWL were also used to contain the injected oxidant. To try and minimize the amount of oxidant lost from the treatment system, the injection flow rate was decreased over time. The total injection and extraction flow rates are presented in Figure 3.11.

3.7.2 Injection/extraction well time-series monitoring

Time-series oxidant concentration data from samples collected from the injection feed, and the total extracted flow are presented in Figure 3.12. Due to the operational difficulties previously mentioned, the concentration of the injected oxidant was extremely variable over the course of the field trial with an average concentration of 8.1 g/L. The initial lag in oxidant breakthrough of 20-27 days resulted from consumption of the injected oxidant by the aquifer reduction capacity. In contrast, bromide breakthrough in the extraction wells during the pre-oxidant tracer test occurred after only 6 days.

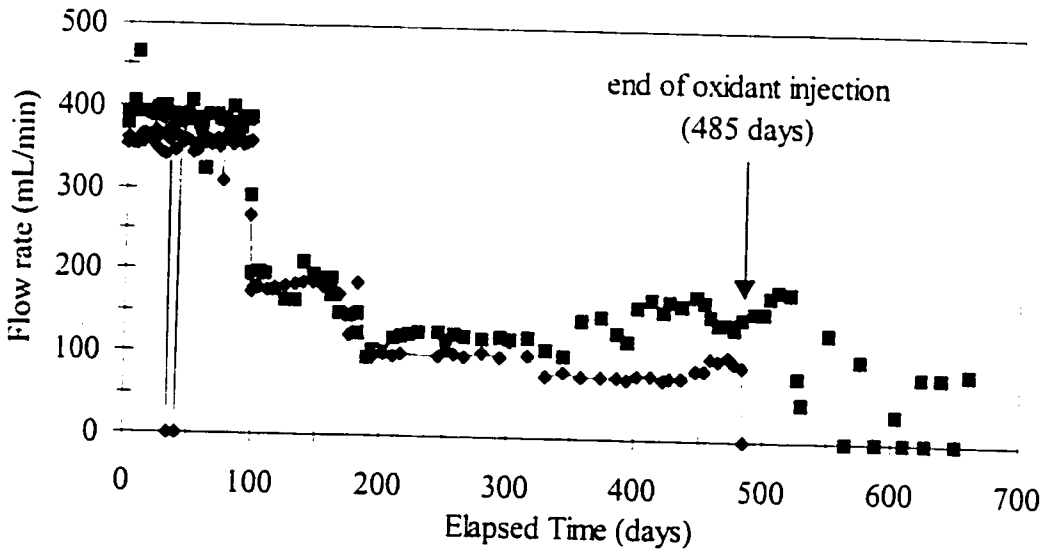

Figure 3.11 Total extraction (■) and injection feed (◆)flow rates during the oxidant flush.

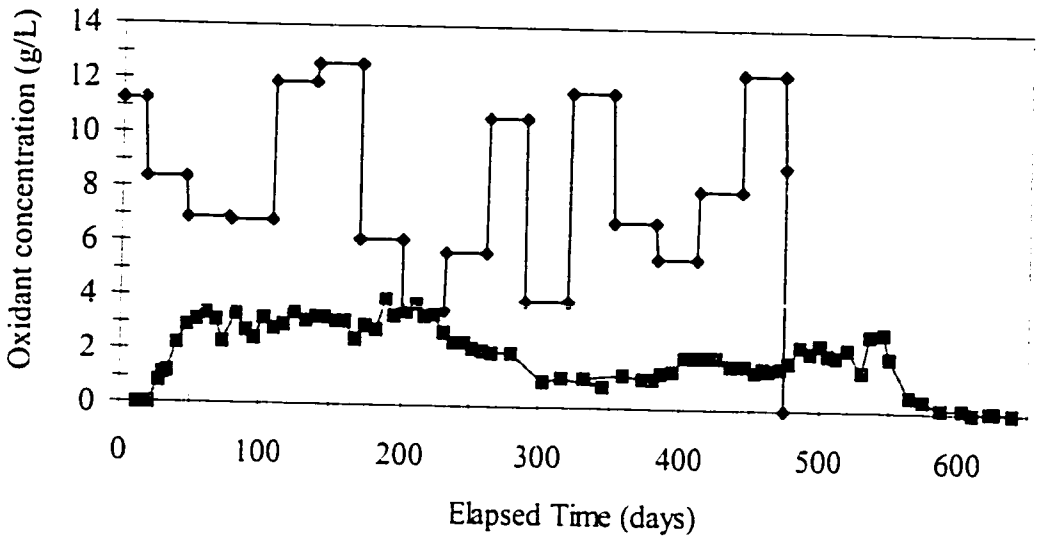

Figure 3.12 Oxidant concentrations in the total extraction flow (■) and the monthly average injection feed (◆).

Over the entire period of oxidant injection, the extracted oxidant concentration varied slightly with the trend in the mean injected oxidant concentration; however, the oxidant concentration of the total extraction flow was substantially lower than the injected oxidant concentration. The average oxidant concentration of the effluent was 2.1 g/L, which was less than the mean injected concentration in spite of attempts to improve oxidant recovery by reducing the injection flow rate and installing additional extraction wells. After oxidant injection ceased, oxidant remained in the effluent for ~100 days and then dropped to a negligible concentration.

The total extraction and injection feed time-series chloride concentration data are presented in Figure 3.13. In the above-ground treatment system, the variability of the extracted chloride concentration was dampened by storage in the equalization tank for several days prior to re-injection. Accordingly, the injected chloride concentration was less variable than the extraction concentration. Initial breakthrough of chloride produced by solvent oxidation occurred in XW2

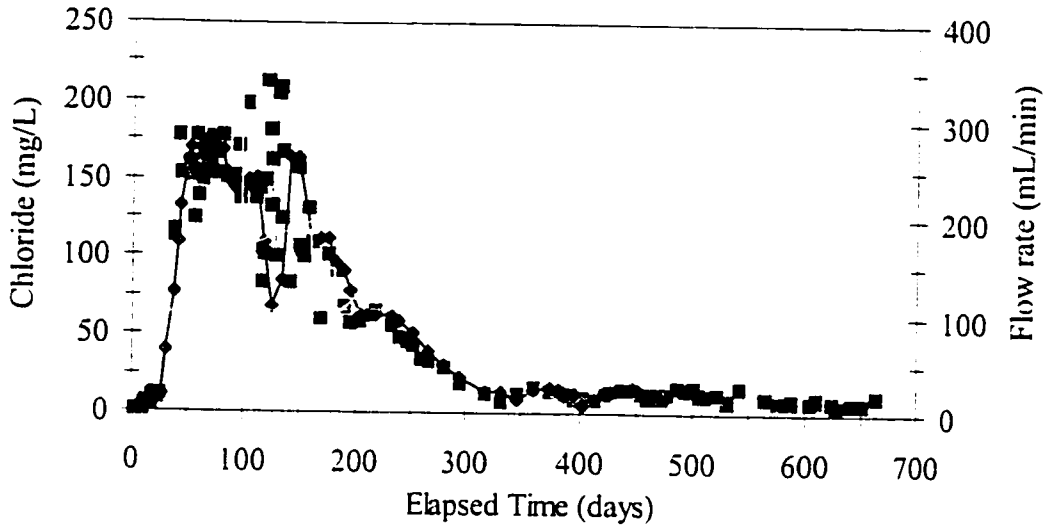

Figure 3.13 Chloride concentration in the total extraction (■) and injection feed flow (◆). Total extraction flow rate is shown for comparison (solid line).

between 17-20 days. The chloride concentration in the total extraction flow rose after 50 days to a peak of ~150 mg/L and remained at this concentration for ~100 days. Following this time, the effluent chloride slowly decreased until it was indistinguishable from the background aquifer chloride concentration after 300 days. The drop in chloride concentration resulted from fluid losses from the treatment zone, indicating that the system was not completely closed.

If the treatment zone behaved as an ideal plug-flow system, the concentrations of chloride and oxidant in the extraction flow should lag the concentrations in the injection feed by the residence time in the treatment zone; however, this system was poorly mixed with non-uniform flow. In previous investigations, the complication of chloride recycling was overcome by a comparison of the injected (recycled) chloride and extracted chloride breakthrough data (e.g., Schnarr et al., 1998). While the feed solution contained chloride, any increase in the chloride concentration above this background level while in the treatment zone could be attributed to removal of DNAPL by the oxidation reaction. While a slight lag in effluent response was evident during the initial breakthrough of permanganate and chloride, the variability of the effluent data relative to the injected concentration made a quantitative comparison impossible.

Causes of the variability included loss of the injected solution from the treatment zone, transient changes in groundwater flow, heterogeneity of the DNAPL distribution, and high variability of the concentration of the injected oxidant solution. Qualitatively, it was possible to draw some conclusions from the chloride concentration data. After 300 days of oxidant flushing, the variability of the effluent chloride concentration decreased and a consistent comparison between the injected and extraction chloride concentrations was possible. The small differences between the chloride concentration in the injection feed and total extraction flow (<1 mg/L) suggested that little oxidation and DNAPL removal was occurring.

The variation in the extracted chloride concentration suggested that the rate of DNAPL mass removal changed over the duration of the oxidant flush. As in previous investigations, the sharp increase in chloride concentration indicated that the maximum rate of DNAPL removal occurred as the oxidant first reached the source zone. The following phase during which a relatively constant chloride was observed (50-150 days) suggested that the rate of chloride production by DNAPL removal was comparable to the rate of chloride loss from the treatment zone by migration outside of the capture zone of the extraction wells. The subsequent drop in chloride concentration suggested that the rate of DNAPL removal also dropped.

The oxidant mass loading through the recirculation system is presented in Figures 3.14. While lower oxidant concentrations were observed in the extraction wells, in part this was due to the higher flow rates in these wells diluting the extracted concentration. The effluent oxidant load was consistently lower than the injection load, indicating that oxidant mass was lost through either losses from the treatment zone or an unexpected chemical reaction that consumed permanganate. After permanganate was observed down-gradient of the extraction wells, the total injection and extraction flow rates were decreased over time to minimize any vertical gradients around the injection wells and to reduce the total mass of oxidant required and the additional extraction wells were installed. However, it was difficult to assess the efficacy of these improvements given the variability of the oxidant concentration in the feed solution. Estimated total oxidant inputs and losses during the oxidant flush are summarized in Table 3.4.

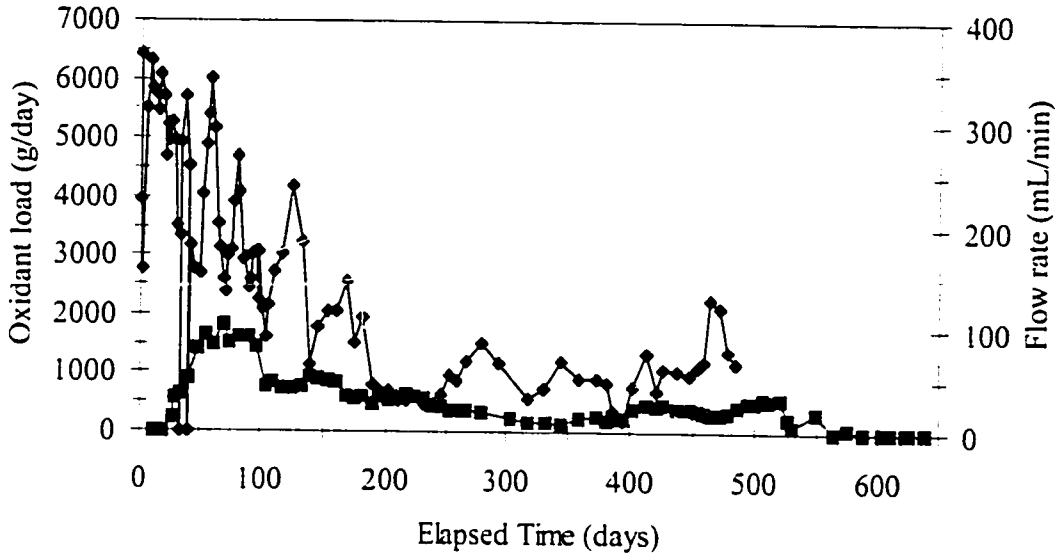

Figure 3.14 Oxidant loads in the total extraction (■) and injection feed flow(◆). Monthly average extraction flow rate (line) is shown for comparison.

Table 3.4 Oxidant balance for emplaced source oxidant flush.

System Input/Output			*Source*
Cumulative Oxidant Injected	892	kg	injection feed sampling
Cumulative Oxidant Extracted	303	kg	effluent sampling
Aquifer Oxidant Demand			
ES *foc*	0.035	%	Rivett et al. (1992)
PV	19.2	m^3	tracer test
Bulk Density	1810	kg/m^3	Ball et al. (1991)
Oxidant Demand	65	g/kg/%*foc*	Appendix A
Treatment Zone Oxidant Demand	78	kg $KMnO_4$	
DNAPL Source Oxidant Demand	15.4	kg $KMnO_4$	based on DNAPL mass estimated by Frind et al. (1999)
Total Inputs	892396496	kg $KMnO_4$	
Total Outputs/Losses		kg $KMnO_4$	
Net Deficit		kg $KMnO_4$	

The recovered oxidant solution was contained within 133 $m^3$of effluent with an average concentration of ~2 g/L. Several mechanisms may have resulted in the apparent loss of oxidant from the treatment zone. The injected oxidant solution may have migrated outside the treatment zone as a result of density-driven advection or transient changes in groundwater flow in the upper Borden aquifer. The density of the solution would have increased as a result of solution concentrations as high as 8,000 mg/L of chloride and 8 g/L of permanganate, resulting in a downward component to groundwater flow. This was supported by limited data indicating the presence of concentrated oxidant in deep sampling points down-gradient of the extraction wells. However, a reactive mechanism may have caused some portion of the oxidant loss. Rees (1987) observed that a slow autocatalytic reaction with MnO_2(s) resulted in unstable aqueous permanganate standards. Since MnO_2(s) was present in the treatment zone as a result of reactions with the VOCs and the natural oxidant demand, autocatalytic decomposition of the permanganate may have resulted in an oxidant sink.

Over the entire duration of the field trial, 892 kg $KMnO_4$ were injected while 303 kg $KMnO_4$ were recovered. Only a small fraction of this difference could be attributed to source zone oxidation. Based on the mass of solvent present at the start of the oxidant flush and the known stoichiometric requirement for the oxidation of TCE and PCE, DNAPL oxidation would require 15.4 kg $KMnO_4$ (1.7% of the total oxidant mass injected). The mass of oxidant consumed by the reduction capacity of the sand aquifer was calculated using the treatment zone pore volume (19.1 m^3) estimated by the second tracer test (see Section 3.8.2) and the measured oxidant demand of the Borden sand. Rivett et al. (1991) reported a mean *foc* of 0.035% in cores taken from the immediate area of the ES site. Based on the oxidant demands for sandy soils reported in Appendix A, the specific oxidant demand of natural organic carbon was estimated to be 65 g $KMnO_4$/kg sand/*%foc*. Accordingly, the oxidant demand of the treatment zone was estimated to be 78 kg $KMnO_4$ (9.9% of total oxidant mass).

The fraction of the oxidant pulse contained by the extraction system was calculated as,

$$f_r = \frac{M_{extract}}{M_{inject} - M_{aquifer} - M_{DNAPL}}$$

where $M_{extract}$ is the cumulative oxidant mass extracted, $M_{aquifer}$ is the oxidant demand exerted by the aquifer solids, M_{DNAPL} is the oxidant demand exerted by the DNAPL source zone, and M_{inject} is the cumulative oxidant mass injected. For this field trial f_r was estimated to be 0.40, indicating that there was a oxidant loss; however, it is not clear that any of this loss could be attributed to a reactive sink rather than migration outside the recirculation system. However, the field experiment conducted by Schnarr (1992), conducted in a completely enclosed cell without recycle, resulted in f_r=0.59, while the fraction of oxidant recovered during the bench scale experiment completed by MacKinnon (1998) was f_r = 0.77. While it was evident that some oxidant migrated outside of the capture zone of the extraction wells during the current field experiment, the fact that the oxidant recovery fractions estimated for all three experiments were substantially below unity suggested that much of the oxidant loss may be attributed to a reactive mechanism.

The chloride loading profile (Figure 3.15) provided additional evidence of ongoing DNAPL mass removal. The chloride load in the extraction system effluent was higher than the injected chloride load until ~300 days into the oxidant flush. For the remainder of the flush, the extracted chloride load, while generally slightly higher than the injection load, was less than the solvent load (expressed as the stoichiometric equivalent chloride load) during the pre-oxidant tracer test (3,585 g/day Cl^-), which suggested that the oxidant flush was not resulting in a dissolution enhancement above that expected without the addition of the oxidant.

3.7.3 Time series monitoring in the 1-m fence

Due to the variability and the small differences between the injected and extracted chloride concentrations, few inferences about the degree of source removal could be made. At that sampling scale, oxidation of the source zone appeared to have stopped after ~300 days. To confirm this results, chloride concentration profiles from the 1-m multilevel fence, where

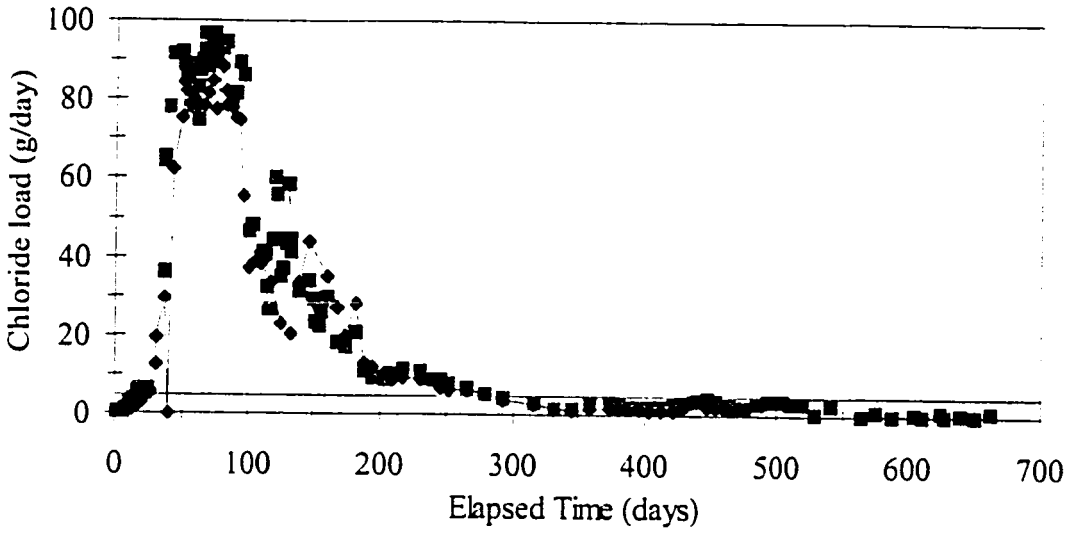

Figure 3.15 Chloride loading in the total extraction (■) and injection feed flows (◆). The pre-oxidant flush solvent loading (on an equivalent chloride basis) is shown for comparison (solid line).

samples could be collected using a finer sample resolution, provided additional data on the extent of DNAPL mass removal.

For the multilevels located immediately to either side of the source (ML1 and ML5), the breakthrough chloride concentrations were similar to the injected Cl^- concentration, indicating that only recycled chloride was observed at these locations (Figure 3.16). The chloride plume generated by the oxidation reaction within the source zone, however, was consistently observed in the centre multilevel (ML3). The upper sampling location (ML3-4) followed a similar trend as the injected concentration while the central point (ML3-7) had an elevated chloride concentration for a short time then declined to the background chloride concentration. Groundwater samples collected from ML3-10 consistently contained chloride concentrations above the background concentration and included the highest chloride concentrations measured at any time during this experiment (8,361 mg/L in ML3-10). After 300 days, no difference between the extracted and injected chloride loading in the recirculation system was evident;

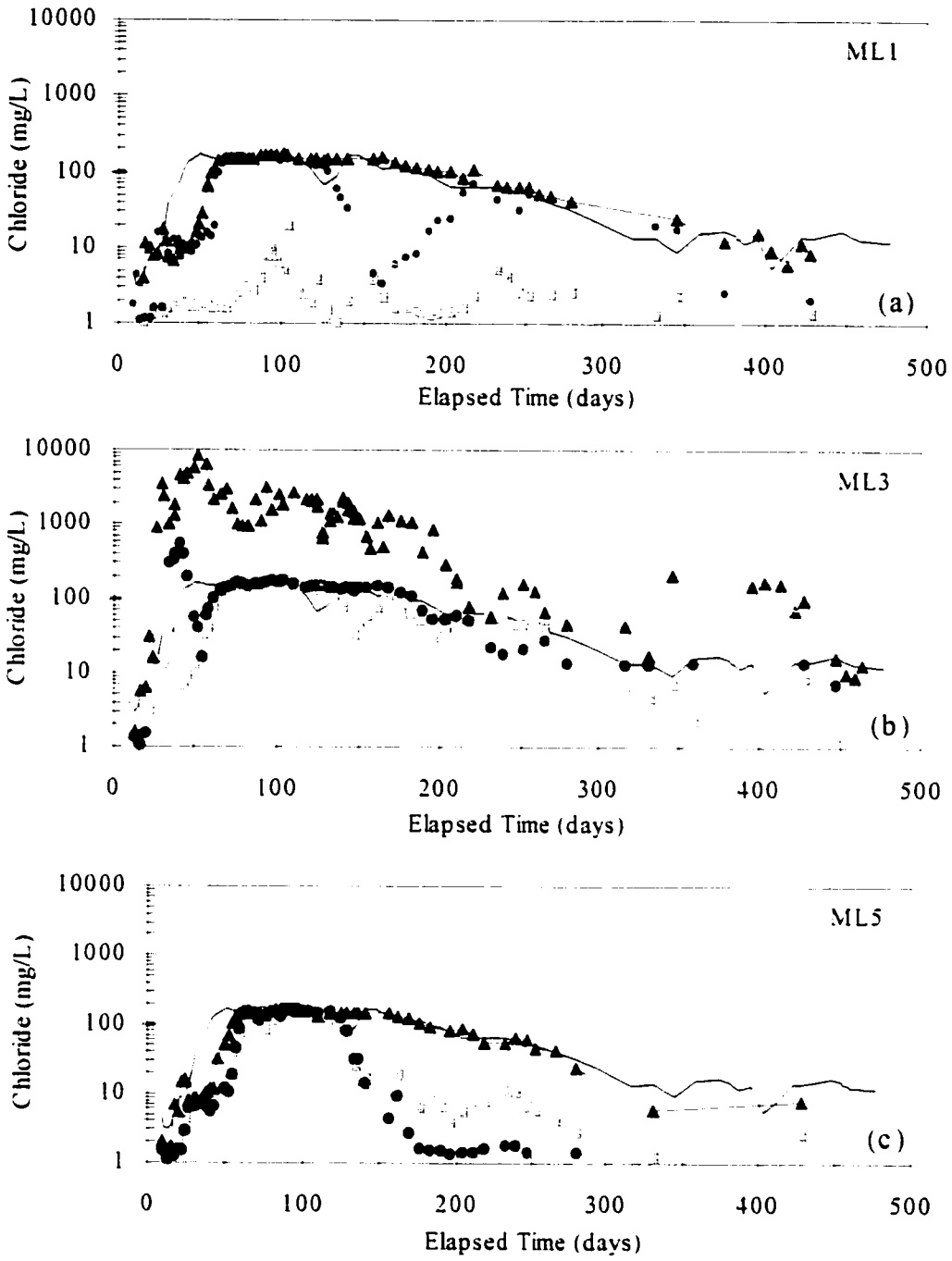

Figure 3.16 Chloride concentration data (log scale) for the 1-m fence multilevels (see Figure 3.6 for locations) for (a) ML1, (b) ML3, and (c) ML3. Sampling points shown are -4 (■), -7 (●), and -10(▲). Recycled chloride concentration (line) shown for comparison.

however, elevated chloride concentrations were measured in ML3-10 up until 450 days. The discrepancy between the sampling scales suggested that after 300 days of oxidant injection the rate of solvent mass removal was slow and produced a small but concentrated chloride plume which was not evident in the extraction wells.

3.7.4 Synoptic sampling of the 1-m fence

Synoptic samples were collected from the 1-m fence to evaluate the spatial distributions of permanganate and chloride in the treatment zone. The chloride plume loading across the 1-m fence was not determined using the snapshot method previously described for the solvent plume since the groundwater velocities at the 1-m fence under forced-gradient conditions throughout the oxidant flush were not measured.

The spatial distributions of chloride and oxidant concentrations at various times during the oxidant flush (Figures 3.17, 3.18, and 3.19) provided fine-resolution sampling data from which the location of the injected oxidant was inferred and the relative rates of DNAPL mass removal assessed. In spite of a large reduction in the injection flow rate after 100 days, the asymmetrical oxidant pulse extended below the 1-m fence monitoring network. The peak chloride concentration was typically very high relative to the injected chloride concentration and roughly corresponded to the known location of the source. In contrast to the oxidant distribution, the chloride plume was small and located only 10-20 cm below the source zone. The consistent appearance of the chloride plume in the vicinity of the source, in contrast to the large spread of the oxidant plume, suggested that the spreading of the oxidant plume occurred up-gradient of where chloride was produced in the source zone. While some of the spreading of the injected oxidant may have resulted from high injection flow rates and density driven advection, divergence of flow around and below the source zone may also have been caused by a permeability decrease on the up-gradient side of the source.

The snapshots shown in Figures 3.17 (a) and (b) represented the oxidant distribution during the

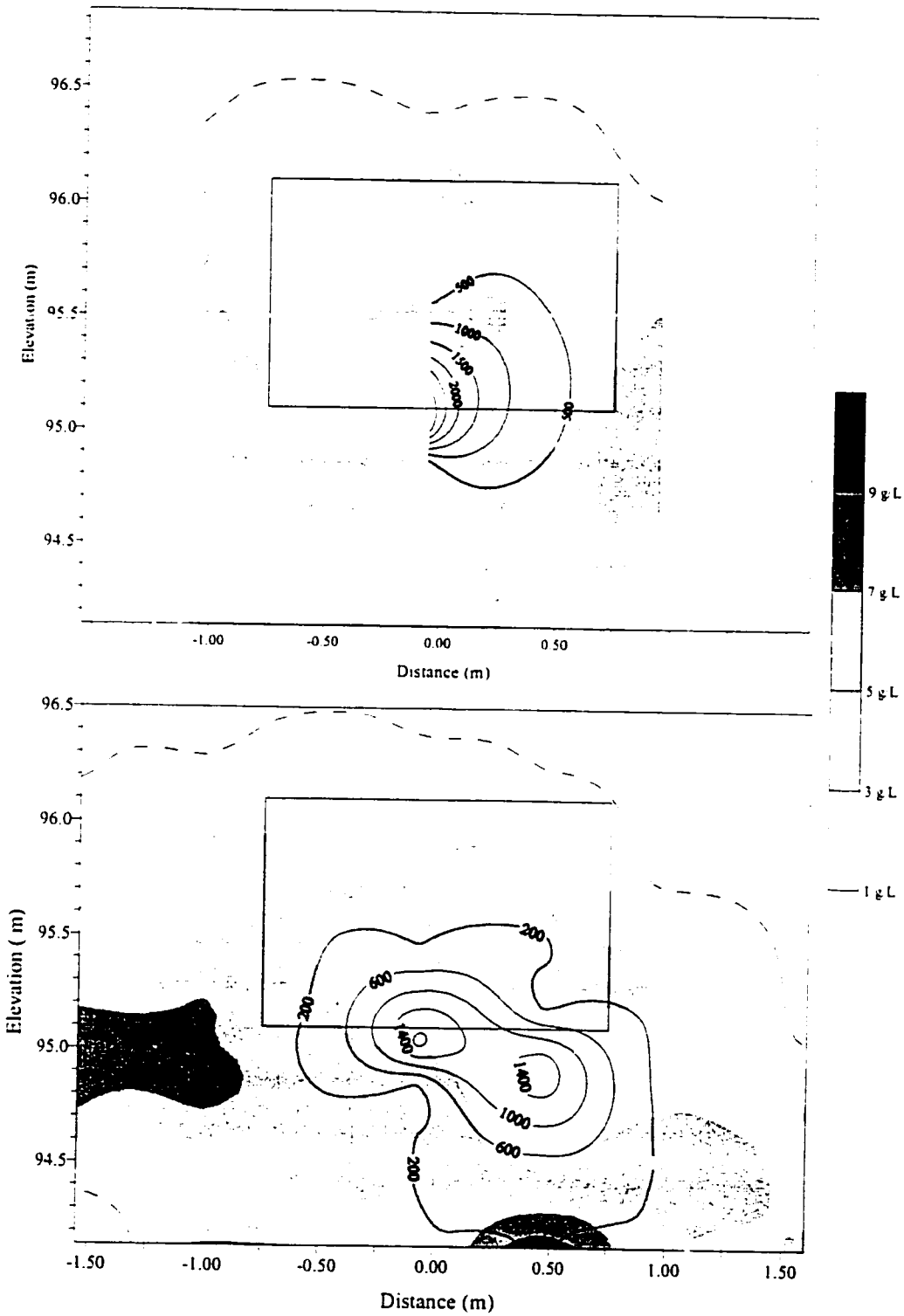

Figure 3.17 Chloride (contours in mg/L) and oxidant (shading in g/L) snapshots collected from the 1-m fence after (a) 98 and (b) 118 days (source location shown).

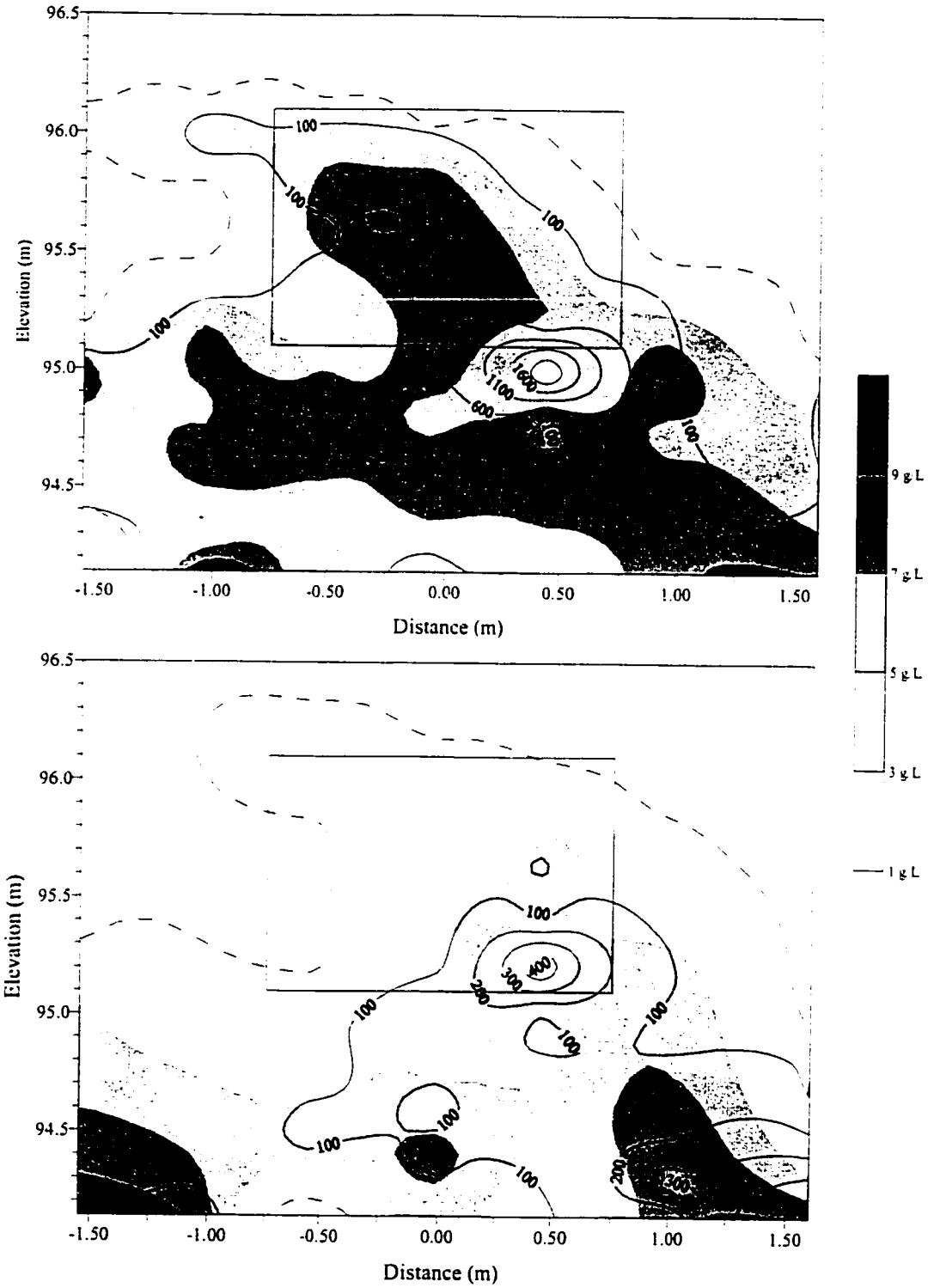

Figure 3.18 Chloride (contours in mg/L) and oxidant (shading in g/L) snapshots collected from the 1-m fence after (a) 161 and (b) 210 days (source location shown).

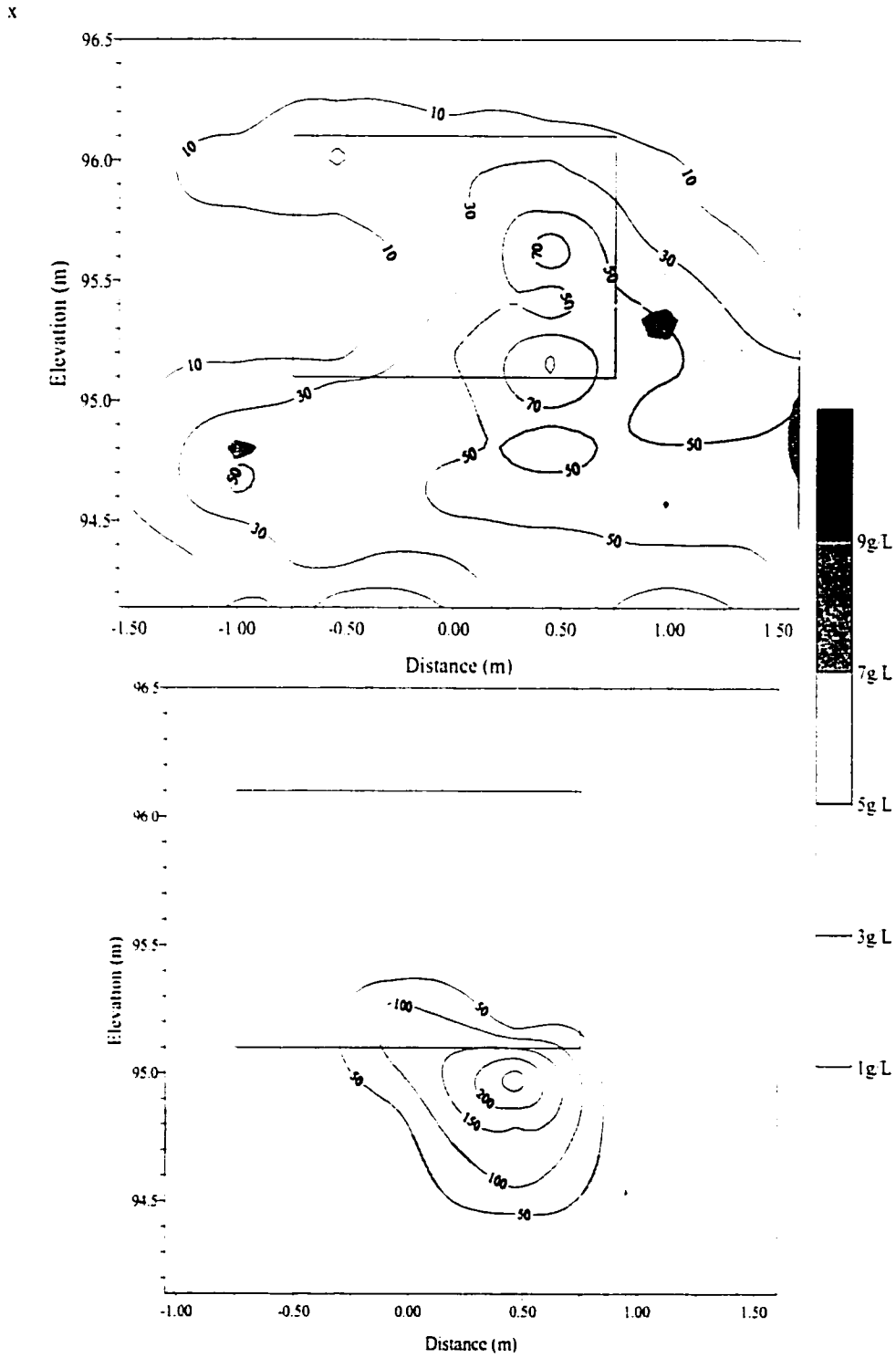

Figure 3.19 Chloride (contours in mg/L) and oxidant (shading in g/L) snapshots collected from the 1-m fence after (a) 280 and (b) 427 days (source location shown).

highest injection and extraction flow rates. At these times, the oxidant pulse was widest and appeared to extend below the monitoring system. In both Figures 3.17 and 3.18, the chloride peak coincided with low oxidant concentrations, which suggested that the oxidant was being depleted by the reaction.

A distinct chloride peak was not evident in the snapshot collected at 280 days (Figure 3.19a); however, a small chloride plume was observed in the following snapshot which suggested that oxidation was continuing with a peak concentration above the background concentration. This result was consistent with time-series data collected from ML3-10 (Figure 3.16b),where elevated chloride concentrations were observed up until to 450 days. Repeated sampling of the multilevels failed to detect a chloride plume after this time. If DNAPL mass removal was still occurring, the chloride plume was sufficiently small that it passed within the sampling resolution of the 1-m fence.

3.7.5 Source zone profiling

Once chloride concentrations in ML3-10 dropped to near-background concentrations, a finer sampling scale was employed to monitor the progress of the oxidant flush. Vertical profiles of oxidant and chloride concentrations in groundwater were collected from one location within the source zone. The profiling location was at the approximate centre of the source and was repeatedly profiled, potentially creating a disturbed zone along the drivepoint trajectory. The extent that this influenced the monitoring results was impossible to ascertain. In addition to the centre profiling location, several additional profiles were collected at different locations ~0.2 m down-gradient of the source.

Source zone profiles collected from the centre of the source during the oxidant flush are shown in Figure 3.20. Additional profiles collected immediately down-gradient of the source are presented in Figure 3.21. Several general observations were evident from the profiling data. The oxidant profiles varied in peak concentration but indicated that a concentrated oxidant solution was present in the source zone. Peak oxidant concentrations in the profiles ranged

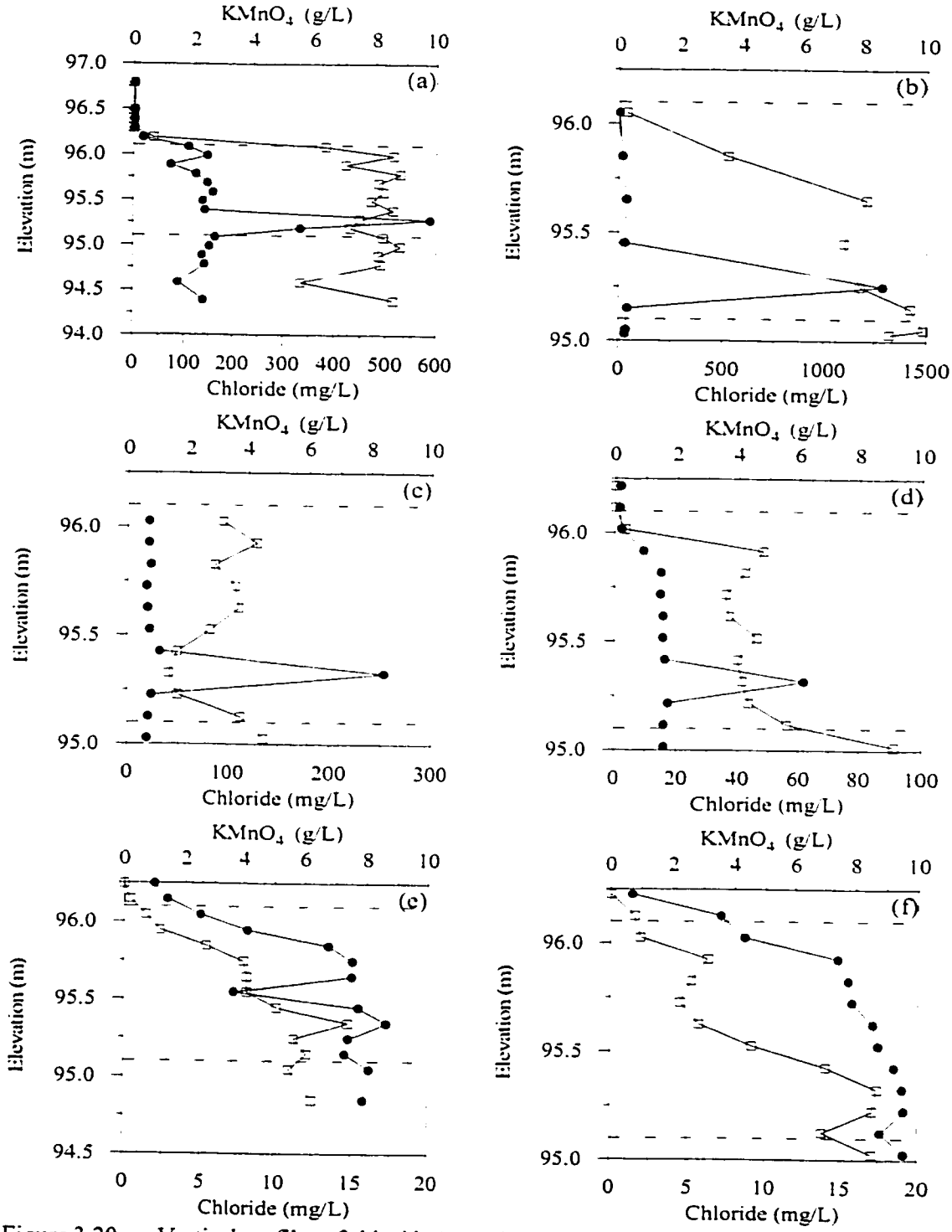

Figure 3.20 Vertical profiles of chloride (•) and permanganate (□) through the centre of the emplaced source collected after (a) 168, (b) 294, (c) 323, (d) 345, (e) 387, and (f) 427 days (dashed lines represent the upper and lower limits of the ES).

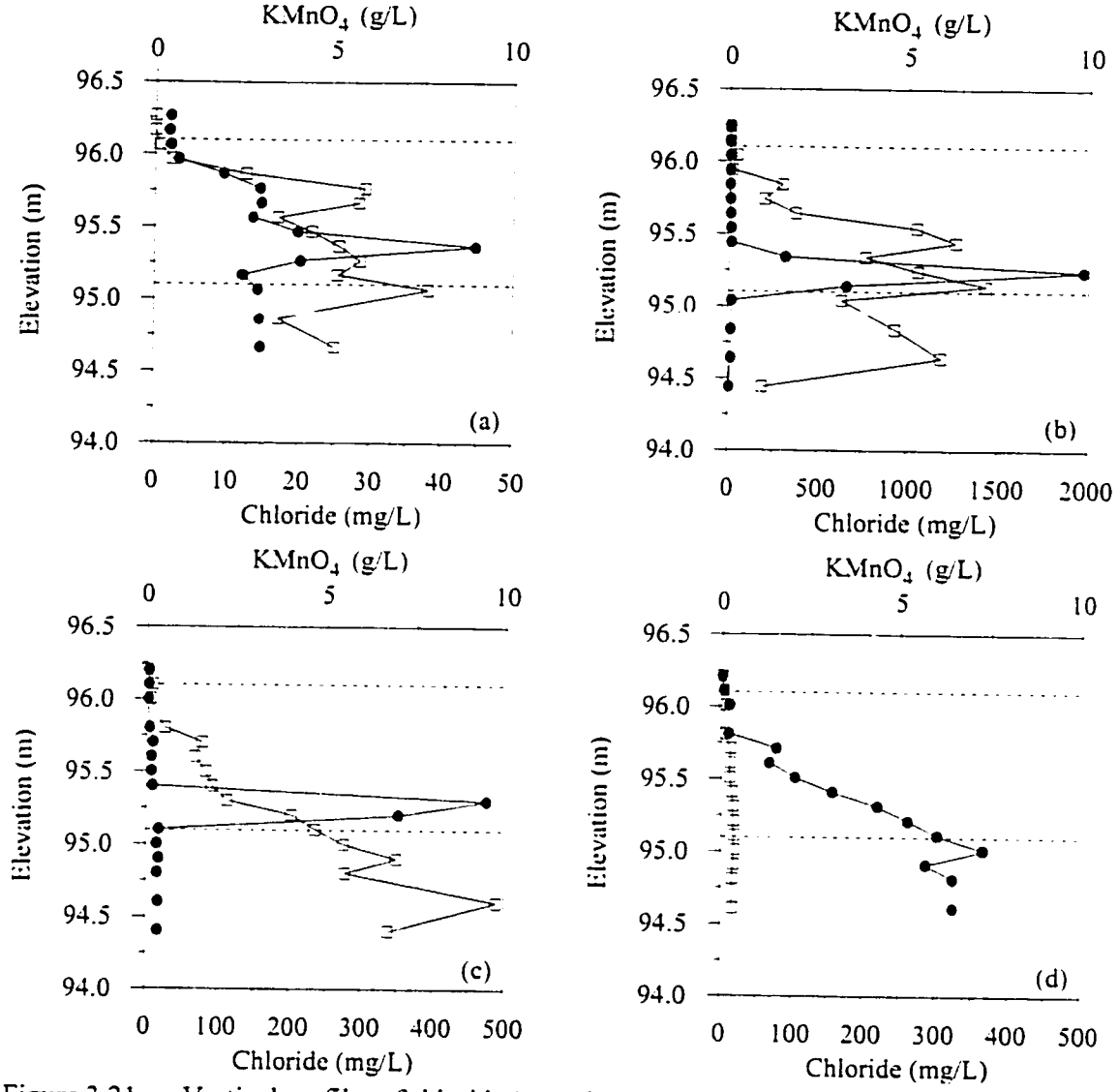

Figure 3.21 Vertical profiles of chloride (•) and permanganate (□), collected <10 cm down-gradient of the source. Profiles (a) and (b) were collected at 381 days and were 25 cm apart. Profiles (c) and (d) were collected at 478 days 37 cm apart (dashed lines represent the upper and lower limits of the ES).

from ~4-10 g/L. In general, the oxidant concentrations increased with depth through the source: low concentrations were observed at the upper edge of the source. The chloride signature was consistently located in a narrow interval centred ~25 cm above the bottom of the source, suggesting the presence of a small DNAPL zone. The peak concentration of the chloride signature declined over time and after 345 days of flushing was indistinguishable from the

recycled chloride concentration, indicating that no oxidation was occurring. Additional concentration profiles were collected on the down-gradient edge of the source zone on the assumption that any solvent mass between the down-gradient face and the centre of the source (the location of previous profiles) would continue to produce a chloride signature. Closely spaced profiles had large differences in peak chloride concentration which suggested that a small chloride plume was being produced by the source after 478 days of oxidant flushing (Figure 3.21c).

The presence of a distinct chloride plume (~450 mg/L) at 478 days was evidence of ongoing oxidation. Given that no chloride was observed in the centre profiles, and that the plume was apparently small enough that it was not observed in either the extraction wells or the 1-m fence, these data suggested that a small DNAPL zone remained on the down-gradient side of the source zone.

3.8 Post-oxidant flush testing

3.8.1 Summary of system operation

A second tracer test was performed to characterize groundwater flow and the plume solvent load in the recirculation system. The flow rates and configuration of the recirculation system were identical to the pre-oxidation tracer test except that an improved tracer injection system was used and operation of the system continued until the effluent tracer pulse was recovered through the extraction wells. Prior to the tracer addition, the system ran for three weeks to establish steady-state flow within the treatment zone. The injection flow was dosed with a concentrated bromide solution through a low-flow, precision peristaltic pump. The concentrated tracer solution of reagent grade NaBr (366,676 mg/L Br^-) was added to the injection feed at 0.29 mL/min for 117 hours. The concentration of the injected tracer pulse was 300 mg/L (total Br^- mass of 754 g). VOC samples were regularly collected from the total extraction flow, which was treated using activated carbon and collected in a storage tank. The effluent tracer solution was not recycled and was periodically discharged. The mean injection flow rate was 348±12 mL/min while the mean extraction flow rate was 386±34 mL/min (Figure 3.22).

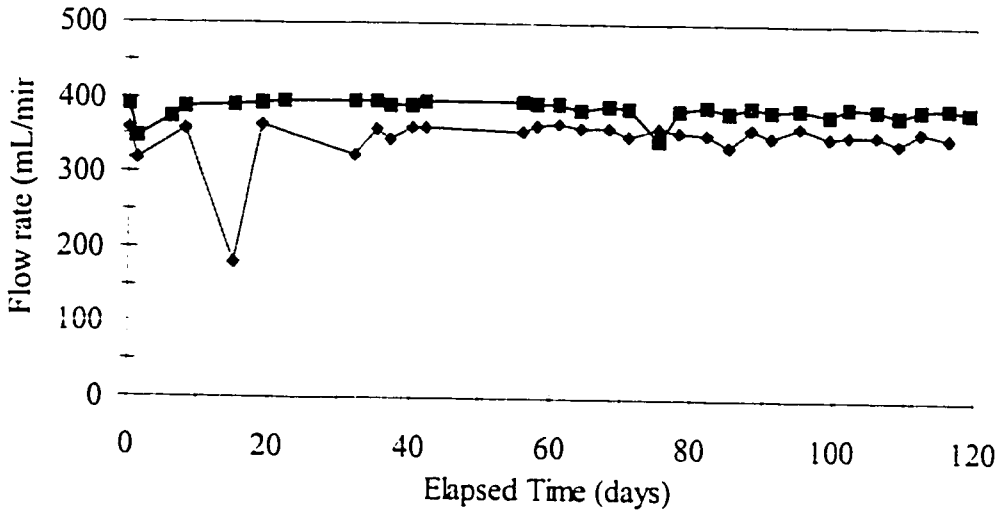

Figure 3.22 Summary of total extraction (■) and injection feed (♦)flow rates from the post-oxidant flush tracer test.

3.8.2 Extraction system tracer testing

The bromide breakthrough curve in the total extraction flow reached a peak of 37 mg/L after ~30 days (Figure 3.23). The breakthrough curve was asymmetric. Distinct tailing of the effluent pulse was evident which was attributed to slower velocities and longer path lengths along the edge of the treatment zone and dispersion of the injected tracer slug.

Data from the post-oxidation tracer test were used to calculate the average residence time of the injected tracer pulse in the treatment system. The estimated treatment zone residence time was 34.5 days, corresponding to an equivalent pore volume of 19.1 m^3. Over this distance between the extraction and injection wells (3.8 m), the residence time indicated that the mean velocity in the treatment zone was 11 cm/day, a result which was only slightly lower than that estimated with the pre-oxidant flush tracer test.

The fraction of the injected tracer mass recovered with the extraction system was used as a measure of the effectiveness of the recirculation system. The recovered fraction was calculated

as.

$$M_r = \frac{1}{M_{total}} \sum_{i=1}^{n} C_i Q_i \Delta t_i \qquad (3.10)$$

where M_{total} is the total mass of tracer injected in the recirculation system, C_i is the mean effluent tracer concentration over time interval Δt_i, and Q_i is the mean extraction flow rate. The mass of tracer recovered during the post-oxidant flush tracer test was 82% of the injected mass. While the bromide concentration was non-zero at the end of the tracer test, extrapolation of the effluent bromide concentration suggested that continued extraction would recover <1% of the total tracer mass. Since this was a dilute tracer solution without the density increase caused by the presence of oxidant and chloride, this recovery fraction represented the maximum recovery of the injected solution during the oxidant flush.

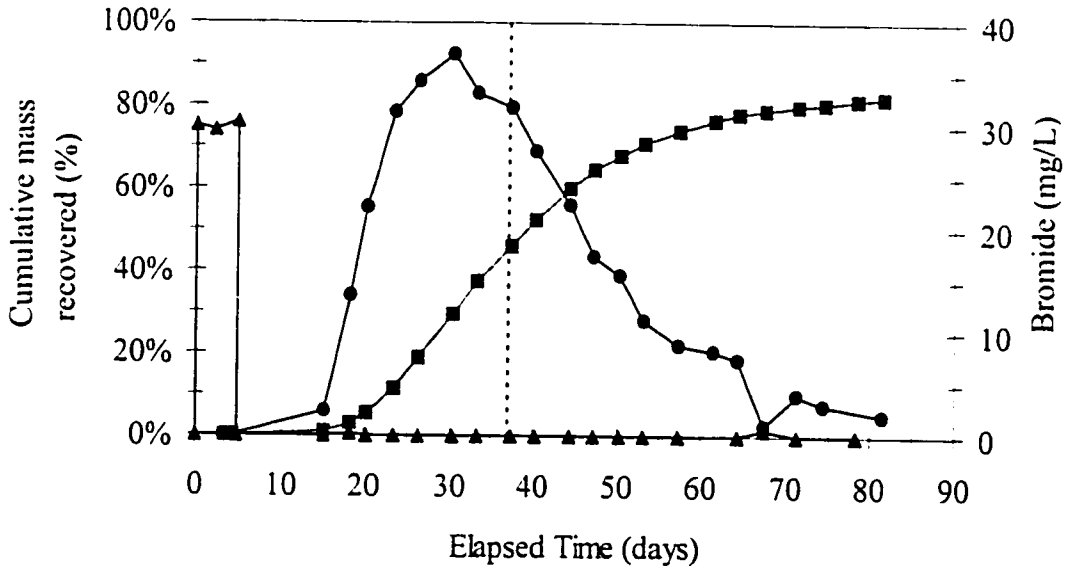

Figure 3.23 Breakthrough profiles of bromide in the injected tracer pulse (▲), and total extraction flow (●), and the cumulative tracer mass recovery (■). Actual injected tracer concentrations are 10X those shown on axis; dashed line represents pulse centroid.

3.8.3 Solvent plume load

Multilevel snapshot plume load

Following closure of the injection system to allow ambient flow in the aquifer, a second snapshot of VOC concentrations was collected from the 1-m fence (Figure 3.24). The peak concentrations of TCE and PCE in the snapshot were 2 and 31 mg/L, respectively. The post-oxidation TCE plume load, calculated using the method previously described in Section 3.6.3, was 7 mg/day while the PCE plume load was 98 mg/day. The plume loads of both TCE and PCE were lower than those estimated before the oxidant flush. Similar to the pre-oxidant flush snapshots, these plumes were centred on the lower-right quadrant of the source zone.

Extraction system solvent load

The VOC data gathered during the post-oxidation tracer testing appeared to vary over time (Figure 3.25). The mass loads for TCE and PCE, calculated using the average of the last five measurements, were 17 mg/day and 222 mg/day, respectively. The concentration of TCE in the effluent decreased over time while the concentration of PCE increased. The changes in concentration ratio suggested that the solvent mass depleted from the source during the tracer test changed the fractional composition of the remaining DNAPL. For this to occur, the total solvent mass in the source would have to be small. Using the method described by Feenstra (1990), the mass of DNAPL remaining in the source was calculated using the mass of each solvent depleted during the tracer test and the change in the PCE:TCE concentration ratio and was determined to be 91 g PCE and 3 g TCE.

3.9 Source zone sampling and excavation

The spatial distributions of the remaining DNAPL and $MnO_2(s)$ within the source zone were determined following the oxidant flush. Samples were collected by excavating to ~30 cm above the source and driving 5-cm ID aluminium core tubes into the source zone until the core tube was refused by the underlying steel pan. The core tubes were sealed with a rubber stopper to form a vacuum, manually withdrawn, capped, sealed with duct tape, and labelled. Cores were

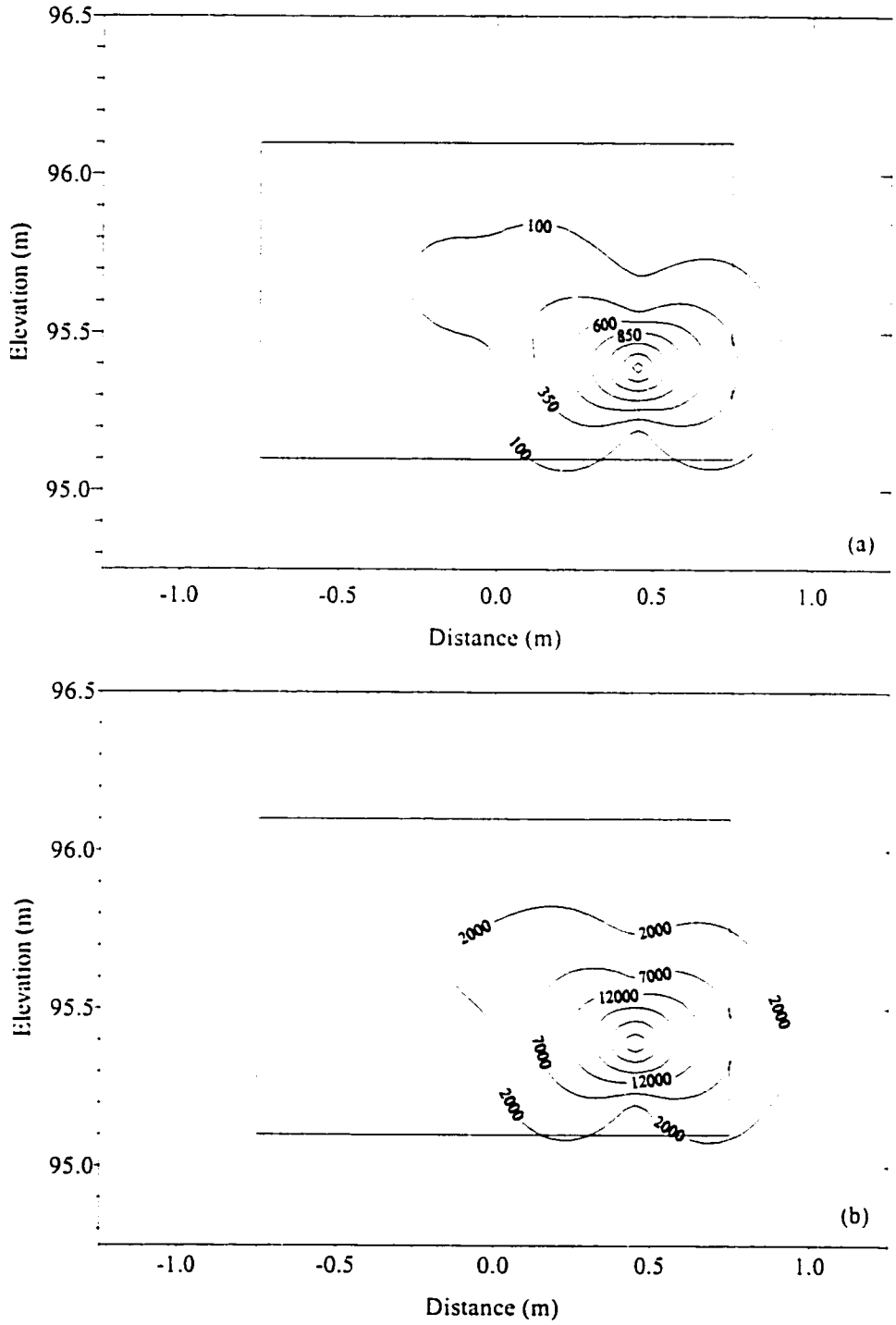

Figure 3.24 Snapshot of (a) TCE and (b) PCE collected from 1-m fence in October 1996 (contours in µg/L). Viewpoint is from down-gradient of the source.

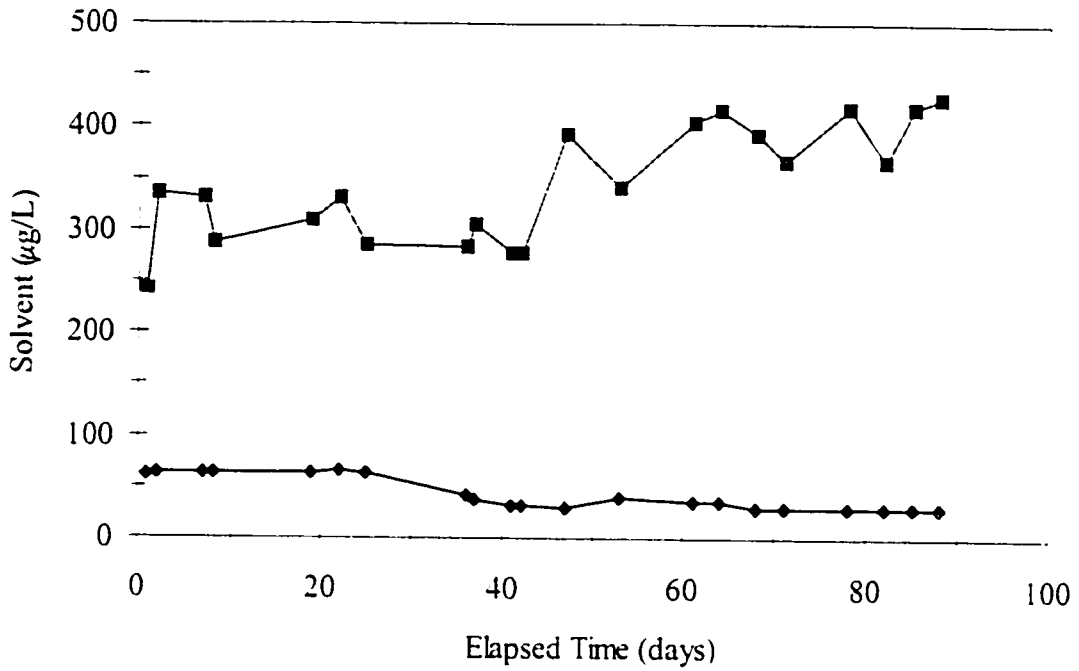

Figure 3.25 Effluent TCE (♦) and PCE (■) concentrations during the post-oxidation tracer test.

oriented in three rows along the length of the source (Figure 3.26). During excavation a plastic sheet, which was assumed to be level based on the reported installation method, was found over the top surface of the source zone. The small section of plastic found in the individual cores was later used to determine the elevation of each core.

The cores were sliced lengthwise and sub-sampled using a precleaned micro-sampling tool (Figure 3.27). The location of the plastic cutout within each core was measured relative to the bottom of the core barrel. Similarly, the location of distinct stains and the length of recovered sample were also recorded. Manganese dioxide stains, evident as dark brown-to-black soil discolouration, were present as distinct horizontal lenses. Duplicate subsamples were collected at 5 cm intervals. The first sample, used for bulk VOC soil concentration, was placed in a 20 mL VOA vial containing 10 mL of methanol as an extraction solvent while the second was put into a 40 mL VOA vial for bulk total Mn analysis (assumed to be present as MnO_2).

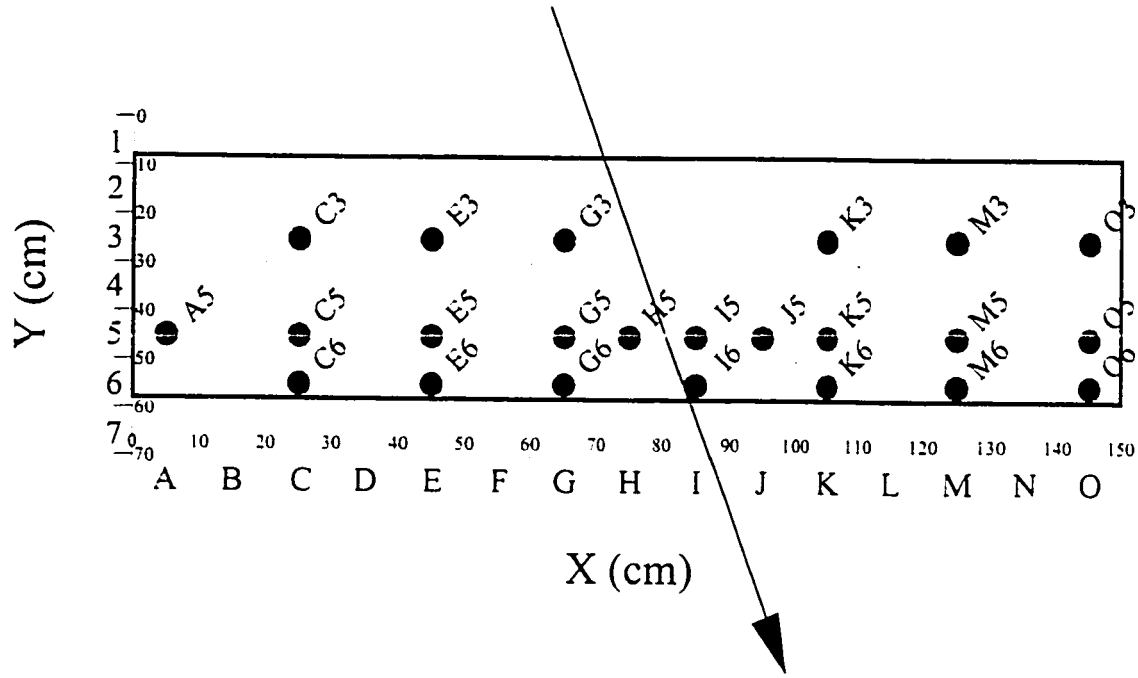

Figure 3.26 Location of cores (●) collected from the source (outline indicates the extent of the source zone while arrow indicates the direction of flow).

3.9.1 Source zone contaminant distribution

The raw concentration data was interpolated onto a regular grid using Tecplot v7.5 (Amtec Engineering, Inc., 1998) and numerically integrated to estimate the total contaminant mass. Sectional plots of the MnO_2(s) distributions are shown in Figure 3.28. Since only a few meaningful detections of TCE or PCE were measured, these data were not plotted.

The background Mn content of the Borden sand is <8.2 mg/kg (Ball et al., 1990). In comparison, bulk soil concentrations of MnO_2(s) in samples collected from the source zone ranged from 197 to 13,442 mg/kg (as MnO_2) with a mean concentration of 1,728 mg/kg (428 samples). The highest detections were primarily located on the up-gradient edge of the source with the centre being the region of highest concentration. Assuming a maximum density of ρ=5.1 g/cm3, the maximum concentration of MnO_2(s) corresponds to ~1% of the total pore volume. Only low concentrations of MnO_2(s) were observed in the top and bottom 10 cm of the source zone. Typically, stains were either visibly continuous through most of the length of

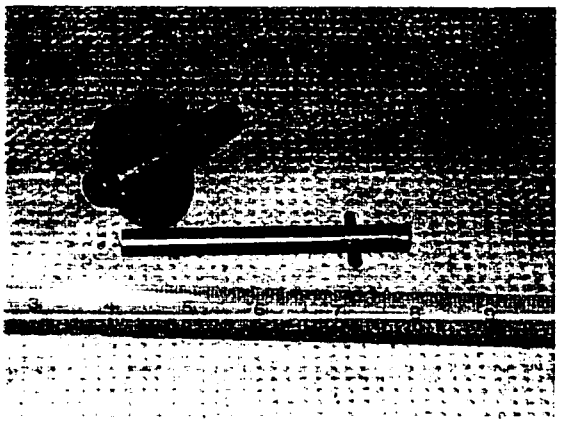

Figure 3.27 Core micro-sampling tool.

the core or present in small distinct lenses surrounded by almost unstained core material, suggesting that DNAPL within that horizon had been oxidized. Some cementation of the soil grains was observed in the most highly stained regions. The mass of $MnO_2(s)$, strongly correlated with the presence of DNAPL at the start of the oxidant flush, could be stoichiometrically converted to the equivalent mass of DNAPL. The total mass of $MnO_2(s)$ in the source (3,295 g) was equivalent to either 2,490 g or 4,714 g of TCE or PCE, respectively. The initial mass of solvent in the source (9.0 kg PCE and 1.6 kg TCE) corresponded to a mass of 10.1 kg of $MnO_2(s)$. The unexpectedly low $MnO_2(s)$ mass measured within the source zone indicated that either the initial solvent mass was overestimated, DNAPL mass remained within the source, or that some $MnO_2(s)$ was deposited down-gradient of the source.

A total of 339 samples from the cores were analysed to determine the concentration of TCE and PCE in soil. Bulk soil concentrations of TCE ranged from ND-30.9 mg/kg with a mean concentration of 0.2 mg/kg. In comparison, PCE concentrations were higher and ranged from ND-163.1 mg/kg with a mean of 25.1 mg/kg. The mean TCE concentration was significantly lower than the mean PCE concentration, consistent with the smaller mass of TCE at the start of the oxidant flush and the higher solubility and oxidation rate of TCE. The few significant detections of TCE and PCE were erratically scattered on the down-gradient side of the source while, in contrast, $MnO_2(s)$ was deposited on the up-gradient edge of the source zone.

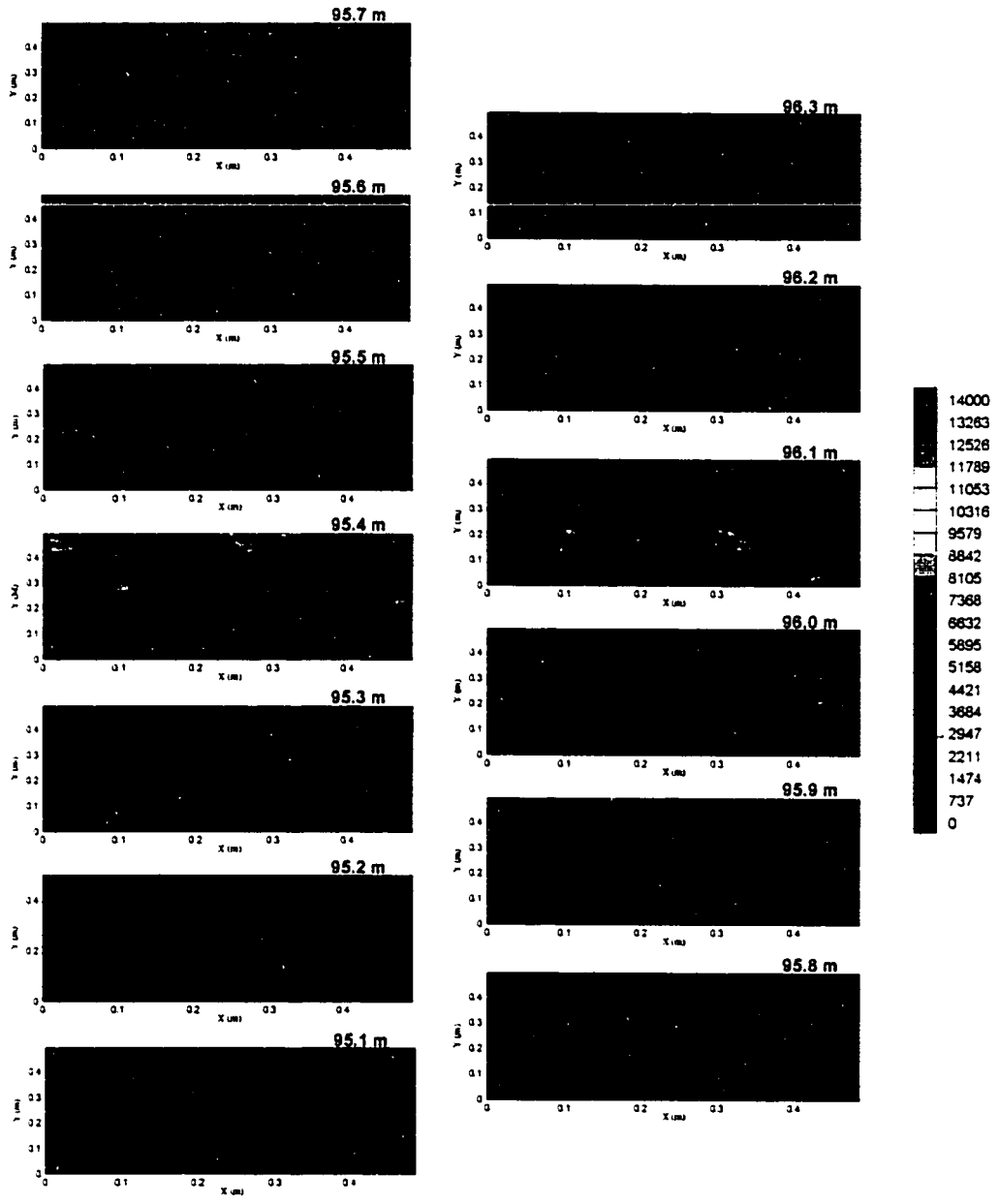

Figure 3.28 Distribution of $MnO_2(s)$ in horizontal sections (section elevation in bold type) interpolated from source sampling data (note that y = 0 is the up-gradient face of the source zone.

Partitioning calculations were performed to estimate the apparent bulk concentration at which the presence of pure phase solvent could be inferred. Assuming that the water phase was at the aqueous solubility limit and equilibrium partitioning to the solid phase, bulk concentrations of TCE (263 mg/kg) and PCE (220 mg/kg) were determined. The fact that very few of the solvent measurements approached these phase limits indicating the presence of pure phase suggested that the solvent mass was primarily present as a sorbed phase.

3.9.2 Source zone core hydraulic conductivity

Two of the twenty-three source zone cores were reserved for permeameter testing prior to sub-sampling for MnO_2(s) analysis. Hydraulic conductivity (K) in cores M6 and K3 (Figure 3.26 for locations) was measured at 5 cm intervals using a multiport permeameter system described by Tomlinson (1998).

Hydraulic conductivity (temperature corrected to 10 °C) and MnO_2(s) concentration profiles are presented in Figures 3.29 and 3.30. The arithmetic mean hydraulic conductivity of the post-oxidation source cores was 1.9×10^{-5} m/s, a result almost six times higher than the pre-oxidation hydraulic conductivity (3.0×10^{-6} m/s) reported by Feenstra (1997) and consistent with the increase in hydraulic conductivity following PCE oxidation observed by Schnarr (1992). The conventional permeameter testing method of Feenstra (1997), which used homogenized and repacked core sub-samples, overestimated the undisturbed conductivity, suggesting that the actual change in hydraulic conductivity between the source coring events was even larger. The increased source conductivity was consistent with DNAPL depletion from the source and dissolution of carbonate minerals from the acidity generated by the oxidation reactions. A correlation of hydraulic conductivity with MnO_2(s) concentration could not be discerned from the natural variability of hydraulic conductivity; however, it appeared that any decrease in conductivity resulting from MnO_2(s) deposition was offset by DNAPL removal and carbonate dissolution.

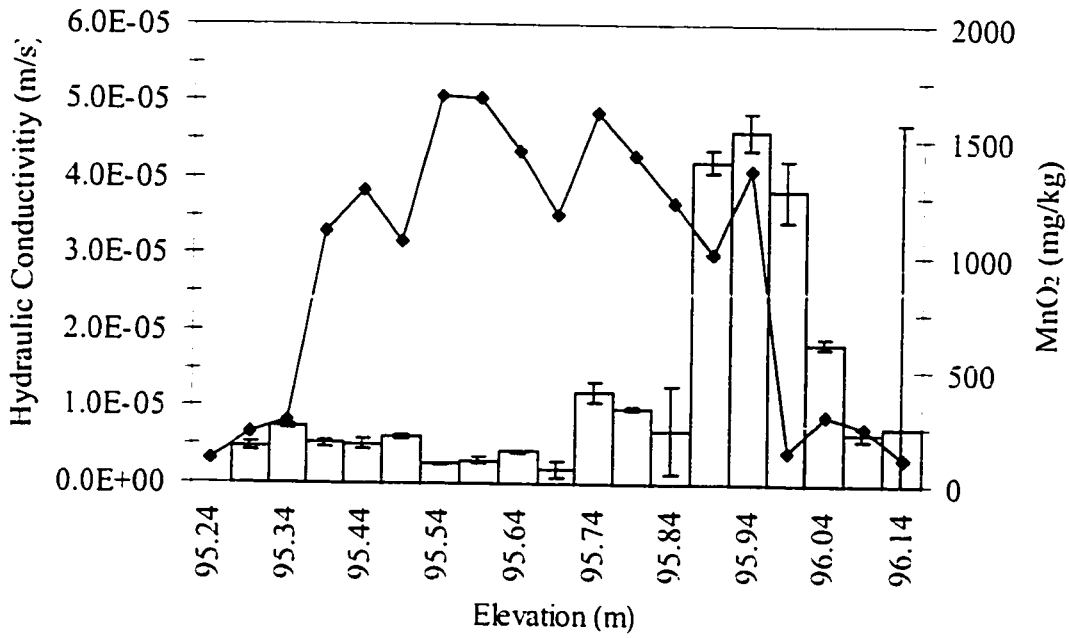

Figure 3.29 Mean hydraulic conductivity (error bars represent one standard deviation of triplicate measurements) and bulk MnO_2(s) concentration (◆) in soil samples from core K3

The measured increase in hydraulic conductivity contrasted with the modelling results of Frind et al. (1999) which suggested that average permeability of the source zone was less than that of the aquifer by a factor of 10 to 20. In addition, the breakthrough curve data collected during the pre-oxidant flush tracer test and oxidant concentration data collected during the oxidant flush suggested that groundwater flow was diverted around the source zone. These results were not entirely inconsistent with the measured increase in hydraulic conductivity. If a low-permeability calcite front formed on the up-gradient face of the source, it was unlikely that either of the cores collected in this study sampled the front. The front however, may have decreased the average horizontal hydraulic conductivity of the entire source, even though the hydraulic conductivity of the remainder of the source zone increased.

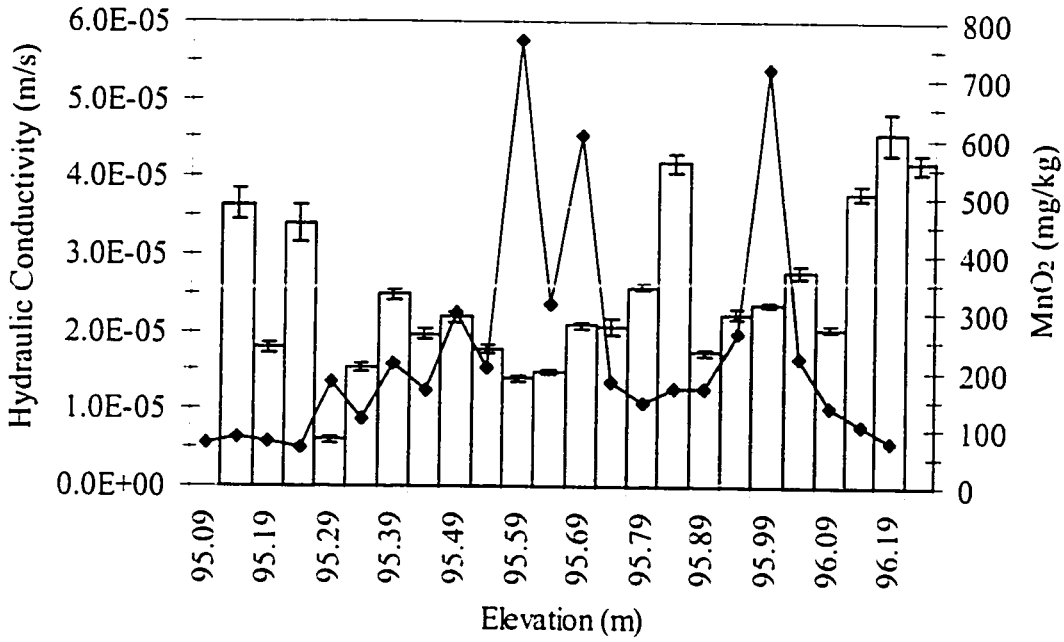

Figure 3.30 Mean hydraulic conductivity (error bars represent one standard deviation of triplicate measurements) and bulk MnO_2(s) concentration (◆) in soil samples from core M6.

3.10 Discussion

3.10.1 Recirculation system performance

The two tracer tests conducted at the field site provided useful data on the performance of the groundwater recirculation system. These tests, in which breakthrough of a conservative tracer pulse was monitored at nine multilevel sampling points and three extraction wells, were operated under conditions comparable to the oxidant flush. The tests were run using the same injection flow rate as the first 100 days of the oxidant flush. During the pre-oxidant flush tracer test breakthrough was observed in eight of nine sampling points, however,~18% of the injected tracer mass had migrated outside of the extraction system's capture zone during the post-oxidant flush tracer test. The tracer data indicated that the injected tracer pulse was effectively delivered to the entire source zone but that the recirculation system did not operate as a completely closed-loop system.

The tracer test data were also used to estimate travel times between sampling points, and the hydraulic residence time (or equivalent pore volume) in the subsurface. While the breakthrough data collected from the 1-m fence multilevels suggested that the injected solution effectively flushed the entire source, the variation in arrival times demonstrated some heterogeneity, likely resulting from a change of the hydraulic conductivity of the source zone within the treatment zone. The hydraulic conductivity variations may have resulted from the source construction procedure and changes in porewater geochemistry. A significant velocity enhancement above the natural gradient velocity (8.3 cm/day) was achieved during both the pre- and post-oxidation tracer tests. The velocities estimated during the pre- and post-oxidation tracer tests were 13 and 11 cm/day, which corresponded to increases of 33 and 57%, respectively. The increase in groundwater velocities in the source zone had important implications for the potential rate of DNAPL removal during the oxidant flush. Higher groundwater velocities increased the mass transfer rate (Equation 2.9) by continuously flushing the source zone with water free of solvents and containing a high oxidant concentration. During the oxidant flush, the higher velocity minimized the effect of oxidant depletion in the source zone.

Several differences between the tracer tests and the oxidant flush make direct extrapolation of the tracer results to the oxidant flush difficult. However, the tracer results provide a limiting case that was useful for comparative purposes. For most of the oxidant flush, the injection and extraction flow rates were less than those during the tracer tests suggesting that the volume of porous media flushed by the injected oxidant solution would also be smaller. As well, the porewater density during the oxidant flush was dissimilar to that observed during the tracer test. The injected oxidant solution contained an average oxidant concentration of ~8 g/L, which corresponds to an increase in solution density of ~0.5% (CRC Handbook of Chemistry and Physics, 55th ed.). In addition, the reaction produced high chloride concentrations which would also increase the solution density. Since the tracer tests employed a dilute tracer concentration unlikely to significantly contribute to the solution density, the recovery of the tracer represented "best-case" conditions for oxidant recovery. While the lower flow rates during the oxidant flush would have less effect on the average groundwater velocity in the treatment zone, the flow rates

were still above the natural gradient velocity in the aquifer. The volumetric flow through the area of the aquifer intercepted by the injection wells was approximately 45 mL/min; the lowest injection flow rate used during the oxidant flush was ~90 mL/min.

3.10.2 Loading reduction and mass removal

Given the difficulties in evaluating the effectiveness of any remedial technology, four separate approaches were employed to compare pre- and post-oxidation contamination (Table 3.5). Samples from the 1-m fence provided peak plume concentration and solvent plume load under natural gradient conditions, tracer effluent data provided a comparable measure of plume load, and analysis of soil samples provided an estimate of the solvent mass present following the oxidant flush.

There were minor differences between the plume loading measurement methods. The effluent flow load measurements were higher than the snapshot load estimates. The consistent ratio between the effluent and snapshot load estimates indicated that the two measurement methods were reproducible and suggested that the methods and the assumptions underlying their use were reasonable. For the four available comparisons (pre- and post-oxidation, TCE and PCE), the solvent load estimated using the snapshot method averaged 42% of that measured with the effluent method, a difference that was consistent with the difference in groundwater velocity between forced-gradient tracer test and the natural-gradient snapshots at the 1-m fence.

Table 3.5 Summary of remediation performance measures.

	Pre-oxidation		Post-oxidation		% Reduction	
	TCE	*PCE*	*TCE*	*PCE*	*TCE*	*PCE*
Load[1] (mg/day)	2099	2218	17	222	99.2	99
Load[2] (mg/day)	836	854	7	98	99.2	88.6
Peak Plume Concentration[3] (µg/L)	142	61	2	31	98.8	49.3
Solvent Mass (g)	9028	1619	0	0	>99.99	>99.99

Notes:
1. Calculated using time-averaged effluent flow loading.
2. Calculated using synoptic samples from the 1-m multilevel fence.
3. Peak concentration observed in 1-m multilevel fence snapshot.

Of the two methods used to estimate the plume load, the effluent load method was preferred since it avoids the uncertainty in the spatial variability of the velocity estimate implicit in the snapshot method and provided a repeatable measurement of plume load which could be statistically evaluated. Accordingly, the quantitative comparisons of source zone strength in the following section employ the measurements of effluent solvent loading.

In addition to the difference between the measurement methods, differences in the ratio of TCE and PCE in the total solvent load were also evident. Prior to the oxidant flush, the measured plume loads for TCE and PCE were statistically identical (n_{TCE}=11; n_{PCE}=11; p=0.01). In contrast, the average TCE load after the oxidant flush was 7% of the PCE load, indicating that the oxidant flush had disproportionately removed TCE from the source zone. Preferential removal of TCE was consistent with the low TCE fraction in the initial source composition and the high solubility and reaction rate of TCE relative to PCE favouring quicker depletion. The oxidant flush resulted in a statistically significant (n_{pre}=11; n_{post}=5; p=0.01) decrease in the effluent loading of TCE and PCE that suggested that the measured reductions reflect the effect of the oxidant flush rather than random sampling variations. The reductions in solvent loads following the oxidant flush were 99.2% for TCE and 88.6% for PCE.

The peak concentrations measured in 1-m fence sampling snapshots were also used as a measure of remediation performance. The reductions in peak concentration of TCE and PCE following the oxidant flush were 98.8% and 49.3%, respectively, which were generally comparable to the reductions in solvent load. However, the reliability of the peak concentration in the 1-m fence was suspect since the location of the peak concentration in the plume may not be coincident with a sampling point.

The decrease in the solvent mass present in the Emplaced Source was estimated to be >99.99% based on a comparison of the simulated change in DNAPL mass at the start of the oxidant flush (Frind et al., 1998) and mass estimated using core samples collected from the source zone

following the oxidant flush. However, several factors indicated that a significant amount of contaminant mass remained with the source including the high chloride concentration observed in the drive-point profile at the end of the oxidant flush, the relatively high dissolved phase concentrations observed following the oxidant flush, and the gradual change in the TCE:PCE ratio in the effluent during the tracer test. The contaminant mass was present as either sorbed phase mass (consistent with the measured VOC concentrations) or as a small zone of DNAPL that was missed by the source zone cores. If the mass was present as a sorbed phase, intraparticle diffusion processes may limit the desorption rate (Wood et al., 1990; Pavlostathis and Mathavan, 1992). While some mass was undoubtedly present in the source as a sorbed phase, this was insufficient to account for the groundwater loads of TCE and PCE observed following the oxidant flush. The small solvent plume present after the oxidant flush most likely resulted from dissolution of a small zone of DNAPL, suggesting that the post-oxidation solvent mass estimates presented in Table 3.5 underestimate the actual mass within the source zone. Removal of the remaining DNAPL mass during the oxidant flush was likely controlled by diffusive transport limitations rather than mass transfer; however, the mechanism that caused the diffusion limitation is not known. While it may have been caused by $MnO_2(s)$ deposition reducing the permeability of the source zone, changes in the groundwater geochemistry caused by the dissolution of gypsum may also have played a role. Since the background aquifer porewater was saturated with respect to calcite, dissolution of the gypsum in the source zone would result in concurrent calcite precipitation. Rivett et al. (1992) estimated a plume source concentration of 510 mg SO_4^- mg/L. Assuming equilibrium exchange of calcite for gypsum, the mass of calcite precipitated since 1989 to the start of the oxidation field study would be ~160 kg or ~25% of the source pore volume. In the event a low permeability calcite front was deposited on the up-gradient face of the ES, the diverging flow field would create a stagnation zone where removal of the DNAPL mass within would be controlled by diffusive transport.

An estimate of the mass of DNAPL oxidized based on the detailed chloride monitoring could not be made. In a best case scenario where the recirculation system was perfectly closed and no chloride losses from the treatment system occurred, the total chloride mass resulting from

contaminant oxidation could be estimated; however, this would only be meaningful in the unlikely event that the initial DNAPL mass and composition was accurately known. Instead, monitoring strategies during the oxidant flush focussed on characterizing the transient changes in the chloride plume produced by removal of the DNAPL source. For a fully closed and recycled treatment system, the rate of DNAPL removal would be comparable to the rate of increase in the chloride concentration. If the efficiency of the extraction system was known, the change in chloride concentration could be corrected for the losses from the treatment zone to estimate the rate of DNAPL removal. However, this could not be done for the data collected during the oxidant flush. While the efficiency of the extraction system was determined to be 82% of the injected tracer mass, this efficiency was not representative of conditions during the oxidant flush. The flow rate during the oxidant flush was similar to the flow rate of the tracer test for only the first 120 days of oxidant injection and was then decreased for the duration of the field experiment. In addition, the density of the oxidant solution, containing a high concentration of both permanganate and chloride, was significantly higher than that of the tracer solution (300 mg/L Br^-), suggesting that the recovery of the extraction system would be lower as a result of density-driven advection below the capture zone of the extraction wells.

The effluent load measurement provided some clear guidance on appropriate and effective performance monitoring strategies. DNAPL is an inappropriate measurement approach since the high heterogeneity of most DNAPL sources make collection of representative samples difficult. Further, at the field-scale DNAPL mass provides minimal information about the benefits of reducing the extent of a groundwater plume with oxidant flushing. Plume loads measured using the effluent method provided a direct measure of the ability of a DNAPL source to generate a groundwater plume. While the effluent plume load measurements assume that a comparable fraction of the plume was extracted during both the pre- and post-oxidant flush plume loading measurements, this is was minor in comparison to the limitations of the snapshot plume loading measurement method. The spatial density of data required for the snapshot measurement was comparatively expensive in terms of the number of samples necessary. In addition, the snapshot plume load employed the average annual linear groundwater velocity (8.5

cm/day) to estimate the velocity normal to the 1-m fence; however considerable seasonal variability in the hydraulic gradient occurs at this site (Figure 3.2). Furthermore, the spatial variability of hydraulic conductivity in the Borden aquifer suggests similar variability in the groundwater velocity that would be difficult to measure. The two methods also differ in terms of evaluating the measurement uncertainty. While the statistical uncertainly in the snapshot method could only be determined by collected replicate snapshots, the effluent plume load estimates require far fewer samples and readily permits statistical analysis of the uncertainty in the measurement.

The reduction in peak solvent concentration did not agree favourably with the reductions in solvent loading, likely as a result of the small spatial extent of the VOC plumes in comparison to the spacing of sample points in the 1-m fence. The use of peak concentrations is not an appropriate approach given the degree of temporal variability observed by previous studies (Feenstra, 1997). An alternative approach at the field scale may be a before-and-after comparison of the mean concentration in a number of sampling points located within the groundwater plume.

3.10.3 Remediation objectives

The experimental results provided insight on methods of assessing technology performance. Current practice focuses on reducing plume concentration at selected monitoring sites and removing mass. The number of spatial and temporal plume samples required can make this an expensive approach. Further, the presence of a small amount of DNAPL in the vicinity of a sample point can easily result in misleadingly high concentrations.

Some field and experimental source remediation efforts have used mass removal as a conceptual measure of aquifer restoration and frequently site engineers report the progress of the remediation strategy by reporting the cumulative solvent mass removed. At field sites, it may be difficult to estimate the mass removed, let alone the DNAPL mass remaining in the aquifer. Factors complicating mass removal estimates include incomplete historical spill reporting,

sparse monitoring data, the sensitive response of DNAPL flow to heterogeneity, and difficulty in interpolating the DNAPL distribution. Recent emphasis has been placed on mass removal since several studies have suggested that little risk reduction is achieved unless at least an order of magnitude reduction in the solvent mass occurs (Freeze and McWhorter, 1997; Sale, 1999). While it is conceivable that source mass could be estimated at some simple sites, the distribution and quantity of DNAPL mass at most DNAPL sites cannot be accurately determined using conventional site characterization techniques. In fact, the highly heterogenous pure phase distributions observed in relatively homogeneous sites like the Borden aquifer suggest that accurate source mass estimates will be infeasible except with expensive and complex *in situ* partitioning tracer tests coupled with inverse models.

In this field experiment, solvent loading and peak plume concentration had similar reductions following the oxidant flush and were both representative measures of remediation effectiveness. This may have been a result of the uncommonly high spatial sampling density employed in this study. With sparser data collection at industrial sites, the estimate of peak plume concentration at a hydrogeologically complex field site might be influenced by changes in the hydraulic gradient. Like the measurement of plume load, the only meaningful assessment of remediation efficacy that may be made using discrete spatial samples is the reduction in concentration at individual monitoring points following an oxidant flush. This has several implications for monitoring at field sites. It requires that steady-state conditions occur before and after the oxidant flush. While frequently there would be sufficient baseline monitoring data to establish a pre-oxidant flush steady-state concentration, monitoring following an oxidant flush may be problematic. The presence of any residual oxidant in the treatment zone will tend to negatively bias a performance assessment, since any residual oxidant could significantly lower the aqueous concentration of a contaminant. Accordingly, VOC monitoring following an oxidant flush should employ multiple sampling points where steady-state VOC concentrations have been previously demonstrated to occur, and should continue at regular intervals until statistical evidence suggests that there is no change in concentration over time at each point. Monitoring following an oxidant flush should rigorously demonstrate a steady-state over a period of at least

one residence time in the treatment zone.

Even with such an approach, however, discrete point concentration measurement provides less information about the extent or potential impact of a solvent plume on a down-gradient receptor than solvent plume load. Plume loading measurement overcomes the constraints of spatial concentration variability by physically integrating the solvent concentration over the capture zone of the extraction system. Assuming that the capture zone completely encompassed the plume, effluent mass loading provides a definitive measurement of the source zone's ability to generate a contaminant plume and the plume's potential impacts on down-gradient receptors.

3.10.4 Oxidant recycling

The potential environmental impacts of the flushing reagent are a major limitation of *in situ* chemical oxidation. Economic and toxicological considerations will likely require containment and treatment of any oxidant that is injected into the subsurface. Containment can minimize down-gradient migration of permanganate, chloride, and soluble Mn(II) and may provide the opportunity to reduce the cost of effluent treatment and additional oxidant through effluent recycling.

The effectiveness of the oxidant containment and recycling system was evaluated using three parameters which included the recovered fraction of the injected oxidant mass, the mass of residual oxidant recycled (or the avoided cost of new oxidant), and the volume of residual oxidant solution for which treatment was avoided. The fraction of the oxidant mass recovered (f_r) was estimated as 49%, with the remaining fraction lost by either migrating outside of the treatment zone or through a reactive mechanism. The oxidant loss emphasised that field applications of ISCO which employ a closed-loop recirculation approach require careful design and monitoring to minimize oxidant losses from the treatment zone. The mass of oxidant required was reduced by recycling 249 kg (31% of the oxidant total mass), a savings that represented a small part of the total cost of this field experiment. In comparison, the mass of oxidant contained in a single pore volume was ~155 kg while the mass of permanganate

required to oxidize the porous media and the contaminants was ~104 kg. A significant benefit was realized by avoiding the requirement to treat the extracted oxidant solution during the oxidant flush. While effluent treatment of 20.5 m^3 was required after oxidant injection was complete, it was substantially less than the 133.5 m^3 of effluent produced during the 484 day oxidant flush. The reduced treatment volume meant that during the oxidant flush only infrequent batch treatment of effluent oxidant was required with large treatment volumes being produced only after oxidant injection was stopped. It is likely the reduced treatment volume would be similarly significant at larger sites, even though the size of the treatment zone would be much larger.

It had been anticipated, based on earlier field experiments that concurrent recycling of chloride along with the oxidant would complicate interpretation of the chloride monitoring data. While it clearly influenced the concentrations observed in the effluent wells, the effect of recycling on the multilevel and profiler observations was minor since the recycled concentration of chloride was small relative to the high concentrations observed in these discrete interval samples. The recycled chloride provided a built-in recirculation system tracer that indicated the spatial extent of the injected oxidant in the treatment zone.

3.10.5 Monitoring source remediation

The monitoring strategy for chloride used three distinct sampling scales. The extraction wells provided an integrated mesoscale approach that was able to identify high rates of source removal but unable to resolve small differences between the injected and the extracted chloride concentrations. The multilevel fence permitted observation of a spatially distinct chloride signature that better indicated source removal. The relatively large chloride signature consistently detected in ML3-10 avoided the need for regular sampling of a large number of the sampling points; however, once the plume became smaller than the sampling scale (i.e., within the spatial resolution of the sampling grid) only erratic detections of the chloride signature were observed. The disappearance of the chloride plume at this sampling scale implied that either oxidation had ceased or that the chloride loading from the source was small. Using the

'microscale' sampling resolution possible with the profiling tool, it was evident that a small chloride plume was still being produced at the end of the oxidant flush. The relatively high chloride concentrations suggested that the plume was being produced by a small DNAPL zone. Discrete sampling tools such as the Waterloo profiler may be particularly appropriate for monitoring source zone remediation since they permit sampling in close proximity to the source zone.

3.11 Implications for other sites

Freeze and McWhorter (1997) completed a qualitative analysis of risk reduction as a result of DNAPL mass removal from low permeability soils and concluded that "very high total mass removal efficiencies are required to achieve significant long-term risk reduction" and suggested that these mass removal efficiencies were not attainable. In a similar effort, Sale (1999) examined pool removal using an analytical approach to evaluate risk reduction and offered similar conclusions. These results, based on analyses assuming equilibrium partitioning, are partly reinforced by the results of this experiment. In contrast to the expectations of Freeze and McWhorter (1997), high mass removals were achieved; however, this removal resulted in a comparatively modest plume loading reduction. This experiment and that of Schnarr et al. (1998), demonstrated that the high mass removals necessary for significant risk reduction are attainable in at least some hydrogeological settings.

The large reduction in solvent load suggests that a substantial benefit was achieved by the oxidant flush. For example, the pump and treat system at the emplaced source used several extraction wells along the length of the plume but was operated with only a single pumping well for several years prior to closure. The average effluent TCE and PCE concentrations from the pumping wells during the final two years of data collection (Nov-93 to Nov-95) were 506 µg/L and ~191 µg/L at the beginning of the oxidant flush. Given the measured plume load reductions for the two solvent components contained by the pump and treat system (99.2% for TCE and 90% PCE), the solvent concentrations expected in the pump-and-treat system would be 4 µg/L TCE and 19 µg/L PCE. A comparable reduction in the operation and maintenance cost of the

treatment process associated with the pump-and-treat system would be anticipated. In the event that this reduction was achieved at a large field site, the cost saving over the operating life of a pump and treat system, even though a groundwater plume remained, could be significantly larger than the original cost of the oxidant flush.

Chapter 4
Model Development and Application

4.1 Introduction

A limited number of field applications of ISCO have been reported in the literature that provide useful design and performance data. As a consequence, little guidance is available to assess the relative effectiveness of alternative design strategies for ISCO using permanganate. Most of the reported ISCO field demonstrations using permanganate, including the present study, have employed forced-gradient schemes to flush the contaminated soil (West et al., 1997; Schnarr et al., 1998). At these field sites, the conceptual design of the flushing system consisted of oxidant injection wells on the up-gradient side of the source zone with extraction wells located down-gradient to contain the reaction products and residual oxidant. The complex interaction of groundwater flow in a forced-gradient flow system with kinetic chemical reactions and rate-limited mass transfer suggests that sophisticated modelling tools are required to compare oxidant flushing system designs and analyse laboratory and pilot test data.

The design of an effective and appropriate ISCO treatment system is controlled by a variety of interrelated factors including:

- economic constraints, such as the cost of oxidant required to flush the zone of contamination and the costs of constructing and operating the flushing system;

- regulatory requirements to protect groundwater resources from injected reagents, reaction products, or other negative impacts on water quality;

- the extent of monitoring data describing the groundwater flow system, background geochemistry, and the spatial extent of the DNAPL; and

- the ability to deliver concentrated oxidant to the contaminated soil.

These design factors suggest that flushing systems should deliver the minimum volume of oxidant solution to treat the DNAPL zone without extending into uncontaminated portions of the aquifer. In the absence of extensive empirical data, effective design of a ISCO system is only possible by comparing the performance of design alternatives through numerical modelling. Development of a model also provides an opportunity to improve the scientific understanding of a complex treatment technology. The results of a model which mathematically incorporates the relevant processes may be compared to experimental data to test the fundamental physico-chemical concepts from which the model was developed.

A three-dimensional numerical model was developed to simulate the ISCO remedial process. The model presented in this research was based on the comprehensive 3D3PT model developed by Thomson (1995), which simulates transient three-dimensional flow and multi-component reactive transport. The transport solution in 3D3PT permits rate-limited mass transfer from a multi-component non-aqueous phase. The model developed during the current research (FLUSH) was adapted from 3D3PT to include:

- transport of additional aqueous phase components representing a non-specific oxidant and a single reaction product;

- kinetic terms describing the reaction between the oxidant and solvent species connected by the stoichiometric mass ratios of two reactants and the product;

- a kinetic term representing the reaction between the oxidant and organic carbon present in porous media;

- a kinetic term representing rate-limited mass transfer from the non-aqueous phase to the aqueous phase that permits the use of one of several empirical correlations for the mass transfer rate coefficient; and

- periodic updating of the aqueous phase flow field at an interval dependent upon the maximum change in the DNAPL saturation.

The modifications were necessary to adequately describe the physico-chemical process models described in Chapter 2. The intent of the model development process was to create an analysis tool that could be applied to the design and analysis of field-scale ISCO treatment systems. FLUSH incorporates a two-stage solution process which is described in detail in Section 4.2. In the initial phase of the solution, the two-phase flow equations (NAPL and water) are solved until a near steady-state condition occurs, permitting the simulation of physically realistic NAPL source zones within the domain. In the second phase of the solution, the solute transport equations for the relevant chemical species are solved. During the transport solution, the aqueous phase flow field is periodically updated to accommodate changes in the relative permeability caused by depletion of the non-aqueous phase. The non-aqueous phase is assumed to be immobile, a reasonable assumption since the NAPL mass providing the driving force for flow is depleted by the oxidation reaction during the simulation.

4.1 Model assumptions and limitations

Early transport models assumed that dissolution was essentially instantaneous and employed the local equilibrium assumption to describe the mass transfer process. Subsequent studies (described in Chapter 2), however, have resulted in empirical expressions to relate the mass transfer rate coefficient to soil properties and the non-aqueous phase saturation (i.e., Powers et

al., 1994). In addition, recent numerical analysis of Borden field data has suggested that both equilibrium and rate-limited conditions can occur (Frind et al., 1998). Given the mass transfer enhancements observed in ISCO experiments, rate-limited mass transfer is a significant process; however, the applicability of the various mass transfer expressions to the high mass transfer rates occurring in a highly concentrated oxidant solution is unknown.

The model assumes that the porosity and permeability of the porous medium are constant in time. This simplification was made despite the known formation of $MnO_2(s)$ by the oxidation reactions in the void space. The precipitate reduces the porosity, which proportionately increases the average linear groundwater velocity but decreases the water volume available for mass transfer. These competing effects may offset one another. In the case of low or residual DNAPL saturations, removal of the pure phase from the void space and carbonate dissolution stimulated by the acid produced by the reaction are counter-balancing factors which may also minimize the change in porosity. Several means of correlating changes in porosity with permeability are available in the literature. For example, the Carmen-Kozeny equation correlates permeability and porosity. Using another empirical approach, Sanford and Konikow (1989) incorporated changes in porosity and permeability resulting from calcite dissolution in a modeling study of saline intrusion into a freshwater aquifer. Porosity changes were directly calculated from equilibrium speciation of calcite and the corresponding change in permeability was calculated using an empirical correlation derived from data collected as part of petroleum reservoir studies. These empirical approaches may tend to underestimate the change in permeability caused by $MnO_2(s)$ deposition since the precipitate will change the interconnectivity of the pore bodies in addition to decreasing the average pore diameter.

Changes in porosity and permeability are likely to be of great importance in the case of porous media containing high DNAPL saturations. There is substantial anecdotal evidence to suggest that permanganate flushing can encapsulate regions of high DNAPL saturation in an impermeable shell of $MnO_2(s)$ (e.g., Mackinnon (1998), Tunnicliffe (1999), Urynowicz and Siegrist (2000), and S. Reitsma, personal communication, 23 May 2000), a process which will

prevent advection through the DNAPL zone and limit mass transfer to a rate sustained by diffusion of the contaminant through the dense MnO_2(s) shell.

While these studies have helped define the difficulty in incorporating the formation of MnO_2(s) into the model, they indicate the further investigate the impact of MnO_2(s) on mass transfer rates and permeability. While it appears evident that the formation of MnO_2(s) is an important process that will have significant effects on permeability and mass transfer rates, there is currently no experimental basis to develop a relationship that captures this process. Until appropriate experiments are completed, inclusion of MnO_2(s) formation, colloidal transport, and deposition in this model would not be appropriate.

Several further assumptions were made which simplified incorporation of the chemical reactions in FLUSH. While Yan and Schwartz (1999) identified unstable intermediate organic compounds resulting from oxidation of chlorinated alkenes, the reactions incorporated within FLUSH assumed that the degradation rates of these intermediates were instantaneous relative to the degradation rate of the parent contaminant. This assumption implies that the rate of chloride production is equivalent to the rate of contaminant degradation multiplied by the molar yield of chloride ions per mole of contaminant.

Reaction rate constants were assumed to be independent of solution pH. While it has been demonstrated that the reaction rate of TCE was essentially constant over pH 4-8, the validity of this assumption in the highly acidic solution (pH<1) observed by MacKinnnon (1999) is not known. In a highly acidic solution, permanganic acid may be the active oxidant rather permanganate (Stewart, 1973); however, no data is available describing the kinetics of this oxidant. Under extremely low pH conditions, the geochemistry is complicated since the reactivity of several mineral phases, including manganese dioxide and carbonate minerals, are also influenced by pH. At low pH, carbonate minerals rapidly dissolve and the stability of MnO_2(s) decreases in favour of soluble Mn(II). The divalent manganese may then be reoxidized by permanganate, which reduces the mass of permanganate available for contaminant degradation. While this effect may be sufficiently minimized by the buffering capacity of the

aquifer so that this process is not significant, incorporating these reactions in the model was beyond the scope of this thesis.

Finally, numerical solution of multi-phase flow problems challenges the fundamental assumption of the continuum approach. DNAPL flow is influenced by slight contrasts in soil properties which can vary over a few millimetres. This scale is inconsistent with typical model discretization where grid blocks are $\sim 10^{-1}$ m and violates the assumption that each grid block represents the macroscopic properties of the porous media. The applicability of multi-phase flow models employing this approach is uncertain but the violation is of some consequence for the transport component of the model. The contrast in scales suggests that rate-limited mass transfer compensates for averaging of the DNAPL saturation within the grid block and, as a result, is a scale-dependent phenomenon. With coarse discretization, mass transfer will increase in importance, while with finer discretization transport phenomena will dominate DNAPL mass removal.

4.2 Governing Equations

As part of the model development process, quantitative expressions for phase and solute conservation were derived. This section presents the governing equations that describe multiphase flow and transport of n_c+2 solutes in porous media. The governing equation representing flow of water and a homogeneous NAPL are (Bear, 1972),

$$\frac{\partial (\phi \rho_\beta S_\beta)}{\partial t} = \frac{\partial}{\partial x_i} \left[\frac{\rho_\beta \, k_{ij} \, k_{r\beta}}{\mu_\beta} \left(\frac{\partial P_\beta}{\partial x_j} - \rho_\beta \, g \, e_j \right) \right] + \Gamma_\beta \qquad i,j = 1,2,3 \qquad (4.1)$$

where β represents either the water (w) or NAPL (nw) phases; ϕ is the porosity, ρ_β is the phase density, S_β is the phase saturation, k_{ij} is the intrinsic permeability field, $k_{r\beta}$ is the relative permeability, μ_β is the absolute viscosity, P_β is the pressure, g is the gravitational acceleration, e_j are the components of a unit vector in the positive z-coordinate direction $<0,0,1>$, and Γ_β is a mass sink or source. Details of Equation 4.2 and the accompanying constitutive equations are presented by Thomson (1995).

The mass conservation equation incorporating advection and dispersion formed the basis of the transport solution for multiple transport species with kinetic source and sink terms. The transport species considered were organic contaminants (of which an arbitrary number of contaminants are contained within a homogenous non-aqueous phase mixture) with kinetic mass transfer between the aqueous and non-aqueous phases, a single oxidant which reacts with the organic contaminant(s) in the aqueous phase, and a single conservative reaction product. Since the oxidation rate was dependent on the concentration of the oxidant and the organic species, transport of both was included. Transport of a conservative reaction product was included since most applications of ISCO have involved extensive chloride monitoring. The remaining reaction products (CO_2 and MnO_2) are not included in the model since they would be of limited use as reaction tracers.

The NAPL phase was assumed to consist of a homogeneous mixture with n_c constituents. The total number of transport components are given by (n_c+2), where the $(n_c+1)th$ component is an oxidant and the $(n_c+2)th$ component is a conservative reaction product. The partial differential equation for mass continuity incorporating aqueous phase advective-dispersive transport is given by Bear (1972),

$$\frac{\partial(\phi S_w C_n)}{\partial t} - \frac{\partial}{\partial x_i}\left[\phi S_w (D_{ij})_n \frac{\partial C_n}{\partial x_j}\right] - q_i \frac{\partial}{\partial x_i}(C_n) \pm \gamma_n = 0 \qquad n = 1,\ldots,n_c+2 \tag{4.2}$$

where x_i and x_j are the Cartesian coordinates, C_n is the mass concentration of component n, D_{ij} the hydrodynamic dispersion tensor, q_i is the Darcy flux, ϕ is the medium porosity, S_w is the aqueous phase saturation, and γ_n represents either sources or sinks of component n. The source and sink terms represent chemical reactions such as oxidation, hydrophobic partitioning between the aqueous and solid phases, mass transfer between the non-aqueous and aqueous phases, and well boundary conditions.

The terms of the hydrodynamic dispersion tensor are given by (Bear, 1972),

$$D_{ij} = \alpha_t |q| \delta_{ij} + (\alpha_l - \alpha_t) \frac{q_i q_j}{|q|} + \phi S_w (D_m)_\alpha \tau \delta_{ij} \qquad (4.3)$$

with,

$$\tau_w = \frac{(\phi S_w)^{7/3}}{\phi^2} \qquad (4.4)$$

where α_l and α_t are the longitudinal and transverse dispersivities, δ_{ij} is the Kronecker delta function, D_m represents the free molecular diffusion coefficient, and τ is the medium tortuosity given by (Millington, 1959).

Dissolution was described using the well-known stagnant film model described in Section 2.2.2,

$$\gamma_n^{NAPL-w} = -\lambda_n (C_n^{sat} - C_n) \qquad n = 1 \ldots n_c \qquad (4.5)$$

where λ_n is the lumped dissolution mass transfer rate coefficient and C_n^{sat} is the effective aqueous solubility of component n. The mass transfer rate coefficient may be evaluated using any of the approaches described in Chapter 2.

The reaction terms for each of the n_c solvent components are based on rate and stoichiometric data for oxidation of chlorinated alkenes by permanganate reported in Chapter 2. The reaction rate was assumed to be irreversible and first-order with respect to each reactant, such that,

$$\gamma_n \equiv -\phi S_w k_n C_n C_{n_c+1} \qquad n = 1, \ldots n_c \qquad (4.6)$$

where k_n is the second-order reaction rate constant for component n. Estimates of k_n used in the current study are based on the kinetic data summarized in Table 2.2. The corresponding rate of oxidant consumption is represented by the sum of the rates of oxidant consumption required by the n_c organic components plus the rate of consumption by the aquifer solids (as an initial

approximation the rate of consumption by the solids was assumed to be first-order with respect to concentrations of the oxidant and the organic carbon in the soil). Oxidant consumption and chloride production are described by,

$$\gamma_{n_c-1} \equiv -\phi S_w \left[\sum_{n=1}^{n_c} \left(M_{f_{n,n_c-1}} k_n C_n C_{n_c-1} \right) + k_{foc} C_{foc} C_{n_c-1} \right] \tag{4.7}$$

with,

$$C_{foc} = (foc)\, O_D\, \rho_{bulk} \phi \tag{4.8}$$

and,

$$\gamma_{n_c-2} = \phi S_w \sum_{n=1}^{n_c} M_{f_{n,n_c-2}} k_n C_n C_{n_c-1} \tag{4.9}$$

where k_{foc} is an assumed second-order rate constant for oxidation of soil organic matter, C_{foc} is the concentration of organic matter expressed as an oxidant demand per unit volume of void space, O_D is the specific oxidant demand per unit mass of dry soil per *%foc* (defined in Appendix A), ϕ is the porosity, and $M_{f_{n,n_c-1}}$ and $M_{f_{n,n_c-2}}$ are the stoichiometric mass ratios of permanganate decomposed or chloride produced relative to a unit mass of solvent component n oxidized. No data for k_{foc} are available although the results of the column experiments reported in Appendix A suggest that the oxidation of organic carbon and reduced minerals in sand is a rapid reaction.

4.2.1 Numerical solution methodology

The governing equations were approximated utilizing a control volume numerical approach that employed a flexible system of assigning boundary conditions. To reduce the computational burden, a sequential approach was used to simulate flow and transport components within the model. Decoupling of the flow and transport equations was efficiently achieved by updating the aqueous phase flow solution during transport after any grid block exceeded a specified change in non-aqueous phase saturation since the previous flow solution. This procedure, consistent with the small changes in the water-phase relative permeability expected for this

criterion, required relatively few solutions of the discretized flow equations. The resulting set of highly non-linear equations were solved using a full-Jacobian iterative approach in conjunction with a preconditioned conjugate-gradient solver.

Conservation of non-aqueous phase mass was achieved through direct calculation of the mass transfer rates such that,

$$\phi S_w \frac{\partial M_{mw}}{\partial t} - \gamma_n^{NAPL-w} = 0 \tag{4.10}$$

where M_n is the mass of component n per unit volume of porous medium. Cumulative mass balances were calculated for each of the n_c+2 solutes at the end of each time step. For each solute, the mass balance was calculated as,

$$\Delta M = M_w - M_s - M_{NAPL} - M_{input} - M_{output} \tag{4.11}$$

where ΔM is the change in solute mass, M_w is the mass in the aqueous phase, M_s is mass in the sorbed phase, M_{NAPL} is the mass in the NAPL phase, M_{input} is the total mass entering the domain and M_{output} is the total mass exiting the domain. Accordingly, ΔM includes the change in solute mass caused by the oxidation reactions in addition to numerical error. For simulations where all species were assumed to be conservative (i.e., k_{foc} and k_n are zero), numerical accuracy was indicated by the magnitude of ΔM. In simulations with non-zero reaction rates, mass balances were checked by calculating the ratio of ΔM to the oxidant and chloride species over the change in contaminant mass, which should be identical to the stoichiometic mass ratios ($M_{fn\ n-1}$ and $M_{fn\ n-2}$) assigned for each component.

4.2.2. Relative significance of oxidation and dissolution kinetics

Applying the equations of mass conservation to an elementary volume of porous media provides some preliminary insight into the interaction of the oxidation and dissolution rates. In particular, the effect of changes in the oxidation rate, which is controlled in part by the design

of an oxidant flush, can be compared to changes in mass transfer rate. Assuming a batch system, the solvent mass conservation equation for a unit volume of porous media containing a single non-aqueous phase component is,

$$\frac{\partial C_1}{\partial t} = \lambda(C_1^{sat} - C_1) - k_2 C_1 C_2 \tag{4.12}$$

where C_1 is the solvent concentration, and C_2 is the oxidant concentration. At steady-state, the oxidant concentration is constant such that $k=k_2C_2$ and the equilibrium concentration of the solvent is given by,

$$\frac{C_1}{C_1^{sat}} = \frac{1}{(1 - k/\lambda)} \tag{4.13}$$

From inspection of the limits taken with respect to the oxidation rate constant, the steady-state solvent concentration approaches the solubility limit as $k \to 0$ or $\lambda \to \infty$ and approaches zero as $k \to \infty$ or $\lambda \to 0$. While the effect of the mass transfer rate coefficient appears obvious, the real significance of Equation (4.13) are the implications for the rate of NAPL mass removal as a function of the oxidation rate. If C_1 is large (i.e., because a particular oxidation reaction has a low rate constant or the oxidant concentration is low), Equation (4.13) suggests that the small dissolution gradient caused by the high equilibrium solvent concentration will result in a low mass removal rate. The opposite situation occurs for a small C_1 up to a maximum mass transfer rate of . Overall, the mass removal rate will be controlled by the ratio of the rate coefficients for oxidation and dissolution. As shown in Figure 4.1, as k/λ becomes large, the small change in C_1 has a negligible effect on the mass removal rate. A typical value of the mass transfer rate coefficient estimated by the correlation of Powers et al. (1990) is 10^{-4} sec^{-1}. Substituting the degradation rate of PCE mixed with 10 g/L permanganate, the ratio of k/λ is $\sim 10^{-1}$-10^{0}. In this range, the value of C/C^{sat} is sensitive to the rate ratio; however, at higher reaction rates, DNAPL mass removal is controlled by the mass transfer rate coefficient and the aqueous solubility limit, and is insensitive to the reaction rate. In this range, criteria other than reaction rate, such as reagent safety, reactivity with site-specific contaminants and natural reductants, and the

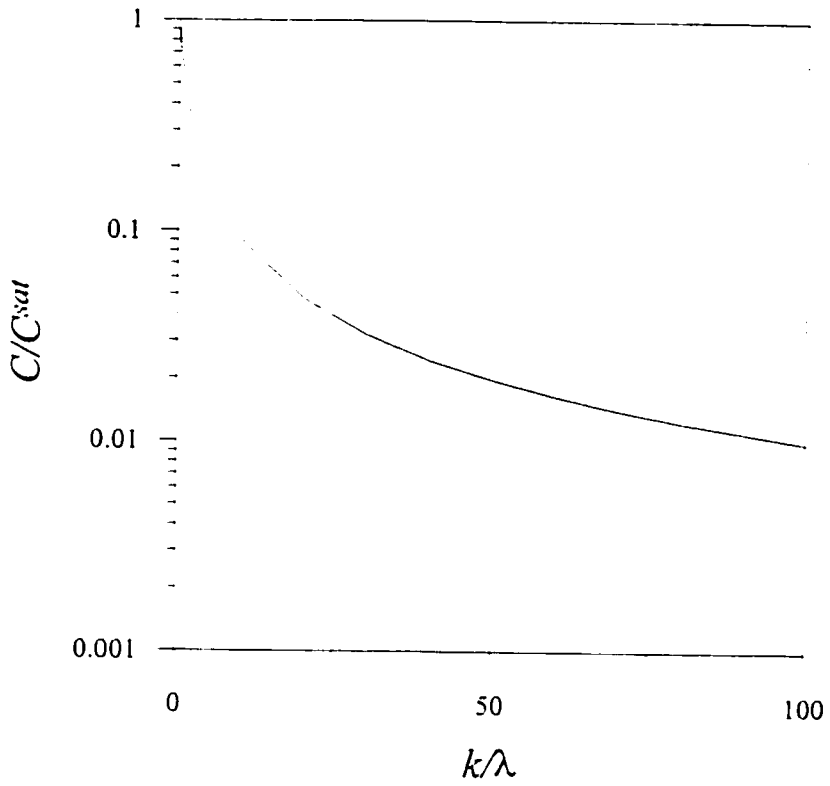

Figure 4.1 Impact of the rate constant ratio (k/λ) on steady-state aqueous solvent concentration for a constant oxidant concentration.

formation of reaction products (precipitates, heat, gas, etc.) govern oxidant selection.

4.3 Model testing

4.3.1 Reaction rate and stoichiometry

The kinetic reaction terms and stoichiometry incorporated into the numerical model were tested using a homogeneous one-dimensional domain without advection (essentially a homogeneous batch reaction system). Initial concentrations of 0 mg/L Cl^-, 1 g/L $KMnO_4$ and 100 mg/L PCE (k_{PCE} = 2.45 M^{-1} min^{-1}) were specified throughout the domain. The simulated results were compared to an analytical solution of the rate law for PCE degradation (Equation 2.34) given by,

$$[PCE](t) = \frac{A[PCE]_0}{[MnO_4^-]_0 e^{(Ak_{PCE}\, t)} - M_{f_{PCE,\ MnO_4^-}}[PCE]_0} \qquad (4.14)$$

where $A = [MnO_4^-]_0 - M_{f_{PCE,\ MnO_4^-}}[PCE]_0$. Based on the change in PCE concentration determined using Equation (4.14), the corresponding changes in the chloride and oxidant concentrations were stoichiometrically calculated and compared to results generated with FLUSH (Figure 4.2). The close agreement between the model results and the analytical solution indicated that model correctly solved the rate and stoichiometry of the oxidation reaction for each of the three simulated transport components.

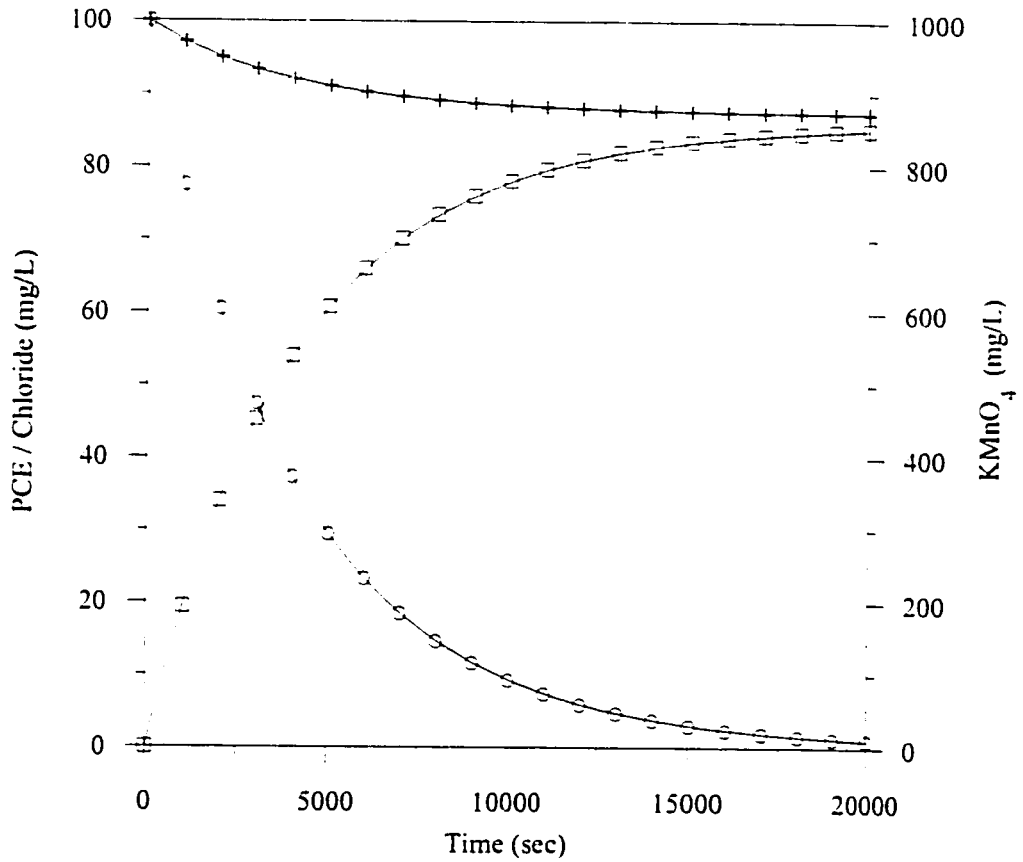

Figure 4.2 Comparison of FLUSH (lines), and analytical solution (symbols) for chloride (□), permanganate (✚), and PCE (○).

4.3.2 Mass balances: one-dimensional column

A comparison of the model results against an analytical solution of the advection-dispersion equation and mass balances were used to check the numerical accuracy of the solution and to verify the numerical approach employed in the model. Simulations were completed examining a horizontal one-dimensional domain (0.3 m long x 0.05 m wide x 0.05 m thick) composed of 60 x 1 x 1 control volumes (Figure 4.3); however, the total domain length extended to 0.6 m to simulate a 30 cm semi-infinite domain. The left and right sides of the domain were assigned constant water phase heads equivalent to a hydraulic gradient of 0.2 m/m, resulting in a Darcy flux of 3.1×10^{-6} cm/s (corresponding to a linear groundwater velocity of 6.6 cm/day) through the column. Longitudinal dispersivity was assigned a constant value of 2 cm while the contaminant species was assigned the properties of PCE (C_{sat}=237 mg/L, r=1.62 g/cm^3, $M_{PCE,\ MnO_4^-}$=1.27, $M_{PCE,\ Cl^-}$=-0.86). The transport boundary conditions applied to the left boundary are described in the following.

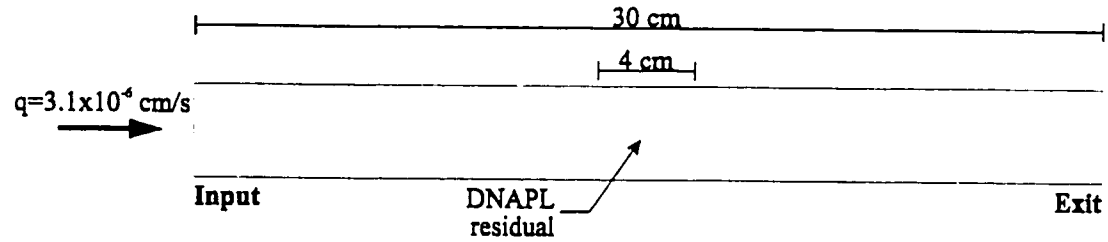

Figure 4.3 Model domain for one-dimensional simulations.

In the first simulation, constant concentrations (250 mg/L) of three non-reactive, non-sorbing solutes were specified at the left boundary. The breakthrough curve determined with FLUSH agreed closely with that calculated using the Ogata-Banks solution (Freeze and Cherry, 1979; Figure 4.4a), indicating that FLUSH solved the advective-dispersive transport problem accurately under this set of conditions.

A second simulation (Figure 4.4b) was completed with constant concentrations of 237 mg/L PCE, 500 mg/L $KMnO_4$, and 0 mg/L chloride specified at the input boundary. A non-zero

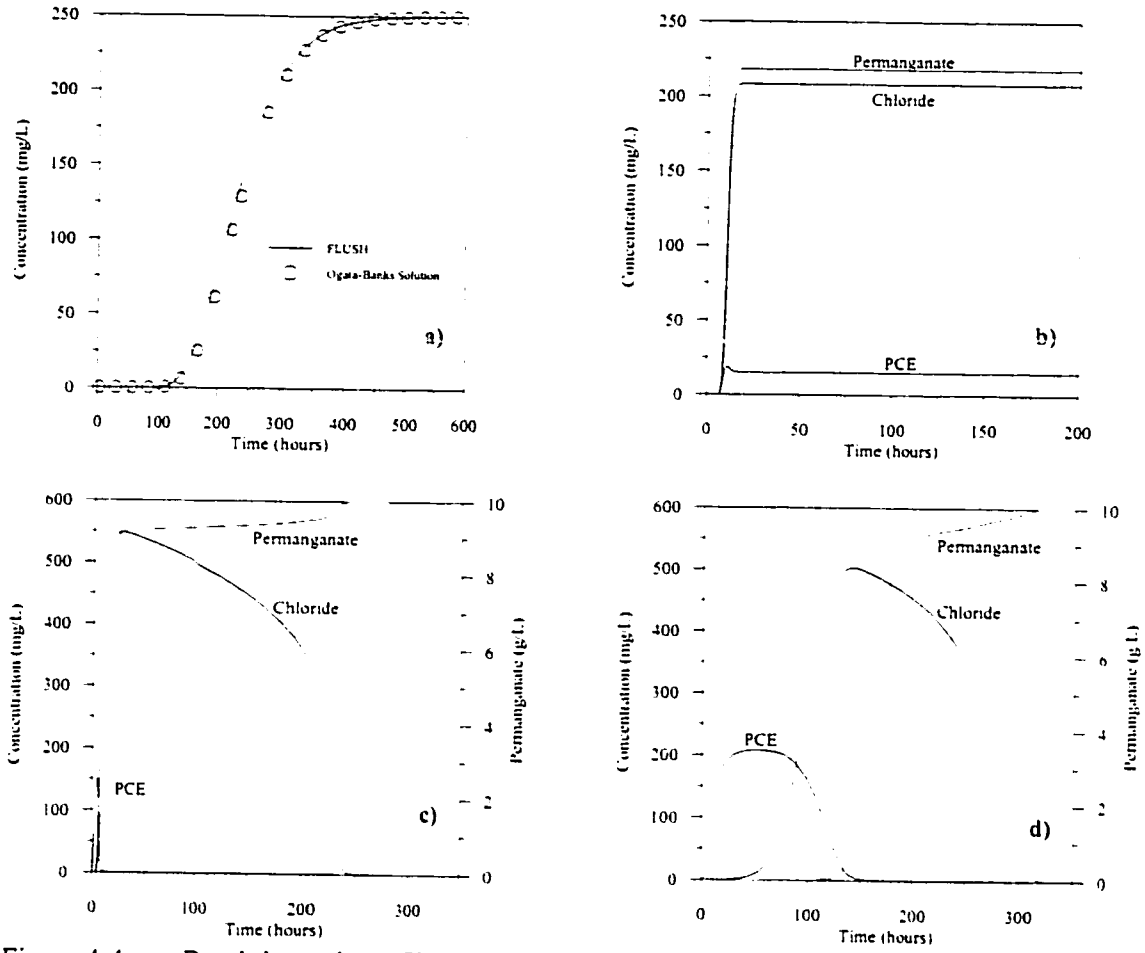

Figure 4.4 Breakthrough profiles one-dimensional simulations a) comparing FLUSH to the Ogata-Banks solution; b) specified concentrations for three reactive solutes at the input boundary; c) 10 g/L of permanganate at the input boundary with a zone of DNAPL residual (no reaction with soil); and d) 10 g/L of permanganate at the input boundary with a zone of DNAPL residual (reaction with soil).

oxidation rate was specified using the specific rate constant for PCE (k_{PCE}=2.45 M^{-1} min^{-1}). PCE was assumed to be non-sorbing and the porous media was considered non-reactive. At the exit boundary of the domain, breakthrough of the high concentration permanganate front was followed immediately by the PCE and chloride fronts. At breakthrough, the concentration of PCE was slightly higher than the steady-state concentration since breakthrough of the steady-state permanganate concentration had not yet occurred. After ~15 hours, the concentration of each species was steady-state. A low concentration of PCE (~15 mg/L) exited the domain since

the residence time and the concentration of permanganate was insufficient to completely degrade the input concentration.

In the remaining two simulations, the influence of soil oxidant demand on DNAPL removal was demonstrated. A 4 cm zone of homogeneous residual DNAPL (S_{nw}= 6%) was specified at the centre of the domain and flushed with 10 g/L permanganate. Mass transfer rate coefficients for the DNAPL were estimated using the correlation presented by Powers et al. (1994). One simulation was completed with non-reactive non-sorbing porous medium (Figure 4.4c) while the other (Figure 4.4d) contained a reactive sorbing porous medium (*foc*= 0.3%, O_D= 100 g/kg/%*foc*). Sorption was modelled using a linear isotherm. In the simulation with non-reactive porous media, a small pulse of dissolved phase PCE exited the column and was truncated once the oxidant front migrated through the source zone. As the oxidant front passed the source zone, the oxidant concentration throughout the PCE source zone was sufficiently high that the dissolved phase PCE was completely oxidized to chloride before exiting the domain. Breakthrough of the oxidant front was only slightly delayed relative to the chloride front as a result of oxidant consumption by the reaction with PCE in the source zone. At the same time, the concentration of the effluent chloride increased to a maximum and then steadily decreased as mass was depleted from the source zone. Once the DNAPL was completely removed, the chloride concentration rapidly dropped to zero while the oxidant concentration increased to the input concentration of 10 g/L. The inclusion of the oxidation reaction with the porous media provided a comparable result that reflects the effect of natural organic carbon on DNAPL removal. Figure 4.4(d) presents the results of a simulation with a reactive porous medium where both the soil-oxidant reaction and PCE sorption were included. In comparison to the non-reactive case, the initial effluent PCE pulse exited the column later and was of longer duration and higher concentration since migration of the oxidant front through the column was delayed by the reaction with the porous media. Similarly, there was longer lag between breakthrough of the chloride and oxidant fronts as the oxidant front was depleted by the reaction with the soil between the source and the exit boundary. As in the non-reactive case, chloride was rapidly produced as the pure phase was depleted from the column.

While these simulations demonstrated that the modelling results were qualitatively consistent with the column experiments reported by Schnarr et al. (1998), the non-linearity and interdependent reaction kinetics of the model made further validation possible only by direct comparison to reliable experimental data. The one-dimensional simulations presented above (particularly Figure 4.4d) are based on the column experiments conducted by Schnarr et al. (1998); however, only qualitative comparisons of the model can be made to these experiments since matching the experimental data exactly proved difficult (results not shown). While it may be that a conceptual weakness of the model was responsible for the poor fits, the lack of sufficient detail describing the DNAPL distribution and the properties of the porous media (especially *foc*) suggested that the limitations of the data set may have been partially responsible for the poor comparisons.

As a check of the numerical accuracy of these simulations, the two mass balance formulations discussed in Section 4.2.1 were calculated (Table 4.1). In the non-reactive simulation, the calculated mass balance errors were $\sim 10^{-17}$, a small error that is less than the numerical convergence tolerances specified for the solver package, which indicated that the transport solution conserved solute mass correctly. The second check of mass balance for the reactive simulations (b, c, and d) were the ratios of the chloride and permanganate mass balance to the

Table 4.1 Summary of 1D column simulation mass balance results (outline indicates reactive simulations).

	Rxn with PCE?	Rxn with soil?	Mass transfer?	Species Mass Balance			Calculated		$\Sigma Cl/Cl_0$
				PCE	Oxidant	Chloride	$M_{PCE\ ox}$	$M_{PCE\ Cl}$	
a)	No	No	No	-8.67e-16	-8.67e-16	-8.67e-16	-	-	1.000
b)	Yes	No	No	-1.61e-03	-2.04e-03	1.38e-03	1.27	-0.86	1.000
c)	Yes	No	Yes	-2.71e-03	-3.42e-03	2.33e-03	1.26	-0.86	0.995
d)	Yes	Yes	Yes	-2.24e-03	-5.83e-02	1.91e-03	NA[1]	-0.85	0.993

solvent mass balance, which should match the stoichiometric mass ratios ($M_{fa\ n-1}$ and $M_{fa\ n-2}$) specified during input. In all cases the mass balance ratios were within 1% of those specified, indicating that the solutions were correct. The largest errors in mass ratios occurred for simulations where a DNAPL phase was present. This may resulted from the small error in the conservation of water phase mass introduced by depleting DNAPL mass and artificially introducing water in between the flow updates to maintain saturated conditions in each control volume; the resulting increase in water mass in the domain replacing the DNAPL may artificially have introduced a small quantity of additional solute mass of each transport species.

4.4 Application: One dimensional diffusion with reaction

In many geologic environments, dissolution is limited by diffusive transport processes rather than the dynamic influence of mass transfer. A simplified conceptual model of diffusion limited mass transfer from a hydraulically isolated DNAPL blob is shown in Figure 4.5; while a fracture is shown, the same general concept is equally applicable to diffusion-limited mass transfer in porous media occurring as a result of heterogeneity. Similar to the conceptual model describing the mechanism through which the mass transfer enhancement during ISCO occurs (Figure 2.11), Figure 4.5 represents a scenario in which diffusion of the aqueous phase solvent from the phase interface to the region of advective flow limits dissolution of the trapped DNAPL. Under conditions of natural groundwater flow, the advective zone contains some concentration of aqueous contaminant and mass transfer is limited by the path length that each solvent molecule must travel before entering advective flow outside of the fracture. Since mass removal is through diffusion, the mass flux of solvent is inversely proportional to the path length and the solvent concentration in the advective zone. However, if the advective zone contains a high concentration of an oxidant such as permanganate, the oxidant can diffuse into the fracture where it reacts with the aqueous solvent, steepens the concentration gradient, and increases the solvent mass flux across the phase interface. This process of counter or two-way diffusion can result in a mass transfer enhancement.

The effect of this phenomenon on DNAPL mass removal rates was examined using a simplified

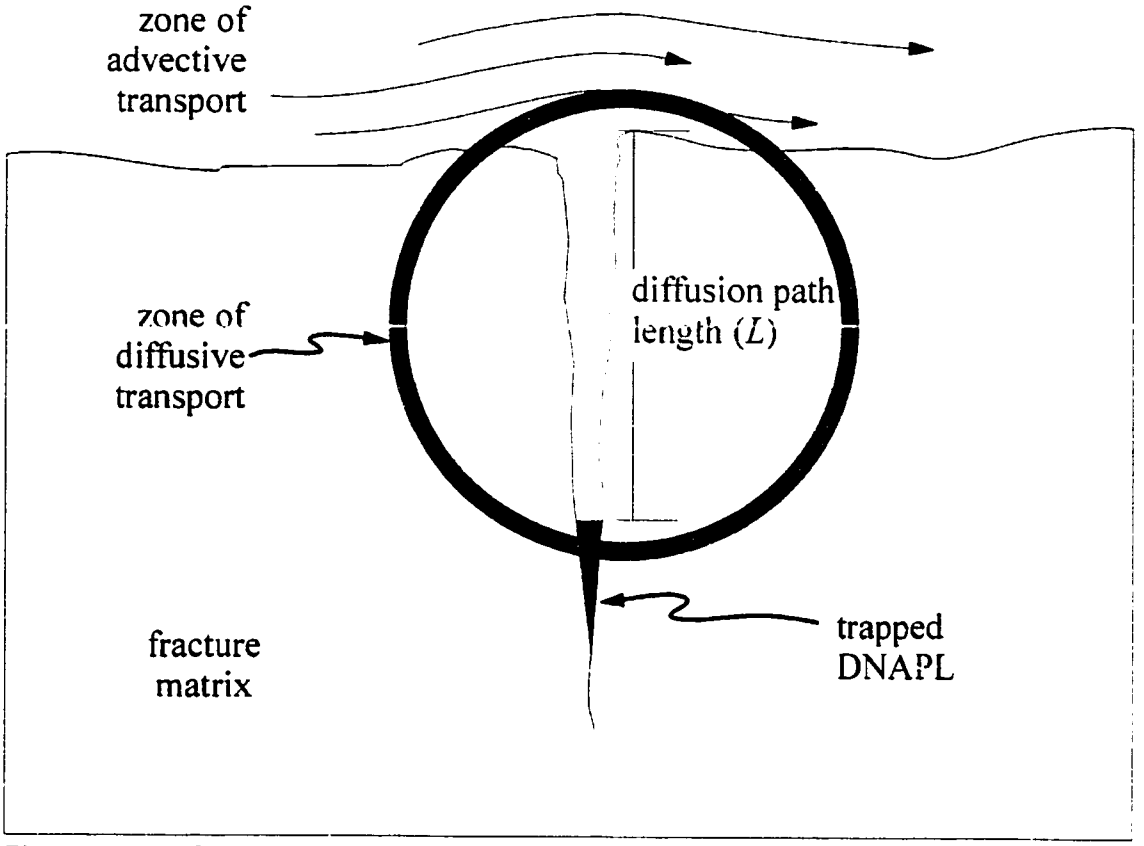

Figure 4.5 Conceptual diagram of diffusion-limited mass transfer from DNAPL in a hydraulically isolated region.

one-dimensional domain (100 control volumes of variable size) without advection. A zone containing a high DNAPL saturation (PCE) was specified near one boundary. On the opposite boundary, a constant oxidant concentration was specified (500 mg/L $KMnO_4$); zero-concentration gradients formed the remaining boundary conditions. The reaction rate for PCE was specified and the porous media was assumed to be non-reactive. Simulations using five diffusion path lengths (5, 10, 20, 30, and 60 cm) were run until steady-state rates of DNAPL mass removal were observed. A sixth simulation was performed to demonstrate the effect of mass transfer limitations on DNAPL removal by specifying a constant oxidant concentration (500 mg/L) across the domain. This simulation represented the case where perfect oxidant delivery occurred and only mass transfer limited DNAPL removal.

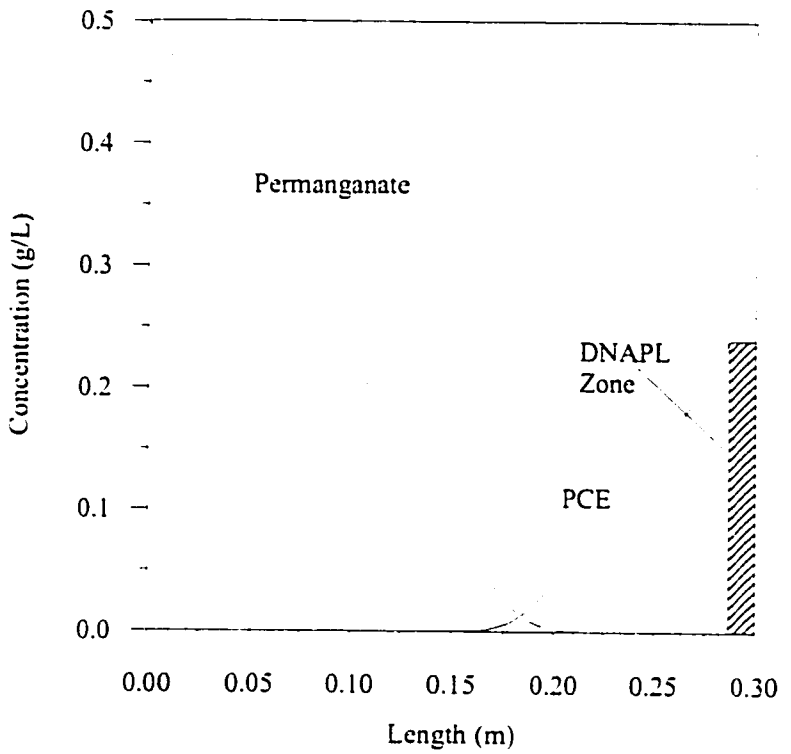

Figure 4.6 Spatial distributions of PCE and permanganate concentrations in the zone of diffusive transport after steady-state DNAPL mass depletion rates occur.

The steady-state spatial distribution of the three solutes (solvent, oxidant, and product/chloride) for a path length of 30 cm, which is representative of the results of the other simulations, is presented in Figure 4.6. On the right edge of the domain, the small zone where the solvent concentration is at the aqueous solubility limit indicates the location of the DNAPL residual. At steady-state, both the solvent and the oxidant concentration varied almost linearly.

For each path length, the mass of DNAPL present as a function of time is shown in Figure 4.7. The rates of steady-state mass depletion (Figure 4.8) decreased asymptotically to zero as the A sixth simulation was performed to demonstrate the effect of mass transfer limitations on DNAPL removal by specifying a constant oxidant concentration path length increased and the

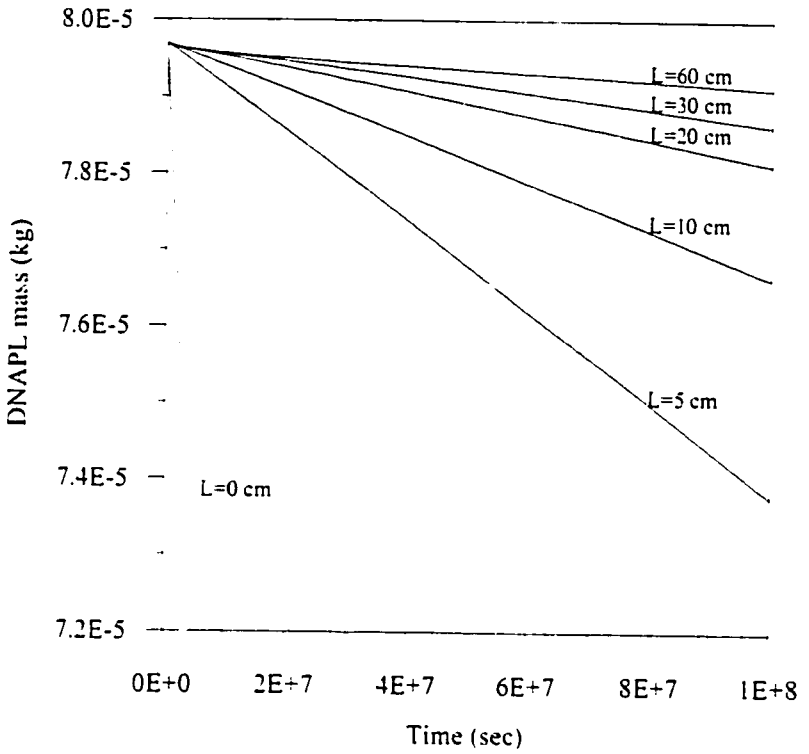

Figure 4.7 Diffusion-controlled DNAPL mass depletion for a range of diffusion path lengths.

concentration gradient at the DNAPL interface asymptotically approached zero. As the path length decreased, the steeper concentration gradients resulted in higher diffusive flux of oxidant into the domain. For shorter path lengths, the mass depletion rate increased rapidly and should continue to increase until the mass transfer rate limited the rate of DNAPL removal. In the mass transfer limited simulation (corresponding to a path length of zero), the DNAPL mass was depleted from the source after only 3.8×10^7 sec.

The data, which suggested slightly different spatial distributions of the solvent and oxidant concentration at steady-state than those shown in Figure 2.11, have important implications for remediation. The diffusion of the oxidant into the diffusion-limited zone enhanced dissolution by an amount that was dependant on the path length. For short diffusion lengths, like those that might be encountered in an relatively homogeneous aquifer, the presence of the oxidant

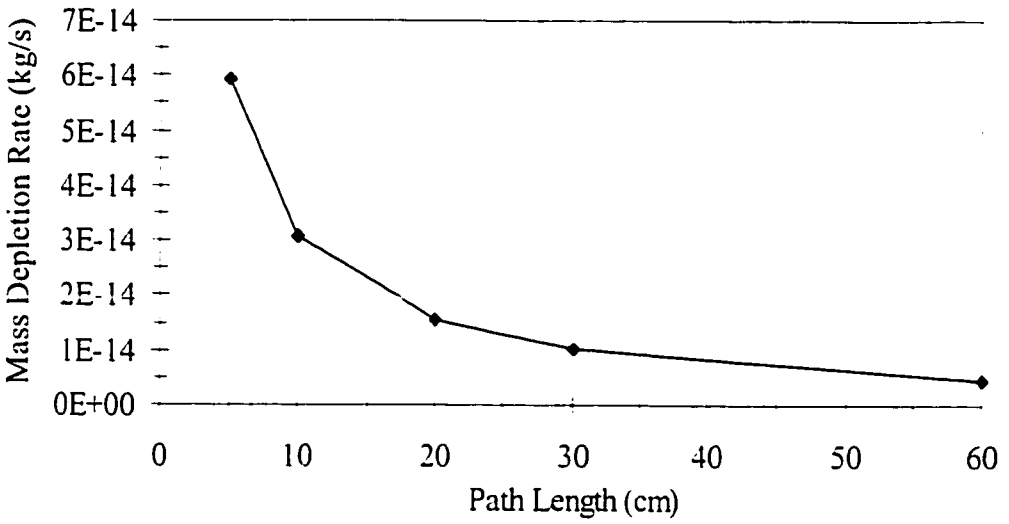

Figure 4.8 Effect of path length on steady-state DNAPL mass depletion rate.

enhanced dissolution; however, beyond path lengths on the order of 10^{-2}-10^{-1} m, the presence of the oxidant resulted in a negligible increase in the rate of mass removal. While oxidant flushing would not appreciably accelerate the removal of DNAPL separated from advective flow by a long diffusion path length, a similar argument may be made to infer that the isolated DNAPL is unlikely to significantly contribute to groundwater contamination.

4.5 Application: two-dimensional heterogeneous aquifer

Few research studies have carefully characterized the effectiveness of potassium permanganate as part of an in situ treatment strategy. As a consequence, little performance or design guidance is available to assess the relative effectiveness of various flushing alternatives. Effective design of a flushing system is controlled by a variety of interrelated factors; however, two of the most significant are the injected oxidant concentration and the groundwater velocity in the treatment zone. Oxidant concentration is often selected either arbitrarily or based on limited data from small-scale column studies; however, the complex kinetics make it difficult to extrapolate from column studies to a realistic expectation of contaminant mass removal at field sites.

Groundwater velocity in the treatment zone is also subject to control through the design process. Passive oxidant addition, the most common and least evaluated method, uses the natural groundwater velocity and density-driven advection to deliver oxidant while forced advection or active oxidant flushing, as used in the field trial described in Chapter 3, increases the velocity in the treatment zone above the existing natural gradient velocity. In either approach, the groundwater velocity is controlled by the boundary conditions of the flow system. In the case of active flushing, the hydraulic boundary conditions are imposed by injection and extraction wells.

In addition to design parameters, uncertainty in the estimates of various input coefficients can also impact the predicted performance of a oxidant flushing strategy,. Estimates of the mass transfer rate coefficient, the oxidation reaction rate coefficients, and the dispersivity coefficients are available with varying degrees of reliability. The existing empirical performance data provides little assistance in focussing data collection on those coefficients which are most likely to have a meaningful impact on the effectiveness of an oxidant flush.

To address these gaps in the current understanding of some factors which may influence the performance of ISCO, a set of general simulations examining the ISCO remediation process for a large DNAPL release into a confined aquifer were conducted. Simulations of heterogeneous DNAPL remediation in non-reactive porous media were used to evaluate the change in the groundwater concentrations of a contaminant, permanganate and chloride that may occur before, during, and after an oxidant flush. The simulation results were used to quantify the numerical sensitivity of remediation performance measures to changes in operational parameters and model coefficients including the hydraulic gradient (dh/dl) through the treatment zone, injected oxidant concentration (C_{in}), mass transfer rate coefficient (λ), oxidation rate constant (k_2), and transverse dispersivity coefficient (a_T). The two performance measured employed were the fraction of the DNAPL mass removed by the oxidant and the decrease in the aqueous solvent mass following the oxidant flush relative to the peak aqueous solvent mass before the oxidant flush. The sensitivity analysis provided insight into the factors limiting the effectiveness of

flushing systems and an understanding of the relative importance of model coefficients for which accurate data are often difficult to obtain from the literature and unavailable from standard site investigation programs.

The model was applied to a two-dimensional (20 m long by 10 m deep by 1 m thick) synthetic scenario consisting of a sandy aquifer overlying an aquitard (Figure 4.9). The model domain was discretized into 20,000 control volumes (100 x 200 x 1) with dimensions of 0.2 m in the horizontal direction and 0.1 m in the vertical direction. The boundaries of the domain, Γ_1, Γ_2, and Γ_3, were assigned constant water phase heads equivalent to a hydraulic gradient of 0.005 m/m, which was held constant throughout these simulations. For the transport solution, a constant concentration of permanganate (C_{in}) was specified on Γ_1. A random spatially-correlated permeability field (Figure 4.10) was generated using the algorithm developed by Robin et al. (1993) based on the Fast Fourier Transform spectral technique. The permeability field was generated using geostatistics representative of the well-characterized Borden aquifer (presented in Table 3.1, ln-transformed mean of -25.7 m^2, ln-variance of 1.0 m^2, and correlation lengths of 2.0 m and 0.2 m in the horizontal and vertical directions, respectively). The average linear groundwater velocity through the domain was ~9 cm/day.

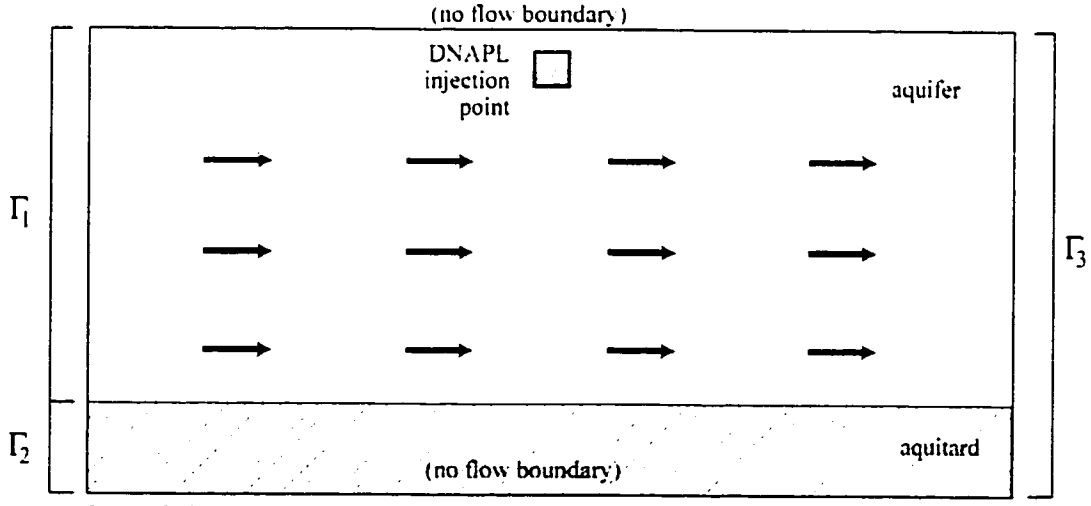

Figure 4.9 Schematic diagram of model domain and boundary conditions.

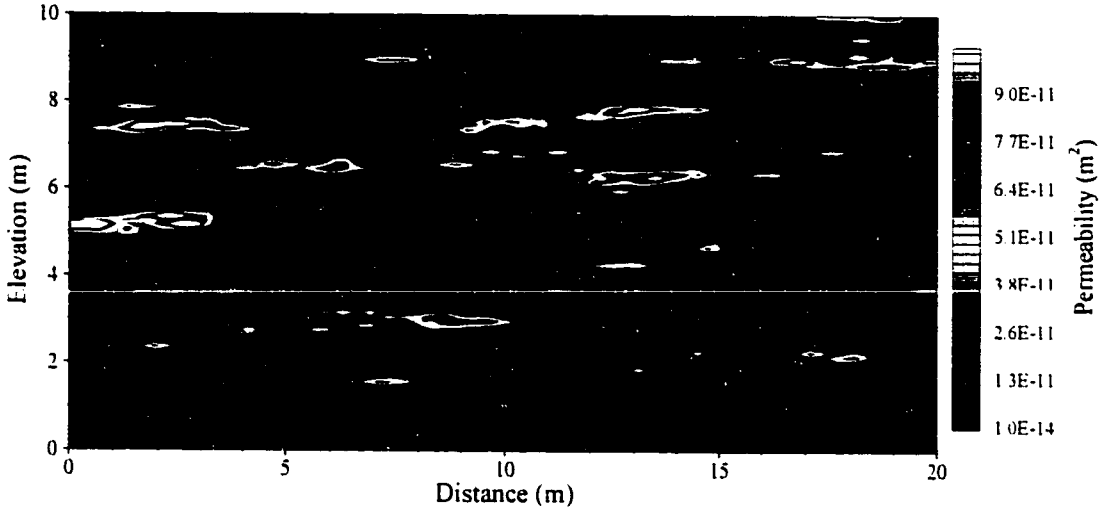

Figure 4.10 Random correlated permeability field with geostatistical properties based on those of the Borden aquifer.

The multi-phase flow component of FLUSH was used to simulate two-phase flow of a 405 kg release of a homogeneous DNAPL assigned the physical and chemical properties of perchloroethylene. The DNAPL was introduced into the domain at the location shown in Figure 4.9 at a constant flow rate of $5x10^{-7}$ m^3/s for ~6 days and allowed to redistribute for an additional 30 days. The resulting heterogeneous DNAPL spatial distribution (the source zone) was comprised of pools and residual regions with non-aqueous phase saturations as high as 84% v/v (Figure 4.11). This pure phase was identical for each of the oxidant flushing simulations considered in the following sections. The general simulation approach consisted of the formation of a DNAPL source zone followed by water flushing for 350 days to establish a baseline solvent plume, oxidant flushing for 450 days, and a second water flush for 470 days.

4.5.2 Base case results

The input parameters for all simulations are summarized in Table 4.2 unless otherwise noted. The temporal variations of the aqueous phase mass of PCE, permanganate, and chloride over the 1270 day simulation period are shown in Figure 4.12(a) to (c) while Figure 4.12(d) provides the corresponding changes in DNAPL mass. The irregularity of the up-gradient edge of the

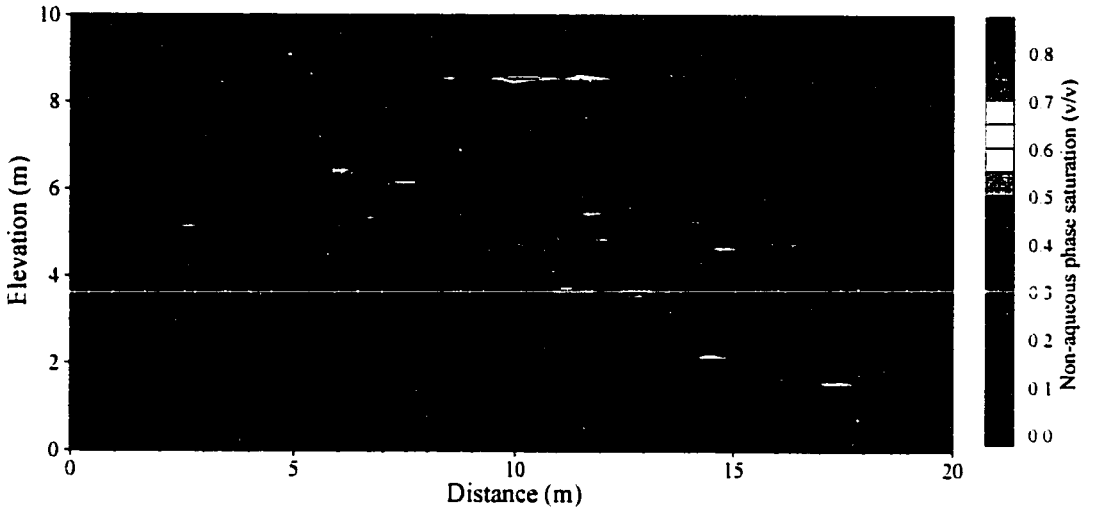

Figure 4.11 Spatial distribution of non-aqueous phase PCE in domain after 36 days.

aqueous PCE plume, shown in Figure 4.13, reflects the heterogeneity of the initial DNAPL distribution (Figure 4.11). As the permanganate penetrated into the DNAPL zone, the mass of the aqueous PCE plume rapidly decreased (Figure 4.12a). The reaction with the aqueous phase solvent simultaneously depleted the oxidant concentration resulting in a gradual increase in the permanganate mass in solution to the maximum possible within the domain (Figure 4.12b). During the latter portion of the oxidant flush, the permanganate was slowly depleted by the oxidation reaction and migrated completely through the source zone in some locations (Figure 4.14). The chloride plume at the end of the oxidant flush is presented in Figure 4.14. Like the aqueous PCE plume, the distribution of chloride in the treatment zone (Figure 4.15) was consistent with the distribution of the pure phase PCE, suggesting that the degradation reaction occurred adjacent to the pure phase interfaces.

The peak chloride concentration (~6,300 mg/L) was thirty times higher than the solvent solubility (237 mg/L) in equivalent units, demonstrating that a significant dissolution enhancement occurred. The peak chloride concentration corresponded to the depletion of 9.3 g/L of permanganate, indicating that essentially all of the permanganate delivered to the DNAPL in that region was used to degrade PCE.

Table 4.2 Summary of base case model input parameters.

Model Parameter		*Value*
PCE density	ρ_{nw}	1430 kg/m^3
PCE viscosity	μ_{nw}	5.7x10^{-4} Pa•s
water density	ρ_w	1000 kg/m^3
water viscosity	μ_w	1x10^{-3} Pa•s
longitudinal dispersivity	α_L	0.05 m
transverse dispersivity	α_T	0.01 m
free diffusion coefficient in water	D^*	1x10^{-10} m^2/s
mole fraction of PCE in DNAPL		1.0
gram molecular weight of PCE		0.166 kg/mole
Solubility		0.240 kg/m^3
Mass yield of chloride	$M_{fPCE,Cl}$	0.86 kg/kg
Mass yield of permanganate	$M_{fPCE,MnO4}$	1.27 kg/kg
PCE degradation rate		2.59x10^{-4} L kg^{-1}sec^{-1}
foc		0.00 g/g
bulk density of soil	ρ_{soil}	1810 kg/m^3
hydraulic gradient		0.005 m/m
convergence tolerance (*S*, *P*, *C*)		10^{-5}, 10^0, 10^{-8}
solver convergence tolerance		10^{-10}

The mass of chloride resulting from mineralization of PCE increased to a maximum as permanganate migrated into the source zone and corresponds with the rate of oxidant depletion. As time progressed, the chloride mass in the domain gradually decreased (Figure 4.12c) as a result of a decrease in the mass transfer dissolution rate caused by lower non-aqueous phase saturations, short-circuiting of permanganate through regions of the source zone where all of the pure phase was removed, and a decrease in the contact time between the oxidant and PCE as DNAPL was depleted from the up-gradient side of the source zone. During the water flush following oxidant addition, the mass of oxidant and chloride rapidly decreased; however, trace amounts of both solutes remained within the low-permeability lens due to diffusion. After 1270

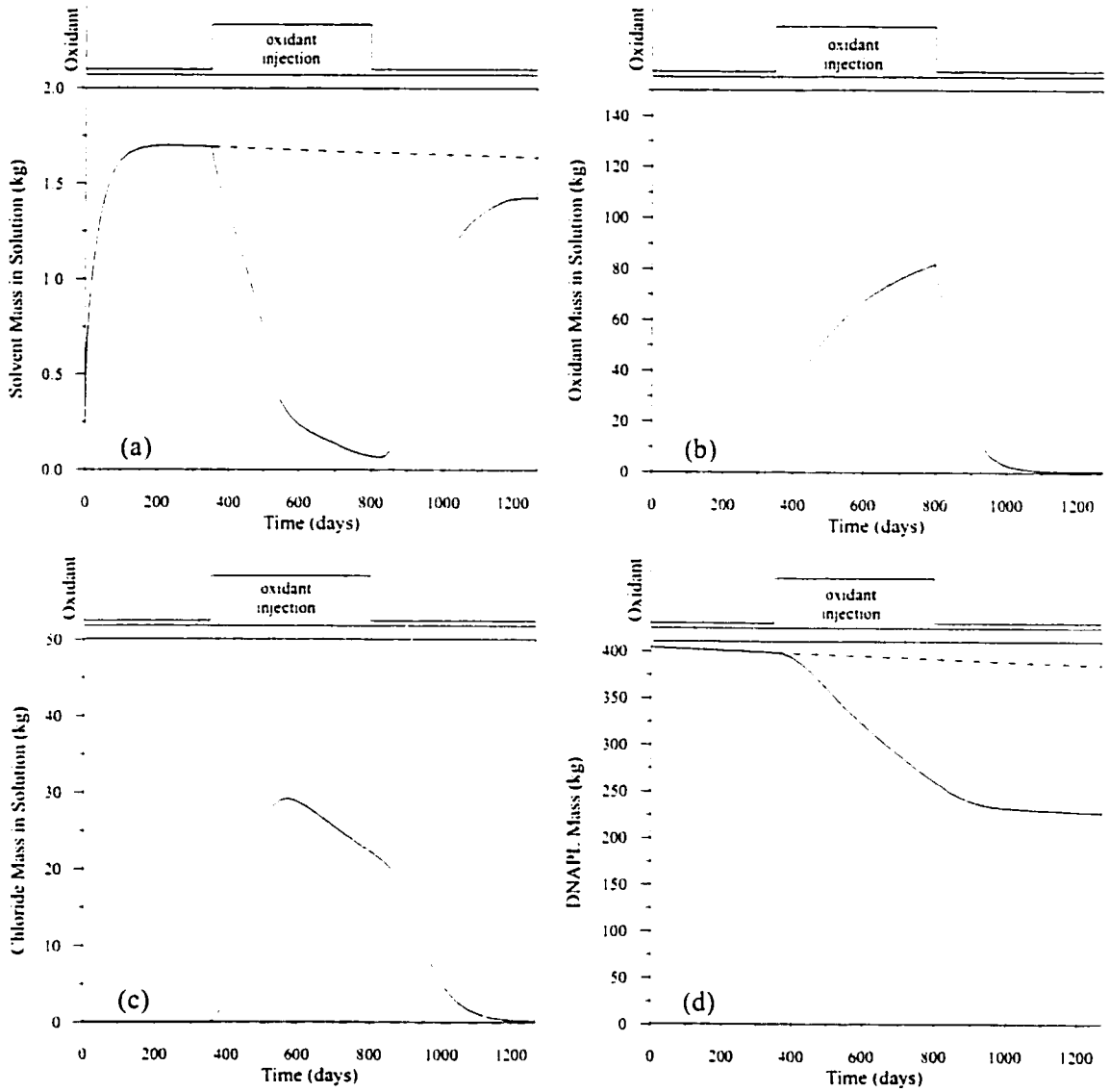

Figure 4.12 Time-series data of simulated a) solvent mass in solution, b) oxidant mass in solution,) chloride mass in solution, and d) DNAPL mass for base case simulation (duration of oxidant injection shown above).

days of flushing with both oxidant solution and water, a total of 227 kg of PCE (56%) was removed from the source zone.

In contrast to the permanganate flush, during a continuous water flush over the 1270 day period the aqueous phase PCE mass in solution decreases gradually as DNAPL mass was depleted

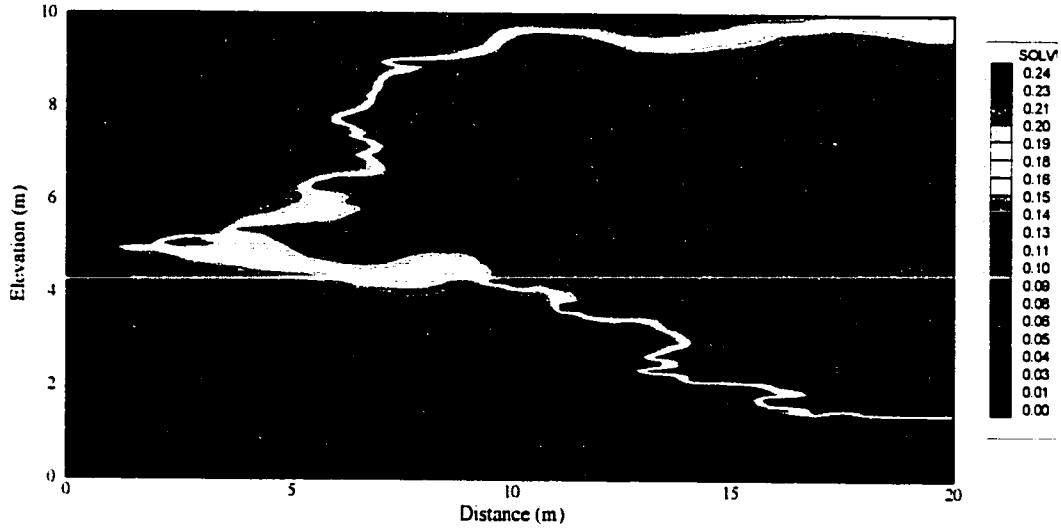

Figure 4.13 Solvent plume distribution at the peak aqueous solvent mass after 350 days of water flushing.

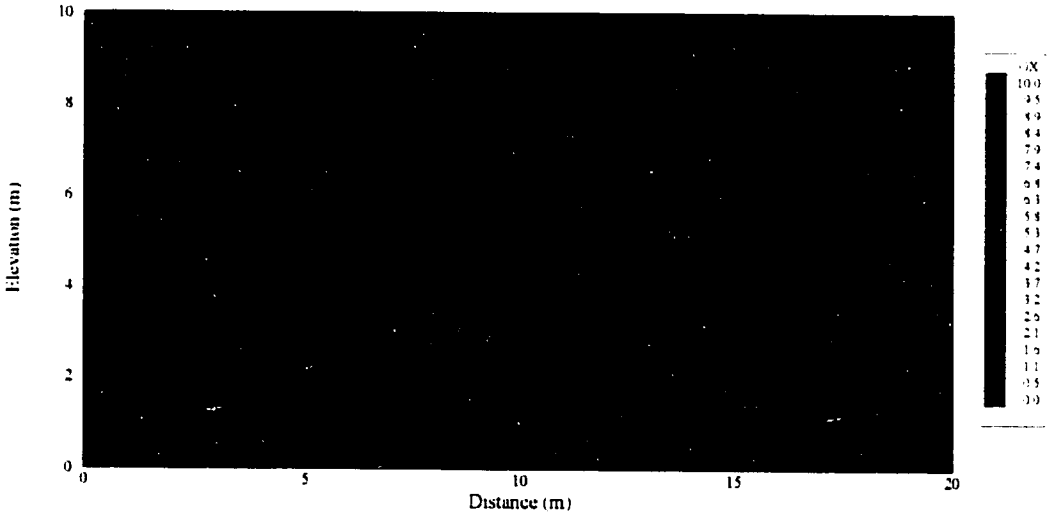

Figure 4.14 Oxidant concentration distribution at the end of the base case oxidant flush.

from the domain (Figure 4.12d). In total, 20 kg of pure phase PCE was removed, a result consistent with the low aqueous solubility of PCE. In comparison, the water flush removed 9% as much pure phase PCE as the oxidant flush.

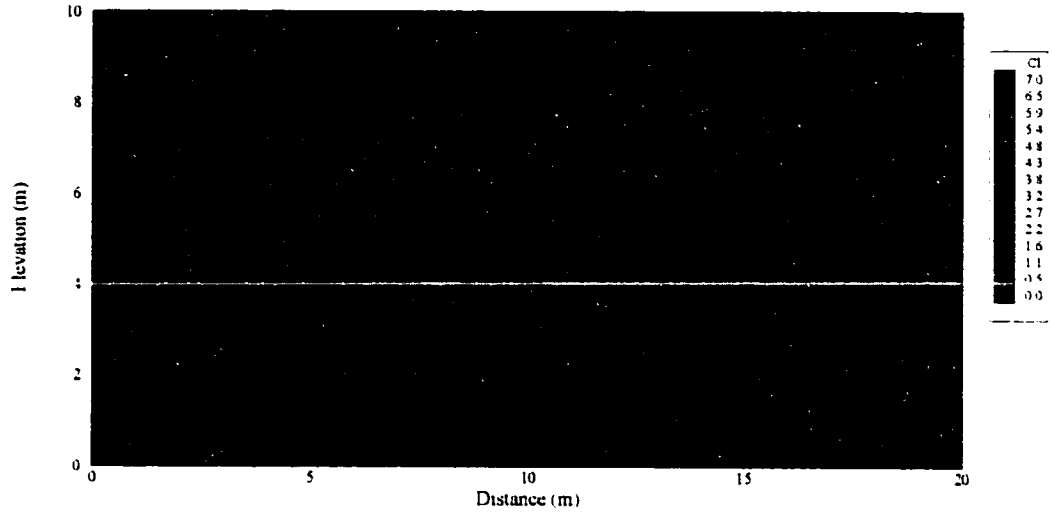

Figure 4.15 Chloride concentration distribution at the end of the base case oxidant flush.

4.5.2 Sensitivity analysis

A limited sensitivity analysis was conducted by individually perturbing a selected set of input parameters and coefficients and observing the change in the selected remediation performance measures. Normalized marginal sensitivity coefficients (C_{nm}) were determined by (Thomson, 2000),

$$C_{nm} = \frac{(\varepsilon_1 - \varepsilon_0)/\varepsilon_0}{(\theta_1 - \theta_0)/\theta_0} \tag{4.15}$$

where ε is an output measure, θ is a model input parameter, and the subscripts 0 and 1 represent base and perturbed states, respectively. The model output measures used in this analysis include the fraction of the initial DNAPL mass removed by the oxidant flush in excess of the DNAPL mass removed by the equivalent water flush (i.e., the simulation without oxidant addition), and the decrease in aqueous solvent mass in solution after the oxidant flush relative to the peak aqueous solvent mass before the oxidant flush.

A summary of the simulations that were performed is presented in Table 4.3. The reductions

Table 4.3 Summary of perturbed parameters for the sensitivity analysis (perturbed parameters are outlined).

Parameter Examined	*Mass Transfer Scale Factor*	$[MnO_4^-]$ *(g/L)*	k_2 *($kg^{-1} \cdot s^{-1}$)*	*dh/dl (m/m)*	α_T *(m)*
Base case oxidant flush	1.0	10	2.59×10^{-4}	0.005	1.0
Base case water flush	1.0	0	2.59×10^{-4}	0.005	1.0
Increase λ by 50%	1.5	10	2.59×10^{-4}	0.005	1.0
Decrease λ by 50%	0.5	10	2.59×10^{-4}	0.005	1.0
Increase $[MnO_4^-]$ by 50%	1.0	15	2.59×10^{-4}	0.005	1.0
Decrease $[MnO_4^-]$ by 50%	1.0	5	2.59×10^{-4}	0.005	1.0
Increase k_2 by 50%	1.0	10	3.89×10^{-4}	0.005	1.0
Decrease k_2 by 50%	1.0	10	1.30×10^{-4}	0.005	1.0
Increase *dh/dl* by 50%	1.0	10	2.59×10^{-4}	0.0075	1.0
Decrease *dh/dl* by 50%	1.0	10	2.59×10^{-4}	0.0025	1.0
Increase α_T by 50%	1.0	10	2.59×10^{-4}	0.005	1.5

in DNAPL mass, aqueous mass, and the normalized marginal sensitivity coefficients associated with these performance variables are summarized in Table 4.4. Input parameters were perturbed by ±50% to provide a sufficiently large response in the output measures. The mass transfer rate coefficient was calculated using the correlation presented by Powers et al. (1994) (Equation 2.6); perturbation of this parameter was achieved by scaling the correlation by the appropriate factor. Since this correlation contains the Reynold's number, the mass transfer rate coefficient was also a function of the hydraulic gradient.

Oxidant concentration

The relative impact of changes in the oxidant concentration on the performance of ISCO was examined by performing simulations using injected oxidant concentrations of 5, 10, and 15 g/L. The temporal variations of the aqueous phase mass of PCE, permanganate, and chloride during the simulations examining the effects of oxidant concentration are presented in Figure 4.16(a) to (c) while the corresponding change in DNAPL mass is provided in Figure 4.16(d). The oxidant concentration affected mass removal through two processes; higher oxidant

Table 4.4 Summary of the results of the sensitivity analysis (outline indicated the most sensitive parameters).

Parameter	*Fraction of DNAPL Mass Removed*	*Sensitivity Coefficient*	*Reduction of Aqueous Phase Solvent Mass After Oxidant Flush*	*Sensitivity Coefficient*
Water Flush	0.05	-	0.97	-
Base Oxidant Flush	0.44	-	0.84	-
Decrease λ	0.35	0.41	0.89	-0.10
Increase λ	0.47	0.16	0.80	-0.11
Decrease $[MnO_4^-]$	0.30	0.61	0.87	-0.07
Increase $[MnO_4^-]$	0.50	0.28	0.83	-0.02
Decrease k_2	0.44	0.02	0.85	-0.01
Increase k_2	0.44	0.00	0.84	-0.00
Decrease *dh/dL*	0.28	0.74	0.90	-0.16
Increase *dh/dL*	0.54	0.46	0.78	-0.14
Increase α_T	0.44	0.02	0.85	-0.02

concentrations caused faster oxidation rates that degraded the PCE more rapidly and provided a larger oxidant flux into the source zone that minimized oxidant depletion.

In general, higher oxidant concentrations improved remediation performance. The reduction in the aqueous phase plume mass was less sensitive to changes in the oxidant concentration than the reduction in DNAPL mass. DNAPL mass removal was less sensitive to the higher oxidant concentration (15 g/L) than the lower concentration (5 g/L) which suggested that DNAPL mass removal was limited by mass transfer at the higher concentration and oxidant depletion at the lower concentration. A similar result was observed for the reduction in aqueous phase plume mass. The high aqueous solvent mass present during the 5 g/L permanganate flush (Figure 4.16(a) indicated that the oxidant was completely depleted within the source zone and that the low oxidant flux limited the effectiveness of the oxidant flush rather than mass transfer or reaction rates. This conclusion was supported by the chloride profile for the 5 g/L simulation; the flat profile indicated that the rate of DNAPL removal was constant in spite of changes in the non-aqueous phase saturation. In the 5 g/L simulation, the sharp drop in aqueous solvent mass near the end of the oxidant flush occurred as oxidant finally migrated past the source zone,

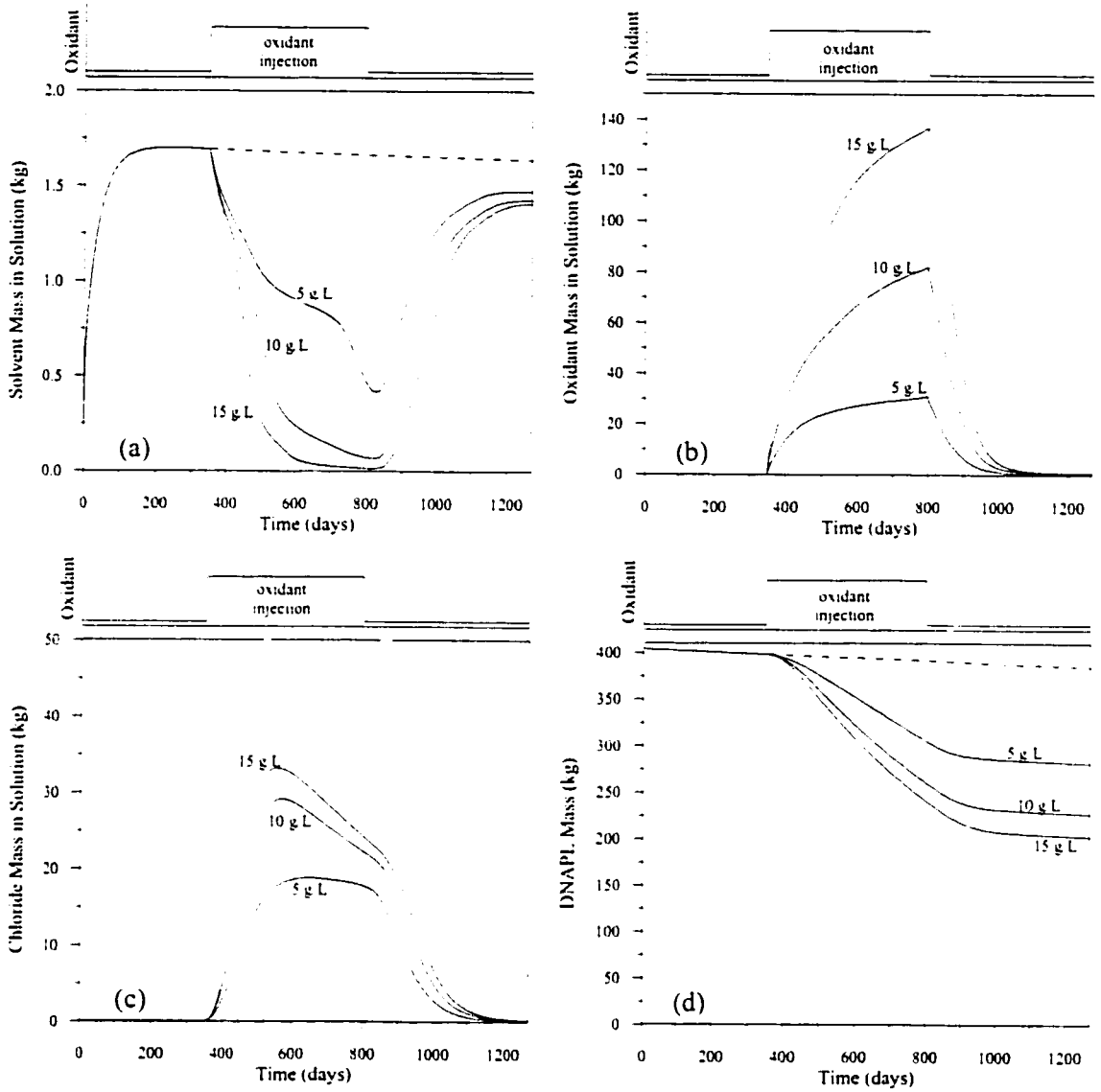

Figure 4.16 Time-series data of simulated a) solvent mass in solution, b) oxidant mass in solution, c) chloride mass in solution and d) DNAPL mass for injected oxidant concentrations of 5, 10, and 15 g/L (solid lines) and without oxidant (dashed) for oxidant concentration sensitivity simulations (duration of oxidant injection shown above).

cutting off plume formation from the entire DNAPL source zone.

Hydraulic gradient

The influence of the hydraulic gradient on the simulated remediation performance measures was

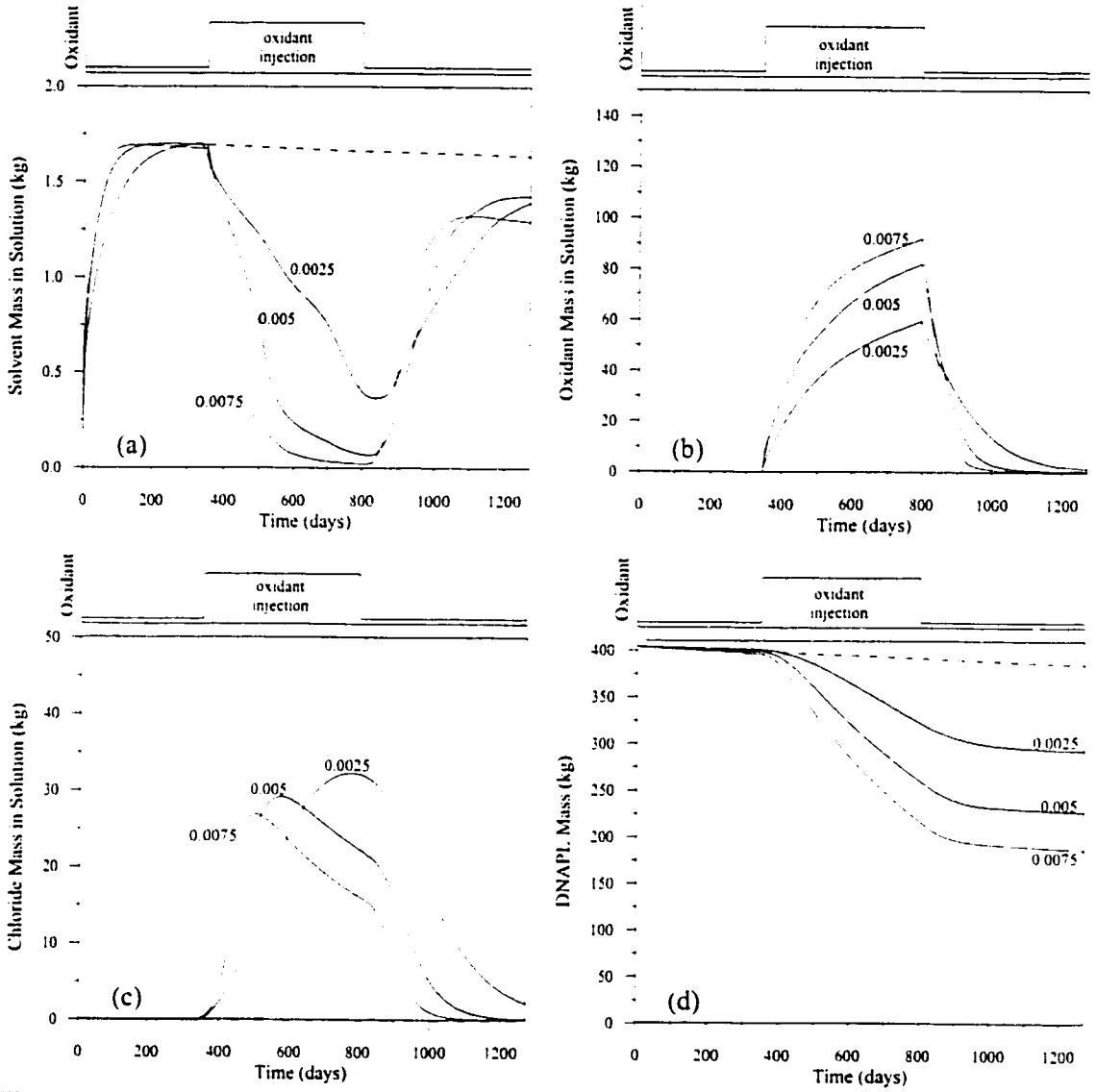

Figure 4.17 Time-series data of simulated a) solvent mass in solution, b) oxidant mass in solution, c) chloride mass in solution and d) DNAPL mass for hydraulic gradients of 0.0025, 0.0050, and 0.0075 m/m (solid lines) and without oxidant (dashed) for hydraulic gradient sensitivity simulations (duration of oxidant injection shown above).

examined by performing simulations with constant hydraulic gradients of 0.0025, 0.005, and 0.0075 m/m across the domain. The temporal variations of the aqueous phase mass of PCE, permanganate, and chloride during the simulations examining the effects of hydraulic gradient are shown in Figure 4.17(a) to (c) while the corresponding change in DNAPL mass is provided

in Figure 4.17(d). The oxidant fluxes into the domain produced using these three gradients were comparable to those in the previous section produced using oxidant concentrations of 5, 10, 15 g/L. Like oxidant concentration, the hydraulic gradient was important since it was a parameter that could be engineered by the design of the oxidant flushing system, which could include forced-gradient advection. The hydraulic gradient has two major influences on the remediation process. Like the oxidant concentration, an increase in hydraulic gradient increases the advective oxidant flux into the source zone and minimizes the effect of oxidation depletion; however, the maximum oxidation rate remains unchanged since the oxidant concentration is constant. In addition, since the correlation describing the mass transfer rate coefficient (Equation 2.6) is a function of the Reynolds number, higher hydraulic gradients result in a higher mass transfer rate coefficient and an enhancement in the overall mass transfer rate above that caused by an equivalent increase in the oxidant flux by increasing the oxidant concentration.

Mass transfer rate coefficient

Simulations examining the sensitivity of the simulated remediation performance measures to changes in the mass transfer rate coefficient were completed by scaling the rate coefficient predicted using the correlation of Powers et al. (1994) by ±50%. The temporal variations of the aqueous phase masses of PCE, permanganate, and chloride during the simulations examining the effects of the mass transfer rate coefficient are presented in Figure 4.18(a) to (c) while the corresponding change in DNAPL mass is provided in Figure 4.18(d). Given the analysis summarized in Figure 4.1, it was anticipated that the modelling results would be sensitive to the mass transfer rate coefficient; higher rates of mass transfer would provide additional aqueous solvent mass in solution which would be available to react with the injected oxidant mass. This effect, however, could potentially be limited by the oxidant flux into the source zone.

The reduction in DNAPL mass was less sensitive to changes in the mass transfer coefficient than changes in the injected oxidant concentration or hydraulic gradient. In contrast, the reduction in aqueous solvent mass was more sensitive to the mass transfer coefficient than the

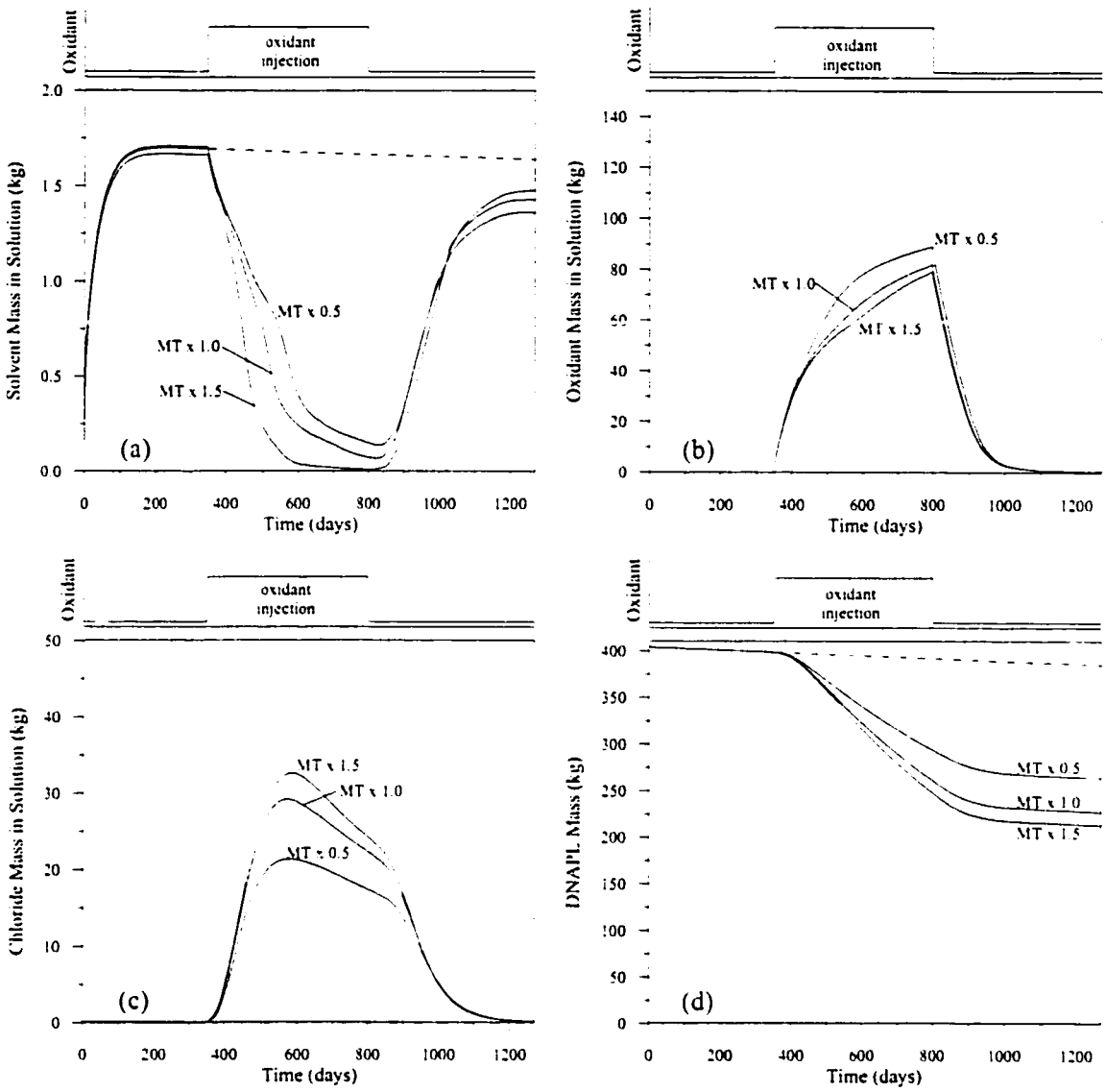

Figure 4.18 Time-series data of simulated a) solvent mass in solution, b) oxidant mass in solution, c) chloride mass in solution and d) DNAPL mass for mass transfer rate coefficients of 0.5λ, 1.0λ, and 1.5λ (solid lines) and without oxidant (dashed) for mass transfer rate sensitivity simulations (duration of oxidant injection shown above).

injected oxidant concentration. This difference may be attributed to the mechanisms controlling the extent of the plume forming after DNAPL is removed. DNAPL removal during the oxidant flush appeared to be limited by the oxidant flux into the source zone (which is controlled by C_{in}); however, the mass of PCE in the aqueous plume after the oxidant flush was controlled by

the mass transfer rate. While the sensitivity of the aqueous mass reduction was similar for both the increase and decrease in mass transfer rate, the DNAPL mass reduction was more sensitive to the decrease in mass transfer rate. The non-linear response may have resulted from a change in the factors controlling DNAPL mass removal. For example, at the higher mass transfer coefficient DNAPL removal may have been limited by the available mass of oxidant while at the lower mass transfer coefficient, DNAPL mass removal may have been limited by the mass transfer rate.

Reaction rate

The sensitivity of the simulated remediation performance measures to the reaction rate constant was examined by modifying the reaction rate by ±50% (1.30×10^{-4}, 2.59×10^{-4}, and 3.89×10^{-4} M^{-1} s^{-1}). The model results (not shown) were essentially identical to the base case simulation. Based on the conceptual model for the micro-scale processes occurring during ISCO presented in Figure 2.11, a high reaction rate decreases the solvent concentration, increases the solvent concentration gradient, and enhances mass transfer from the DNAPL. In these simulations, changes in the reaction rate had no effect on the rate of DNAPL mass removal, a result that suggested that mass removal was limited by the flux of oxidant into the source zone and the mass transfer rate. For the base case investigated here, the mass transfer rate was sufficiently high that the injected oxidant was depleted regardless of the reaction rate, suggesting that in comparison to the groundwater transport rates that the reaction was essentially instantaneous and that a large degree of uncertainty in the actual reaction rate can be tolerated without appreciable impact on the simulation results. These results further imply that conducting experiments using site-specific groundwater and geochemical condition to measure the contaminant degradation rate is likely of little value.

As demonstrated in Figure 4.1, above a minimum oxidation rate there is a negligible increase in the DNAPL mass removal rate. The simulation results suggest that the oxidation rates employed in these simulations are above this minimum rate and that the efficiency of the oxidant flush was limited by other factors, including oxidant flux and mass transfer kinetics.

Transverse dispersivity

A simulation assessing the sensitivity of the simulated remediation performance measures model to a change in the transverse dispersivity was performed where the transverse dispersivity coefficient was increased by 50% from 1.0 cm to 1.5 cm. The model results (not shown) were identical to the base case simulation. The conceptual model shown in Figure 2.11 suggested that transverse dispersivity may influence remediation by limiting the dispersive fluxes of oxidant towards and solvent away from a DNAPL pool interface. The synthetic model domain contained a number of trapped zones of high non-aqueous phase saturation, indicating that this was a potentially important mass removal process. Over the range investigated, the model was insensitive to changes in the transverse dispersivity coefficient, which indicated that dispersive transport processes did not limit mass transfer under the conditions of this simulation. Advective transport through regions of high non-aqueous phase saturation was significant in spite of the reduction in non-aqueous phase saturation. However, mass removal may be limited by transverse dispersion where the DNAPL resides above a low permeability capillary barrier that impedes aqueous phase flow.

4.5.3 Summary

In general, over the range of conditions examined the performance measures were insensitive to changes in the transverse dispersivity coefficient and the oxidation reaction rate constant and sensitive to changes in the mass transfer rate coefficient, the injected oxidant concentration, and the hydraulic gradient. As well, the sensitivity of the reduction in the aqueous solvent mass was small in comparison to the reduction in DNAPL mass, a result which emphasized the requirement to remove a large mass of DNAPL to produce a significant reduction in the size and extent of the solvent plume. In general, the sensitivity of the aqueous phase mass reduction to changes in the various model parameters was in order of (from most sensitive to least),

$$\frac{\partial h}{\partial l} > \lambda > C_{in} > \alpha_T > k_2 \qquad (4.16)$$

while the sensitivity of DNAPL mass removal was given by,

$$\frac{\partial h}{\partial l} > C_{in} > \lambda > \alpha_T > k_2 \qquad (4.17)$$

Both DNAPL and aqueous mass reductions were more sensitive to the hydraulic gradient than the oxidant concentration. This result indicated that while the hydraulic gradient resulted in a effect comparable to oxidant concentration in terms of controlling the oxidant flux into the source zone, the hydraulic gradient also proportionately changed the rate of mass transfer. The combined effects of the increased oxidant flux into the source zone and the increased mass transfer rates suggested that above a minimum oxidant flux, the effectiveness of the oxidant flush was more sensitive to changes in the hydraulic gradient than the injected oxidant concentration.

Since the reaction rate was not an important model coefficient as the rate of mass removal was either controlled by the mass transfer kinetics or depletion of the injected oxidant mass, it appears that determination of site-specific oxidation rates is not essential design information. The insensitivity of the model to reaction rate also suggested that the reaction rate for permanganate and PCE, the chlorinated ethene which degrades the slowest, is sufficiently high that degradation was essentially instantaneous in comparison to the slow groundwater transport rates. While the rate of oxidation of chlorinated ethenes by Fenton's reagent may be orders of magnitude higher than the rate of degradation by permanganate, these data suggested that reaction rate alone was not an appropriate rationale on which to base oxidant selection.

While the empirical data underlying the development of the mass transfer rate coefficient correlation used in these simulations appears to be fundamentally sound, the correlation may not be applicable to the analysis of field-scale dissolution problems. At this scale, the conditions and mechanisms of dissolution differ from those occurring in the column experiments from which the correlation was derived. The correlation presented by Powers et

al. (1994) was determined from observations of columns containing a styrene residual (0.045 v/v) flushed at a Darcy velocity of 3.5 m/day. It is difficult to extrapolate from these experimental conditions to those in the synthetic spatial domain used in these simulations. In addition, the specific DNAPL interfacial surface areas formed during these column experiments likely differed from those in a field scale problem that includes DNAPL pools. The columns contained a minimum residual saturation with the DNAPL primarily in the smallest pore spaces. At the field scale, however, substantial quantities of undrained or partially-drained DNAPL are present. As a result, in a field-scale release, the DNAPL resides in the largest pore spaces, reducing the relative permeability. Accordingly, mass transfer from porous media containing high DNAPL saturations is likely to be influenced by transient changes in the water-phase relative permeability, and the wide distribution of pore sizes containing non-aqueous phase. It would be reasonable to expect that diffusion may limit mass transfer; as DNAPL mass is depleted, the increasing diffusion path length causes a decline in the mass transfer rate. In DNAPL pools, the decline in mass transfer rate may occur while a large fraction of the initial DNAPL mass remains. These differences in the dissolution processes of residual and pools suggest that the mass transfer rate coefficient correlations may be of limited applicability to real-world DNAPL problems. Accordingly, accurate prediction of mass removal may require either site specific calibration data or a substantial improvement in the understanding of the fundamental processes controlling mass transfer at the field scale.

The sensitivity analysis provided useful guidance on design strategies for oxidant flushing systems. While minimizing the volume of the treatment zone, selection of an oxidant concentration and design of a flushing system should emphasise:

- increasing the flux of oxidant into the source zone to avoid depletion and ensure that mass transfer or diffusion limit contaminant mass removal; and,

- enhancing mass transfer by increasing the groundwater velocity through the source zone.

Chapter 5
Conclusions and Recommendations

5.1 Conclusions from the in situ chemical oxidation field trial

This research investigated the performance of oxidant flushing to remediate groundwater contaminated with DNAPL compounds such as TCE and PCE. An in situ chemical oxidation treatment system was constructed to recirculate a concentrated solution of potassium permanganate through a DNAPL source zone at an experimental site at CFB Borden. Down-gradient of the source zone, the concentrations of permanganate and chloride were monitored during the oxidant flush to assess the delivery of the oxidant solution to the source zone and to determine an appropriate endpoint for the oxidant flush. The performance of the oxidant flush was evaluated using several approaches including the decrease in the flux of contaminants in the groundwater and the fraction of the initial DNAPL mass removed. This experiment was the first highly monitored pilot-scale experiment of its type to operate for a prolonged period of time.

The use of the oxidant recirculation system was found to be an effective means of delivering oxidant solution to the source zone. The groundwater recirculation system resulted in an increase in the average linear groundwater velocity in the treatment zone from 8.5 cm/day to 11-13 cm/day while providing containment of the majority of the injected tracer solution. During a tracer test, the recirculation system recovered 82% of the injected tracer mass; however, the recovery during the oxidant flush was likely lower due to density effects. Monitoring data

confirmed that oxidant was flushed throughout the source zone. The loss of oxidant solution from the treatment zone emphasized the importance of the recirculation system design in ensuring effective and economic application of ISCO.

Recycling was a cost-effective approach to managing the residual oxidant contained in the effluent from the extraction wells. In addition to conserving a significant mass of permanganate, the cost of continuous treatment to remove residual permanganate from the effluent was avoided. During the field experiment, 109 m^3 of oxidant solution was reinjected rather than treated.

A permanganate mass balance suggested that a substantial fraction of the injected permanganate mass was lost from the treatment system. While it is likely that much of this mass simply migrated outside of the capture zone of the extraction wells, the loss was consistent with that observed in other studies with completely closed treatment zones, which suggests that some of the oxidant loss may result from a reactive mechanism. While the specific reaction mechanism was not identified, decomposition of the permanganate solution may have been catalysed by $MnO_2(s)$.

Monitoring of the progress of DNAPL removal was complicated by the loss of the oxidant solution from the treatment zone and recycling of the chloride in the effluent along with in the residual permanganate. Accordingly, interpretation of the difference between the injected and extracted chloride concentration data was difficult. Discrete depth sampling was used to identify the presence of a concentrated chloride signature indicating DNAPL removal. In spite of the high concentration of chloride in the recycled oxidant solution, the chloride signature was clearly distinguishable. The peak chloride concentration measured during the field trial was higher than the recycled chloride concentration by a factor of ~50 and clearly demonstrated that DNAPL mass removal was occurring although locating the chloride signature required an extensive sampling effort. However, fine-resolution samples collected immediately down-gradient of the source zone located a chloride signature that was not evident in either the 1-m

fence or the extraction wells, suggesting that the total load of the chloride plume was small.

While DNAPL was not observed in soil samples collected from the source zone, the monitoring data suggested that a localized zone of DNAPL was present in the source. However, following the oxidant flush the loads of TCE and PCE in the down-gradient groundwater plume were reduced by 99%. and 90%, respectively. These results emphasized the difficulty in achieving complete restoration of groundwater quality; however, the reduction in plume load was a significant benefit that has important implications for performance monitoring and the role of ISCO as part of a comprehensive remediation strategy

5.2 Model development and applications

As part of this research, a comprehensive numerical model that captures the essential aspects of the ISCO remediation technology was developed, tested, and applied to a number of problems to demonstrate the processes influencing remediation and controlling the effectiveness of the design of ISCO treatment systems. The model included both the multi-phase flow and multi-component reactive transport equations. The transport of three species (contaminant, oxidant/permanganate, and product/chloride) solutes was simulated using kinetic mass transfer and reaction rates. The simulation included oxidation of both the contaminant and the natural oxidant demand of the porous media by permanganate.

Comparison of the transport component of the model to analytical solutions indicated that the simulated solutions for the degradation rate and reaction stoichiometry and advective-dispersive solute transport were correct. Due the non-linear nature of the reactive transport problem, direct comparison of reactive transport to an analytical solution was not possible.

A process by which counter diffusion of the oxidant into a non-advective zone enhances mass transfer from advectively-isolated DNAPL was demonstrated. In general, the magnitude of the enhancement was shown to be dependent upon the diffusion path length; however, the increase in mass transfer rate was negligible for path lengths greater than ~10^{-1} m.

Using a hypothetical ISCO application, a sensitivity analysis was used to elucidate the processes controlling the effectiveness of this technology and to determine the relative significance of key model parameters. The effectiveness of the oxidant flush was insensitive to the reaction rate and transverse dispersivity and was sensitive to hydraulic gradient, oxidant concentration, and the mass transfer rate coefficient. Over the range of conditions evaluated, the sensitivity analysis suggested that technology performance was primarily controlled transport limitations on oxidant delivery to the contaminant and the mass transfer rate.

In each simulation the reduction in DNAPL mass was large in comparison to the reduction in aqueous plume mass. The most effective results were achieved when the oxidant flux into the source zone was sufficiently large that the oxidant migrated through the source zone without being depleted. Under this condition, mass transfer limited the rate of DNAPL mass removal rather than depletion of the oxidant. Increasing the hydraulic gradient had a larger affect on the performance of the oxidant flush than increasing the oxidant concentration since the mass transfer rate increased while providing a higher oxidant flux into the source zone.

The model results reinforced the conceptual model for the expected changes in groundwater concentration of contaminant, permanganate, and chloride during an oxidant flush and demonstrated the mechanism of enhanced DNAPL removal. The results suggested that recirculation cells operating under forced-gradient conditions will be more effective than pulse or passive injection systems relying upon natural gradient flushing, emphasizing the importance of oxidant flushing system designs that increase the hydraulic gradient while containing the oxidant within the treatment zone.

5.3 Recommendations

The applicability of in situ chemical oxidation using permanganate to degrade typical industrial contaminants should be determined experimentally since wide gaps in the experimental data exist and the reactivity of only a few common groundwater contaminants has been rigorously

evaluated. While some contaminants will be completely mineralized, others will be only partially degraded and an assessment of the eventual environmental fate and toxicity of the products relative to the parent contaminant may be necessary. Testing protocols to assess the reactivity should characterize the reaction products resulting from the reaction and provide an approximate estimate of the reaction rate.

Limitations of the existing correlation models for the mass transfer rate coefficient were identified which suggest that the mass transfer rate coefficients predicted using these correlations may not be applicable to dissolution kinetics from DNAPL present in high non-aqueous phase saturations (pools). The applicability of these correlations to pooled DNAPL should be experimentally assessed to refine the current conceptual understanding of DNAPL mass transfer. Given the emphasis on transverse dispersivity in the literature describing pool dissolution, further evaluation of the conditions under which this process limits mass transfer and the relevance of these conditions to typical field sites is necessary.

While a number of pilot-scale demonstrations of active flushing with permanganate have been reported in the scientific literature, results from a carefully monitored field-scale application have yet to be reported. Additional performance and design data from industrial sites where ISCO has been utilized are necessary to evaluate the potential effectiveness of the remediation technology, provide typical construction and operation costs, and assess the utility of alternative flushing system design approaches. Given the cost of full-scale application and the difficulty in properly evaluating the effectiveness of this technology, future field-scale research directions should emphasize conducting long-term performance audits of oxidant flushes previously completed.

Oxidant losses in the field experiment reported in the current study and other experimental studies may have been caused by a reactive mechanism where permanganate was chemically reduced in a slow reaction catalysed by $MnO_2(s)$. The extent and kinetics of the reactive mechanism and its impact on geochemistry require further investigation, including an

assessment of the reaction's impact on field-scale applications of ISCO. Potential ameliorating techniques, such as pulsed injection of a sacrificial reductant to remove $MnO_2(s)$ from the treatment zone, should be investigated. Similarly, additional work is required to characterize the natural oxidant demand exerted by aquifer materials by correlating the oxidant demand (in terms of mass of permanganate required per mass of oxidized soil) with the organic carbon, iron, manganese, and sulfide content of the soil, and determining the kinetics of the reaction.

Model validation suffered from a lack of reliable bench-scale experimental data with which to compare simulated results. Carefully controlled permanganate flushing experiments with columns containing a controlled DNAPL source (e.g., similar to the method of Powers et al., 1994) are required to provide a basis for model validation and parameter calibration. In addition to rigorously controlling the DNAPL source zone, addition experimental controls should be used to provide information on mass transfer and soil oxidation rates are necessary.

At the field scale, monitoring strategies should focus on measuring the long-term reduction in contaminant flux resulting from an oxidant flush. While previous field experiments have demonstrated that complete mass removal may occur (e.g., Schnarr et al., 1998), the most likely outcome at a field site is a substantial decrease in the contaminant load in the groundwater plume which suggests that this technology may be particularly effective when paired with a passive technology (e.g., permeable reactive barriers, monitored natural attenuation) capable of degrading the remaining aqueous mass.

The development of the model revealed some limitations in the current conceptual understanding of the remediation process. The effect of $MnO_2(s)$ and $CO_2(g)$ on the removal of high DNAPL saturations should be investigated and quantitative expressions describing the impact of the $MnO_2(s)$ shell and $CO_2(g)$ gas binding on the permeability of the porous medium to water and the diffusion of oxidant towards and contaminant away from DNAPL interfaces should be developed.

5.4 Research contributions

This research has included one of the few pilot-scale field demonstrations that has carefully evaluated the performance of this innovative technology and has demonstrated the limited capacity of ISCO to completely restore contaminated groundwater. Performance measures included in this study included the fraction of DNAPL removed, and the reduction of the groundwater plume, which was measured using the decrease in the maximum contaminant concentration and the reduction in the groundwater plume solvent load. This research provided a clear measurement of the long-term benefit of the oxidant flush used at this site. The field experiment demonstrated that active recirculation of the injected oxidant solution was an economic approach that effectively delivered permanganate to the source zone. While oxidant recycling achieved only a modest benefit in terms of reducing the mass of oxidant required, the volume of effluent requiring treatment to remove residual permanganate was significantly reduced.

Based on a conceptual model derived from previous experimental data, a numerical model that captured the essential physico-chemical processes of the remediation process was developed, tested, and applied to several synthetic scenarios. The process of two-way or counter oxidant diffusion was demonstrated to cause a mass transfer enhancement in DNAPL isolated from advective flow. Preliminary design guidance was provided along with general recommendations for the design of oxidation treatment systems.

References

Aiken, G.R., D. McKnight, R. Wershaw, and P. MacCarthy, *Humic substances in soil, sediment and water: geochemistry, isolation and characterization*, John Wiley & Sons, Toronto, 1985.

Allen-King, R.M., R.M. Halket, D.R. Gaylord, and M.J.L. Robin, Characterizing the heterogeneity and correlation of perchloroethylene sorption and hydraulic conductivity using a facies-based approach, *Water Resour. Res.*, 34(3):385-396, 1998.

Amer, A.M., and A.A. Awad, Permeability of cohesionless soils, *J. Geotechnical Engineering*, 100:GT12, 1309-1316.

American Public Health Association, American Water Works Association and Water Pollution Control Federation, *Standard methods for the examination of water and wastewater*, 19th ed., American Public Health Association, Washington DC,1995.

Amtec Engineering, Inc., *User's manual, Version 7 Tecplot*, Amtec Engineering, Inc. Bellevue, WA, 1996.

Ball, W.P., C.H. Buehler, T.C. Harmon, D.M. Mackay, and P.V. Roberts, Characterization of sandy aquifer material at the grain scale, *J. Contam. Hydrol.*, 5(3):253-295, 1990.

Ball, W.P. and P.V. Roberts, Long term sorption of halogenated organic chemicals by aquifer material. 1. equilibrium, *Environ. Sci. Technol.*, 25(7):1223-1236, 1991.

Banerjee, S., Solubility of organic mixtures in water, *Environ. Sci. Technol.*, 18(8):587-591, 1984.

Barbaro, S.E., H-J. Albrechtsen, B.K. Jensen, C.I. Mayfield and J.F. Barker, Relationships between aquifer properties and microbial populations in the Borden aquifer, *Geomicrobiol. J.*, (12):203-219, 1994.

Barbee, G.C., Fate of chlorinated aliphatic hydrocarbons in the vadose zone and ground water, *Ground Water Mon. Remediat.*, 14(1):129-140, 1994.

Barcelona, M.J., T.R. Holm, M.R. Schock, and G.K. George, Spatial and temporal gradients in aquifer oxidation-reduction conditions, *Water Resour. Res.*, 25(5):991-1003, 1989.

Barcelona, M.J., and T.R. Holm, Oxidation-reduction capacities of aquifer solids, *Environ. Sci. Technol.*, 25(9):1565-1572, 1991.

Bear, J., *Dynamics of fluids in porous media*, American Elsevier Pub. Co., New York, 1972.

Beck, A.G., Determination of residual permanganate and permanganate demand, *Water Waste Eng.*, December, 1968

Belavin, B.V., E.I. Kresova, A.P. Moravskii, and A.E. Shilov, Oxidation of methane in potassium permanganate solution, *Kinetika I Kataliz*, 31(3):764, 1990.

Bellamy, W.D., G.T. Hickman, P.A. Mueller, and N. Ziemba, Treatment of VOC-contaminated groundwater by hydrogen peroxide and ozone oxidation, *Res. J. WPCF*, 63(2):120-128, 1991.

Bolha, J., *A sedimentological investigation of a progradational foreshore sequence*, M.Sc. Thesis, Department of Earth Sciences, University of Waterloo, Waterloo, ON, 1986.

Brandes, D. and K.J. Farley, Importance of phase behaviour on the removal of residual DNAPLs from porous media by alcohol flooding, *Water Environ. Res.*, 65(7):869-878, 1993.

Brewster, M.L. and A.P. Annan, Ground-penetrating radar monitoring of a controlled DNAPL release: 200 MHz radar, *Geophysics*, 59(8):1211-1221, 1994.

British Standards Institution, *Methods of test for soils for civil engineering purposes* (BS1377), Test 8 - Determination of the organic matter content, London, England, April 1975.

Broholm, K., S. Feenstra, and J.A. Cherry, Dissolution of heterogeneously distributed solvent residuals: a field experiment, in the proceedings of *the Fourth International KfK/TNO Conference on Contaminated Soil*, Berlin, Germany, May 1993.

Brooks, R.H., and A.T. Corey, Hydraulic properties of porous media, *Hydrol. Papers No. 3*, Colorado State University, Fort Collins, CO, 1964.

Carlson, K.H., and W.R. Knocke, Modeling manganese oxidation with $KMnO_4$ for drinking water treatment, *J. Environ. Eng.*, 123(10):892-896, 1999.

Carus Chemical, CAIROX, Available: http:// www.caruschem.com/INDEX1.HTM [March14, 1999], 1997.

Cherry, J.A., R.W. Gillham, E.G. Anderson and P.E. Johnson, Migration of contaminants in groundwater at a landfill: a case study 2. groundwater monitoring devices, *J. Hydrol.*, 63(1-2):31-49, 1983.

Cherry, J.A., S. Feenstra, B.H. Kueper, and D.W. McWhorter, Status of in situ technologies for cleanup of aquifers contaminated by DNAPLs below the water table, in the proceedings of *the International Specialty Conference on How Clean is Clean? Cleanup Criteria*

for Contaminated Soil and Groundwater, Air and Waste Management Association, November 6-9, 1990.

Cherry, J.A., S. Feenstra, and D.M. Mackay, Developing a conceptual framework and rational goals for groundwater remediation at DNAPL sites, in the proceedings of *the Subsurface Restoration Conference, Third International Conference on Ground Water Quality Research*, Dallas, TX, June 21-24, 1992.

Cherry, J.A., J.F. Barker, S. Feenstra, R.W. Gillham, D.M. Mackay, and D.J. Smyth, The Borden site for groundwater contamination experiments: 1978-1995, in the proceedings of *In Situ Subsurface Remediation: Research and Strategies*, Stuttgart, Germany, September 24-25, 1995.

Cho, S.H., and A.R. Bowers, Treatment of toxic or refractory aromatic compounds by chemical oxidants, *On-Site Bioreclamation Processes for Xenobiotic and Hydrocarbon Treatment*, R.E. Hinchee and R.F. Olfenbuttel (eds), Boston, MA, Butterworth-Heinemann, 273-292, 1991.

Cline, S.R., O.R. West, R.L. Siegrist, and W.L. Holden, Performance of in situ chemical oxidation field demonstrations at DOE sites, in the proceedings of *the ASCE Geotechnical Conference, Special Publication No. 71*, Minneapolis MN, October 5, 1997.

Colthurst, J.M. and P.C. Singer, Removing trihalomethane precursors by permanganate oxidation and manganese dioxide precipitation, *J. Amer. Water Works Assoc.*, 71(2):78-83, 1982.

Connor, J.A, C.J. Newell and D.K. Wilson, Assessment, field testing and conceptual design for managing dense nonaqueous phase liquids (DNAPL) at a Superfund site, in the proceedings of *the Conference on Petroleum Hydrocarbons and Organic Chemicals in Groundwater: Prevention, Detection and Restoration*, National Water Well Association, Houston TX, 1989.

Cowie, A. M. and M. F. Weider, In situ remediation of formalin release at Monsanto, Springfield, Massachusetts, in the proceedings of *the Hazardous Materials Spills Conference*, 1986.

Curtis, G.P., P.V. Roberts, and M. Reinhard, A natural gradient experiment on solute transport in a sand aquifer 4. sorption of organic solutes and its influence on mobility, *Water Resour. Res.*, 22(13):2059-2067, 1986.

Doty, C.B. and C.C. Travis, *The effectiveness of groundwater pumping as a restoration technology*, ORNL/TM-11866, Oak Ridge National Laboratory, Oak Ridge, TN, May

1991.

Eilbeck, W.J. and G. Mattock. *Chemical processes in wastewater treatment*, John Wiley & Sons, Toronto, 1987.

Feenstra, S., Evaluation of multi-component DNAPL sources by monitoring of dissolved-phase concentrations, presented at the conference on *Subsurface Contamination by Immiscible Fluids* (IAH), Calgary, AB, April 18-20, 1990.

Feenstra, S., Data Compilation from the Emplaced Source Field Experiment, Department of Earth Sciences, University of Waterloo, 1997.

Ficek, K.J., Manganese removal using potassium permanganate in low pH, low hardness waters, Carus Chemical Co., Ottawa, IL, 1986.

Foley, S., *Influence of sand microbeds on hydraulic response of an unweathered clay aquitard*, M.Sc. Project, Department of Earth Sciences, University of Waterloo, Waterloo, ON, 1992.

Fountain, J.C., R.C. Starr, T. Middleton, M. Beikirch, C. Taylor, and D. Hodge, A controlled field test of surfactant-enhanced aquifer remediation, *Ground Water*, 34(5):910-916, 1996.

Freeze, R.A. and J.A. Cherry, *Groundwater*, Prentice-Hall Ltd, Englewood Cliffs, NJ, 1979.

Freeze, R.A. and D.B. McWhorter, A framework for assessing risk reduction due to DNAPL mass removal from low-permeability soils, *Ground Water*, 35(1):111-123, 1997.

Freyberg, D.L, A natural gradient experiment on solute transport in a sand aquifer, 2. spatial moments and the advection and dispersion of nonreactive tracers, *Water Resour. Res.*, 22(13):2031-2046, 1986.

Frind, E.O., J.W. Molson, M. Schirmer, and N. Guiguer, Dissolution and mass transfer of multiple organics under field conditions: the Borden emplaced source, *Water Resour. Res.*, 35(3):683-694, 1999.

Gates, D.D., and R.L. Siegrist, In situ chemical oxidation of trichloroethylene using hydrogen peroxide, *J. Environ. Eng.*, (121):639-644, 1995.

Geller, J.T., and J.R. Hunt, Mass transfer from nonaqueous phase organic liquids in water-saturated porous media, *Water Resour. Res.*, 29(4):833-845, 1993.

Gillham, R.W. and D.R. Burris, In situ treatment walls - chemical dehalogenation,

denitrification and bioaugmentation, in the proceedings of *the Subsurface Restoration Conference, Third International Conference on Ground Water Quality Research*, Dallas, TX, June 21-24, 1992.

Glaze, W.H. and J.W. Kang, Advanced oxidation processes for treating groundwater contaminated with TCE and PCE: laboratory studies, *J. Amer. Water Works*, 80(5):57-63, 1988.

Grubb, D.G. and N. Sitar, *Evaluation of technologies for in situ cleanup of DNAPL contaminated sites*, EPA/600/R-94/120, R.S. Kerr Environmental Research Laboratory, Ada, OK, 1994.

Guiguer, N., *Dissolution and mass transfer processes for residual organics in the saturated groundwater zone : numerical modelling*, Ph.D. Thesis, Department of Earth Sciences, University of Waterloo, Waterloo, ON, 1992.

Haines, A.H, *Methods for the oxidation of organic compounds: alkanes, alkenes, alkynes and arenes*, Academic Press, Toronto, 1985.

Hayes, M., P MacCarthy, R. Malcolm, and R. Swift, *Humic substances II - in search of structure*, John Wiley & Sons, Toronto, 1989.

Hoigné, J. and H. Bader, Role of hydroxyl radical reaction in ozonation processes in aqueous solutions, *Water Res.*, (10):377, 1976.

Hood, E.D., N.R. Thomson, and G.J. Farquhar, In situ oxidation: an innovative treatment strategy to remediate trichloroethylene and perchloroethylene DNAPLs in porous media, in the proceedings of *the 6th Symposium on Groundwater and Soil Contamination*, Montreal, QC, 1997.

Hood, E.D., N.R. Thomson, D. Grossi and G.J. Farquhar, Experimental determination of the kinetic rate law for oxidation of perchloroethylene by potassium permanganate, *Chemosphere*, 40(12):1383-1388, 1999.

Huang, K.C., G.E. Hoag, P. Chheda, B.A. Woody and G.M. Dobbs, Kinetic study of oxidation of trichloroethylene by potassium permanganate, *Environ. Eng. Sci.*, 16(4):265-274, 1999.

Imhoff, P.T., P.R. Jaffé, and G.F. Pinder, An experimental study of complete dissolution of a nonaqueous phase liquid in saturated porous media, *Water. Resour. Res.*, 30(2):307-320, 1994.

Johnson, R.L. and J.F. Pankow, Dissolution of dense chlorinated solvents into groundwater.

2. Source functions for pools of solvent, *Environ. Sci. Technol.*, 26(5): 896-901, 1992.

Johnson, R.L., P.C. Johnson, D.B. McWhorter, R.E. Hinchee, and I. Goodman, An overview of in situ air sparging, *Ground Water Monit. Remed.*, (Fall):127-135, 1993.

Korom, S.F., M.J. McFarland, and R.C. Sims, Reduced sediments: a factor in the design of subsurface oxidant delivery systems, *Ground Water Monit. Remed.*, 16(1):100-105, 1996.

Kueper, B.H., W. Abbott, and G.J Farquhar, Experimental observations of multiphase flow in heterogeneous porous media, *J. Contam. Hydrol.*, 5(1):83-95, 1989.

Kueper, B.H. and E.O. Frind, Two-phase flow in heterogeneous porous media 2. model application, *Water Resour. Res.*, 27(6):1059-1070, 1991.

Kueper, B.H., D. Redman, R.C. Starr, S. Reitsma and M. Mah, A field experiment to study the behavior of tetrachloroethylene below the water table: spatial distribution of residual and pooled DNAPL, *Ground Water*, 31(5):756-766, 1992.

Larson, R.A. and J. Cervini-Silva, Electron transfer to organochlorine compounds by an iron (II) porphyrin-dithionite system, in the proceedings of *the First International Conference on Remedation of Chlorinated and Recalcitrant Compounds*, Monterey, CA, May 18-21, 1998.

Lee, D.G., Oxidation of organic compounds by permanganate ion and hexavalent chromium, Open Court Publishing Co., LaSalle, IL, 1980.

Lesage, S. and S. Brown, Observation of the dissolution of NAPL mixtures, *J. Contam. Hydrol.*, 15(1-2):57-71, 1994.

Lesage, S., S. Brown, and K. Millar, Vitamin B12-catalyzed dechlorination of perchloroethylene present as residual DNAPL, *Ground Water Monit. Remed.*, 16(4):76-85, 1996.

Leverett, M.C., Capillary behaviour in porous solids, *Trans. AIME*, (142):152-169, 1941.

Lowry, G., M. Reinhard, and W. McNab, Jr., Dehalogenation of chlorinated solvents using a palladium catalyst hydrogen gas, in the proceedings of *the First International Conference on Remediation of Chlorinated and Recalcitrant Compounds*, Monterey, CA, May 18-21, 1998.

Lunn, G., E.B. Sansone, M DeMeo, M. Laget, and M. Castegnaro, Potassium permanganate can be used for degrading hazardous compounds, *Amer. Ind. Hyg. Assoc. J.*, 55(2):167-171,

1994.

Macfarlane, D.S., J.A. Cherry, R.W. Gillham, and E.A. Sudicky, Migration of contaminants in groundwater at a landfill: 1, a case study, *J. Hydrol.*, 63(1-2):1-29, 1983.

Mackay, D., W.Y. Shiu,, A. Maijanen, and S. Feenstra, Dissolution of non-aqueous phase liquids in groundwater, *J. Contam. Hydrol.*, 8(1):23-42, 1991.

MacKay, D., A. Hewitt, S. Reitsma, J. LaChance, and R. Baker, *In situ* oxidation of trichloroethylene using potassium permanganate: part 2. pilot study, in proceedings of *the First International Conference on Remediation of Chlorinated and Recalcitrant Compounds*, Monterey, CA, May 18- 21, 1998.

Mackay, D.M. and J.A. Cherry, Groundwater contamination: pump-and-treat remediation, *Environ. Sci. Technol.*, 23(6):630-636, 1989.

Mackay, D.M. and L.A. Smith, Agricultural chemicals in groundwater: monitoring and management in California, *J. Soil Water Conserv.*, 45(2):253-256, 1990.

Mackay, D.M., D.L. Freyberg and P.V. Roberts, A natural gradient experiment on solute transport in a sand aquifer, 1. approach and overview of plume movement, *Water Resour. Res.*, 22(13):2017-2029, 1986.

MacKinnon, L.K., *In situ oxidation of a PCE pool*, M.A.Sc. Thesis, Department of Civil Engineering, University of Waterloo, Waterloo, ON, 1999.

Marvin, B.K., C.H. Nelson, W. Clayton, K. M. Sullivan and G. Skladany, In situ chemical oxidation of pentachlorophenol and polycyclic aromatic hydrocarbons: from laboratory tests to field demonstrations, in the proceedings of *the First International Conference on Remediation of Chlorinated and Recalcitrant Compounds*, Monterey, CA, May 18-21, 1998.

Mercer, J.W. and R.M Cohen, A review of immiscible fluids in the subsurface: properties, models, characterization and remediation, *J. Contam. Hydrol.*, 6(2):107-163, 1990.

Michalski, A., M.N. Metlitz,and I.L. Whitman, A field study of enhanced recovery of DNAPL pooled below the water table, *Ground Water Mon. Rev.*, 15(1):90-100, 1995.

Middlemas, R.E., and K.J. Ficek, Controlling the potassium permanganate feed for taste and odour treatment, in the proceedings of the *AWWA Annual Conference*, Denver, CO, June 26, 1986.

Miller, C.T., Poirier-McNeill, M.M., and A.S. Mayer, Dissolution of trapped nonaqueous phase

liquids: mass transfer characteristics, *Water Resour. Res.*, 26(11):2783-2796, 1990.

Millington, R.J., Gas diffusion in porous media, *Science*, 130:100-102, 1959.

Montgomery, J.M, Consulting Engineers, *Water Treatment Principles and Design*, John Wiley & Sons, Toronto, 1985.

Moody, D.W, Groundwater contamination in the United States, *J. Soil Water Conserv.*, 45(2):170-179, 1990.

Moyers, B. and J.S. Wu, Removal of organic precursors by permanganate oxidation and alum coagulation, *Water Res.*, 19(3):309-314, 1985.

National Research Council, *Alternatives for ground water cleanup*, National Academy Press, Washington, DC, 1994.

Newell, C.J., J.A. Connor, D.K. Wilson and T.E. McHugh, Impact of dissolution of dense non-aqueous phase liquids (DNAPLs) on groundwater remediation, in the proceedings of *Petroleum Hydrocarbons and Organic Chemicals in Ground Water: Prevention, Detection, and Restoration*, November 20-22, Houston, TX, 1991.

O'Hannesin, S.F. and R.W. Gillham, A permeable reaction wall for in situ degradation of halogenated organic fluids, in the proceedings of *the 45th Canadian Geotechnical Conference*, Toronto, ON, October 26-28, 1992.

Oolman, T., S.T. Godard, G.A. Pope, M. Jin, and K. Kirchner, DNAPL flow behaviour in a contaminated aquifer: evaluation of field data, *Ground Water Monit. Remed.*, 15(1):125-137, 1995.

Pankow, J.F., and R.L. Johnson, Dissolution of dense chlorinated solvents into groundwater 2. source functions for pools of solvent, *Environ. Sci. Technol.*, 26(5):896-908, 1992.

Pankow, J.F. and J.A. Cherry, *Dense chlorinated solvents and other DNAPLs in Groundwater*, Waterloo Press, Guelph, ON, 1996.

Pankow, J.F., R.L. Johnson and J.A. Cherry, Air sparging in gate walls, cutoff walls and trenches for control of plumes of volatile organic compounds (VOCs), *Ground Water*, 31(4):654-663, 1993.

Pavlostathis, S.G., and K.J. Jaglal, Desorptive behaviour of TCE in contaminated soil, *Environ. Sci. Technol.*, 25(2):274-279, 1991.

Pitkin, S.E., J.A. Cherry, R.A. Ingleton, and M. Broholm, Field demonstrations using the

Waterloo ground water profiler, *Ground Water Monit. Remed.*, 19(2):122-131, 1999.

Plumb, R.H., A comparison of ground water monitoring data from CERCLA and RCRA sites, *Ground Water Mon. Rev.*, 7(4):94-100, 1987.

Plumb, R.H., The occurrence of Appendix IX organic constituents in disposal site ground water, *Ground Water Mon. Rev.*, 11(2):157-165, 1991.

Perry, R.H., D. Green, and J.O. Maloney (eds.), *Perry's Chemical Engineers' Handbook*, 6th Ed., McGraw-Hill, Inc., New York, 1984.

Poulsen, M.M. and B.H. Kueper, A field experiment to study the behaviour of tetrachloroethylene in unsaturated porous media, *Environ. Sci. Technol.*, 26(5):889-895, 1992.

Powers, S.E., L.M. Abriola, and W.J. Weber, Jr., An experimental investigation of nonaqueous phase liquid dissolution in saturated subsurface systems: Transient mass transfer rates, *Water Resour. Res.*, 30(2):321-332, 1994.

Rajaram, H., and L.W. Gelhar, Three-dimensional spatial moments analysis of the Borden tracer test, *Water Resour. Res.*, 27(6):1239-1251, 1991.

Ravikumar, J. X. and M. D. Gurol, Chemical oxidation of chlorinated organics by hydrogen peroxide in the presence of sand, *Environ. Sci. Technol.*, 28(3):395-400, 1994.

Rees, T., The stability of potassium permanganate solutions, *J. Chem. Ed.*,64(12):1058, 1987.

de Renzo, D.J., *Unit operations for treatment of hazardous industrial wastes*, Noyes Data Corporation, Park Ridge, NJ, 1978.

Rinehart, K.L, *Oxidation and reduction of organic compounds*, Prentice-Hall, Inc., Englewood Cliffs, NJ, 1973.

Rivett, M.O., A field evaluation of pump-and-treat remediation, in the proceedings of *the Joint CSCE-ASCE National Conference on Environmental Engineering*, Montreal, QC, July 12-14, 1993.

Rivett, M.O., S. Feenstra, and J.A. Cherry, Field experimental studies of a residual solvent source emplaced in the groundwater zone, in proceedings of *the Conference on Petroleum Hydrocarbons and Organic Chemicals in Groundwater, National Water Well Association*, Houston, TX, November 20-22, 1991.

Rivett, M.O., S. Feenstra, and J.A. Cherry, Groundwater zone transport of chlorinated solvents:

a field study, in the proceedings of *Modern Trends in Hydrogeology*, Hamilton, ON, May 10, 1992.

Rivett, M.O., S. Feenstra, and J.A. Cherry, Comparison of Borden natural gradient tracer tests, in the proceedings of *the IAHR Symposium on Transport and Reactive Processes in Aquifers*, Zurich, Switzerland, April 11-15, 1994.

Roberts, J.R., J.A. Cherry, and F.W. Schwartz, *Water Resour. Res.*, 18:525-534, 1982.

Roberts, P.V., M.N. Goltz and D.M. Mackay, A natural gradient experiment on solute transport in a sand aquifer 3. retardation estimates and mass balances for organic solutes, *Water Resour. Res.*, 22(13):2047-2058, 1986.

Robin, M.J.L., A.L. Gutjahr, E.A. Sudicky, and J.L. Wilson, Cross-correlated random field generation with the direct Fourier transform method, *Water Resour. Res.*, 29(7):2385-2397, 1993.

Sale, T.C., *Interphase mass transfer from single component DNAPLs*, Ph.D. Thesis, Department of Chemical and Bioresource Engineering, Colorado State University, Fort Collins, CO, 1999.

Sanford, W.E. and L.F. Konikow, Simulation of calcite dissolution and porosity changes in saltwater mixing zones in coastal aquifer, *Water Resour. Res.*, 25(4):655-667, 1989.

Sawhney, B.L., J.J. Pignatello and S.M. Steinberg, Determination of 1,2-dibromoethane (EDB) in field soils: implications for volatile organic compounds, *J. Environ. Qual.*, 17(1):149-152, 1988.

Schnarr, M.J. and G.J. Farquhar, An in situ oxidation technique to destroy residual DNAPL from soil, in the proceedings of *the Third International Conference on Ground Water Quality*, Dallas, TX, June 21-24, 1992.

Schnarr, M.J., *An in-situ oxidative technique to remove residual DNAPL from soils*, M.A.Sc. Thesis, Department of Civil Engineering, University of Waterloo, Waterloo, ON, 1992.

Schnarr, M.J., C.L. Truax, G.J. Farquhar, E.D. Hood, T. Gonullu and B. Stickney, Laboratory and controlled field experiments using potassium permanganate to remediate trichloroethylene and perchloroethylene DNAPLs in porous media, *J. Contam. Hydrol.*, 29(3):205-224, 1998.

Schwarzenbach, R.P., P.M. Gschwend, and D.M. Imboden, *Environmental organic chemistry*, J. Wiley & Sons, New York, 1993.

Schwille, F., *Dense chlorinated solvents in porous and fractured media : model experiments*, Lewis Publishers, Chelsea, MI, 1988.

She, H.Y. and B.E. Sleep, Removal of perchloroethylene from a layered soil system by steam flushing, *Ground Water Monit. Remed.*, 19(2):70-77, 1999.

Siegrist, R.L., K.S. Lowe, L.C. Murdoch, T.L. Case, and D.A. Pickering, In situ oxidation by fracture emplaced reactive solids, *J. Environ. Eng.*, 125(5):429-440, 1999.

Singer, P.C, J.H Borchardt, and J.M. Colthurst, The effects of permanganate pretreatment on trihalomethane formation in drinking water, *J. AWWA Res. Technol.*, 70(10):573-578, 1980.

Sleep, B.E. and J.F Sykes, Modeling the transport of volatile organics in variably saturated media, *Water Resour. Res.*, 25(1):81-92, 1989.

Smith, B.E and J.F. Sykes, Recovery of DNAPL-theory and practice, in the proceedings of *the Fifth National Conference on Hazardous Wastes and Hazardous Materials*, April 19-21, Las Vegas, NV, 1988.

Solomon, D.K., R.J. Poreda, S.L. Schiff and J.A. Cherry, Tritium and He^3 as groundwater age tracers in the Borden aquifer, *Water Resour. Res.*, 28(3):741-755, 1991.

Starr, R.C. and J.A. Cherry, In situ remediation of contaminated ground water: the funnel-and-gate system, *Ground Water*, 32(3):465-476, 1994.

Stewart, R., *Oxidation in organic chemistry: oxidation by permanganate*, K.Wiberg, ed., Academic Press, New York, 1973.

Sudicky, E.A. J.A.Cherry, and E.O. Frind, Migration of contaminants in groundwater at a landfill: a case study; 4. A natural-gradient dispersion test, *J. Hydrol.*, 63(1-2):81-108, 1983.

Sudicky, E.A., A natural gradient experiment on solute transport in a sand aquifer: spatial variability of hydraulic conductivity and its role in the dispersion process, *Water Resour. Res.*, 22(13):2069-2082, 1986.

Thomson, N.R., 3D3PT Manual, Department of Civil Engineering, University of Waterloo, Waterloo, ON, 1995.

Thomson, N.R., ENV473 - Contaminant Transport Course Notes, Department of Civil Engineering, University of Waterloo, Waterloo, ON, 2000.

Tomlinson, D.W., *A performance assessment of in situ air sparging*, M.A.Sc. Thesis, Department of Civil Engineering, University of Waterloo, Waterloo, ON, 1998.

Turcke, M.A., and B.H. Kueper, Geostatistical analysis of the Borden aquifer hydraulic conductivity field, *J. Hydrol.*, 178(1-4):223-240, 1996.

Tratnyek, P.G., T.L. Johnson, S.D. Warner, H.S. Clarke, J.A. Baker, In situ treatment of organics by sequential reduction and oxidation, in the proceedings of *the First International Conference on Remediation of Chlorinated and Recalcitrant Compounds*, Monterey, CA, May 18-21, 1998.

Truax, C.T.L., *Investigation of the in situ $KMnO_4$ oxidation of residual DNAPLs located below the groundwater table*, M.A.Sc. Thesis, Department of Civil Engineering, University of Waterloo, Waterloo, ON, 1994.

Tunnicliffe, B.S., *Mass removal from a rough-walled fracture: experimental investigation using permanganate*, M.A.Sc. Thesis, Department of Civil Engineering, University of Waterloo, Waterloo, ON, 1999.

Underwood, J.L., K.A. Debelak, D.J. Wilson, and J.M. Means, Soil clean up by in situ surfactant flushing. V. micellar solubilization of some aromatic contaminants, *Sep. Sci. Technol.*, 28(8):1527-1537, 1993.

Urynowicz, M.A., and R.L. Siegrist, Chemical degradation of TCE DNAPL by permanganate, in the proceedings of *the Second International Conference on Remedation of Chlorinated and Recalcitrant Compounds*, Monterey, CA, May 22-25, 2000.

United States Environmental Protection Agency, Inert ingredients in pesticide products: policy statement, *Federal Register*, 52(77):13305-13309, 1987.

Vella, P.A., G. Deshinsky, J.E. Boll, J.A. Munder, and W.M. Joyce, Treatment of low level phenols (mg./L) with potassium permanganate, *J. WPCF*, 62(7):907-914, 1990.

Vella, P.A. and J.A Munder, A comparison of the oxidants potassium permanganate, chlorine dioxide, and Fenton's reagent on the oxidation and toxicity of substituted phenols, in the proceeding of *Emerging Technologies for Hazardous Waste Management*, Atlanta, GA, October 1-3, 1991.

Vella, P.A. and B. Veronda, Oxidation of trichloroethylene: a comparison of potassium permanganate and Fenton's reagent, in the proceedings of *the Third International Symposium on Chemical Oxidation Technology for the Nineties*, Vanderbuilt University, Nashville, TN, 1992.

Vendkatadri, R. and R.W. Peters, Chemical oxidation technologies: ultraviolet light/hydrogen peroxide, Fenton's reagent, and titanium dioxide-assisted photocatalysis, *Haz. Waste & Haz. Mat.*, 10(2):107-144, 1993.

Watts, R.J., M.D. Udell, S. Kong, and S.W. Leung, Fenton-like soil remediation catalyzed by naturally occurring iron minerals, *Environ. Eng. Sci.*, 16(1):93-103, 1999.

West, O.R, In situ oxidation by well injection and recirculation of potassium permanganate, *summary of presentation at the Water Environment Federation (WEFTEC) Workshop on In Situ Oxidation for Site Remediation*, Chicago, IL, October 1997.

Westrick, J.J, J.W. Mello, and R.F Thomas, The groundwater supply survey, *J. Amer. Water Works Assoc.*, 76(5):52-59, 1984.

Yan, Y.E, and F. Schwartz, Oxidation of chlorinated solvents by permanganate, in the proceedings of *the First International Conference on Remediation of Chlorinated and Recalcitrant Compounds*, Monterey, CA, May 18-21, 1998.

Yan, Y.E, and F. Schwartz, Oxidative degradation and kinetics of chlorinated ethylenes by potassium permanganate, *J. Contam. Hydrol.*, 37(3):343-365, 1999.

Walkley, A. and I.A. Black, An examination of the Degtjareff method for determining soil organic matter, and a proposed modification of the chromic acid titration method, *Soil Sci.*, (37):29-37, 1935.

West, O.R., S.R. Cline, W.L. Holden, F.G. Gardner, B.M. Schlosser, J.E. Thate, D.A. Pickering, and T.C. Houk, A full-scale demonstration of in situ chemical oxidation through recirculation at the X-701B: field operations and TCE degradation, Environmental Sciences Division, Oak Ridge National Laboratory, Oak Ridge TN, 1997.

Wilson, R.D., and D.M. Mackay, A method for passive release of solutes from an unpumped well, *Ground Water*, 33(6):936-945, 1995.

Wood, W.W., T.F. Kraemer, and P.P. Hearn Jr., Intragranular diffusion: an important mechanism influencing solute transport in clastic aquifers?, *Science*, (247), March 1990.

Woodbury, A.D. and E.A. Sudicky, The geostatistical characteristics of the Borden aquifer, *Water Resour. Res.*, 27(4), 533-546, 1991.

Zhu, K., C. Hui, L. Guanche, and L. Zhaochang, In situ remediation of petroleum compounds in groundwater aquifer with chlorine dioxide, *Water Res.*,32(5):1471-1480, 1998.

Appendix A

Measurement of the Oxidant Demand of Sandy Soils

A.1 Introduction

The amount of oxidant required to oxidize uncontaminated soils can be a significant fraction of the total oxidant mass required during in situ chemical oxidation (ISCO). The soil oxidant demand (or reduction capacity) appears to primarily result from the oxidation of naturally-occurring organic carbon compounds known as humic substances that comprise the organic carbon content (*foc*). The presence of reduced mineral forms of iron, manganese and sulfur can also result a oxidant demand, although in comparison to *foc* this is a relatively minor contribution (Holm and Barcelona, 1991). In the case of permanganate, the oxidant demand can be characterized using one of several soil oxidant demand measurement methods developed and tested during the course of the current research. This Appendix presents a description of the test methods, presents preliminary results of measurements of oxidant demand made on a number of sand samples, and examines the relationship between the oxidant demand and the soil organic carbon content.

A.2 Materials and Measurement Methods

A.2.1 Characterization of Sand Samples

The characteristics of each soil sample used in this study are summarized in Table A.1. Measurements of *foc* were made at the University of Waterloo Earth Sciences Geochemistry Laboratory using an analytical method developed by Churcher and Dickhout (1987). The detection limit of the method was 0.03% (mass of organic carbon per dry mass of sand).

A.2.2 Column Measurement of Oxidant Demand

A column test method was devised to determine the oxidant demand of a representative soil sample under redox conditions representative of those occurring during an oxidant flush. A representative soil sample was dried and homogenized with a riffle splitter. Particles larger than 2 mm were removed using a #10 standard sieve. The riffle splitter was also used to collect homogeneous subsamples of the original sand sample. The measurement apparatus, which is shown in Figure A.1, was constructed in a light-opaque closet to minimize light-catalysed decomposition of the permanganate solution. A small column that was fitted with a fine stainless steel screen to contain fines was packed with a preweighed subsample in one cm lifts. The column was flushed with CO_2 to remove air from the void spaces and was then flushed with a standardized permanganate solution. Permanganate solutions were standardized by titration with oxalate (Standard Methods, 16th ed.). A micro-flow peristaltic pump delivered the oxidant feed solution through either Norprene or Teflon tubing to the column. The volumetric flow rate of the permanganate solution was measured using a 1 mL graduated pipet and a stopwatch while

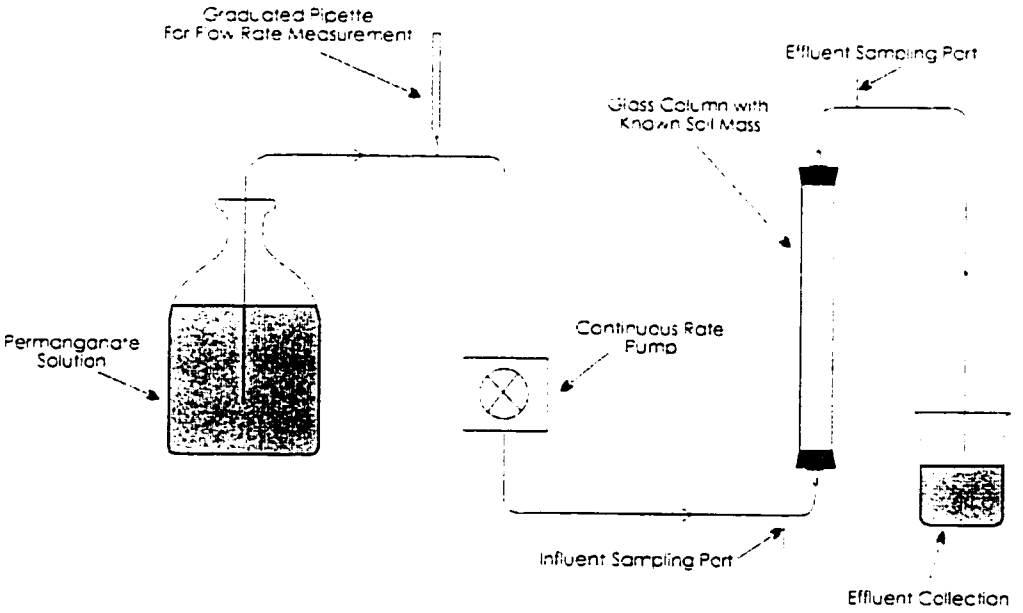

Figure A.1 Schematic of column apparatus for measuring soil oxidant demand.

the influent and effluent permanganate concentrations were measured using the spectrophotometric method described in Chapter 3. The average linear groundwater velocity in the column was ~ 0.3 m/day. Following oxidant breakthrough in the effluent, samples were collected and immediately analysed to determine the permanganate concentration. Each test ran until the effluent permanganate concentration was indistinguishable from the influent concentration. The mass of oxidant consumed by the sample was calculated as the difference between the total mass of permanganate contained in the influent and effluent flows.

A.2.3 Walkley-Black Titration to Determine Organic Content

As a simple alternative to the column method described in the previous section, soil oxidant demand measurements were made using a titration method comparable to the conventional chemical oxygen demand (COD) measurement used for analysis of wastewater. Titration measurements were made using a standard method [described in detail by the British Standards Institution (1975)] that is based upon an experimental method developed by Walkley and Black (1935).

The method uses a preliminary digestion step followed by volumetric titration. The soil sample is dried and pulverized and a weighed portion(0.2-5.0 g to the nearest 0.001 g) transferred to a flask. The sample is digested with 10 mL of 1 N potassium dichromate and 20 mL of concentration sulfuric acid for 30 min, after which 200 mL deionized water, 10 mL of 85% orthophosphoric acid, and 1 mL of sodium diphenylaminesulphonate indicator solution are added. The mixture is titrated with a standardized ferrous sulfate solution (~0.5 N) until the colour of the solution changes from blue to green. The volume of ferrous sulfate titrant is used to calculate the volume of dichromate solution reduced by the soil, which may be converted using equivalent units to an oxidant demand in terms of potassium permanganate.

Several species are known to interfere with the determination of the dichromate endpoint. The presence of high chloride or sulfide concentrations in the soil will tend to result in an overestimate of the actual organic matter content.

A.3 Results

Results of the titration and column measurement of soil oxidant demand are presented in Table A.2 The average specific oxidant demand was determined to be 65 g/kg/%*foc*. The soil oxidant demand measured with the column method as a function of the *foc* is presented in Figure A.2. In contrast to prior experiments conducted by Barcelona and Holm (1991), the soil oxidant demand appears to be only weakly correlated with the organic carbon content (r^2=0.20). Given the number of analysts and the evolving nature of the column measurement apparatus during the time that these measurements were made, it may be that much of the variability in these results is caused by experimental errors. Of particular interest is the difference between samples taken from the saturated and unsaturated zones in the Borden aquifer. The oxidant demand of the unsaturated zone sample was ~ 10 times that of the unsaturated zone sample. The difference may be attributed to several factors including the relatively recent deposition of the shallow sediment, and the availability of unweathered organic material (including vegetative fragments) near the surface.

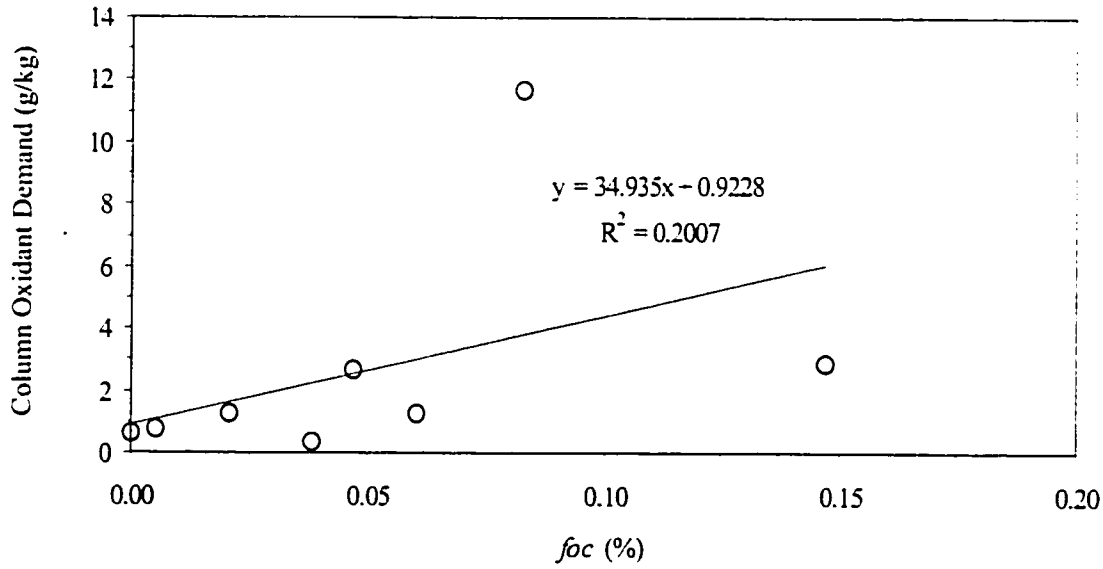

Figure A.2 Correlation of soil oxidant demand measured using the column method with organic carbon content.

In contrast to the column measurements, the soil oxidant demands measured using the Walkley-Black titration method are substantially larger and vary linearly (r^2=0.94) with the organic carbon content (Figure A.3). The average specific oxidant demand estimated using the titration method was 213 g/kg/%*foc*, a result that was significantly higher than that estimated using the column method. Only three samples were tested using both methods (Borden A, Borden B, and Seagram). The oxidant demand results obtained using both test method appeared to be linearly correlated (Figure A.4) although the small number of samples made this difficult to confirm. The oxidant demands measured using the Walkley-Black method were approximately twice those estimated using the column method.

A.4 Discussion and Recommendations

While the column results appeared to be only weakly correlated with organic carbon content, this result may reflect a methodological problem rather than one caused by reactions between the injected permanganate solution and the soil. The various column measurements employed

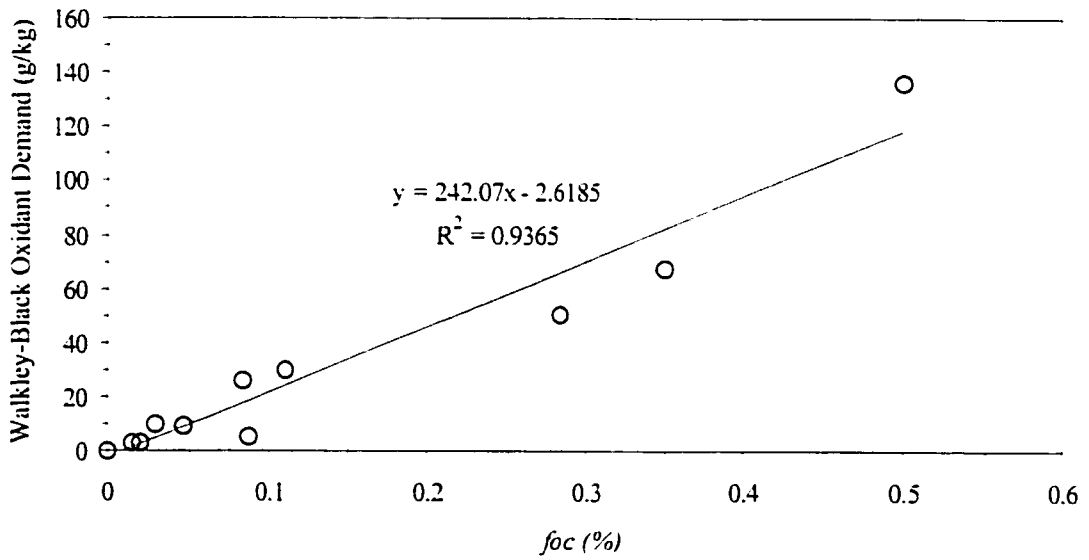

Figure A.3 Correlation of the soil oxidant demand measured using the Walkley-Black titration method with organic carbon content.

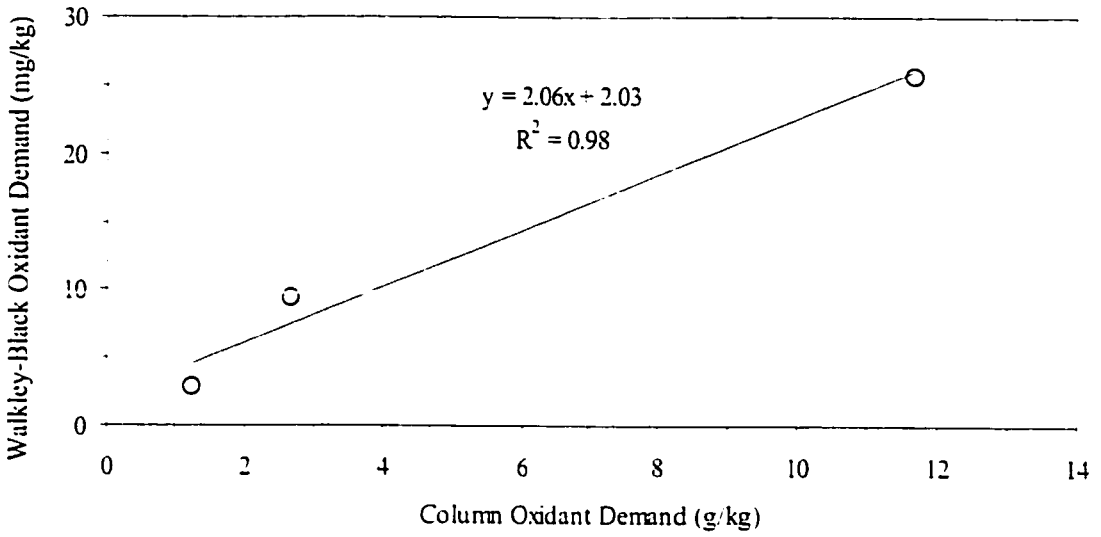

Figure A.4 Correlation between soil oxidant demands estimated using the column and Walkley-Black titration methods.

a method and measurement apparatus that varied over time. Further, the level of effort required to complete a single measurement precluded extensive testing to verify the reproducibility of the column method. In the earlier columns, oxidation of the materials used (especially Norprene) and autocatalytic decomposition of the permanganate solution caused by exposure to light may have resulted in significant oxidant consumption in comparison to the soil sample. Further, some of the column tests may not have run for a sufficiently long period of time to completely satisfy the oxidant demand. In many of the column tests, the final effluent permanganate concentration was ~99% of the influent permanganate concentration. While the influent and effluent concentrations were statistically indistinguishable, it is possible that the small difference was significant in terms of the total oxidant demand exerted by the sample.

Several improvements to the test methods are recommended. The columns should be redesigned to provide a substantially longer residence time to ensure that the permanganate has sufficient time to react with any oxidizable fraction of the soil. To make the feed solution more

representative of field conditions, the alkalinity and the dissolved gas content of the feed solution should be adjusted so that it is geochemically similar to real groundwater. As a test of the reproducibility of the column measurement method, blank column tests containing fired silica sand should be performed to ensure that the measured oxidant demand reflects the oxidant demand exerted by the sample rather than the materials used to construct the measurement apparatus. Finally, a number of sand samples over a range of organic carbon contents should be tested using both the column and titration methods to determine any correlation between the two methods. In the event that consistent and linear correlation between the methods can be established, the use of the complex column method could then be discarded in favour of the rapid and highly reproducible titration method.

Table A.1
Description and Characterization of Sand Samples

Sample ID	Location	Groundwater Interval	Depth	Textural Description	Colour	Contamminated? (Y/N)	*foc* (%)
Borden A	CFB Borden, ON	vadose	~1.5 m below ground surface	SPu, uniform, medium fine	tan, orange	N	0.0833
Borden B	CFB Borden, ON	saturated	~0.5 m below water table	SPu, uniform, medium fine	white to grey	N	0.021[a]
Seagram	Waterloo, ON	vadose	~0.75 m below ground surface	SM silty	grey	N	0.0467
Rocky Mountain Arsenal	Commerce City, CO	NA	homogenized sample from 59.87' bgs	SPu, uniform, medium fine, with pebbles	light tan	N	0.005
Field Site No. 1	Texas	saturated	NA	easily fragmented sandstone	reddish	N	0.038
Field Site No. 2	Peterborough, ON	saturated	2 m bgs	fine to coarse sand	dark brown to grey	N	0.06
Field Site No. 3	Nova Scotia	saturated/unsaturated transitional zone	2 m bgs	silty sand and gravel	reddish brown	NA	0.147
Field Site No. 4	Mississauga, ON	saturated	2 m bgs	uniform fine	dark brown	N	
Muskoka Field Site	Bracebridge, ON	vadose	0.48-1.25 m bgs	SPu, uniform, medium fine	brown	Y[d]	0.0867
Muskoka Field Site	Bracebridge, ON	vadose	0-0.52 m bgs	SW, well-graded	brown	Y[d]	0.5
Lampton	Lampton, ON	vadose	1.85 m bgs	SPu, uniform, medium fine	tan/brown	Y[d]	NA
Lambton	Lampton, ON	vadose	0.35-0.85 m bgs	SPu, uniform, medium fine	brown	Y[d]	0.11
Cambridge	Cambridge, ON	vadose	0.35-0.75 m bgs	SPu, uniform, medium fine	tan/brown	Y[d]	0.2833
Cambridge	Cambridge, ON	vadose	0-0.75 m bgs	SPu, uniform, medium fine	brown	Y[d]	0.35
Columbia River	Oregon	surface	surface	SPu, uniform, medium fine	dark grey	N	0.015[b]
Oregon Beach	Oregon	surface	surface	SPu, uniform, medium fine	tan	N	0.03
Silica Sand	NA	laboratory[c]	NA	SPu, uniform, medium fine	white	N	0

Notes:

bgs - below ground surface

fos - fractional organic carbon content

NA - Not applicable/available

[a] Sample was below method detection limit, value reported that by Ball et al. (1990)

[b] The sample *fos* was below method detection limit, value reported as half MDL

[c] The silica sand was fired in the Muffle furnace at ~600 Celcius to combust any organic matter

[d] Samples were collected as part of an investigation of septic systems. While the samples were reported to represent background conditions, they may contain contaminants associated with sewage

Table B.2
Summary of Soil Oxidant Demands Measured
Using Walkley-Black Titration
and Column Measurement Methods

Sample	*foc* (%)	Oxidant Demand			
		Walkley Black		Column	
		(g/kg)[1]	(g/kg/%*foc*)	(g/kg)[1]	(g/kg/%*foc*)
Borden A	0.0833	25.7	309	11.7	140
Borden B	0.021[a]	2.9	138	1.2	59
Seagram	0.0467	9.4	201	2.6	57
Rocky Mountain Arsenal	0.005			0.7	149
Field Site No. 1	0.038			0.3	9
Field Site No. 2	0.060			1.2	21
Field Site No. 3	0.147			2.9	20
Field Site No. 4				0.7	-
Muskoka Field Site	0.0867	5.4	62		
Muskoka Field Site	0.5	136.4	273		
Lampton	NA	66.7			
Lambton	0.11	30.1	274		
Cambridge	0.2833	50.7	179		
Cambridge	0.35	67.5	193		
Columbia River	0.015[b]	2.7	183		
Oregon Beach	0.03	9.6	319		
Silica Sand	0	0.1			
		Average =	**213**		**65**

Notes:

foc - fractional organic carbon content

NA - Not applicable available

[1] Oxidant demand reported as g $KMnO_4$ required to oxidize 1 kg of dry sample.

Appendix B

Summary of Data Collected During ISCO Field Trial

List of Tables

TABLE B-1

Spatial Coordinates of Multilevel Sampling Points, Monitoring Well Screens and the Emplaced Source Zone (Page 1 of 3)

Coordinate ID	*Description of Coordinate*	*X (m)*	*Y (m)*	*Elevation (m)*
1-1	multilevel sampler	0.95	-1.04	96.740
1-2	multilevel sampler	0.95	-1.04	96.540
1-3	multilevel sampler	0.95	-1.04	96.340
1-4	multilevel sampler	0.95	-1.04	96.140
1-5	multilevel sampler	0.95	-1.04	95.940
1-6	multilevel sampler	0.95	-1.04	95.740
1-7	multilevel sampler	0.95	-1.04	95.540
1-8	multilevel sampler	0.95	-1.04	95.340
1-9	multilevel sampler	0.95	-1.04	95.140
1-10	multilevel sampler	0.95	-1.04	94.940
1-11	multilevel sampler	0.95	-1.04	94.740
1-12	multilevel sampler	0.95	-1.04	94.540
1-13	multilevel sampler	0.95	-1.04	94.340
1-14	multilevel sampler	0.95	-1.04	94.140
2-1	multilevel sampler	0.45	-1.04	96.790
2-2	multilevel sampler	0.45	-1.04	96.590
2-3	multilevel sampler	0.45	-1.04	96.390
2-4	multilevel sampler	0.45	-1.04	96.190
2-5	multilevel sampler	0.45	-1.04	95.990
2-6	multilevel sampler	0.45	-1.04	95.790
2-7	multilevel sampler	0.45	-1.04	95.590
2-8	multilevel sampler	0.45	-1.04	95.390
2-9	multilevel sampler	0.45	-1.04	95.190
2-10	multilevel sampler	0.45	-1.04	94.990
2-11	multilevel sampler	0.45	-1.04	94.790
2-12	multilevel sampler	0.45	-1.04	94.590
2-13	multilevel sampler	0.45	-1.04	94.390
2-14	multilevel sampler	0.45	-1.04	94.190
3-1	multilevel sampler	-0.05	-1.04	96.840
3-2	multilevel sampler	-0.05	-1.04	96.640
3-3	multilevel sampler	-0.05	-1.04	96.440
3-4	multilevel sampler	-0.05	-1.04	96.240
3-5	multilevel sampler	-0.05	-1.04	96.040
3-6	multilevel sampler	-0.05	-1.04	95.840
3-7	multilevel sampler	-0.05	-1.04	95.640
3-8	multilevel sampler	-0.05	-1.04	95.440
3-9	multilevel sampler	-0.05	-1.04	95.240
3-10	multilevel sampler	-0.05	-1.04	95.040
3-11	multilevel sampler	-0.05	-1.04	94.840
3-12	multilevel sampler	-0.05	-1.04	94.640
3-13	multilevel sampler	-0.05	-1.04	94.440
3-14	multilevel sampler	-0.05	-1.04	94.240
4-1	multilevel sampler	-0.55	-1.04	96.790
4-2	multilevel sampler	-0.55	-1.04	96.590
4-3	multilevel sampler	-0.55	-1.04	96.390
4-4	multilevel sampler	-0.55	-1.04	96.190
4-5	multilevel sampler	-0.55	-1.04	95.990
4-6	multilevel sampler	-0.55	-1.04	95.790
4-7	multilevel sampler	-0.55	-1.04	95.590

TABLE B-1
Spatial Coordinates of Multilevel Sampling Points, Monitoring Well Screens and the Emplaced Source Zone (Page 2 of 3)

Coordinate ID	*Description of Coordinate*	*X (m)*	*Y (m)*	*Elevation (m)*
4-8	multilevel sampler	-0.55	-1.04	95.390
4-9	multilevel sampler	-0.55	-1.04	95.190
4-10	multilevel sampler	-0.55	-1.04	94.990
4-11	multilevel sampler	-0.55	-1.04	94.790
4-12	multilevel sampler	-0.55	-1.04	94.590
4-13	multilevel sampler	-0.55	-1.04	94.390
4-14	multilevel sampler	-0.55	-1.04	94.190
5-1	multilevel sampler	-1.05	-1.04	96.780
5-2	multilevel sampler	-1.05	-1.04	96.580
5-3	multilevel sampler	-1.05	-1.04	96.380
5-4	multilevel sampler	-1.05	-1.04	96.180
5-5	multilevel sampler	-1.05	-1.04	95.980
5-6	multilevel sampler	-1.05	-1.04	95.780
5-7	multilevel sampler	-1.05	-1.04	95.580
5-8	multilevel sampler	-1.05	-1.04	95.380
5-9	multilevel sampler	-1.05	-1.04	95.180
5-10	multilevel sampler	-1.05	-1.04	94.980
5-11	multilevel sampler	-1.05	-1.04	94.780
5-12	multilevel sampler	-1.05	-1.04	94.580
5-13	multilevel sampler	-1.05	-1.04	94.380
5-14	multilevel sampler	-1.05	-1.04	94.180
28-1	multilevel sampler	1.60	-1.04	97.300
28-2	multilevel sampler	1.60	-1.04	97.100
28-3	multilevel sampler	1.60	-1.04	96.900
28-4	multilevel sampler	1.60	-1.04	96.700
28-5	multilevel sampler	1.60	-1.04	96.500
28-6	multilevel sampler	1.60	-1.04	96.300
28-7	multilevel sampler	1.60	-1.04	96.100
28-8	multilevel sampler	1.60	-1.04	95.900
28-9	multilevel sampler	1.60	-1.04	95.700
28-10	multilevel sampler	1.60	-1.04	95.500
28-11	multilevel sampler	1.60	-1.04	95.300
28-12	multilevel sampler	1.60	-1.04	95.100
28-13	multilevel sampler	1.60	-1.04	94.900
28-14	multilevel sampler	1.60	-1.04	94.700
30-1	multilevel sampler	-1.55	-1.04	97.420
30-2	multilevel sampler	-1.55	-1.04	97.220
30-3	multilevel sampler	-1.55	-1.04	97.020
30-4	multilevel sampler	-1.55	-1.04	96.820
30-5	multilevel sampler	-1.55	-1.04	96.620
30-6	multilevel sampler	-1.55	-1.04	96.420
30-7	multilevel sampler	-1.55	-1.04	96.220
30-8	multilevel sampler	-1.55	-1.04	96.020
30-9	multilevel sampler	-1.55	-1.04	95.820
30-10	multilevel sampler	-1.55	-1.04	95.620
30-11	multilevel sampler	-1.55	-1.04	95.420
30-12	multilevel sampler	-1.55	-1.04	95.220
30-13	multilevel sampler	-1.55	-1.04	95.020
30-14	multilevel sampler	-1.55	-1.04	94.820

TABLE B-1

Spatial Coordinates of Multilevel Sampling Points, Monitoring Well Screens and the Emplaced Source Zone (Page 3 of 3)

Coordinate ID	*Description of Coordinate*	*X (m)*	*Y (m)*	*Elevation (m)*
source	corner	-0.75	0.25	96.100
source	corner	0.75	0.25	96.100
source	corner	0.75	-0.25	96.100
source	corner	-0.75	-0.25	96.100
source	corner	-0.75	0.25	95.100
source	corner	0.75	0.25	95.100
source	corner	0.75	-0.25	95.100
source	corner	-0.75	-0.25	95.100
source	centre/grid origin	0.00	0.00	95.600
IW1	top of screen	-0.99	1.51	96.185
IW1	bottom of screen	-0.99	1.51	94.966
IW2	top of screen	-0.62	1.51	96.209
IW2	bottom of screen	-0.62	1.51	94.990
IW3	top of screen	-0.25	1.51	96.313
IW3	bottom of screen	-0.25	1.51	95.094
IW4	top of screen	0.23	1.51	96.207
IW4	bottom of screen	0.23	1.51	94.988
IW5	top of screen	0.58	1.51	96.206
IW5	bottom of screen	0.58	1.51	94.987
IW6	top of screen	0.96	1.51	96.199
IW6	bottom of screen	0.96	1.51	94.980
XW1	top of screen	0.72	-2.29	96.228
XW1	bottom of screen	0.72	-2.29	95.009
XW2	top of screen	0.17	-2.29	96.209
XW2	bottom of screen	0.17	-2.29	94.990
XW3	top of screen	-0.33	-2.29	96.195
XW3	bottom of screen	-0.33	-2.29	94.976
BWL	top of screen	-0.42	-4.82	93.968
BWL	bottom of screen	-0.42	-4.82	92.444
BWU	top of screen	-0.27	-4.82	95.192
BWU	bottom of screen	-0.27	-4.82	93.668

Notes:

1) Elevation referenced to local benchmark of 100 m.

TABLE B-2
Summary of Injection Flow Rates During Pre-oxidant Flush Tracer Test

Measurement Date (mm/dd/yy)	*Elapsed Time (days)*	*Initial Flow Rate (mL/min)*	*Reset Flow Rate (mL/min)*	*Avg. Flow Rate (mL/min)*	*Cumulative Volume (L)*
11/2/95	0	360	360	360	0
11/4/95	2	370	360	365	1106
11/7/95	5	353	360	357	2721
11/10/95	8	357	360	359	4280
11/13/95	11	361	360	361	5794
11/16/95	14	370	360	365	7327
11/18/95	16	340	360	350	8388
11/21/95	19	361.5	360	361	9903
11/24/95	22	375	360	368	11557
11/27/95	25	370	360	365	13134
11/28/95	26	351	360	356	13605
11/28/95	26	376	360	368	13691
11/28/95	27	357	360	359	13777
11/29/95	27	360	360	360	13864
11/29/95	27	240	360	300	13999
12/2/95	30	360	360	360	15656
12/4/95	32	363	360	362	16714
12/7/95	35	355	360	358	18247
12/10/95	38	351	361	356	19826
12/17/95	45	366	362	364	23441
1/1/96	60	350	358	356	30858
1/4/96	63	328	359	343	32340
1/8/96	67	363	362	361	34701
1/12/96	71	354	358	358	36484

Notes

1) Reported flow rates are the total volumetric flow injected into the six injection wells (IW1 to IW6).

2) Flow rates were measured at the beginning (initial) and end (reset) of each site visit to estimate the average flow rate for the periods between site visits.

3) Mean injection flow rate of 357 ± 13 mL/min (%RSD=3.7%).

TABLE B-3
Summary of Extraction Flow Rates During Pre-oxidant Flush Tracer Test

Measurement Date (mm/dd/yy)	*Elapsed Time (days)*	*Initial Flow Rate (mL/min)*	*Reset Flow Rate (mL/min)*	*Avg. Flow Rate (mL/min)*	*Cumulative Volume (L)*
11/2/95	0	NR	368	368	0
11/4/95	2	NR	379	379	1148
11/7/95	5	375	403	377	2856
11/10/95	8	375	405	389	4548
11/13/95	11	397	398	401	6233
11/16/95	14	390	390	394	7887
11/18/95	16	390	390	390	9069
11/21/95	19	398	385	394	10724
11/24/95	22	395	390	390	12479
11/27/95	25	382.5	390	386	14147
11/29/95	27	385	385	388	15176
12/2/95	30	375	395	380	16863
12/4/95	32	396	395	396	18020
12/5/95	33	398	392	397	18544
12/5 95	33	398	392	395	18544
12/6/95	34	395	395	394	19146
12/7 95	35	392	395	394	19712
12/8/95	36	392	392	394	20263
12/9/95	37	396	396	394	20831
12/10/95	38	396	396	396	21464
12/12/95	40	396	396	396	22628
12/14/95	42	394	394	395	23731
12/17/95	45	415	413	405	25435
12/19/95	47	390	390	402	26592
12/21 95	49	377	391	384	27748
1/4/96	63	380	396	386	35173
1/8/96	67	397	390	397	37766
1/12/96	71	385	405	388	39696
1/16/96	75	387	387	396	41977

Notes

1) Reported flow rates are the total volumetric flows extracted from the extraction wells (XW1, XW2, and XW3).

2) Flow rates were measured at the beginning (initial) and end (reset) of each site visit to estimate the average flow rate for the periods between site visits.

3) Mean total extraction flow rate of 391 ± 8 mL/min (%RSD=2.0%).

TABLE B-4
Summary of Inorganic Analytical Data Collected During
the Pre-oxidant Flush Tracer Test (Page 1 of 5)

Sample Location	*Sampling Date (mm/dd/yy)*	*Elapsed Time (days)*	*Bromide (mg/L)*	*Chloride (mg/L)*	*Sulfate (mg/L)*
1-10	11/28/96	-1	0	22	140
1-10	12/02/96	3	0	22	146
1-10	12/03/96	4	0	22	147
1-10	12/04/96	5	0	22	150
1-10	12/05/96	6	0	22	149
1-10	12/06/96	7	0	22	151
1-10	12/07/96	8	0	22	149
1-10	12/08/96	9	0	22	147
1-10	12/09/96	10	0	22	152
1-10	12/10/96	11	2	23	153
1-10	12/11/96	12	3	23	154
1-10	12/12/96	13	24	23	159
1-10	12/13/96	14	41	23	158
1-10	12/14/96	15	59	22	159
1-10	12/15/96	16	87	22	158
1-10	12/17/96	18	60	20	158
1-10	12/18/96	19	33	17	145
1-10	12/19/96	20	21	16	134
1-10	12/20/96	21	14	13	0
1-10	12/21/96	22	0	12	0
1-10	12/22/96	23	0	15	0
1-10	12/23/96	24	1	13	131
1-10	12/24/96	25	1	13	128
1-10	12/26/96	27	0	12	0
1-10	12/27/96	28	0	13	172
1-4	11/28/96	-1	0	21	108
1-4	12/02/96	3	0	21	135
1-4	12/03/96	4	0	22	137
1-4	12/04/96	5	0	22	140
1-4	12/05/96	6	0	22	143
1-4	12/06/96	7	0	22	143
1-4	12/07/96	8	0	22	143
1-4	12/08/96	9	0	22	145
1-4	12/09/96	10	0	22	145
1-4	12/10/96	11	0	22	147
1-4	12/11/96	12	0	22	147
1-4	12/12/96	13	0	22	148
1-4	12/13/96	14	0	22	149
1-4	12/14/96	15	0	22	152
1-4	12/15/96	16	0	22	151
1-4	12/17/96	18	7	22	153
1-4	12/18/96	19	24	23	154
1-4	12/19/96	20	38	23	157
1-4	12/20/96	21	54	22	156
1-4	12/21/96	22	69	21	153
1-4	12/22/96	23	4	13	131

TABLE B-4
Summary of Inorganic Analytical Data Collected During
the Pre-oxidant Flush Tracer Test (Page 2 of 5)

Sample Location	*Sampling Date (mm/dd/yy)*	*Elapsed Time (days)*	*Bromide (mg/L)*	*Chloride (mg/L)*	*Sulfate (mg/L)*
1-4	12/23/96	24	4	13	132
1-4	12/24/96	25	4	13	131
1-4	12/26/96	27	4	13	131
1-4	12/27/96	28	1	13	127
1-7	11/28/96	-1	0	17	81
1-7	12/02/96	3	0	21	126
1-7	12/03/96	4	0	22	134
1-7	12/04/96	5	0	22	137
1-7	12/05/96	6	0	21	137
1-7	12/06/96	7	0	21	140
1-7	12/07/96	8	0	22	140
1-7	12/08/96	9	0	22	142
1-7	12/09/96	10	0	22	143
1-7	12/10/96	11	0	22	145
1-7	12/11/96	12	0	22	146
1-7	12/12/96	13	0	22	147
1-7	12/13/96	14	1	22	147
1-7	12/14/96	15	2	22	147
1-7	12/15/96	16	3	22	148
1-7	12/17/96	18	4	22	148
1-7	12/18/96	19	8	22	152
1-7	12/19/96	20	16	22	152
1-7	12/20/96	21	25	22	153
1-7	12/21/96	22	33	22	153
1-7	12/22/96	23	23	16	147
1-7	12/23/96	24	23	16	145
1-7	12/24/96	25	28	16	150
1-7	12/26/96	27	28	17	152
1-7	12/27/96	28	9	14	138
1-7	12/28/96	29	10		
1-7	12/29/96	30	5		
1-7	12/30/96	31	5		
1-7	01/01/97	33	3		
1-7	01/04/97	36	3		
3-10	12/02/96	3	0	22	145
3-10	12/03/96	4	0	22	151
3-10	12/04/96	5	0	22	147
3-10	12/05/96	6	0	22	146
3-10	12/07/96	8	0	23	149
3-10	12/08/96	9	0	22	150
3-10	12/09/96	10	0	22	149
3-10	12/10/96	11	1	22	152
3-10	12/12/96	13	22	22	156
3-10	12/13/96	14	36	22	154
3-10	12/14/96	15	48	21	151
3-10	12/15/96	16	53	20	146

TABLE B-4
Summary of Inorganic Analytical Data Collected During
the Pre-oxidant Flush Tracer Test (Page 3 of 5)

Sample Location	*Sampling Date (mm/dd/yy)*	*Elapsed Time (days)*	*Bromide (mg/L)*	*Chloride (mg/L)*	*Sulfate (mg/L)*
3-10	12/17/96	18	49	17	139
3-10	12/18/96	19	35	16	139
3-10	12/19/96	20	21	15	137
3-10	12/21/96	22	4	13	129
3-10	12/22/96	23	0	13	132
3-10	12/23/96	24	0	13	131
3-10	12/24/96	25	1	13	131
3-10	12/26/96	27	1	13	128
3-10	12/27/96	28	1	13	133
3-10	12/28/96	29	0	22	139
3-4	11/28/96	-1	0	26	0
3-4	12/02/96	3	0	0	0
3-4	12/03/96	4	0	22	157
3-4	12/04/96	5	0	23	148
3-4	12/05/96	6	0	22	144
3-4	12/07/96	8	0	21	0
3-4	12/08/96	9	4	22	0
3-4	12/09/96	10	0	22	147
3-4	12/10/96	11	1	20	0
3-4	12/12/96	13	0	0	0
3-4	12/13/96	14	0	24	144
3-4	12/14/96	15	0	24	157
3-4	12/15/96	16	0	24	169
3-4	12/17/96	18	0	0	0
3-4	12/18/96	19	0	21	0
3-4	12/19/96	20	0	20	0
3-4	12/21/96	22	0	17	0
3-4	12/22/96	23	1	13	125
3-4	12/23/96	24	1	12	0
3-4	12/24/96	25	1	12	0
3-4	12/26/96	27	0	11	0
3-4	12/27/96	28	0	12	0
3-7	11/28/96	-1	1	17	0
3-7	12/02/96	3	0	16	0
3-7	12/03/96	4	0	20	0
3-7	12/04/96	5	1	19	0
3-7	12/05/96	6	0	24	0
3-7	12/07/96	8	0	24	0
3-7	12/08/96	9	0	22	175
3-7	12/09/96	10	0	21	166
3-7	12/10/96	11	0	21	168
3-7	12/12/96	13	0	21	165
3-7	12/13/96	14	1	22	173
3-7	12/14/96	15	0	22	163
3-7	12/15/96	16	2	22	172
3-7	12/17/96	18	6	22	167

TABLE B-4
Summary of Inorganic Analytical Data Collected During
the Pre-oxidant Flush Tracer Test (Page 4 of 5)

Sample Location	*Sampling Date (mm/dd/yy)*	*Elapsed Time (days)*	*Bromide (mg/L)*	*Chloride (mg/L)*	*Sulfate (mg/L)*
3-7	12/18/96	19	25	22	164
3-7	12/19/96	20	53	22	164
3-7	12/21/96	22	50	19	161
3-7	12/22/96	23	4	13	128
3-7	12/23/96	24	4	13	128
3-7	12/24/96	25	3	13	126
3-7	12/26/96	27	3	12	125
3-7	12/27/96	28	2	13	129
5-10	11/28/96	-1	0	24	146
5-10	12/02/96	3	0	22	148
5-10	12/03/96	4	0	22	149
5-10	12/04/96	5	0	22	150
5-10	12/05/96	6	0	22	149
5-10	12/06/96	7	0	22	149
5-10	12/07/96	8	0	22	151
5-10	12/08/96	9	0	22	151
5-10	12/09/96	10	0	22	152
5-10	12/10/96	11	9	22	154
5-10	12/11/96	12	24	22	155
5-10	12/12/96	13	76	22	158
5-10	12/13/96	14	95	22	161
5-10	12/14/96	15	136	22	160
5-10	12/15/96	16	154	22	159
5-10	12/17/96	18	110	18	151
5-10	12/18/96	19	69	15	134
5-10	12/19/96	20	38	14	135
5-10	12/20/96	21	21	13	130
5-10	12/21/96	22	10	13	127
5-4	12/02/96	3	0	22	147
5-4	12/03/96	4	0	22	148
5-4	12/04/96	5	0	22	149
5-4	12/05/96	6	0	22	149
5-4	12/06/96	7	0	22	148
5-4	12/07/96	8	0	22	149
5-4	12/08/96	9	0	22	150
5-4	12/09/96	10	0	22	151
5-4	12/10/96	11	0	23	154
5-4	12/11/96	12	0	22	152
5-4	12/12/96	13	13	23	157
5-4	12/13/96	14	28	22	158
5-4	12/14/96	15	44	22	158
5-4	12/15/96	16	75	22	158
5-4	12/17/96	18	133	22	161
5-4	12/18/96	19	78	19	157
5-4	12/19/96	20	33	17	146
5-4	12/20/96	21	16	14	137

TABLE B-4
Summary of Inorganic Analytical Data Collected During
the Pre-oxidant Flush Tracer Test (Page 5 of 5)

Sample Location	*Sampling Date (mm/dd/yy)*	*Elapsed Time (days)*	*Bromide (mg/L)*	*Chloride (mg/L)*	*Sulfate (mg/L)*
5-4	12/21/96	22	6	13	130
5-4	12/22/96	23	1	13	132
5-4	12/23/96	24	2	13	164
5-4	12/24/96	25	1	13	132
5-7	11/28/96	-1	0	22	142
5-7	11/28/96	-1	0	22	143
5-7	12/02/96	3	0	22	146
5-7	12/03/96	4	0	22	147
5-7	12/04/96	5	0	22	148
5-7	12/05/96	6	0	22	149
5-7	12/06/96	7	0	22	149
5-7	12/07/96	8	0	22	150
5-7	12/08/96	9	0	22	148
5-7	12/09/96	10	0	22	151
5-7	12/10/96	11	17	14	131
5-7	12/10/96	11	0	22	152
5-7	12/11/96	12	0	22	152
5-7	12/13/96	14	3	23	158
5-7	12/13/96	14	0	23	160
5-7	12/14/96	15	13	22	159
5-7	12/15/96	16	60	22	155
5-7	12/17/96	18	137	21	161
5-7	12/18/96	19	95	20	159
5-7	12/19/96	20	43	16	144
5-7	12/21/96	22	7	13	124
5-7	12/22/96	23	2	13	158
5-7	12/23/96	24	2	13	157
5-7	12/24/96	25	1	13	133

Notes

1) Sulfate data is above the limit of linearity (LOL=100 mg/L sulfate) and should be considered qualitative.

2) Chloride detections were attributed to contamination from existing municipal landfill plume.

3) Tracer pulse was injected over 21.25 hours starting 11/28/96 12:30 PM.

TABLE B-5

Summary of Injection Flow Rates During Emplaced Source Oxidant Flush (Page 1 of 3)

Measurement Date (mm/dd/yy)	*Elapsed Time (days)*	*Measured Flow Rates (mL/min)*						*Total Flow (mL/min)*	*Cumulative Volume (L)*	*Monthly Avg. Flow Rate (mL/min)*
		IW1/2 Initial	*IW1/2 Reset*	*IW3/4 Initial*	*IW3/4 Reset*	*IW5/6 Initial*	*IW5/6 Reset*			
05/14/96	0		120		120		120	360	0	
05/15/96	0	115	120	110	120	120	120	353	159	
05/17/96	2	120	120	120	120	120	120	360	1195	
05/20/96	5	116	120	112	120	120	120	354	2725	
05/23/96	8	114	122	116	120	116	118	353	4250	
05/25/96	10	126	120	122	120	120	120	364	5298	
05/27/96	12	108	121	122	121	121	121	356	6322	
05/29/96	14	120	120	124	120	122	121	365	7372	
05/31/96	16	118	120	122	121	121	121	361	8411	358
06/03/96	19	112	120	122	122	120	120	358	9958	
06/05/96	21	106	119	113	120	120	120	351	10967	
06/06/96	22	130	120	126	120	126	120	371	11501	
06/07/96	23	121	121	120	120	118	118	360	12018	
06/10/96	26	96	120	111	120	120	120	343	13500	
06/13/96	29	126	118	124	120	121	121	366	15079	
06/14/96	30	108	119	104	119	110	120	341	15570	
06/16/96	33	119	0	119	0	120	0	358	17073	
06/17/96	34	0	120	0	121	0	121	0	17073	
06/18/96	34	125	120	128	120	126	121	371	17384	
06/21/96	37	112	120	106	121	112	120	346	18877	
06/23/96	40	120	0	121	0	120	0	361	20393	
06/24/96	41	0	120	0	119	0	120	0	20393	
06/26/96	42	122	120	116	120	117	118	357	21186	
06/28/96	44	120	120	121	121	112	122	356	22209	340
07/01/96	47	118	120	118	121	118	121	359	23758	
07/03/96	49	116	119	115	120	116	120	355	24779	
07/05/96	51	96	115	114	121	116	118	343	25766	
07/08/96	54	114	119	112	120	112	120	346	27260	
07/10/96	56	118	122	120	120	112	122	355	28281	
07/12/96	58	120	120	123	120	121	121	364	29330	
07/15/96	61	117	120	115	120	119	119	356	30867	
07/17/96	63	119	119	120	120	119	119	359	31900	
07/19/96	65	116	122	118	122	116	120	354	32919	

TABLE B-5

Summary of Injection Flow Rates During Emplaced Source Oxidant Flush (Page 2 of 3)

Measurement Date (mm/dd/yy)	*Elapsed Time (days)*	*Measured Flow Rates (mL/min)*						*Total Flow (mL/min)*	*Cumulative Volume (L)*	*Monthly Avg. Flow Rate (mL/min)*
		IW1/2 Initial	*IW1/2 Reset*	*IW3/4 Initial*	*IW3/4 Reset*	*IW5/6 Initial*	*IW5/6 Reset*			
07/22/96	68	120	120	116	120	114	122	357	34462	
07/24/96	70	122	122	122	122	116	122	361	35501	
07/26/96	72	108	120	114	121	112	120	350	36509	
07/29/96	75	113	121	89	121	55	121	309	37844	
07/31/96	77	120	120	120	120	121	121	362	38887	351
08/02/96	79	116	122	119	119	118	120	357	39915	
08/05/96	82	122	121	116	120	108	118	354	41442	
08/07/96	84	126	122	126	121	132	120	372	42512	
08/09/96	86	121	121	119	119	117	122	360	43549	
08/12/96	89	120	120	115	115	118	118	358	45093	
08/14/96	91	114	122	120	120	118	118	353	46108	
08/16/96	93	120	120	119	119	114	122	357	47135	
08/19/96	97	119	119	118	118	118	118	358	48950	
08/19/96	97	60	60	59	59	60	60	267	48990	358
08/21/96	98	55	61	54	60	59	59	174	49334	
08/23/96	100	61	61	60	60	57	62	179	49849	
08/26/96	103	60	60	56	60	59	59	179	50623	
08/28/96	105	60	60	60	60	59	59	179	51138	179
09/02/96	110	56	60	62	59	56	59	177	52409	
09/09/96	117	59	59	62	62	60	60	180	54218	
09/16/96	124	62	62	61	61	60	60	182	56053	
09/24/96	132	62	62	61	61	61	61	184	58167	182
10/01/96	139	62	62	64	64	61	61	186	60037	
10/08/96	146	63	61	61	61	61	61	186	61911	
10/16/96	154	59	59	58	58	61	61	181	63991	
10/22/96	160	60	60	60	60	62	62	180	65546	
10/29/96	167	52	60	48	0	62	61	172	67280	180
11/05/96	174	61	61	0	61	61	61	122	68505	
11/12/96	181	60	33	65	33	65	33	187	70384	187
11/19/96	188	32	32	28	33	34	34	97	71357	
11/25/96	194	33	33	32	32	33	33	99	72208	98

TABLE B-5

Summary of Injection Flow Rates During Emplaced Source Oxidant Flush (Page 3 of 3)

Measurement Date (mm/dd/yy)	*Elapsed Time (days)*	*Measured Flow Rates (mL/min)*						*Total Flow (mL/min)*	*Cumulative Volume (L)*	*Monthly Avg. Flow Rate (mL/min)*
		IW1/2 Initial	*IW1/2 Reset*	*IW3/4 Initial*	*IW3/4 Reset*	*IW5/6 Initial*	*IW5/6 Reset*			
12/03/96	202	33	33	37	33	33	33	101	73366	
12/10/96	209	33	33	34	34	31	34	99	74359	
12/17/96	216	34	34	34	34	33	33	101	75377	100
01/15/97	245	30	33	29	33	35	35	98	79449	
01/21/97	251	34	34	40	34	36	34	106	80360	
01/28/97	258	34	34	31	34	33	33	100	81368	103
02/04/97	265	28	33	33	33	34	34	98	82356	
02/18/97	279	35	35	34	34	37	37	103	84432	103
03/04/97	293	32	33	29	31	28	33	98	86398	
03/13/97	302	35	35	68	32	36	33	118	87927	
03/27/97	316	35	26	33	25	33	25	101	89953	107
04/10/97	330	28	26	23	25	23	25	75	91465	
04/24/97	344	28	25	28	25	28	25	80	93078	80
05/08/97	358	26	26	27	27	26	26	77	94630	
05/23/97	373	23	15	26	26	25	35	77	96283	76
06/05/97	386	13	13	28	26	33	33	75	97687	
06/13/97	394	15	15	27	27	35	35	75	98545	
06/21/97	402	16	16	28	26	35	35	78	99444	76
07/01/97	412	15	15	29	24	34	34	78	100560	
07/10/97	421	15	15	23	25	34	34	73	101499	
07/15/97	426	17	17	28	25	34	34	77	102050	
07/25/97	436	16	19	24	35	37	35	77	103152	75
08/04/97	446	18	20	32	35	33	33	86	104390	
08/11/97	453	20	25	35	40	31	35	87	105267	
08/16/97	458	24	24	40	40	35	35	100	105983	
08/21/97	463	24	24	40	40	32	32	98	106685	
08/29/97	471	24	24	43	43	44	32	104	107878	97
09/03/97	476	22	22	37	37	32	32	95	108562	
09/10/97	483	22	0	37	0	32	0	91	109479	91

Notes

1) Injection wells were turned off on 10/9/97

TABLE B-6

Summary of Extraction Flow Rates During Emplaced Source Oxidant Flush (Page 1 of 4)

Measurement Date	*Elapsed Time*	XW_{total}		*BWU*		*XW1*		*XW2*		*XW3*		*BWL*		*Avg. Flow Rate*	*Cumulative*
(mm/dd/yy)	*(days)*	*Initial*	*Reset*	*Initial*	*Reset*	*Initial*	*Reset*	*Initial*	*Reset*	*Initial*	*Reset*	*Initial*	*Reset*	*(mL/min)*	*Volume (L)*
05/14/96	0		390											390	0
05/15/96	0	365	392											378	170
05/17/96	2	392	392											392	1299
05/20/96	5	415	393											404	3042
05/23/96	8	540	394											467	5057
05/25/96	10	388	393											391	6183
05/27/96	12	390	390											392	7311
05/29/96	14	393	393											392	8438
05/31/96	16	390	390											392	9566
06/03/96	19	390	390											390	11251
06/05/96	21	385	385											388	12367
06/06/96	22	397	397											391	12930
06/07/96	23	395	395											396	13500
06/10/96	26	405	400											400	15228
06/13/96	29	400	390											400	16956
06/14/96	30	380	380											385	17510
06/17/96	33	380	385											380	19152
06/19/96	35	390	390											388	20268
06/20/96	36	390	390											390	20830
06/21/96	37	390	390											390	21391
06/24/96	40	355	380											373	23000
06/26/96	42	390	390											385	24109
06/28/96	44	380	380											385	25218
07/01/96	47	400	390											390	26903
07/03/96	49	425	380											408	28076
07/05/96	51	385	385											383	29178
07/08/96	54	385	385											385	30841
07/10/96	56	370	370											378	31928
07/12/96	58	380	385											375	33008
07/15/96	61	260	390											323	34402
07/17/96	63	390	390											390	35525
07/19/96	65	390	390											390	36648
07/22/96	68	388	388											389	38328

TABLE B-6

Summary of Extraction Flow Rates During Emplaced Source Oxidant Flush (Page 2 of 4)

Measurement Date	*Elapsed Time*	XW_{total}		*BWU*		*XW1*		*XW2*		*XW3*		*BWL*		*Avg. Flow Rate*	*Cumulative*
(mm/dd/yy)	*(days)*	*Initial*	*Reset*	*Initial*	*Reset*	*Initial*	*Reset*	*Initial*	*Reset*	*Initial*	*Reset*	*Initial*	*Reset*	*(mL/min)*	*Volume (L)*
07/24/96	70	390	390											389	39449
07/26/96	72	380	380											385	40558
07/29/96	75	387	387											384	42214
07/31/96	77	380	380											384	43319
08/02/96	79	370	391											375	44399
08/05/96	82	410	390											401	46129
08/07/96	84	370	370											380	47223
08/09/96	86	367	381											369	48285
08/12/96	89	365	390											373	49896
08/14/96	91	385	385											388	51012
08/16/96	93	385	385											385	52121
08/19/96	97	390	390											388	54085
08/19/96	97	195	195											293	54129
08/21/96	98	195	195											195	54515
08/23/96	100	190	190											193	55070
08/26/96	103	198	200											194	55908
08/28/96	105	195	195											198	56477
09/01/96	109	195	195											195	57600
09/09/96	117	160	200											178	59645
09/16/96	124	130	205											165	61308
09/24/96	132	124	205											165	63203
10/01/96	139	215	200											210	65320
10/08/96	146	190	190											195	67285
10/16/96	154	190	190											190	69474
10/22/96	161	190	192											190	71235
10/22/96	160	152	152											172	71148
10/29/96	167	146	146											149	72632
11/05/96	174	150	150											148	74124
11/12/96	181	147	147											149	75620
11/12/96	182	103	103	10	10			43	43			50	50	125	75718
11/19/96	188	87	110	9	10			22	50			56	50	95	76601
11/25/96	194	100	104	10	10			43	46			47	50	105	77509
12/03/96	202	103	115	7	7			45	45			52	65	104	78701

TABLE B-6

Summary of Extraction Flow Rates During Emplaced Source Oxidant Flush (Page 3 of 4)

Measurement Date	*Elapsed Time*	XW_{total}		*BWU*		*XW1*		*XW2*		*XW3*		*BWL*		*Avg. Flow Rate*	*Cumulative*
(mm/dd/yy)	*(days)*	*Initial*	*Reset*	*Initial*	*Reset*	*Initial*	*Reset*	*Initial*	*Reset*	*Initial*	*Reset*	*Initial*	*Reset*	*(mL/min)*	*Volume (L)*
12/10/96	209	123	122	7	7			44	45			63	70	119	79900
12/17/96	216	124	124	6	6			44	44			73	73	123	81140
12/23/96	222	124	129	5	5			44	44			69	75	124	82212
12/31/96	230	126	126											128	83680
01/15/97	245	130	126	7	7			45	45			79	74	128	86445
01/21/97	251	108	125	4	7			43	43			45	75	117	87456
01/28/97	258	124	122	5	8			44	44			75	75	125	88711
02/04/97	265	125	120	0	8			43	43			80	76	124	89956
02/18/97	279	118	126	10	5			45	45			62	73	119	92355
03/04/97	293	121	124	8	5			43	45			70	74	124	94845
03/13/97	302	116	122	6	6			45	45			67	72	120	96400
03/27/97	316	124	124	7	7			44	44			75	75	123	98880
04/10/97	330	94	93	9	9			43	43			45	45	109	101077
04/24/97	344	108	155	9	5			44	75			54	75	101	103103
05/08/97	358	134	154	0	10			60	75			78	78	145	106016
05/23/97	373	146	168	5	5			69	74			75	91	150	109256
06/05/97	386	92	176	0	5			0	74			92	92	130	111690
06/13/97	394	66	168	0	3			0	69			66	94	121	113084
06/21/97	402	156	173	5	5			66	72			90	96	162	114950
07/01/97	412	168	170	5	5			72	72			93	93	171	117405
07/10/97	421	142	174	0	5			68	73			76	93	156	119427
07/15/97	426	166	184	5	5			79	77			87	95	170	120651
07/25/97	436	142	178	0	5			72	72			71	98	163	122998
08/04/97	446	173	172	4	4			70	70			96	96	176	125525
08/11/97	453	164	154	0	5			64	51			96	96	168	127219
08/16/97	458	152	148	5	0			47	47			99	99	153	128320
08/21/97	463	134	138	0	12			43	43			90	90	141	129336
08/29/97	471	146	146	13	13			30	30			104	104	142	130971
09/03/97	476	129	129	12	12			28	28			94	94	138	131961
09/10/97	483	170	170	20	20			22	22			132	132	150	133468
09/19/97	492	143	150	12	16			22	26			115	122	157	135497
09/26/97	499	164	166	16	16			36	36			114	114	157	137079
10/02/97	505	187	187	15	15			65	65			114	114	177	138604

TABLE B-6

Summary of Extraction Flow Rates During Emplaced Source Oxidant Flush (Page 4 of 4)

Measurement Date (mm/dd/yy)	*Elapsed Time (days)*	*XW_{total}*		*BWU*		*XW1*		*XW2*		*XW3*		*BWL*		*Avg. Flow Rate (mL/min)*	*Cumulative Volume (L)*
		Initial	*Reset*	*Initial*	*Reset*	*Initial*	*Reset*	*Initial*	*Reset*	*Initial*	*Reset*	*Initial*	*Reset*		
10/08/97	511	180	180	17	17					66	66	103	103	184	140190
10/17/97	520	184	158	15	12					63	34	112	112	182	142548
10/23/97	526	0	57									0	57	79	143231
10/26/97	529	36	132	5	5					34	34	0	96	47	143432
11/15/97	549	132	0											132	147233
11/30/97	564	0	67											0	147233
12/10/97	574	67	0							16	0	54	0	100	148666
12/23/97	587	0	57									0	57	0	148666
01/08/98	603	67	0									67	0	34	149438
01/14/98	609	0	82									0	82	0	149438
01/28/98	623	81	0									81	0	82	151081
01/31/98	626	0	72									0	72	0	151081
02/12/98	638	89	0									89	0	81	152472
02/23/98	649	0	82									0	82	0	152472
03/07/98	661	89	0									89	0	86	153950

Notes

1) All flow rates in mL/min.

TABLE B-7
Oxidant Concentrations in Monitoring Wells
During the Oxidant Flush (Page 1 of 2)

Measurement Date (mm/dd/yy)	*Elapsed Time (days)*	*XW1 (g/L)*	*XW2 (g/L)*	*XW3 (g/L)*	*XWT (g/L)*	*BWL (g/L)*	*BWU (g/L)*
05/25/96	11	0.0	0.0	0.01	0.0		
05/27/96	13	0.0	0.0	0.03	0.0		
05/29/96	15	0.0	0.0	0.05	0.0		
06/03/96	20	0.0	0.1	0.12	0.0		
06/10/96	27	0.5	0.2	1.87	0.8		
06/13/96	29	0.9	0.4	2.26	1.1		
06/17/96	33	1.4	0.6	2.33	1.2		
06/24/96	40	1.6	1.0	2.9	2.2		
07/01/96	47	3.4	2.0	5.0	2.9		
07/08/96	54	3.5	2.4	5.4	3.1		
07/15/96	61	0.2	2.9	3.8	3.4		
07/22/96	68	0.2	2.6	3.1	3.1		
07/27/96	73	0.2	4.4	4.9	2.3		
08/05/96	82	0.2	2.5	3.5	3.3		
08/12/96	89	0.2	2.5	3.3	2.7		
08/19/96	96	0.2	2.1	3.5	2.5		
08/26/96	103	0.2	2.5	3.5	3.2		
09/01/96	109	2.0	3.2	3.2	2.8		
09/09/96	117	2.1	3.5	3.5	3.0		
09/16/96	124	3.2	2.7	4.1	3.4		
09/24/96	132	2.8	3.1	3.5	3.1		
10/01/96	139	3.7	5.3	3.4	3.2	3.8	
10/08/96	146	2.3	4.4	3.1	3.3	3.6	
10/16/96	154	2.3	3.7	2.7	3.1	4.6	
10/22/96	160	2.6	3.8	2.7	3.1	3.5	3.5
10/29/96	167	2.3	3.9	2.9	2.5		
11/05/96	174	2.8	2.9	2.6	3.0	6.2	0.6
11/12/96	181	2.9	3.6	2.0	2.8	5.0	0.7
11/19/96	188		3.3		3.9	4.8	0.1
11/25/96	194		2.9		3.3	4.2	0.0
12/03/96	202		2.4		3.5	4.8	0.0
12/10/96	209		3.0		3.8	5.0	
12/17/96	216		2.5		3.3	3.8	0
12/23/96	222		2.5		3.4	3.9	0
12/31/96	230		2.4		2.7	3.0	0
01/07/97	237		2.2		2.4	0.5	
01/15/97	245		2.7		2.3	2.4	
01/21/97	251		2.5		2.2	2.1	0
01/28/97	258		2.6		2.1	1.7	0
02/04/97	265		2.4		2.0	1.7	0
02/18/97	279		2.4		2.0	2.0	0
03/13/97	302		0.8		1.0	1.1	0
03/27/97	316		1.1		1.1	1.2	0
04/24/97	344		0.8		0.8	1.0	0
04/11/97	331	1.2			1.1	1.3	0
05/08/97	358	1.5			1.3	1.1	0
05/23/97	373				1.1		

TABLE B-7
Oxidant Concentrations in Monitoring Wells
During the Oxidant Flush (Page 2 of 2)

Measurement Date (mm/dd/yy)	*Elapsed Time (days)*	*XW1 (g/L)*	*XW2 (g/L)*	*XW3 (g/L)*	*XWT (g/L)*	*BWL (g/L)*	*BWU (g/L)*
05/30/97	380				1.1		
06/05/97	386				1.4		
06/13/97	394	0.6			1.4	2.1	
06/21/97	402	1.2			1.9	2.5	
07/01/97	412	1.2			1.9	2.7	0
07/10/97	421	1.2			1.9	2.7	0
07/15/97	426	1.2			1.9	2.6	0
07/25/97	436	0.9			1.6	2.4	0
08/04/97	446	0.7			1.6	2.4	0
08/11/97	453	0.5			1.4	2.2	0
08/16/97	458	0.3			1.5	2.1	0
08/21/97	463	0.3			1.5	1.9	0
08/29/97	471	0.3			1.6		0.1
09/04/97	477				1.8		
09/12/97	485	0.3			2.4	2.9	0.1
09/19/97	492	0.2			2.1	2.8	0.10
09/26/97	499			1.2	2.4	2.8	0.15
10/02/97	505			1.1	2.1	3.0	0.12
10/08/97	511			0.9	2.0	2.9	0.15
10/17/97	520			0.6	2.3	3.0	0.10
10/26/97	529			0.6	1.5	1.7	0.12
11/01/97	535				2.8	2.9	
11/11/97	545				2.9	2.8	
11/15/97	549				2.0	2.1	0.51
11/30/97	564			0.1	0.6	0.8	
12/10/97	574			0.0	0.4		
12/23/97	587				0.1	0.1	
01/08/98	603				0.2		
01/14/98	609				0.04	0.04	
01/28/98	623				0.08	0.08	
01/31/98	626				0.06	0.06	
02/12/98	638				0.03	0.03	

TABLE B-8

Summary of Time-series Chloride Data Collected During the Emplaced Source Oxidant Flush (Page 1 of 4)

ML1-4		ML1-7		ML1-10		ML3-4		ML3-7		ML3-10	
Date	Cl (mg/L)	Date	Cl (mg/L)	Date	Cl (mg/L)	Date	Cl (mg/L)	Date	Cl (mg/L)	Date	Cl (mg/L)
05/23/96	1	05/23/96	2	05/23/96	0	05/23/96	1	05/23/96	1	05/23/96	1
05/25/96	1	05/25/96	5	05/25/96	1	05/25/96	1	05/25/96	1	05/25/96	1
05/27/96	1	05/27/96	1	05/27/96	1	05/27/96	1	05/27/96	1	05/27/96	2
05/29/96	1	05/29/96	1	05/29/96	4	05/29/96	1	05/29/96	1	05/29/96	1
05/31/96	1	05/31/96	1	05/31/96	12	05/31/96	1	05/31/96	1	05/31/96	6
06/03/96	1	06/03/96	1	06/03/96	10	06/03/96	1	06/03/96	2	06/03/96	6
06/05/96	2	06/05/96	2	06/05/96	8	06/05/96	3	06/17/96	306	06/05/96	32
06/07/96	2	06/07/96	16	06/07/96	8	06/07/96	8	06/20/96	333	06/07/96	16
06/10/96	1	06/10/96	2	06/10/96	18	06/10/96	14	06/21/96	391	06/10/96	922
06/13/96	2	06/13/96	6	06/13/96	13	06/13/96	13	06/24/96	544	06/13/96	349
06/14/96	2	06/14/96	8	06/14/96	8	06/14/96	13	06/26/96	402	06/14/96	219
06/14/96	2	06/17/96	13	06/14/96	7	06/17/96	39	06/28/96	194	06/17/96	101
06/17/96	2	06/20/96	10	06/17/96	7	06/20/96	7	07/03/96	57	06/20/96	134
06/20/96	2	06/21/96	8	06/20/96	12	06/21/96	7	07/05/96	40	06/21/96	183
06/21/96	2	06/24/96	10	06/21/96	10	06/24/96	7	07/08/96	16	06/24/96	476
06/24/96	2	06/26/96	10	06/24/96	10	06/26/96	8	07/10/96	58	06/26/96	411
06/26/96	2	06/28/96	9	06/26/96	10	06/28/96	9	07/12/96	75	06/28/96	485
06/28/96	2	07/01/96	11	06/28/96	11	07/01/96	13	07/15/96	103	07/03/96	575
07/01/96	2	07/03/96	14	07/01/96	17	07/03/96	13	07/19/96	130	07/05/96	836
07/03/96	2	07/05/96	14	07/03/96	21	07/05/96	17	07/19/96	132	07/10/96	644
07/03/96	2	07/08/96	16	07/05/96	29	07/08/96	33	07/22/96	142	07/12/96	336
07/05/96	2	07/10/96	14	07/08/96	67	07/10/96	39	07/26/96	154	07/15/96	213
07/08/96	2	07/12/96	19	07/08/96	65	07/12/96	38	07/29/96	164	07/19/96	249
07/10/96	2	07/15/96	98	07/10/96	97	07/15/96	78	08/02/96	158	07/22/96	306
07/12/96	2	07/19/96	157	07/12/96	108	07/19/96	123	08/05/96	150	07/26/96	170
07/15/96	2	07/22/96	158	07/15/96	139	07/22/96	145	08/09/96	160	07/29/96	101
07/19/96	2	07/26/96	158	07/19/96	145	07/26/96	159	08/12/96	160	08/02/96	95
07/22/96	2	07/29/96	160	07/22/96	149	07/29/96	154	08/12/96	162	08/05/96	97
07/26/96	3	08/05/96	145	07/26/96	153	08/02/96	152	08/16/96	165	08/09/96	221
07/29/96	3	08/09/96	154	07/26/96	151	08/05/96	146	08/19/96	173	08/12/96	111
08/02/96	3	08/12/96	159	07/29/96	147	08/09/96	152	08/23/96	172	08/16/96	316
08/05/96	3	08/16/96	165	08/02/96	152	08/12/96	161	08/26/96	173	08/19/96	158
08/09/96	4	08/19/96	166	08/05/96	150	08/16/96	164	09/01/96	157	08/23/96	251
08/12/96	8	08/21/96	142	08/09/96	164	08/19/96	166	09/09/96	144	08/26/96	188
08/16/96	10	08/21/96	141	08/12/96	166	08/23/96	167	09/12/96	147	09/01/96	267
08/19/96	7	08/23/96	164	08/16/96	168	08/26/96	175	09/16/96	148	09/09/96	213
08/23/96	8	08/26/96	149	08/19/96	168	09/01/96	151	09/19/96	148	09/12/96	217
08/26/96	20	09/01/96	144	08/23/96	171	09/09/96	143	09/24/96	144	09/12/96	204
09/01/96	2	09/09/96	125	08/26/96	165	09/12/96	144	09/26/96	144	09/16/96	220
09/09/96	2	09/12/96	124	09/01/96	151	09/16/96	130	10/01/96	133	09/16/96	175
09/12/96	4	09/16/96	117	09/09/96	151	09/19/96	136	10/04/96	141	09/19/96	77
09/16/96	1	09/19/96	102	09/12/96	149	09/24/96	130	10/08/96	128	09/19/96	65
09/19/96	2	09/24/96	62	09/16/96	143	09/26/96	113	10/11/96	139	09/24/96	139
09/29/96	1	09/26/96	46	09/19/96	146	10/01/96	78	10/16/96	144	09/24/96	114
09/26/96	1	10/01/96	34	09/24/96	147	10/08/96	32	10/22/96	150	09/26/96	143
10/01/96	2	10/16/96	5	10/01/96	147	10/11/96	48	10/29/96	146	09/28/96	127
10/16/96	4	10/22/96	3	10/16/96	148	10/16/96	58	11/05/96	123	10/01/96	234
10/22/96	2	10/29/96	6	10/22/96	153	10/22/96	74	11/12/96	109	10/01/96	201
10/29/96	2	11/05/96	7	10/29/96	132	10/29/96	115	11/19/96	72	10/04/96	197
11/05/96	2	11/12/96	9	11/05/96	120	11/05/96	64	11/25/96	52	10/04/96	159
11/12/96	1	11/19/96	17	11/12/96	114	11/12/96	51	12/03/96	55	10/08/96	147
11/19/96	1	11/25/96	23	11/19/96	106	11/19/96	51	12/10/96	59	10/08/96	123
11/25/96	1	12/03/96	25	11/25/96	103	11/25/96	30	12/17/96	51	10/18/96	46
12/03/96	1	12/10/96	53	12/03/96	103	12/03/96	40	12/31/96	22	10/11/96	235
12/10/96	2	12/17/96	71	12/10/96	85	12/10/96	54	01/07/97	18	10/16/96	135
12/17/96	2	12/31/96	43	12/17/96	110	12/17/96	64	01/07/97	18	10/22/96	215
12/31/96	5	01/07/97	60	12/31/96	67	12/31/96	63	01/21/97	21	10/25/96	100
01/07/97	4	01/15/97	31	01/07/97	62	01/07/97	54	02/04/97	28	10/29/96	272
01/15/97	3	01/21/97	53	01/15/97	64	01/15/97	46	02/18/97	14	11/05/96	221
01/21/97	2	01/15/97	31	01/21/97	63	01/21/97	47	03/27/97	13	11/12/96	216
02/04/97	2	01/21/97	53	01/28/97	51	01/28/97	44	04/10/97	13	11/19/96	84
02/18/97	3	01/28/97	49	02/04/97	50	02/04/97	40	05/08/97	13	11/25/96	173
04/24/97	2	02/04/97	45	02/18/97	42	02/18/97	44	07/15/97	14	12/03/96	59
04/10/97	1	02/18/97	38	04/24/97	25	03/27/97	6	08/04/97	7	12/10/96	168
07/15/97	1	04/24/97	17	05/23/97	12	04/10/97	4			12/10/96	189
		04/10/97	20	06/13/97	16	04/24/97	7			12/17/96	80
		05/23/97	3	06/21/97	9	05/08/97	2			12/31/96	58
		07/15/97	2	07/01/97	6	07/15/97	8			01/07/97	119
				07/10/97	12	08/04/97	1			01/21/97	160
				07/15/97	8					01/28/97	124

TABLE B-8

Summary of Time-series Chloride Data Collected During the Emplaced Source Oxidant Flush (Page 2 of 4)

ML3-10		ML5-4		ML5-7		ML5-10		BWL		BWU	
Date	Cl (mg/L)	Date	Cl (mg/L)	Date	Cl (mg/L)	Date	Cl (mg/L)	Date	Cl (mg/L)	Date	Cl (mg/L)
02.04.97	68	05.23.96	2	05.23.96	2	05.23.96	2	08.27.96	4	10.22.96	36
02.18.97	47	05.25.96	1	05.25.96	2	05.25.96	1	09.02.96	45	10.29.96	48
03.27.97	44	05.27.96	1	05.27.96	1	05.27.96	1	09.09.96	63	11.05.96	29
04.10.97	17	05.29.96	1	05.29.96	1	05.29.96	2	09.16.96	94	11.12.96	39
04.24.97	212	05.31.96	1	05.31.96	1	05.31.96	7	09.24.96	84	11.19.96	9
06.13.97	148	06.03.96	2	06.03.96	1	06.03.96	5	10.01.96	235	11.25.96	7
06.21.97	165	06.05.96	3	06.05.96	1	06.05.96	15	10.08.96	189	12.03.96	5
07.01.97	163	06.05.96	3	06.05.96	1	06.05.96	15	10.16.96	139	12.10.96	4
07.10.97	70	06.07.96	4	06.07.96	3	06.07.96	15	10.22.96	115	12.17.96	5
07.15.97	99	06.07.96	4	06.07.96	3	06.07.96	15	10.29.96	139	12.31.96	6
08.04.97	16	06.10.96	8	06.10.96	6	06.07.96	15	11.05.96	125	01.15.97	4
08.11.97	10	06.10.96	8	06.10.96	6	06.07.96	15	11.12.96	118	01.21.97	3
08.16.97	9	06.13.96	9	06.13.96	6	06.10.96	8	11.19.96	93	02.04.97	2
08.21.97	13	06.13.96	9	06.13.96	6	06.10.96	8	11.25.96	86	02.18.97	1
		06.14.96	8	06.14.96	7	06.13.96	8	12.03.96	79	03.04.97	1
		06.21.96	7	06.14.96	7	06.13.96	8	12.10.96	81	04.10.97	1
		06.24.96	6	06.21.96	6	06.14.96	8	12.17.96	79	04.24.97	1
		06.26.96	10	06.24.96	6	06.14.96	8	12.31.96	61	05.23.97	2
		07.03.96	14	06.26.96	6	06.14.96	8	01.07.97	59	06.21.97	1
		07.05.96	15	07.03.96	11	06.14.96	8	01.15.97	47	07.01.97	1
		07.08.96	40	07.03.96	12	06.17.96	8	01.21.97	41	07.10.97	1
		07.08.96	19	07.03.96	12	06.20.96	10	01.28.97	33	07.15.97	2
		07.10.96	63	07.05.96	11	06.21.96	10	02.04.97	29	07.15.97	2
		07.10.96	46	07.05.96	11	06.24.96	12	02.18.97	27	07.25.97	2
		07.12.96	77	07.08.96	19	06.26.96	12	03.04.97	21	07.25.97	2
		07.12.96	86	07.10.96	46	06.28.96	32	03.27.97	14	08.04.97	2
		07.15.96	105	07.12.96	85	07.03.96	52	04.10.97	10	08.04.97	2
		07.19.96	122	07.15.96	134	07.05.96	70	04.24.97	9	08.16.97	2
		07.22.96	120	07.19.96	158	07.08.96	101	05.08.97	12	08.18.97	2
		07.26.96	97	07.22.96	143	07.08.96	102	05.23.97	12	08.21.97	2
		07.29.96	82	07.26.96	121	07.10.96	127	06.13.97	14	08.29.97	2
		08.02.96	119	07.26.96	118	07.12.96	148	06.21.97	13	09.12.97	3
		08.05.96	114	07.29.96	131	07.15.96	158	07.01.97	15	09.19.97	2
		08.09.96	163	08.02.96	147	07.19.96	151	07.15.97	17	09.26.97	2
		08.12.96	166	08.02.96	147	07.22.96	147	07.10.97	18	10.02.97	2
		08.16.96	154	08.05.96	153	07.26.96	144	07.10.97	17	10.17.97	2
		08.19.96	157	08.05.96	156	07.29.96	142	07.25.97	21	11.01.97	1
		08.23.96	156	08.09.96	128	08.02.96	154	07.25.97	20		
		08.26.96	152	08.12.96	169	08.05.96	164	08.04.97	20		
		09.01.96	143	08.16.96	167	08.09.96	161	08.04.97	20		
		09.09.96	117	08.19.96	165	08.12.96	165	08.11.97	15		
		09.16.96	81	08.23.96	156	08.16.96	167	08.16.97	15		
		09.19.96	76	08.26.96	153	08.19.96	156	08.21.97	15		
		09.24.96	25	09.01.96	148	08.23.96	153	09.12.97	20		
		09.26.96	16	09.09.96	152	08.26.96	152	09.19.97	19		
		10.01.96	17	09.16.96	123	09.01.96	130	09.29.97	18		
		10.16.96	9	09.19.96	80	09.09.96	142	10.02.97	17		
		10.22.96	19	09.24.96	33	09.16.96	146	10.08.97	16		
		11.05.96	6	09.26.96	31	09.19.96	150	10.17.97	15		
		11.12.96	8	10.01.96	14	09.24.96	145	10.26.97	10		
		11.19.96	6	10.16.96	4	09.26.96	144	11.07.97	17		
		11.25.96	4	10.22.96	9	10.01.96	144	11.15.97	13		
		12.03.96	6	10.29.96	3	10.16.96	149	11.30.97	13		
		12.10.96	8	11.05.96	2	10.22.96	129	12.10.97	9		
		12.17.96	8	11.12.96	1	10.29.96	119	12.23.97	9		
		12.31.96	11	11.19.96	1	11.05.96	103	12.23.97	8		
		01.07.97	11	11.25.96	1	11.12.96	90	01.08.98	8		
		01.15.97	6	12.03.96	1	11.25.96	84	01.08.98	8		
		01.21.97	6	12.10.96	1	12.03.96	88	01.14.98	10		
		02.04.97	4	12.17.96	2	12.10.96	71	01.14.98	9		
		02.18.97	3	12.31.96	2	12.17.96	54	01.27.98	7		
		04.10.97	1	01.07.97	2	12.31.96	55	01.31.98	5		
		07.15.97	3	01.15.97	1	01.07.97	63	02.12.98	7		
				01.21.97	1	01.15.97	59	02.23.98	6		
				02.04.97	1	01.21.97	46	03.07.98	11		
				02.18.97	1	02.04.97	42				
				04.10.97	1	02.18.97	24				
						04.10.97	6				
						07.15.97	8				

TABLE B-8
Summary of Time-series Chloride Data Collected During the Emplaced Source Oxidant Flush (Page 3 of 4)

IF		IF		XW1		XW2		XW3		XWT	
Date	Cl (mg L)	Date	Cl (mg L)	Date	Cl (mg L)	Date	Cl (mg L)	Date	Cl (mg L)	Date	Cl (mg L)
05 23 96	5	07 10 97	14	05 23 96	2	05 23 96	1	05 23 96	2	05 16 96	1
05 25 96	3	07 15 97	14	05 25 96	1	05 25 96	2	05 25 96	1	05 21 96	1
05 27 96	3	08 04 97	17	05 27 96	2	05 27 96	2	05 27 96	2	05 22 96	2
05 29 96	4	08 11 97	15	05 29 96	2	05 29 96	4	05 29 96	2	05 23 96	2
05 31 96	5	08 11 97	14	05 31 96	2	05 31 96	9	05 31 96	7	05 24 96	2
06 03 96	8	08 16 97	13	06 03 96	2	06 03 96	30	06 03 96	3	05 25 96	5
06 05 96	9	08 16 97	13	06 05 96	2	06 07 96	34	06 05 96	4	05 26 96	5
06 05 96	9	08 21 97	13	06 05 96	2	06 07 96	34	06 05 96	4	05 27 96	7
06 07 96	9	08 21 97	13	06 07 96	4	06 10 96	40	06 07 96	5	05 28 96	6
06 07 96	9	08 29 97	12	06 07 96	4	06 10 96	40	06 07 96	5	05 30 96	6
06 07 96	9	09 03 97	12	06 10 96	5	06 13 96	44	06 10 96	7	05 30 96	6
06 10 96	12			06 10 96	5	06 13 96	44	06 10 96	7	05 31 96	5
06 10 96	12			06 13 96	8	06 13 96	44	06 13 96	7	05 31 96	10
06 14 96	39			06 13 96	8	06 13 96	44	06 13 96	7	05 31 96	10
06 14 96	39			06 14 96	7	06 14 96	46	06 14 96	7	06 01 96	8
06 21 96	78			06 14 96	7	06 14 96	46	06 14 96	7	06 01 96	8
06 24 96	109			06 21 96	6	06 21 96	96	06 21 96	10	06 02 96	11
06 26 96	133			06 24 96	10	06 24 96	141	06 24 96	15	06 02 96	11
07 03 96	162			06 26 96	6	06 26 96	153	06 26 96	15	06 03 96	10
07 04 96	171			07 03 96	12	07 03 96	137	07 03 96	18	06 05 96	11
07 05 96	162			07 05 96	10	07 05 96	32	07 05 96	22	06 05 96	11
07 08 96	156			07 08 96	12	07 05 96	32	07 08 96	26	06 06 96	10
07 10 96	153			07 10 96	16	07 05 96	52	07 10 96	47	06 06 96	10
07 12 96	151			07 12 96	13	07 08 96	29	07 12 96	60	06 07 96	11
07 15 96	154			07 15 96	4	07 08 96	30	07 15 96	106	06 08 96	12
07 19 96	153			07 19 96	4	07 10 96	35	07 19 96	87	06 08 96	12
07 22 96	165			07 22 96	5	07 12 96	175	07 22 96	101	06 20 96	117
07 26 96	173			07 26 96	9	07 15 96	63	07 26 96	97	06 20 96	116
07 29 96	176			07 29 96	7	07 19 96	46	07 29 96	100	06 21 96	113
08 02 96	169			08 02 96	66	07 19 96	45	07 29 96	99	06 24 96	177
08 05 96	155			08 05 96	11	07 22 96	56	08 05 96	87	06 26 96	153
08 05 96	153			08 09 96	15	07 26 96	83	08 09 96	106	07 03 96	160
08 09 96	148			08 12 96	9	07 29 96	72	08 12 96	133	07 04 96	159
08 12 96	144			08 16 96	30	08 02 96	122	08 12 96	131	07 05 96	161
08 16 96	147			08 19 96	8	08 05 96	81	08 16 96	114	07 05 96	160
08 19 96	141			08 23 96	5	08 09 96	74	08 19 96	121	07 06 96	152
08 26 96	150			08 26 96	10	08 12 96	84	08 21 96	76	07 07 96	156
08 23 96	148			09 01 96	38	08 16 96	55	08 23 96	105	07 08 96	125
09 01 96	150			09 09 96	60	08 19 96	85	08 26 96	137	07 10 96	178
09 09 96	109			09 16 96	162	08 23 96	104	09 01 96	125	07 12 96	152
09 16 96	68			09 24 96	89	08 26 96	122	09 09 96	128	07 12 96	140
09 24 96	85			10 01 96	193	09 01 96	463	09 16 96	86	07 14 96	158
10 01 96	164			10 08 96	69	09 09 96	314	09 24 96	144	07 15 96	163
10 08 96	164			10 16 96	80	09 09 96	302	10 01 96	59	07 16 96	150
10 22 96	109			10 22 96	98	09 16 96	166	10 08 96	74	07 18 96	172
10 29 96	112			10 29 96	123	09 24 96	179	10 16 96	57	07 19 96	174
11 05 96	113			11 05 96	78	10 01 96	224	10 22 96	75	07 20 96	158
11 12 96	96			11 12 96	114	10 08 96	224	10 29 96	86	07 22 96	159
11 19 96	91			04 10 97	10	10 16 96	168	11 05 96	56	07 25 96	177
11 25 96	79			04 24 97	18	10 22 96	149	11 12 96	46	07 26 96	173
12 03 96	64			05 08 97	23	10 29 96	253	09 19 97	1	07 27 96	175
12 10 96	63			05 23 97	18	11 05 96	109	10 26 97	1	07 28 96	153
12 17 96	63			06 13 97	4	11 12 96	116	09 19 97	1	07 29 96	170
12 31 96	63			06 21 97	7	11 19 96	49	09 26 97	3	07 29 96	173
01 07 97	60			07 01 97	5	11 25 96	44	10 02 97	4	07 30 96	167
01 21 97	52			07 10 97	9	12 03 96	45	10 08 97	3	08 02 96	178
02 04 97	40			07 15 97	10	12 10 96	46	10 17 97	3	08 05 96	150
02 18 97	32			07 25 97	10	12 17 96	48	09 30 97	2	08 09 96	152
03 04 97	24			07 25 97	7	12 31 96	31	12 10 97	2	08 12 96	151
03 27 97	14			08 04 97	9	01 07 97	57			08 16 96	172
04 10 97	14			08 04 97	9	01 15 97	52			08 19 96	138
04 24 97	9			08 11 97	7	01 21 97	30			08 23 96	199
05 08 97	16			08 11 97	7	01 28 97	47			08 26 96	146
05 23 97	17			08 16 97	4	02 04 97	39			09 01 96	138
05 30 97	15			08 16 97	4	02 18 97	35			09 03 96	145
06 05 97	12			08 21 97	2	03 04 97	19			09 03 96	145
06 13 97	13			08 21 97	3	03 27 97	12			09 04 96	144
06 21 97	5			08 29 97	3					09 08 96	150
07 01 97	9									09 05 96	145
										09 06 96	84

TABLE B-8

Summary of Time-series Chloride Data Collected During the Emplaced Source Oxidant Flush (Page 4 of 4)

XWT		XWT	
Date	Cl (mg L)	Date	Cl (mg L)
09 07 96	105	10 26 97	9
09 09 96	102	11 07 97	17
09 10 96	213	11 07 97	16
09 12 96	213	11 30 97	10
09 14 96	182	11 30 97	10
09 15 96	132	12 10 97	8
09 16 96	163	12 10 97	8
09 19 96	101	12 23 97	9
09 21 96	205	12 23 97	8
09 23 96	208	01 08 98	8
09 24 96	167	01 08 98	8
09 25 96	125	01 14 98	10
10 01 96	84	01 14 98	9
10 08 96	157	01 27 98	7
10 11 96	107	01 31 98	5
10 13 96	104	02 12 98	7
10 15 96	101	02 23 98	6
10 16 96	105	03 07 98	11
10 17 96	132		
10 22 96	110		
10 29 96	60		
11 05 96	101		
11 12 96	92		
11 19 96	68		
11 25 96	58		
12 03 96	60		
12 10 96	64		
12 17 96	66		
12 31 96	56		
01 07 97	49		
01 15 97	47		
01 21 97	44		
01 28 97	35		
02 04 97	34		
02 18 97	29		
03 04 97	20		
03 27 97	13		
04 10 97	8		
04 24 97	12		
05 08 97	17		
05 23 97	15		
05 30 97	14		
06 05 97	13		
06 13 97	9		
06 21 97	10		
07 01 97	9		
07 10 97	13		
07 15 97	14		
07 25 97	16		
08 04 97	16		
08 11 97	13		
08 11 97	13		
08 16 97	11		
08 21 97	13		
08 21 97	13		
08 29 97	10		
09 03 97	12		
09 12 97	17		
09 12 97	17		
09 19 97	16		
09 19 97	15		
09 26 97	16		
09 26 97	16		
10 02 97	12		
10 02 97	12		
10 08 97	11		
10 08 97	11		
10 17 97	12		
10 17 97	12		
10 26 97	8		

TABLE B-9

Vertical Concentration Profiles In and Adjacent to Emplaced Source (Page 1 of 5)

Date	Sample Depth (m)	Elevation (m)	$CHCl_3$ (g/L)	TCE (g/L)	PCE (g/L)
1994	3.86	145.57	0	43	27
through source	3.96	145.47	0	330	534
	4.06	145.37	79	1599	28872
	4.16	145.27	483	55739	49421
	4.26	145.17	593	205074	159630
	4.36	145.07	488	217483	143961
	4.46	144.97	548	235173	154226
	4.56	144.87	545	306174	180591
	4.66	144.77	517	224349	147721
	4.76	144.67	515	76212	101393
	4.86	144.57	79	6958	18522

	Sample Depth (m)	~Elev. (m)	$KMnO_4$ (g/L)	Cl- (mg/L)
10/29/96	3.1	96.79	0.0	2
through centre of source (0,0)	3.4	96.49	0.0	2
	3.5	96.39	0.0	2
	3.6	96.29	0.0	2
	3.7	96.19	0.6	18
	3.8	96.09	6.4	108
	3.9	95.99	8.6	146
	4.0	95.89	7.0	72
	4.1	95.79	8.8	123
	4.2	95.69	8.1	146
	4.3	95.59	8.2	158
	4.4	95.49	7.9	136
	4.5	95.39	8.6	141
	4.6	95.29	7.5	588
	4.7	95.19	7.2	334
	4.8	95.09	8.2	162
	4.9	94.99	8.8	151
	5.0	94.89	8.1	136
	5.1	94.79	8.2	141
	5.3	94.59	5.6	87
	5.5	94.39	8.6	138

	Sample Depth (m)	~Elev. (m)	$KMnO_4$ (g/L)	Cl- (mg/L)
03/04/97	3.8	96.05	0.2	2
through centre of source (0,0)	4	95.85	3.5	18
	4.2	95.65	8.1	37
	4.4	95.45	7.3	29
	4.6	95.25	7.9	1292
	4.7	95.15	9.5	41
	4.8	95.05	9.9	35
	4.82	95.03	8.8	31

TABLE B-9

Vertical Concentration Profiles In and Adjacent to Emplaced Source (Page 2 of 5)

	Sample Depth (m)	*~Elev. (m)*	*$KMnO_4$ (g/L)*	*Cl- (mg/L)*
04/02/97	3.8	96.03	3.1	20
through centre of source (0,0)	3.9	95.93	4.3	20
	4	95.83	2.9	22
	4.1	95.73	3.6	18
	4.2	95.63	3.7	19
	4.3	95.53	2.7	21
	4.4	95.43	1.6	31
	4.5	95.33	1.3	253
	4.6	95.23	1.6	23
	4.7	95.13	3.8	20
	4.8	95.03	4.5	19

	Sample Depth (m)	*~Elev. (m)*	*$KMnO_4$ (g/L)*	*Cl- (mg/L)*
04/24/97	3.6	96.22	0.0	2
through centre of source (0,0)	3.7	96.12	0.0	2
	3.8	96.02	0.3	2
	3.9	95.92	4.8	9
	4	95.82	4.2	15
	4.1	95.72	3.6	15
	4.2	95.62	3.7	16
	4.3	95.52	4.6	16
	4.4	95.42	4.0	16
	4.5	95.32	4.1	62
	4.6	95.22	4.3	17
	4.7	95.12	5.6	16
	4.8	95.02	9.1	16

	Sample Depth (m)	*~Elev. (m)*	*$KMnO_4$ (g/L)*	*Cl- (mg/L)*
05/30/97	3.6	96.25	0.0	2
through centre of source (0,0)	3.7	96.15	0.0	2
	3.8	96.05	0.8	5
	3.9	95.95	2.5	11
	4	95.85	2.4	10
	4.1	95.75	2.7	12
	4.2	95.65	3.8	13
	4.3	95.55	5.9	14
	4.4	95.45	7.3	15
	4.5	95.35	5.1	8
	4.6	95.25	2.5	5
	4.7	95.15	3.4	8
	4.8	95.05	3.4	3

TABLE B-9

Vertical Concentration Profiles In and Adjacent to Emplaced Source (Page 3 of 5)

	Sample Depth (m)	*~Elev. (m)*	*$KMnO_4$ (g/L)*	*Cl- (mg/L)*
05/30/97	3.6	96.3	0.0	2
downgradient of source (-0.15,-0.35)	3.7	96.2	0.0	2
	3.8	96.1	0.1	2
	3.9	96.0	0.4	3
	4	95.9	2.5	9
	4.1	95.8	5.8	14
	4.2	95.7	5.7	15
	4.3	95.6	3.4	14
	4.4	95.5	4.3	20
	4.5	95.4	5.1	45
	4.6	95.3	5.7	20
	4.7	95.2	5.1	12
	4.8	95.1	7.6	14
	5	94.9	3.4	15
	5.2	94.7	5.0	15

	Sample Depth (m)	*~Elev (m)*	*$KMnO_4$ (g/L)*	*Cl- (mg/L)*
05/30/97	3.6	96.24	0.0	2
downgradient of source (0.10,-0.25)	3.7	96.14	0.0	2
	3.8	96.04	0.2	2
	3.9	95.94	0.1	3
	4.0	95.84	1.5	2
	4.1	95.74	1.0	5
	4.2	95.64	1.8	7
	4.3	95.54	5.2	10
	4.4	95.44	6.3	14
	4.5	95.34	3.8	313
	4.6	95.24	5.3	1971
	4.7	95.14	7.2	663
	4.8	95.04	3.2	15
	5.0	94.84	4.6	12
	5.2	94.64	5.9	13
	5.4	94.44	0.9	4

TABLE B-9

Vertical Concentration Profiles In and Adjacent to Emplaced Source (Page 4 of 5)

	Sample Depth (m)	*~Elev. (m)*	*$KMnO_4$ (g/L)*	*Cl- (mg/L)*	*TCE (g/L)*	*PCE (g/L)*
06/05/97	3.6	96.246	0	2	0	1
downgradient of source (-0.05,-0.24)	3.7	96.146	0.2	3	1	1
	3.8	96.046	0.7	5	0	1
	3.9	95.946	1.1	8	0	1
	4	95.846	2.7	14	0	2
	4.1	95.746	4.0	15	0	11
	4.2	95.646	4.1	15		
	4.3	95.546	4.1	7	0	3
	4.4	95.446	5.1	15	0	2
	4.5	95.346	7.4	17	0	3
	4.6	95.246	5.6	15	0	3
	4.7	95.146	6.1	15	0	2
	4.8	95.046	5.5	16	0	1
	5	94.846	6.2	16	0	2

	Sample Depth (m)	*~Elev. (m)*	*$KMnO_4$ (g/L)*	*Cl- (mg/L)*	*TCE (g/L)*	*PCE (g/L)*
08/29/97	3.6	96.226	0	1	0	7
centre of source (0.0)	3.7	96.126	0.8	7	0	5
	3.8	96.026	0.9	9	0	7
	3.9	95.926	3.1	15	0	7
	4	95.826	2.6	16	0	27
	4.1	95.726	2.2	16	0	113
	4.2	95.626	2.8	17		
	4.3	95.526	4.6	17	0	76
	4.4	95.426	7.0	18	0	14
	4.5	95.326	8.7	19	0	10
	4.6	95.226	8.5	19	0	12
	4.7	95.126	6.9	18	0	7
	4.8	95.026	8.5	19	0	9

TABLE B-9

Vertical Concentration Profiles In and Adjacent to Emplaced Source (Page 5 of 5)

	Sample Depth (m)	*~Elev. (m)*	*$KMnO_4$ (g/L)*	*Cl- (mg/L)*	*PCE (g/L)*
09/04/97	3.6	96.202	0	2	6
downgradient of source (0.22,-0.32)	3.7	96.102	0.2	2	6
	3.8	96.002	0.1	2	
	4	95.802	0.5	4	5
	4.1	95.702	1.5	9	6
	4.2	95.602	1.3	7	5
	4.3	95.502	1.6	8	6
	4.4	95.402	1.8	9	
	4.5	95.302	2.2	474	9
	4.6	95.202	4.0	351	6
	4.7	95.102	4.7	18	
	4.8	95.002	5.5	15	6
	4.9	94.902	7.0	18	6
	5	94.802	5.5	16	6
	5.2	94.602	9.8	18	5
	5.4	94.402	6.7	17	4

	Sample Depth (m)	*~Elev. (m)*	*$KMnO_4$ (g/L)*	*Cl- (mg/L)*	*PCE (g/L)*
09/04/97	3.6	96.21	0	1	5
downgradient of source (0.59,-0.32)	3.7	96.11	0.1	2	5
	3.8	96.01	0.2	3	6
	4	95.81	0.2	4	5
	4.1	95.71	1.5	12	7
	4.2	95.61	1.3	12	8
	4.3	95.51	2.1	12	6
	4.4	95.41	3.1	15	6
	4.5	95.31	4.4	17	6
	4.6	95.21	5.2	17	7
	4.7	95.11	6.1	18	6
	4.8	95.01	7.3	18	6
	4.9	94.91	5.7	18	6
	5	94.81	6.5	16	6
	5.2	94.61	6.5	16	7

TABLE B-10

Summary of Injection Flow Rates During Post-oxidant Flush Tracer Test

Measurement Date (mm/dd/yy)	*Elapsed Time (days)*	*Initial Flow Rate (mL/min)*	*Reset Flow Rate (mL/min)*	*Avg. Flow Rate (mL/min)*	*Cumulative Volume (L)*
07/24/98	37	338	358	346	0
07/27/98	40	364	364	361	1,560
07/29/98	42	358	358	361	2,599
08/12/98	56	356	362	357	9,796
08/14/98	58	368	368	365	10,848
08/17/98	61	365	365	367	12,431
08/20/98	64	361	361	363	13,999
08/24/98	68	364	364	363	16,087
08/27/98	71	340	364	352	17,608
08/31/98	75	360	360	362	19,693
09/03/98	78	353	360	357	21,233
09/07/98	82	347	356	354	23,269
09/10/98	85	320	358	338	24,729
09/13/98	88	364	364	361	26,289
09/16/98	91	336	364	350	27,801
09/20/98	95	364	364	364	29,897
09/24/98	99	339	352	352	31,922
09/27/98	102	357	357	355	33,453
10/01/98	106	349	356	353	35,487
10/04/98	109	330	358	343	36,968
10/07/98	112	360	360	359	38,519
10/11/98	116	344	356	352	40,547

Notes

1) Reported flow rates are the total volumetric flow injected into the six injection wells (IW1 to IW6).

2) Flow rates were measured at the beginning (initial) and end (reset) of each site visit to estimate the average flow rate for the periods between site visits.

3) Mean injection flowrate of 356 ± 7 mL/min (%RSD=2.1%).

TABLE B-11
Summary of Extraction Flow Rates During
Post-oxidant Flush Tracer Test

Measurement Date (mm/dd/yy)	*Elapsed Time (days)*	*Initial Flow Rate (mL/min)*	*Reset Flow Rate (mL/min)*	*Avg. Flow Rate (mL/min)*	*Cumulative Volume (L)*
07/24/98	37	385	385	390	0
07/27/98	40	395	395	390	1685
07/29/98	42	395	395	395	2822
08/12/98	56	395	395	395	10786
08/14/98	58	390	395	393	11916
08/17/98	61	390	393	393	13612
08/20/98	64	380	390	387	15281
08/24/98	68	390	390	390	17528
08/27/98	71	387	385	389	19206
08/31/98	75	308	386	347	21202
09/03/98	78	383	395	385	22863
09/07/98	82	387	387	391	25115
09/10/98	85	380	390	384	26772
09/13/98	88	390	390	390	28457
09/16/98	91	380	394	385	30120
09/20/98	95	385	385	390	32363
09/24/98	99	375	387	380	34552
09/27/98	102	393	393	390	36237
10/01/98	106	385	385	389	38478
10/04/98	109	375	385	380	40119
10/07/98	112	390	390	388	41793
10/11/98	116	390	390	390	44040
10/14/98	119	380	380	385	45703

Notes

1) Reported flow rates are the total volumetric flows extracted from the extraction wells (XW1, XW2, and XW3).

2) Flow rates were measured at the beginning (initial) and end (reset) of each site visit to estimate the average flow rate for the periods between site visits.

3) Mean total extraction flow rate of 387 ± 10 mL/min (%RSD=2.5%).

TABLE B-12
Calculation of Average Injected Tracer Concentration and
Mass - Post-oxidant Flush Tracer Test

A) Calculate mass of tracer based on precise measurement of the concentrated tracer dosing rate.

Sampling Date	*Flow (mL/min)*	*delta time (min)*	*Bromide mass (g)*
24/07/98 17:30	0.288	0	0
27/07/98 12:00	0.297	3990	428
29/07/98 14:00	0.293	3000	752

Bromide in tracer concentrate[1] = 366676 mg/L Br^-

b) Calculate mass of tracer ased on concentration in injected feed solution

Sampling Date	*Flow (mL/min)*	*delta time (min)*	*Bromide mass[2] (g)*
24/07/98 17:30	358	0	0
27/07/98 12:00	361	3990	431
29/07/98 14:00	361	3000	756

Notes

1) Based on nine replicate analyses of subsamples of tracer concentrate solution.

2) Calculated based on mean bromide concentration of feed solution (300.5 mg/L Br-).

TABLE B-13
Summary of Tracer Monitoring Results During
Post-oxidant Flush Tracer Test (page 1 of 8)

Sampling Location	*Measurement Date (mm/dd/yy)*	*Elapsed Time (days)*	*Bromide (mg/L)*
IW	07/24/98	0	0
IW	07/24/98	0	301
IW	07/27/98	2	296
IW	07/29/98	5	305
IW	07/29/98	5	0
IW	08/09/98	15	0
IW	08/12/98	18	1
IW	08/14/98	20	0
IW	08/17/98	23	0
IW	08/20/98	26	0
IW	08/24/98	30	0
IW	08/27/98	33	0.0
IW	08/31/98	37	0.1
IW	09/03/98	40	0.0
IW	09/07/98	44	0.1
IW	09/10/98	47	0
IW	09/13/98	50	0
IW	09/16/98	53	0
IW	09/20/98	57	0
IW	09/27/98	64	0
IW	09/30/98	67	5
IW	10/04/98	71	0
IW	10/11/98	78	0
XW1	08/12/98	18	4
XW1	08/12/98	18	4
XW1	08/14/98	20	15
XW1	08/14/98	20	14
XW1	08/14/98	20	14
XW1	08/17/98	23	21
XW1	08/17/98	23	21
XW1	08/20/98	26	29
XW1	08/20/98	26	29
XW1	08/20/98	26	29
XW1	08/22/98	28	22
XW1	08/22/98	28	22
XW1	08/22/98	28	22
XW1	08/24/98	30	20
XW1	08/24/98	30	21
XW1	08/24/98	30	20
XW1	08/26/98	32	21
XW1	08/26/98	32	21
XW1	08/27/98	33	24
XW1	08/27/98	33	24
XW1	08/29/98	35	24
XW1	08/29/98	35	24
XW1	08/31/98	37	24

TABLE B-13
Summary of Tracer Monitoring Results During
Post-oxidant Flush Tracer Test (page 2 of 8)

Sampling Location	*Measurement Date (mm\dd\yy)*	*Elapsed Time (days)*	*Bromide (mg/L)*
XW1	08/31/98	37	24
XW1	09/02/98	39	36
XW1	09/02/98	39	36
XW1	09/03/98	40	37
XW1	09/03/98	40	37
XW1	09/05/98	42	39
XW1	09/05/98	42	39
XW1	09/07/98	44	40
XW1	09/07/98	44	40
XW1	09/09/98	46	42
XW1	09/09/98	46	42
XW1	09/10/98	47	40
XW1	09/12/98	49	41
XW1	09/12/98	49	41
XW1	09/13/98	50	40
XW1	09/15/98	52	36
XW1	09/16/98	53	38
XW1	09/16/98	53	37
XW1	09/18/98	55	30
XW1	09/18/98	55	30
XW1	09/20/98	57	24
XW1	09/20/98	57	24
XW1	09/20/98	57	23
XW1	09/24/98	61	17
XW1	09/24/98	61	17
XW1	09/24/98	61	17
XW1	09/25/98	62	16
XW1	09/25/98	62	17
XW1	09/27/98	64	15
XW1	09/27/98	64	15
XW1	09/29/98	66	2
XW1	09/29/98	66	8
XW1	09/30/98	67	12
XW1	09/30/98	67	12
XW1	10/04/98	71	7
XW1	10/04/98	71	7
XW1	10/06/98	73	0
XW1	10/06/98	73	0
XW1	10/06/98	73	0
XW1	10/07/98	74	1
XW1	10/07/98	74	1
XW1	10/07/98	74	1
XW1	10/11/98	78	3
XW1	10/11/98	78	3
XW1	10/11/98	78	3
XW1	10/13/98	80	3

TABLE B-13
Summary of Tracer Monitoring Results During
Post-oxidant Flush Tracer Test (page 3 of 8)

Sampling Location	*Measurement Date (mm\dd\yy)*	*Elapsed Time (days)*	*Bromide (mg/L)*
XW1	10/13/98	80	3
XW1	10/14/98	81	3
XW1	10/14/98	81	3
XW2	08/12/98	18	18
XW2	08/12/98	18	18
XW2	08/12/98	18	17
XW2	08/14/98	20	30
XW2	08/14/98	20	31
XW2	08/14/98	20	30
XW2	08/17/98	23	33
XW2	08/17/98	23	33
XW2	08/17/98	23	33
XW2	08/20/98	26	26
XW2	08/20/98	26	26
XW2	08/20/98	26	27
XW2	08/22/98	28	23
XW2	08/22/98	28	23
XW2	08/24/98	30	25
XW2	08/24/98	30	25
XW2	08/24/98	30	25
XW2	08/26/98	32	31
XW2	08/26/98	32	31
XW2	08/27/98	33	32
XW2	08/27/98	33	32
XW2	08/29/98	35	39
XW2	08/29/98	35	39
XW2	08/31/98	37	40
XW2	08/31/98	37	40
XW2	09/02/98	39	41
XW2	09/02/98	39	40
XW2	09/03/98	40	35
XW2	09/03/98	40	36
XW2	09/05/98	42	30
XW2	09/05/98	42	30
XW2	09/07/98	44	24
XW2	09/07/98	44	24
XW2	09/09/98	46	20
XW2	09/09/98	46	20
XW2	09/10/98	47	16
XW2	09/10/98	47	16
XW2	09/12/98	49	15
XW2	09/12/98	49	15
XW2	09/13/98	50	12
XW2	09/13/98	50	12
XW2	09/15/98	52	13
XW2	09/15/98	52	13

TABLE B-13
Summary of Tracer Monitoring Results During
Post-oxidant Flush Tracer Test (page 4 of 8)

Sampling Location	*Measurement Date (mm\dd\yy)*	*Elapsed Time (days)*	*Bromide (mg/L)*
XW2	09/16/98	53	9
XW2	09/16/98	53	9
XW2	09/20/98	57	7
XW2	09/20/98	57	7
XW2	09/22/98	59	9
XW2	09/22/98	59	9
XW2	09/22/98	59	8
XW2	09/25/98	62	7
XW2	09/25/98	62	7
XW2	09/27/98	64	9
XW2	09/27/98	64	9
XW2	09/29/98	66	6
XW2	09/29/98	66	6
XW2	09/30/98	67	1
XW2	09/30/98	67	1
XW2	09/30/98	67	0
XW2	09/30/98	67	1
XW2	09/30/98	67	1
XW2	10/04/98	71	4
XW2	10/04/98	71	5
XW2	10/07/98	74	3
XW2	10/07/98	74	3
XW2	10/11/98	78	1
XW2	10/11/98	78	1
XW2	10/11/98	78	1
XW2	10/13/98	80	2
XW2	10/13/98	80	2
XW2	10/14/98	81	2
XW2	10/14/98	81	2
XW3	08/12/98	18	20
XW3	08/12/98	18	20
XW3	08/14/98	20	33
XW3	08/14/98	20	32
XW3	08/14/98	20	32
XW3	08/17/98	23	40
XW3	08/17/98	23	41
XW3	08/17/98	23	40
XW3	08/20/98	26	80
XW3	08/20/98	26	81
XW3	08/20/98	26	80
XW3	08/22/98	28	93
XW3	08/22/98	28	92
XW3	08/22/98	28	93
XW3	08/24/98	30	85
XW3	08/24/98	30	85
XW3	08/24/98	30	86

TABLE B-13
Summary of Tracer Monitoring Results During
Post-oxidant Flush Tracer Test (page 5 of 8)

Sampling Location	*Measurement Date (mm\dd\yy)*	*Elapsed Time (days)*	*Bromide (mg/L)*
XW3	08/26/98	32	54
XW3	08/26/98	32	54
XW3	08/27/98	33	57
XW3	08/27/98	33	57
XW3	08/29/98	35	43
XW3	08/29/98	35	43
XW3	08/31/98	37	31
XW3	08/31/98	37	31
XW3	09/02/98	39	23
XW3	09/02/98	39	23
XW3	09/03/98	40	20
XW3	09/03/98	40	20
XW3	09/05/98	42	21
XW3	09/05/98	42	20
XW3	09/07/98	44	36
XW3	09/07/98	44	36
XW3	09/09/98	46	63
XW3	09/09/98	46	59
XW3	09/09/98	46	60
XW3	09/10/98	47	69
XW3	09/10/98	47	69
XW3	09/12/98	49	81
XW3	09/12/98	49	80
XW3	09/12/98	49	80
XW3	09/13/98	50	66
XW3	09/13/98	50	66
XW3	09/15/98	52	52
XW3	09/15/98	52	52
XW3	09/16/98	53	35
XW3	09/16/98	53	35
XW3	09/18/98	55	24
XW3	09/18/98	55	24
XW3	09/20/98	57	20
XW3	09/20/98	57	20
XW3	09/20/98	57	20
XW3	09/22/98	59	20
XW3	09/22/98	59	20
XW3	09/22/98	59	20
XW3	09/25/98	62	21
XW3	09/25/98	62	21
XW3	09/27/98	64	16
XW3	09/27/98	64	16
XW3	09/29/98	66	12
XW3	09/29/98	66	12
XW3	09/30/98	67	1
XW3	09/30/98	67	1

TABLE B-13
Summary of Tracer Monitoring Results During
Post-oxidant Flush Tracer Test (page 6 of 8)

Sampling Location	*Measurement Date (mm\dd\yy)*	*Elapsed Time (days)*	*Bromide (mg/L)*
XW3	10/04/98	71	4
XW3	10/04/98	71	4
XW3	10/06/98	73	6
XW3	10/06/98	73	6
XW3	10/06/98	73	6
XW3	10/07/98	74	2
XW3	10/07/98	74	2
XW3	10/07/98	74	2
XW3	10/11/98	78	1
XW3	10/11/98	78	1
XW3	10/11/98	78	1
XW3	10/13/98	80	1
XW3	10/13/98	80	1
XW3	10/14/98	81	1
XW3	10/14/98	81	1
XWT	07/23/98	-2	0
XWT	07/23/98	-2	0
XWT	07/23/98	-2	0
XWT	07/28/98	3	0
XWT	07/28/98	3	0
XWT	07/28/98	3	0
XWT	07/29/98	4	0
XWT	07/29/98	4	0
XWT	07/29/98	4	0
XWT	08/09/98	15	2
XWT	08/09/98	15	2
XWT	08/09/98	15	2
XWT	08/12/98	18	14
XWT	08/12/98	18	14
XWT	08/12/98	18	14
XWT	08/12/98	18	13
XWT	08/12/98	18	13
XWT	08/12/98	18	13
XWT	08/14/98	20	22
XWT	08/14/98	20	22
XWT	08/14/98	20	22
XWT	08/14/98	20	22
XWT	08/14/98	20	22
XWT	08/14/98	20	22
XWT	08/17/98	23	31
XWT	08/17/98	23	32
XWT	08/17/98	23	31
XWT	08/20/98	26	34
XWT	08/20/98	26	34
XWT	08/20/98	26	35
XWT	08/24/98	30	37

TABLE B-13
Summary of Tracer Monitoring Results During
Post-oxidant Flush Tracer Test (page 7 of 8)

Sampling Location	*Measurement Date (mm\dd\yy)*	*Elapsed Time (days)*	*Bromide (mg/L)*
XWT	08/24/98	30	37
XWT	08/24/98	30	37
XWT	08/27/98	33	34
XWT	08/27/98	33	34
XWT	08/27/98	33	34
XWT	08/31/98	37	32
XWT	08/31/98	37	32
XWT	08/31/98	37	32
XWT	09/03/98	40	28
XWT	09/03/98	40	28
XWT	09/03/98	40	28
XWT	09/07/98	44	22
XWT	09/07/98	44	23
XWT	09/07/98	44	22
XWT	09/10/98	47	18
XWT	09/10/98	47	17
XWT	09/10/98	47	18
XWT	09/13/98	50	16
XWT	09/13/98	50	16
XWT	09/16/98	53	11
XWT	09/16/98	53	11
XWT	09/16/98	53	11
XWT	09/20/98	57	9
XWT	09/20/98	57	9
XWT	09/20/98	57	9
XWT	09/24/98	61	7
XWT	09/24/98	61	8
XWT	09/24/98	61	9
XWT	09/27/98	64	5
XWT	09/27/98	64	9
XWT	09/27/98	64	9
XWT	09/30/98	67	1
XWT	09/30/98	67	1
XWT	09/30/98	67	1
XWT	10/04/98	71	4
XWT	10/04/98	71	4
XWT	10/04/98	71	4
XWT	10/04/98	71	4
XWT	10/04/98	71	4
XWT	10/04/98	71	4
XWT	10/07/98	74	2
XWT	10/07/98	74	3
XWT	10/07/98	74	3
XWT	10/07/98	74	3
XWT	10/11/98	78	1
XWT	10/11/98	78	1

TABLE B-13
Summary of Tracer Monitoring Results During
Post-oxidant Flush Tracer Test (page 8 of 8)

Sampling Location	*Measurement Date (mm\dd\yy)*	*Elapsed Time (days)*	*Bromide (mg/L)*
XWT	10/11/98	78	1
XWT	10/14/98	81	2
XWT	10/14/98	81	2

TABLE B-14
Solvent Plume Load Measurement
Plume Snapshot - October 25, 1995 (Page 1 of 2)

Sampling Location	*X (m)*	*Y (m)*	*Elev. (m)*	*TCE (µg/L)*	*PCE (µg/L)*
ES1-1	0.95	-1.04	96.74	74	263
ES1-2	0.95	-1.04	96.54	147	293
ES1-3	0.95	-1.04	96.34	168	410
ES1-4	0.95	-1.04	96.14	59	230
ES1-5	0.95	-1.04	95.94	216	432
ES1-6	0.95	-1.04	95.74	72	447
ES1-7	0.95	-1.04	95.54	3500	2200
ES1-8	0.95	-1.04	95.34	2200	1400
ES1-9	0.95	-1.04	95.14	363	1335
ES1-10	0.95	-1.04	94.94	188	1161
ES1-11	0.95	-1.04	94.74	183	1101
ES1-12	0.95	-1.04	94.54	214	792
ES1-14	0.95	-1.04	94.14	137	516
ES2-3	0.45	-1.04	96.39	85	283
ES2-4	0.45	-1.04	96.19	167	410
ES2-6	0.45	-1.04	95.79	1500	17700
ES2-7	0.45	-1.04	95.59	127300	61000
ES2-8	0.45	-1.04	95.39	142400	36200
ES2-9	0.45	-1.04	95.19	800	1800
ES2-10	0.45	-1.04	94.99	1100	800
ES2-11	0.45	-1.04	94.79	1400	1300
ES2-12	0.45	-1.04	94.59	1200	1300
ES2-13	0.45	-1.04	94.39	1100	1200
ES2-14	0.45	-1.04	94.19	1500	1500
ES3-1	-0.05	-1.04	96.84	70	297
ES3-2	-0.05	-1.04	96.64	56	226
ES3-3	-0.05	-1.04	96.44	197	426
ES3-4	-0.05	-1.04	96.24	152	327
ES3-5	-0.05	-1.04	96.04	171	418
ES3-6	-0.05	-1.04	95.84	18500	45500
ES3-7	-0.05	-1.04	95.64	600	1300
ES3-8	-0.05	-1.04	95.44	7800	43700
ES3-9	-0.05	-1.04	95.24	2200	38400
ES3-10	-0.05	-1.04	95.04	186	702
ES3-11	-0.05	-1.04	94.84	185	450
ES3-13	-0.05	-1.04	94.44	186	693
ES3-14	-0.05	-1.04	94.24	297	609
ES4-1	-0.55	-1.04	96.79	117	272
ES4-2	-0.55	-1.04	96.59	38	239
ES4-4	-0.55	-1.04	96.19	168	370
ES4-5	-0.55	-1.04	95.99	191	387
ES4-6	-0.55	-1.04	95.79	183	516
ES4-8	-0.55	-1.04	95.39	1746	918
ES4-9	-0.55	-1.04	95.19	177	459
ES4-10	-0.55	-1.04	94.99	140	366
ES4-11	-0.55	-1.04	94.79	308	
ES4-12	-0.55	-1.04	94.59	71	432
ES4-13	-0.55	-1.04	94.39	107	624
ES4-14	-0.55	-1.04	94.19	265	

TABLE B-14
Solvent Plume Load Measurement
Plume Snapshot - October 25, 1995 (Page 2 of 2)

Sampling Location	*X (m)*	*Y (m)*	*Elev. (m)*	*TCE (µg/L)*	*PCE (µg/L)*
ES5-1	-1.05	-1.04	96.78	160	300
ES5-2	-1.05	-1.04	96.58	71	355
ES5-3	-1.05	-1.04	96.38	36	203
ES5-4	-1.05	-1.04	96.18	33	147
ES5-5	-1.05	-1.04	95.98	180	388
ES5-6	-1.05	-1.04	95.78	144	376
ES5-7	-1.05	-1.04	95.58	140	308
ES5-8	-1.05	-1.04	95.38	216	419
ES5-9	-1.05	-1.04	95.18	99	585
ES5-11	-1.05	-1.04	94.78	72	354
ES5-12	-1.05	-1.04	94.58	2671	2365
ES5-13	-1.05	-1.04	94.38	75	311
ES28-2	1.60	-1.04	97.10	183	445
ES28-3	1.60	-1.04	96.90	38	129
ES28-4	1.60	-1.04	96.70	152	337
ES28-5	1.60	-1.04	96.50	124	301
ES28-6	1.60	-1.04	96.30	195	
ES28-7	1.60	-1.04	96.10	131	349
ES28-8	1.60	-1.04	95.90	59	251
ES28-9	1.60	-1.04	95.70	67	300
ES28-10	1.60	-1.04	95.50	53	318
ES28-11	1.60	-1.04	95.30	210	445
ES28-12	1.60	-1.04	95.10	191	390
ES28-13	1.60	-1.04	94.90	51	292
ES28-14	1.60	-1.04	94.70	58	328
ES29-2	2.60	-1.04	97.07	45	159
ES29-3	2.60	-1.04	96.87	49	5000
ES29-4	2.60	-1.04	96.67	83	314
ES29-5	2.60	-1.04	96.47	149	332
ES29-6	2.60	-1.04	96.27	24	174
ES29-9	2.60	-1.04	95.67	122	427
ES29-10	2.60	-1.04	95.47	119	362
ES29-11	2.60	-1.04	95.27		87
ES29-12	2.60	-1.04	95.07	54	199
ES30-2	-1.55	-1.04	97.22	207	
ES30-3	-1.55	-1.04	97.02	160	357
ES30-4	-1.55	-1.04	96.82	152	316
ES30-5	-1.55	-1.04	96.62	135	340
ES30-7	-1.55	-1.04	96.22	85	283
ES30-8	-1.55	-1.04	96.02	120	347
ES30-9	-1.55	-1.04	95.82	61	236
ES30-11	-1.55	-1.04	95.42	64	286
ES30-12	-1.55	-1.04	95.22	179	428
ES30-13	-1.55	-1.04	95.02	147	389
ES30-14	-1.55	-1.04	94.82	129	363

TABLE B-15
Solvent Plume Load
Extraction System Effluent Monitoring - 11/2/95 through 12/10/96

Measurement Date (mm/dd/yy)	*Elapsed Time (days)*	*Avg. Flow Rate (mL/min)*	*PCE*[1] *(mg/L)*	*TCE*[1] *(mg/L)*
11/02/95	0	368	10	37
11/04/95	2	379	12	61
11/07/95	5	377	9	40
11/11/95	8	389	6	7
11/12/95	9	401	8	8
11/16/95	13	394	7	7
11/18/95	15	390	9	9
11/21/95	18	394	3	3
11/24/95	21	390	4	4
11/25/95	22	388	4	4
11/27/95	24	386	4	5
11/28/95	25	387	4	5
11/29/95	26	388	4	4
12/02/95	29	380	3	3
12/04/95	31	396	3	3
12/05/95	32	396	3	3
12/07/95	34	394	5	5
12/08/95	35	394	5	6
12/09/95	36	394	2	2
12/10/95	37	396	5	5
		Average VOC Concentration =	3.8	4.0
		Standard Deviation =	1.0	1.0
		Number of Measurements =	11	11

Notes:

1) Based on samples taken from total extraction flow (XWT)

TABLE B-16
Solvent Plume Load Measurement
Plume Snapshot - October 26, 1998 (Page 1 of 2)

Measurement Location	*X (m)*	*Y (m)*	*Elevation (m)*	*TCE (µg/L)*	*PCE (µg/L)*
1-1	0.95	-1.04	96.74	0.3	4.4
1-2	0.95	-1.04	96.54	0.3	2.7
1-4	0.95	-1.04	96.14	0.3	4.5
1-5	0.95	-1.04	95.94	0.3	6.7
1-6	0.95	-1.04	95.74	1.1	54.9
1-7	0.95	-1.04	95.54	8.6	291.1
1-8	0.95	-1.04	95.34	69.5	1923.1
1-9	0.95	-1.04	95.14	6.0	228.8
1-10	0.95	-1.04	94.94	1.2	40.5
1-11	0.95	-1.04	94.74	2.1	59.8
1-12	0.95	-1.04	94.54	2.4	72.3
1-13	0.95	-1.04	94.34	1.0	36.0
1-14	0.95	-1.04	94.14	0.8	35.3
2-1	0.45	-1.04	96.79	2.9	19.0
2-2	0.45	-1.04	96.59	1.1	7.0
2-3	0.45	-1.04	96.39	0.5	9.2
2-4	0.45	-1.04	96.19	0.8	10.7
2-5	0.45	-1.04	95.99	0.8	20.0
2-6	0.45	-1.04	95.79	3.2	360.6
2-7	0.45	-1.04	95.59	194.3	7190.2
2-8	0.45	-1.04	95.39	1720.8	30933.9
2-9	0.45	-1.04	95.19	42.2	548.3
2-10	0.45	-1.04	94.99	4.8	61.2
2-11	0.45	-1.04	94.79	4.3	60.7
2-12	0.45	-1.04	94.59	3.8	48.5
2-13	0.45	-1.04	94.39	3.2	41.5
2-14	0.45	-1.04	94.19	2.9	45.8
3-1	-0.05	-1.04	96.84	19.2	22.9
3-2	-0.05	-1.04	96.64	13.8	7.5
3-3	-0.05	-1.04	96.44	11.8	6.6
3-4	-0.05	-1.04	96.24	12.1	6.3
3-5	-0.05	-1.04	96.04	17.6	10.1
3-6	-0.05	-1.04	95.84	51.5	718.2
3-7	-0.05	-1.04	95.64	328.2	3712.7
3-8	-0.05	-1.04	95.44	36.1	682.0
3-9	-0.05	-1.04	95.24	28.9	295.5
3-10	-0.05	-1.04	95.04	13.6	36.9
3-11	-0.05	-1.04	94.84	15.5	27.6
3-12	-0.05	-1.04	94.64	14.3	38.0
3-13	-0.05	-1.04	94.44	23.7	49.2
3-14	-0.05	-1.04	94.24	15.5	51.2
5-1	-1.05	-1.04	96.78	2.8	12.0
5-2	-1.05	-1.04	96.58	2.8	13.9
5-3	-1.05	-1.04	96.38	2.5	20.3
5-4	-1.05	-1.04	96.18	1.0	5.3

TABLE B-16
Solvent Plume Load Measurement
Plume Snapshot - October 26, 1998 (Page 2 of 2)

Measurement Location	*X (m)*	*Y (m)*	*Elevation (m)*	*TCE (µg/L)*	*PCE (µg/L)*
5-5	-1.05	-1.04	95.98	0.3	1.7
5-6	-1.05	-1.04	95.78	2.4	19.0
5-7	-1.05	-1.04	95.58	1.3	6.9
5-8	-1.05	-1.04	95.38	2.2	9.8
5-9	-1.05	-1.04	95.18	1.8	9.4
5-10	-1.05	-1.04	94.98	1.7	9.9
5-11	-1.05	-1.04	94.78	1.9	9.7
5-12	-1.05	-1.04	94.58	1.3	8.5
5-13	-1.05	-1.04	94.38	1.4	8.9
5-14	-1.05	-1.04	94.18	2.5	19.0
28-3	1.60	-1.04	96.90	1.4	8.9
28-4	1.60	-1.04	96.70	1.3	8.3
28-5	1.60	-1.04	96.50	1.2	6.7
28-7	1.60	-1.04	96.10	1.9	69.6
28-8	1.60	-1.04	95.90	4.5	185.8
28-9	1.60	-1.04	95.70	1.4	24.4
28-10	1.60	-1.04	95.50	1.3	9.1
28-11	1.60	-1.04	95.30	1.2	9.2
28-12	1.60	-1.04	95.10	1.4	7.8
28-13	1.60	-1.04	94.90	1.4	11.4
28-14	1.60	-1.04	94.70	2.5	22.3

TABLE B-17
Solvent Plume Load
Extraction System Effluent Monitoring - 6/19/98 through 9/13/98

Measurement Date (mm/dd/yy)	*Elapsed Time (days)*	*Avg. Flow Rate (mL/min)*	*PCE[1] (mg/L)*	*TCE[1] (mg/L)*
06/19/98	2	348	63	336
06/24/98	7	375	64	332
06/25/98	8	389	63	289
07/06/98	19	393	63	309
07/09/98	22	398	65	332
07/12/98	25	398	63	285
07/23/98	36	395	41	284
07/24/98	37	390	38	305
07/28/98	41	395	33	278
07/29/98	42	395	32	278
08/03/98	47	395	29	392
08/09/98	53	395	40	340
08/17/98	61	393	36	404
08/20/98	64	387	36	416
08/24/98	68	390	29	393
08/27/98	71	389	29	367
09/03/98	78	385	31	419
09/07/98	82	391	29	367
09/10/98	85	384	30	420
09/13/98	88	390	29	429
		Average VOC Concentration =	30	400
		Standard Deviation =	1	31
		Number of Measurements =	5	5

Notes:

1) Based on samples taken from total extraction flow (XWT)